Ulm University, Institute of Neurobiology, Prof. Dr. Annika Herwig

Spontaneous torpor in the Djungarian hamster *(Phodopus sungorus):* systemic prerequisites and acute mRNA regulation within the brain

DISSERTATION

with the aim of achieving the title

Doctor rerum naturalium (Dr. rer. nat.)

at the Faculty of Natural Sciences,

Department of Biology, Ulm University, Germany

Submitted by

ELENA HAUGG

from Pfaffenhofen, Ilm, Germany

April 2022

Faculty Dean: Prof. Dr. Thorsten Bernhardt,

Institute of Surface Chemistry and Catalysis,

Ulm University, Germany

First Reviewer: Prof. Dr. Annika Herwig,

Institute of Neurobiology,

Ulm University, Germany

Second Reviewer: Prof. Dr. Simone Sommer,

Institute of Evolutionary Ecology and Conservation Genomics,

Ulm University, Germany

Day of oral defense: 27.06.2022

“If you are not willing to learn, no one can help you.

If you are determined to learn, no one can stop you.”

(Zig Ziglar)

Index of Content

I General Abbreviations 11

II General Abstract 12

III Allgemeine Zusammenfassung 14

1 General Introduction 16

1.1 From basic research to application 16

1.2 Metabolic downstates in nature 17

1.3 Hibernation versus spontaneous torpor 18

1.4 The Djungarian hamster 19

1.5 The brain as major control center 21

1.6 Aims of thesis 22

2 Body Temperature and Activity Adaptation of Short Photoperiod-Exposed Djungarian Hamsters *(Phodopus sungorus):* Timing, Traits, and Torpor 26

2.1 Main Document 27

2.2 Supplementary Material 47

3 Comparative Transcriptomics of the Djungarian Hamster Hypothalamus during Short Photoperiod Acclimation and Spontaneous Torpor 56

3.1 Main Document 57

3.2 Supplementary Material 74

3.2.1 Supplementary File 1: Supplementary Tables and Figures 74

3.8.2 Supplementary File 2: Processing Pipeline 78

3.8.3 Supplementary File 3: R-Statistics 81

4 Time to Enter Torpor: Transcriptomics of the Djungarian Hamster Hypothalamic Core Areas Suprachiasmatic Nucleus and Paraventricular Nucleus 86

4.1 Abstract 88

4.2 Introduction 89

4.3 Materials and Methods 92

4.3.1 Animal work 92

4.3.1.1 Breeding and housing 92

4.3.1.2 Experimental setup 92

4.3.1.3 Radiotelemetry 92

4.3.1.4 Sampling scheme 93

4.3.2 Lab work 93
4.3.2.1 Preparations 93
4.3.2.2 Sectioning of the brain 94
4.3.2.3 Staining of cell nuclei and Nissl bodies 94
4.3.2.4 Lasermicrodissection of hypothalamic core areas 94
4.3.2.5 From total RNA to sequencing of mRNA 95
4.3.3 Data work 95
4.3.3.1 Bioinformatics 95
4.3.3.2 Data depositories and supplied scripts 96
4.3.3.3 Statistics 96
4.3.3.4 Data interpretation 97
4.3.3.5 Gene expression profiling 97
4.3.3.6 Regulated biological processes 97
4.3.3.7 Screening for indicator genes 98
4.3.3.8 Regulated genes 98
4.4 Results 98
4.4.1 Gene expression profiling 99
4.4.2 Regulated biological processes 99
4.4.3 Screening for indicator genes 99
4.4.4 Genes regulated in both SCN and PVN during torpor entry 99
4.4.5 Genes regulated in SCN during torpor entry 100
4.4.6 Genes regulated in PVN during torpor entry 100
4.5 Discussion 100
4.5.1 Gene expression profiling 101
4.5.2 Regulated biological processes 102
4.5.3 Screening for indicator genes 102
4.5.4 Genes regulated in both SCN and PVN during torpor entry 106
4.5.5 Genes regulated in SCN during torpor entry 107
4.5.5.1 Mitochondria 107
4.5.5.2 Systemic signaling and metabolism 108
4.5.5.3 Transcription and modification 110
4.5.5.4 Cell cycle 111

4.5.5.5 Brain plasticity 111
4.5.5.6 Unclear function 112
4.5.6 Genes regulated in PVN during torpor entry 113
4.6 Conclusion 114
4.7 Tables and Figures 115
4.8 Supplementary Material 123
4.8.1 Supplementary File 1: Supplementary Tables and Figures 123
4.8.2 Supplementary File 2: Processing Pipeline 128
4.8.3 Supplementary File 3: R-Statistics 132
5 General Discussion 136
5.1 Early prediction of torpor behavior using radiotelemetry data 136
5.1.1 Why is torpor expressed in artificial, rich conditions? 137
5.1.2 Does torpor influence circadian rhythm? 139
5.1.3 Is a certain phenotype inherited? 140
5.1.4 Are there forever normothermic hamsters? 140
5.1.5 Is the next torpor bout predictable? 142
5.1.6 Is locomotor activity data reliable? 142
5.1.7 How to express relative locomotor activity data? 144
5.1.8 How do locomotor activity and body temperature relate? 145
5.1.9 Are there alternatives to radiotelemetry? 147
5.1.10 Can radiotelemetry help to refine animal husbandry and reduce animal numbers? 148
5.2 Investigation of hypothalamic control mechanisms by transcriptomics 149
5.2.1 What is mapping of transcriptomes good for? 150
5.2.2 How to unravel torpor-genes? 151
5.2.3 How to identify the relevant data? 152
5.2.4 Are transcriptome studies in hibernators and Djungarian hamsters comparable? 154
5.3 Further Perspectives 156
IV References 159
V Statement of Contribution 187
VI Approvals and Funding 187

VII *Scientific Curriculum Vitae* 188

VIII Danksagung 192

I General Abbreviations

abbreviation	general meaning	dissertation-specific remarks
HT	hypothermia	torpor with Tb < 32 °C for at least 30 minutes
HT-group		hamsters sampled during a torpor bout; kept in SP
log2(FC)	logarithm of fold change to the base 2	per gene, given for the first-named relative to the second-named sampling group of a pairwise comparison
LP	summer-like long photoperiod	artificial conditions with 16:8 hours light:darkness
LP-group		hamsters kept in LP over the course of their lifespan; sampled in NT
NT	normothermia	no torpor given Tb > 32 °C
NT-group		hamsters sampled on a torpor-free day; either kept in LP or SP
padj	adjusted p-value	significance of a genes` regulation; normalized over all samples of a pairwise comparison
photoperiod	daylength	
photophase	daytime hours	
PVN	paraventricular nucleus	
SCN	suprachiasmatic nucleus; circadian master clock	
scotophase	nighttime hours	
SP	winter-like short photoperiod	artificial conditions with 8:16 hours light:darkness
SP-group		hamsters kept in LP for at least 10 weeks; transferred to SP; sampled after at least 10 weeks and at least one torpor bout in HT or NT
Std. Dev.	standard deviation of the mean	
Tb	core body temperature	high-resolute, real-time, remote measurements via radiotelemetry
torpor	a natural, reversible metabolic downstate	
torpor incidence	number of torpor bouts per number of observed days	given for the last full seven days exclusively the day of sampling
ZT	Zeitgeber-time, given in hours after an external cue for entrainment	lights on at ZT0; lights off at ZT16 in LP, lights off at ZT08 in SP; torpor entry around ZT01, deep torpor around ZT04, torpor arousal around ZT07

II General Abstract

Djungarian hamsters (*Phodopus sungorus,* Cricetidae) are small rodents originating from the Siberian steppes, a seasonally variable environment. Since the 1970ies, their internal adjustments to changing external conditions are studied with approaches ranging from systemic to molecular level. The animals maintain energy balance also under energetic challenging winter conditions. This is allowed by a pronounced response in behavior, morphology and physiology to winter-like short photoperiod, which is naturally present in early autumn and winter and can artificially be provided in the lab at any time throughout the year. After about three months, when the hamsters have acclimated their activity, body mass, food intake and fur properties, as well as all underlying physiological processes, spontaneous torpor bouts are expressed by most hamsters. During torpor, metabolic rate and consequently body temperature of this model organism are clearly reduced. Unlike larger, seasonal rodents that hibernate with torpor bouts for days and weeks, torpor bouts in Djungarian hamsters are restricted to the few hours of daylight. However, the photoperiodic, nocturnal hamsters has a high metabolism most of the time.

It is evident, that the comprehensive, systemic preconditions as well as timing and course of torpor episodes are orchestrated within hypothalamic core areas. As response to environmental stimuli, they integrate external and internal cues from the peripheral organs and interact with each other via feedback loops of various neuroendocrine and anatomical pathways to control the output. Findings gained from this growing interdisciplinary basic research allows deeper insight in metabolic control mechanisms of endothermic mammals and might be applied in animal protection, human medicine, and space travel. Furthermore, this profound knowledge might contribute to assess problems such as climate change, food scarcity, or light pollution.

This thesis on expression of spontaneous torpor in the Djungarian hamster contributes with big data sets and state-of-the-art analysis methods to expand this knowledge. Radiotelemetry data provide deeper insight into potential causes and effects of the hamster's individual acclimation to short photoperiod which does not necessarily include torpor expression. Wide, predictive analyzes allow an improved distribution of hamsters to sampling groups with the aim to lower potential bias in the neuroendocrine and molecular data. Monitoring of locomotor activity and core body temperature has the potential to

indicate, whether torpor is expressed, how often and on which days. The radiotelemetry study indicates that the later torpor incidence is related to the initial response to short photoperiod, the strength of gradual acclimation, temporal coincidence of torpor entry with onset of photophase, torpor duration, and minimal body temperature values during a torpor bout. This underlines the already known influence of the major circadian clock on the Djungarian hamsters` energy balance (Chapter 2). Therefore, two transcriptome studies were performed to unraveled torpor-relevant gene regulation in the hypothalamus during deep torpor (Chapter 3) and in the suprachiasmatic and paraventricular nuclei of the hypothalamus during torpor entry (Chapter 4). The regulation of the circadian clock and the metabolism are not only connected but seem to influence each other, as e.g., shown by a synchronized regulation of clock genes with glucose transporters and mitochondrial respiratory chain. These transcriptomic data will be of use to find available anti-mRNA and antibodies which are applicable in the Djungarian hamster for the verification and anatomical localization of regulated genes and their proteins.

III Allgemeine Zusammenfassung

Dsungarische Hamster (*Phodopus sungorus,* Cricetidae) sind kleine Nagetiere aus der Sibirischen Steppe, einer saisonal variablen Umgebung. Ihre internen Anpassungen an die sich verändernden externen Bedingungen werden seit den 1970er Jahren mithilfe verschiedenster methodischer Ansätze studiert, die von systemischer bis molekularer Ebene reichen. Die Hamster halten ihr Energiegleichgewicht auch unter energetisch herausfordernden Winterbedingungen aufrecht. Dies wird durch ausgeprägte Anpassungen von Verhalten, Morphologie und Physiologie als Antwort auf eine winterähnliche kurze Photoperiode ermöglicht, welche natürlicherweise im frühen Herbst und Winter vorherrscht und ganzjährig künstlich im Labor eingestellt werden kann. Nachdem die Hamster über etwa drei Monate hinweg Aktivität, Körpergewicht, Futteraufnahme und Felleigenschaften sowie alle zugrundeliegenden physiologischen Prozesse angepasst haben, zeigen die meisten Hamster spontanen Torpor. Die Stoffwechselrate und folglich die Körpertemperatur dieses Modellorganismus sind während einer Torporepisode deutlich reduziert. Im Gegensatz zu größeren, saisonalen Nagetieren, die mit tage- bis wochenlangen Torporepisoden überwintern, ist Torpor im Dsungarischen Hamster auf die wenigen Tageslichtstunden beschränkt. Jedoch weist der photoperiodische, nachtaktive Hamster die meiste Zeit des Tages einen hohen Stoffwechsel auf.

Es liegt nahe, dass die umfassenden, systemischen Voraussetzungen sowie die Zeitplanung und der Verlauf von Torporepisoden in den Kerngebieten des Hypothalamus reguliert werden. Als Antwort auf Umweltreize integrieren sie externe und interne Signale von peripheren Organen und interagieren miteinander über Rückkopplungsschleifen mannigfaltiger neuroendokriner und anatomischer Leitungsbahnen, um die Reaktion zu kontrollieren. Erkenntnisse, die mit dieser zunehmend interdisziplinären Grundlagenforschung gewonnen werden, erlauben einen besseren Einblick in Kontrollmechanismen des Stoffwechsels endothermer Säugetiere und könnten in Tierschutz, Humanmedizin und Raumfahrt Anwendung finden. Weiterhin könnte dieses fundierte Wissen dazu beitragen, Probleme wie Klimawandel, Nahrungsmittelknappheit oder Lichtverschmutzung zu verstehen.

Diese Thesis zur Expression spontanen Torpors im Dsungarischer Zwerghamster trägt mit großen Datensätzen und modernsten Analysemethoden zur Ausweitung dieses

Wissens bei. Radiotelemetriedaten bieten tiefere Einblicke in mögliche Ursachen und Wirkungen der individuellen Anpassungsleistung eines Hamsters an die kurze Photoperiode, welche nicht unbedingt die Expression von Torporepisoden miteinschließt. Umfassende, prädiktive Analysen erlauben eine verbesserte Verteilung von Hamstern auf Beprobungsgruppen, um etwaige Verzerrungen in den neuroendokrinen und molekularen Daten zu mindern. Die Überwachung von Aktivität und Körperkerntemperatur könnte potenziell anzeigen, ob Torpor exprimiert wird, wie oft, und an welchen Tagen. Die Radiotelemetriestudie deutet darauf hin, dass die spätere Torporinzidenz mit der initialen Antwort auf eine kurze Photoperiode, der Intensität der graduellen Anpassungsleistung, des zeitlichen Zusammenfalls von Torporeintritt mit Beginn der Photophase, der Torpordauer und den minimalen Körpertemperaturwerten während eines Torpors zusammenhängt. Dies betont den bereits bekannten Einfluss der inneren Uhr auf das Energiegleichgewicht des Dsungarischen Hamsters (Kapitel 2). Darum wurden zwei Transkriptomstudien durchgeführt, um Torpor-relevante Genregulation während des tiefen Torpors im Hypothalamus (Kapitel 3) und während des Torporeintritts im suprachiasmatischen und im paraventrikulären Nukleus des Hypothalamus (Kapitel 4) zu begreifen. Die Regulation der inneren Uhr und des Stoffwechsels stehen nicht nur in Verbindung, sondern scheinen sich gegenseitig zu beeinflussen, wie beispielsweise eine synchronisierte Regulation von Uhrengenen mit Glukosetransportern und mitochondrialer Atmungskette aufzeigt. Diese Transkriptomdaten werden hilfreich sein, um verfügbare anti-mRNA und Antikörper zu finden, welche im Dsungarischen Hamster für die Verifizierung und anatomische Lokalisation von regulierten Genen und ihren Proteinen angewandt werden können.

Chapter 1

General Introduction



1.1 From basic research to application

Fascination hypometabolism. Metabolic downstates are defined by a temporary, and therefore reversible, natural depression of metabolic rate, often associated with reduction of core body temperature (Tb), muscle and brain activity, breathing and heart rate [1]. The overarching term of metabolic downstates is torpor, which includes diverse forms of torpor, such as fasting torpor, spontaneous daily torpor, estivation, and hibernation [2,3]. Torpor requires internal prerequisites, including neuroendocrine regulation of reproductivity, body mass and fur properties, which are induced and modulated by environmental cues, such as photoperiod, ambient temperature and food availability [4–7]. Hereby, elementary brain areas must perfectly integrate external and internal stimuli. Blood pressure must be adjusted to allow the initialization, maintenance, and termination of a metabolic downstate, while the blood composition must maintain transport of oxygen and nutrients as well as functionality of the immune system [8–12]. The brain and peripheral organs must compensate challenges as oxidative stress and accumulation of biological waste products [13–15]. Within each organelle, such as cell nuclei and mitochondria, molecular mechanisms, such as transcription, translation, and ubiquitination, must be regulated, respecting the temperature-dependent enzyme activity and further biochemical processes [16–20]. Although growing interdisciplinary research

from systemic to molecular level examined single aspects of regulatory mechanisms, the complexity to orchestrate metabolic downstates impedes a comprehensive understanding [21–23].

Relevance for human. Hypometabolism including hypothermia of endotherms can be observed not only in rodents and hedgehogs, but also in birds, bats, bears, and even primates as lemurs [23–25]. Therefore, knowledge on fine-tuned control of cardiorespiratory, muscular, and neuroendocrine functions is potentially applicable to humans [26–28]. Insights are valuable for translational medicine to understand, prevent and treat e.g., weight issues, sleep problems, dementia, stroke and ischemia-reperfusion damage, besides further metabolic, energetic, cardiovascular, neurological, circadian, and neuroendocrine syndromes and dysregulations [29,30]. Torpor-like states might be reasonably provoked in humans. For long, exhausting surgeries, human bodies are already artificially cooled during a so-called therapeutic hypothermia, aiming to slow down metabolism and thereby gain time [31]. Furthermore, long, exhausting space missions in spaceships might one day be made possible by a maintenance of some sort of metabolic downstate in astronauts, which also implies minimal oxygen and food need [27,28,32].

1.2 Metabolic downstates in nature

Costs and benefits. Drastic metabolic downstates in rodents require tremendous physiological, morphological, and behavioral preparations and impact the entire organism. There is a risk of unpleasant side effects, such as temperature-dependent telomere damage in dormice [33] and hibernation-driven memory loss in European ground squirrels [34]. By contrast, there are several potential benefits [35], while the most important is to wait out unfavorable conditions. For example, estivation is expressed to overcome hot and dry summers, starvation torpor to overcome food scarcity, spontaneous torpor and hibernation to overcome harsh winters [3]. Usually, animals reverse the temporal hypometabolism as well as the preconditions without suffering acute life-threatening harm [23,24,26].

Species-specific adaptations. Since nature provides various extreme environments and situations, there are countless potential model organisms across the animal kingdom to study the spectrum of species- and circumstance-specific adaptations. Hereby, external

factors, as daylength and ambient temperature in the seasonal course, trigger species-specific acclimation mechanisms which enable individual energy saving mechanisms. Given or missing elements of this cascade cause diversity across species and a variety of manifestation within species. For example, the rat (*Rattus norvegicus,* Muridae) is naturally not capable of any form of dormancy [36]. The mouse (*Mus musculus,* Muridae) can use fasting-induced torpor after a certain body mass loss [37,38]. The thirteen-lined ground squirrel (*Ictidomys tridecemlineatus*, Sciuridae) hibernates throughout the winter months [39]. The edible dormouse (*Glis glis,* Gliridae) can express estivation, hibernation and spontaneous torpor [40]. The Djungarian hamster (*Phodopus sungorus,* Cricetidae), also known as Siberian hamster (Pallas 1773), can use starvation torpor and spontaneous torpor, which differ in metabolic rate patterns and hypothalamic gene expression [41,42].

1.3 Hibernation versus spontaneous torpor

Same but different. All metabolic downstates serve to save energy and are characterized in a drastic, reversible reduction of metabolic rate which causes a temporal decline of further biological functions [24,43]. Yet, it is unclear, whether distinct types of heterothermy are based on similar mechanisms [42,44]. For example, hibernation in the garden dormouse (*Eliomys quercinus*, Gliridae) and spontaneous torpor in the Djungarian hamster strongly differ in prerequisites and torpor patterns, although both are used for overwintering [3].

The circannual and circadian clock. In particular, the clock varies between both nocturnal model organisms [45]. The seasonal dormouse is circannual, which means, its acclimatization to natural or acclimation to artificial conditions is largely determined by an internal rhythm [46]. By contrast, the photoperiodic hamster uses the daylength as external cue to adjust its internal clock daily which consequently triggers adaptation mechanisms feasible for the circumstances [47]. This difference might be based on conditions in the particular distribution area, as well as the strive for reproductive success despite the species-specific life expectancy [21,48–50].

Overwintering strategies. Both species underlie gradual, reversible, drastic physiological, morphological, and behavioral changes. These adjustments allow their metabolic downstates. Hereby, dormice and hamsters have different strategies. In

particular, the bigger dormouse gains body mass prior to the anticipated winter to consume energy from fat tissue during hibernation. For example, in 18 late-born juvenile dormice, the body mass was pre-hibernation 82.3 ± 6.7 g, and post-hibernation 61.1 ± 9.6 g [51]. The smaller hamster cannot gain sufficient fat reserves to hibernate. Broadly speaking, its strategy is to save energy by limiting foraging activity. Consequently, the reduced food intake causes a body mass loss between 20 and 40 % prior to torpor expression. For example, although fed *ad libitium,* 12 adult hamsters decreased their average body mass of 35 g to 27 g within three months of acclimation to winter-like short photoperiod [52].

Torpor duration. Once acclimated to winter-like conditions, both species express torpor, however, with an species-specific extent of metabolic reduction [43,44]. The torpor bouts of the dormouse expand to about 14 days. They are interrupted by few hours lasting interbout arousals with normal metabolism [24,53]. By contrast, the normal metabolism of the hamster is interrupted by few hours lasting spontaneous torpor bouts, which are restricted to the daytime hours and synchronized by light [2]. Dependent on housing conditions and monitored data, torpor duration is about 5.7 hours in the hamster [54–56].

Minimal body temperature. In dependency on ambient temperature and torpor duration, species-specific minimal Tb values are maintained. More and more hibernators are found hibernating with Tb values below zero [3]. In dormice, minimal Tb during a torpor bout is about 5 °C when kept without food and water in complete darkness at 4 °C ambient temperature [46]. In hamster, minimal Tb during deep torpor is about 23 ˚C when kept with food and water in short photoperiod at about 18 ˚C ambient temperature [42]. Regardless of the ambient temperature, the Djungarian hamsters' Tb never falls below 12 °C during a torpor bout [55,57–59].

1.4 The Djungarian hamster

Acclimation. The photoperiodic Djungarian hamster anticipates harsh winter-like conditions primarily by changes in daylength, hence photoperiod. Behavior and morphology is acclimated in nature, as soon as photophase duration falls below 13 hours per day, and in artificial conditions, when the light regime is changed from summer-like long photoperiod (e.g., 16:8 hours light:darkness) to winter-like short photoperiod (e.g., 8:16 hours light:darkness) [60–62]. Food intake and body mass are drastically reduced

[4,63,64]. Reproduction is ceased and reproductive organs are receded [65,66]. A white fur is developed for a higher thermal insulation [4,63,64]. Given these and further tremendous, reversible acclimations [2], the summer-like and the winter-like hamster are two distinct model organisms, one fat and reproductive with brown fur, the other lean, and sterile with white fur. Regardless of its acclimation state, the nocturnal hamster is active throughout the nighttime hours, also known as scotophase, and on torpor-free days [67,68].

Daily torpor, but not every day. After about three months of acclimation to short photoperiod, spontaneous torpor is expressed during the daytime hours, also known as photophase [2]. Empirically, torpor incidence, which is the number of torpor bouts per number of observation days [69], differs between hamsters. When kept in 20° C ambient temperature with food *ad libitum*, hamsters without torpor expression are relatively common, while rarely a hamster expresses torpor every day. Hence, the traditional term "spontaneous daily torpor" refers to the hitherto unpredictable and therefore spontaneous torpor bouts of the Djungarian hamster, which are expressed during daylight, but not necessarily every day.

Torpor characteristics. Spontaneous torpor in the Djungarian hamster is characterized by a reduced metabolic rate, which in turn is accompanied by a reduction of Tb, heart rate, and ventilation. The course of Tb values follows the course of metabolic rate values with a temporal delay of about 30 minutes, as exemplary plots showed [41,58,70]. Although torpor is expressed during the resting phase, while the Djungarian hamster lay prone with closed eyes [71], torpor cannot be compared to sleep [27,72–74]. The state of deep torpor, when metabolic rate and Tb values are maintained at a plateau, is resolved by a spontaneous burst of metabolic rate [75]. During torpor arousal, normometabolic and consequently normothermic values are reached by shivering of muscles and non-shivering thermogenesis of mitochondria especially within brown adipose tissue [6,56,76].

Torpor timing. Torpor is initialized, maintained, and reversed within hours [75]. As shown for entrainment after light regime changes, onset and offset of torpor (Tb < 32 °C) are timed with onset and offset of light [54]. When daylength is reduced to four hours per day, torpor does not start earlier, but is expanded into scotophase [55], suggesting onset of light as an important external *Zeitgeber*.

Torpor pattern. To describe torpor, different parameters and definitions were used, according to the method and measurement intervals of monitored data (see also bachelor

thesis of Franziska Heli in 2020/2021 "Definition von Torpor in Dsungarischen Zwerghamstern *(Phodopus sungorus)* anhand von Körpertemperatur und Stoffwechsel"). From experience, the typical pattern of metabolic rate and Tb values varies between individuals and torpor bouts, what impedes comparability and understanding. Timing of torpor entry, deep torpor and arousal, duration of a torpor bout, minimal Tb values, and consequently energy saved, is not predictable.

1.5 The brain as major control center

The photoneuroendocrine pathway. All adaptations in the Djungarian hamster are controlled by photoperiod. The photoneuroendocrine pathway starts with photosensitive ganglion cells within the retina of the eye. The perceived light signal is transmitted via the optic nerve to the suprachiasmatic nucleus (SCN) within the hypothalamus. Consequently, melatonin secretion of the pineal gland within the epithalamus is altered [71,77,78]. Melatonin is exclusively secreted during the scotophase. Thereby, melatonin precisely mirrors night length including changes over the course of a year [66,79,80]. The melatonin signal feeds back to structures in the brain: The pars tuberalis of the pituitary gland to integrate seasonal information, the SCN to entrain circadian rhythmicity, while also the paraventricular nucleus has melatonin receptors [81–85]. The thyroid stimulating hormone (TSHβ) of the pars tuberalis feeds back to the hypothalamus, where it regulates the activity of thyroid hormones (iodothyronine deiodinases II and III) in tanycytes, blood, and several organs. [49,86,87].

Tanycytes. Tanycytes are a specific type of glial cells, lining the third ventricle of the hypothalamus, connecting blood vessels from the median eminence, cerebrospinal fluid, and neurons. Thyroid hormone metabolism in tanycytes is a key regulator of seasonal physiological changes in mammals and birds, as Djungarian hamster, Soay sheep and Japanese quail [65,88,89]. Shape and function of tanycytes change with photoperiod [90,91]. There is evidence, that tanycytes mediate acute and long-term energy metabolism on level of cells, as glucose consumption of neurons, and the whole organism, as thermogenesis of brown adipose tissue [92–94]. Hence, thyroid hormone action is probably involved in torpor control [69,77,95].

The hypothalamus. Functionally, the hypothalamus controls circadian rhythms and sleep, homeostasis of Tb, blood pressure and osmolarity, uptake of food and water, and reproduction [29]. Hence, the hypothalamus integrates external and internal signals to modulate multi-level biological functions appropriate to the external conditions, aiming to maintain an overall energy balance [44,96], making it reasonable to assume that the hypothalamus is also involved in torpor control. The hypothalamic core areas and cell populations play distinct roles in complex physiological contexts, such as photoperiodic acclimations, and, less explored, torpor orchestration [22,32,97]. Several hypothalamic nuclei are of particular interest in torpor control in Djungarian hamsters.

The suprachiasmatic nucleus. The SCN, a hypothalamic core area located bilaterally from the ventral third ventricle, is the circadian clock of all mammals, which is synchronized by the external 24-h-rhythm [98,99]. As pacemaker of the timekeeping system, the self-oscillating neurons within the SCN regulate in a complex feedback loop rhythms of downstream oscillators, such as feeding and sleeping [100–102]. Since torpor bouts are strongly circadian gated, the SCN is likely to be involved in torpor control.

The paraventricular nucleus. Neurons of the SCN project to another hypothalamic core area, the paraventricular nucleus (PVN), which is located bilaterally from the dorsal third ventricle [99,103–105]. Together with the supraoptic nucleus, the PVN influences the sympathetic nervous system via the intermediolateral horn of the spinal cord and controls the release of hormones via the pituitary gland into the bloodstream [103,106,107]. The PVN plays a role in food and water uptake, fat reserves and energy metabolism, circadian rhythm and response to short photoperiod, hence, probably also in torpor control [108–113].

1.6 Aims of thesis

Radiotelemetry. Djungarian hamsters differ in response to short photoperiod in terms of e.g., body mass reduction, winter fur growth, torpor incidence and torpor pattern [5,114]. This broad spectrum of traits as well as unpredictable spontaneous torpor bouts challenges an adequate sampling to unravel the mechanisms behind. Hence, this dissertation should contribute with the further development of analysis methods using available acclimation data inclusively data monitored by a radiotelemetry system. Gained

insights might favor an early recognition of later torpor proneness and enable considerations regarding an improvement of sampling.

In Chapter 2, radiotelemetry data of 60 Djungarian hamsters were analyzed to better understand the interplay of several parameters, namely Tb and locomotor activity during the last seven days before sacrifice as well as body mass and fur index throughout the about three months of acclimation to short photoperiod. Data might help to forecast the next torpor bout and therefore planning of sampling. Eleven of these hamsters were implanted prior to the light regime change from long to short photoperiod. Data might favor to conclude the later torpor behavior by the initial response of Tb and locomotor activity after the light regime change and might improve the equal distribution of hamsters with diverse traits on sampling groups.

Transcriptomics. To unravel mechanisms behind acclimation to short photoperiod and torpor expression on mRNA-level, several transcriptome studies were performed on the hypothalamus in the hibernating thirteen-lined ground squirrel *(Ictidomys tridecemlineatus)* [115,116] and the Djungarian hamster [117,118]. A comprehensive understanding is unclear, since these approaches differ in study design, lab work, data processing and analysis. Hence, this dissertation contributes with two analogously performed transcriptomic studies in the Djungarian hamster. One study faces general mechanisms, driven by photoperiodic acclimation as well as torpor, within the whole hypothalamus. The other study adds specific mechanisms in focusing first-time on the hypothalamic nuclei SCN and PVN.

In Chapter 3, the hypothalamic transcriptome of twelve hamsters sampled four hours after lights on was analyzed to better understand underlying molecular mechanisms of torpor control. Two pairwise comparisons of sampling groups allowed to assess differential gene expression within the hypothalamus. A comparison between normothermic winter-like and normothermic summer-like hamsters should validate mRNA-Seq methods given already known regulation of certain photoperiod-driven gene regulation. A comparison between deep torpor and a torpor-free day in winter-like hamsters might help to investigate mechanisms of torpor. Yet, in this approach on the whole hypothalamus, nucleus-specific mechanisms essential for torpor control might not be discovered.

In Chapter 4, lasermicrodissection allowed to focus on distinct hypothalamic nuclei which are potentially relevant in torpor control. Twelve winter-like hamsters were sampled either during torpor entry or on a torpor-free day. Stained cryosections of the brain allowed to distinguish the hypothalamic nuclei given their different neuronal density. After lasermicrodissection of SCN and PVN, the bioinformatical and statistical pipeline developed in Chapter 3 was applied. For each hypothalamic nucleus, data of the hypothermic group was compared with data of the normothermic group. Hereby, torpor-relevant mechanisms in this nucleus-specific approach might be investigated.

Chapter 2

Body Temperature and Activity Adaptation of Short Photoperiod-Exposed Djungarian Hamsters *(Phodopus sungorus):* Timing, Traits, and Torpor

Published as original research article on 07 July 2021 in Integrative Physiology, a section of the journal Frontiers in Physiology, doi: 10.3389/fphys.2021.626779.

Authors: Elena Haugg, Annika Herwig, Victoria Diedrich

Edited by: Alessandro Silvani, University of Bologna, Italy

Reviewed by: David A. Bechtold, The University of Manchester, United Kingdom, and Rebecca Oelkrug, University of Lübeck, Germany

Copyright © 2021 Haugg, Herwig and Diedrich. This is an open-access article distributed under the terms of the Creative Commons Attribution License (CC BY 4.0, https://creativecommons.org/licenses/by/4.0/). The use, distribution or reproduction in other forums is permitted, provided the original author(s) and the copyright owner(s) are credited and that the original publication in this journal is cited, in accordance with accepted academic practice. No use, distribution or reproduction is permitted which does not comply with these terms.

2.1 Main Document

frontiers in Physiology

ORIGINAL RESEARCH
published: 07 July 2021
doi: 10.3389/fphys.2021.626779



Body Temperature and Activity Adaptation of Short Photoperiod-Exposed Djungarian Hamsters (*Phodopus sungorus*): Timing, Traits, and Torpor

Elena Haugg, Annika Herwig and Victoria Diedrich*

Institute of Neurobiology, Ulm University, Ulm, Germany

To survive the Siberian winter, Djungarian hamsters (*Phodopus sungorus*) adjust their behavior, morphology, and physiology to maintain energy balance. The reduction of body mass and the improvement of fur insulation are followed by the expression of spontaneous daily torpor, a state of reduced metabolism during the resting phase to save additional energy. Since these complex changes require time, the upcoming winter is anticipated *via* decreasing photoperiod. Yet, the extent of adaptation and torpor use is highly individual. In this study, adaptation was triggered by an artificially changed light regime under laboratory conditions with 20°C ambient temperature and food and water *ad libitum*. Two approaches analyzed data on weekly measured body mass and fur index as well as continuously recorded core body temperature and activity during: (1) the torpor period of 60 hamsters and (2) the entire adaptation period of 11 hamsters, aiming to identify parameters allowing (1) a better prediction of torpor expression in individuals during the torpor period as well as (2) an early estimation of the adaptation extent and torpor proneness. In approach 1, 46 torpor-expressing hamsters had a median torpor incidence of 0.3, covering the spectrum from no torpor to torpor every day within one representative week. Torpor use reduced the body temperature during both photo- and scotophase. Torpor was never expressed by 14 hamsters. They could be identified by a high, constant body temperature during the torpor period and a low body mass loss during adaptation to a short photoperiod. Already in the first week of short photoperiod, approach 2 revealed that the hamsters extended their activity over the prolonged scotophase, yet with reduced scotophase activity and body temperature. Over the entire adaptation period, scotophase activity and body temperature of the scoto- and photophases were further reduced, later accompanied by a body mass decline and winter fur development. Torpor was expressed by those hamsters with the most pronounced adaptations. These results provide insights into the preconditions and proximate stimuli of torpor expression. This knowledge will improve experimental planning and sampling for neuroendocrine and molecular research on torpor regulation and has the potential to facilitate acute torpor forecasting to eventually unravel torpor regulation processes.

Keywords: circadian rhythms, metabolism, phenotypes, radiotelemetry, Siberian hamster, spontaneous daily torpor

OPEN ACCESS

Edited by:
Alessandro Silvani,
University of Bologna, Italy

Reviewed by:
David A. Bechtold,
The University of Manchester, United Kingdom
Rebecca Oelkrug,
University of Lübeck, Germany

****Correspondence:***
Elena Haugg
elena.haugg@uni-ulm.de

Specialty section:
This article was submitted to Integrative Physiology, a section of the journal Frontiers in Physiology

Received: *06 November 2020*
Accepted: *24 May 2021*
Published: *07 July 2021*

Citation:
Haugg E, Herwig A and Diedrich V (2021) Body Temperature and Activity Adaptation of Short Photoperiod-Exposed Djungarian Hamsters (Phodopus sungorus): Timing, Traits, and Torpor. Front. Physiol. 12:626779. doi: 10.3389/fphys.2021.626779

INTRODUCTION

The investigation of seasonal winter adaptation, including metabolic downstates like hibernation and daily torpor, in mammals has a long history (Jastroch et al., 2016), with promising implications for human life sciences, medicine, and manned spaceflight (Dave et al., 2012; Choukèr et al., 2019). Diverse species (bears, lemurs, marmots, bats, birds, squirrels, and dormice) in various environmental contexts (season, photophase, temperature, social context, food, and sleep) have been characterized *via* measurements of many different parameters at the whole animal level (behavior, morphology, and physiology) (Geiser, 2008). Over the years, the underlying regulatory mechanisms on the (neuro)endocrine and molecular genetic levels have become of increasing interest, and new analytical methods have opened. These methods either enable the measurement of classical *in vivo* parameters like activity, metabolic rate, body temperature, and body composition with higher resolution or the *in vitro* detection of new parameters like structure or transport proteins, enzymes, and RNA/DNA on the cellular and molecular levels. This rich repertoire offers countless possibilities to characterize the mechanisms of seasonal adaptation with a high degree of precision and standardization, improving comparability and reproducibility. However, the study of torpor regulatory mechanisms has remained complicated since torpor is a sensitive and difficult to anticipate physiological state. Hence, research would benefit from a method that better predicts adaptive strategies, including torpor.

Seasonal adaptations have been thoroughly investigated in the small rodent *Phodopus sungorus* (Pallas 1773). In long photoperiods, Djungarian hamsters are reproductively active and have a high body mass and a light brown summer fur. As soon as photophase length falls below 13 h per day (Hoffmann, 1982), the hamsters start to prepare for the harsh Siberian winter by reducing body mass as well as reproductive organs and by growing a well-insulating, white winter fur, to name only a few adaptation parameters (Scherbarth and Steinlechner, 2010; Cubuk et al., 2016). Approximately 3 months later, the morphological and physiological adaptations are largely completed, and the animals start to express spontaneous daily torpor. They use this metabolic downstate to save additional energy during their resting phase (photophase), while they are normothermic and active during the scotophase (Heldmaier and Steinlechner, 1981b; Diedrich et al., 2020). This complex temporal organization requires sensitivity to photoperiod length, based on daily light information as *zeitgeber*.

Most laboratory Djungarian hamsters are kept indoors in artificial light and subjected to abrupt changes of photoperiod. Independently of the time of year, they are bred in long photoperiod and transferred to short photoperiod to study the adaptation processes and spontaneous daily torpor. Although performed countless times since the beginnings of research in the 1970s, it has not been reported how the hamsters' physiology reacts to this abrupt photoperiod change in the short and long terms.

Timing and the extent of seasonal adaptation in Djungarian hamsters can be highly individual within a hamster population. The morphology and physiology of respective adaptation phenotypes have been thoroughly characterized and categorized as responders, late responders, partial responders, or non-responders (Ruf et al., 1991, 1993; Przybylska et al., 2019), whereby responsiveness refers to the reaction to the change in photoperiod length. Non-responders retain a constant body mass and a brown summer fur and therefore do not express torpor. Responders show the already described morphological and physiological adaptations, yet with a high variability in timing and extent of single adaptive parameters. Even in responders, torpor expression is not obligatory under laboratory conditions. Although parameters like activity or food intake could be related to the incidence of torpor bouts (Ruf et al., 1991), it is still not possible to reliably extrapolate from certain adaptation parameters to later torpor expression.

In most institutes that contributed to the multiple studies on Djungarian hamsters during the last 40 years, torpor research comprises the *in vivo* characterization of responding hamsters and their torpor expression as well as a postmortem organ sampling for *in vitro* molecular analyses. The metabolic state of each hamster can be estimated from body temperature. Spontaneous daily torpor in Djungarian hamsters has been defined as a hypothermic core body temperature (T_b) below 32°C (Ruf and Heldmaier, 1992; Ruf et al., 1993) for more than 30 min (Paul et al., 2005; Diedrich et al., 2015; Cubuk et al., 2017a,b). Single torpor bouts and the expression patterns can be further characterized using parameters like torpor incidence, torpor onset, minimal temperature during a torpor bout, torpor offset, as well as torpor duration (Kirsch et al., 1991; Ruf et al., 1993; Paul et al., 2004).

With continuous radiotelemetry measurements (Scribner and Wynne-Edwards, 1994; Schöttner et al., 2011; Jones et al., 2014), hypothermic hamsters with a body temperature below 32°C (HT, torpor) can be differentiated from normothermic hamsters (NT, no torpor) on the day of sampling (Bank et al., 2015). Usually, the sampling paradigm also comprises a temporal component allowing to differentiate circadian factors (Herwig et al., 2007; Bank et al., 2017; Cubuk et al., 2017a,b). This high degree of sampling standardization is of great value for the *in vitro* characterization of the molecular mechanisms underlying the different stages of torpor expression.

However, the sampling paradigm is based on each hamster's acute torpor expression. The high interindividual variability in torpor incidence as well as the torpor onset or torpor bout duration might affect the desired equal distribution across sampling groups.

To define parameters in order to better predict torpor expression in individuals during the torpor period, the present study examined the existing body temperature and activity datasets of responders, which had been dedicated to molecular organ analyses on torpor regulation. In an additional approach,

Abbreviations: HT, hypothermic—body temperature below 32°C for more than 30 min, spontaneous daily torpor (on day of sampling); NT, normothermic—no spontaneous daily torpor (on day of sampling); LP, long photoperiod—16 h light and 8 h darkness per day; SP, short photoperiod—8 h light and 16 h darkness per day; Std. Dev., standard deviation of the mean; T_b, core body temperature; ZT, *zeitgeber* time, with ZT0 as the beginning of photophase.

data were analyzed over the entire adaptation process to a short photoperiod, aiming at the early estimation of the adaptation extent and torpor proneness. Additionally, winter fur development and body mass reduction were determined over the course of adaptation in all animals. The phenotyping toward torpor incidence may help improve the *a priori* planning of experimental groups for a refined sampling with high standardization. Furthermore, the identification of potential predictors on general torpor capability would enable a preselection of torpor-prone hamsters early during adaptation in favor of animal reduction in future experiments.

MATERIALS AND METHODS

Breeding and Housing

Djungarian hamsters (*P. sungorus*) were bred, raised, and kept at the Institute of Neurobiology, Ulm University, at 20 ± 1°C ambient temperature. Artificial light (150 lx) was provided 16 h per day in long photoperiod (LP) and 8 h per day in short photoperiod (SP). Additional constant red light (<5 lx) enabled animal handling during the scotophase. The hamsters were housed in Makrolon type III cages (26.5 cm × 42.5 cm × 18.0 cm) with wooden bedding and tissue as the nesting material. Tap water and food (Altromin hamster breeding diet 7014, Lage, Germany) were provided *ad libitum*. Additionally, cucumber, oak flakes, and sunflower seeds were fed once a week. The hamsters were bred in artificial long photoperiod by an outbred crossing scheme in accordance with the local ethics committee (35/9185.46-3) at Ulm University, Germany. During breeding, hamster pairs were provided with additional nesting material and a red transparent plastic house. Litters were weaned at an age of 3 weeks and housed in same-gender sibling groups. The hamsters were single housed since the age of 6 weeks. They were transferred to the short photoperiod earliest at 12 weeks of age. The expression of spontaneous daily torpor was expected during the torpor period after adaptation to the short photoperiod was largely completed.

The Experiment

Between 2018 and 2020, 80 adult hamsters were adapted to SP with an average age of 4 months and sampled approximately 4 months later during the torpor period for molecular torpor research. The change of light regime from long to short photoperiod delayed the zeitgeber time 0 (ZT0) by 1 h and advanced the beginning of the scotophase by 7 h to favor the later realization of the described temporal sampling paradigm. The hamsters were approached daily by the caretaker between ZT07 and ZT08 for a visual check. Once a week, the animals were handled just before ZT08 by the experimenter to assess the progress of short photoperiod adaptation. Therefore, the relative body mass change (in percent) with respect to the absolute body mass of the last week in LP was monitored. In addition, the hamsters' fur index was scored from 1 for a light brown summer fur to 6 for a dense white winter fur (Figala et al., 1973). During handling, wooden bedding and nesting material were refreshed every other week.

To measure body temperature and activity, a radiofrequency transmitter [Data Sciences International (DSI), Harvard Bioscience Inc., St. Paul, MN, United States] was implanted intraperitoneally under isoflurane anesthesia (2.5% and 1 ml/min for induction, 0.75–2.0% and 0.4 ml/min for maintenance) and carprofen analgesia (5 mg/kg, i.p.; Rimadyl, Zoetis Deutschland GmbH, Berlin, Germany). Recovery from surgery was supported by additional oat flakes, sunflower seeds, cucumber, and nesting material. Body mass, coat care, posture, and behavior were monitored daily for about 7 days. Experimental and surgical procedures were approved by the Regierungspräsidium Tübingen, Germany (1411).

Twenty hamsters, implanted during the torpor period, expressed spontaneous daily torpor within 2 weeks after implantation and were directly sacrificed. Data of the remaining 60 hamsters were used for this study, which required radiotelemetry data of 1 week after at least 1 week of recovery from surgery.

Approach 1: Torpor Behavior (n = 60)

The torpor behavior of 60 hamsters (41 males and 19 females) was analyzed using radiotelemetry data recorded during the torpor period after SP exposure for 15 ± 2 weeks. For animals that expressed torpor, the last week before sacrifice was chosen as the representative week of analysis. To favor a comparable adaptation state, the first possible week after 1 week of recovery from surgery was chosen as the week of analysis for hamsters that never expressed torpor during their individual total observation interval. Detailed background information on each hamster's age when transferred to SP and the weeks spent in SP at implantation, observation, and sacrifice is listed in the **Supplementary Table 1**.

Torpor incidence was calculated as the number of torpor bouts divided by the number of observation days, i.e., 7 days of the analysis week (**Figure 1A**). Furthermore, a decrease of body temperature to at least 33°C which did not result in a torpor bout per definition is referred to as a torpor bout attempt. The minimal body temperature is the lowest value during a torpor bout. Temporal values are given in hours and minutes after the beginning of the photophase at ZT0. Torpor onset was defined by the time point or ZT when a hamster reached a body temperature of 32°C first and consequently entered a torpor. Torpor offset was defined by the time point or ZT when the body temperature exceeded the threshold of 32°C first during the hamsters' arousal from a torpor bout. Torpor duration was defined as the time between torpor onset and torpor offset (Ruf et al., 1993; Paul et al., 2005).

Approach 2: Change of Light Regime and Adaptation to Short Photoperiod (n = 11)

Eleven of the 60 hamsters analyzed in approach 1 (five females and six males, bred in 2020) had already been implanted in long photoperiod for long-term radiotelemetry measurements until sacrifice for molecular torpor research in SP14. Data acquisition started after one and a half weeks of surgical recovery and comprised 1 week in long photoperiod (referred to as LP baseline or SP00) and 13 weeks in short photoperiod (from SP01 to SP13). The development of body mass, fur index, body temperature,

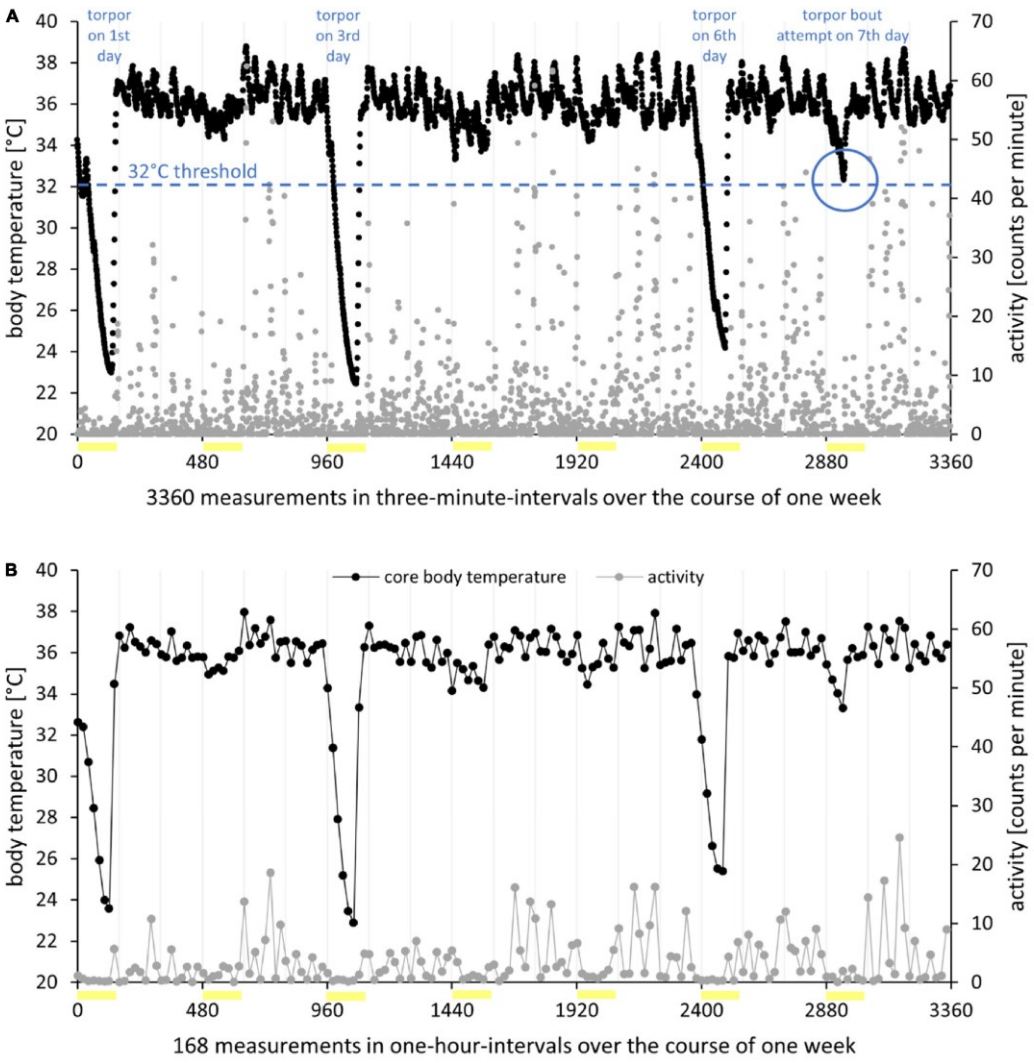

FIGURE 1 | Processing of radiotelemetry data I. Body temperature (in degree Celsius, *black*) and activity (in counts per minute, *gray*) of hamster EH02-27 over the course of 1 week in the short photoperiod (L/D 8:16 h). Photophases are indicated as *yellow bars*. **(A)** High resolution. Real-time raw data recorded in 3-min intervals. Within the 7 days, the hamster expressed three torpor bouts per definition with body temperature below 32°C for at least 30 min, resulting in a torpor incidence of 0.43. On the last day of the analysis week, the hamster showed a torpor bout attempt. While the body temperature hardly changed from one measurement to the next, the activity data were highly variable. **(B)** Low resolution. Processing of raw data to mean values per hour resulted in a smoothing of the body temperature measurements; however, the activity data became more accessible.

and locomotor activity over the course of SP adaptation was shown for individuals and the cohort to provide a visualization of variance within the cohort and statistical analyses of trends.

Data on relative body mass reduction and relative torpor incidence of 10 hamsters (2018 breed) have already been published in another research context (Piscitiello et al., 2021), while studies on molecular analyses of the hamsters' tissues are in progress. Therefore, the radiotelemetry data of this study are not yet published for free use, but can be provided on request.

Radiotelemetry

The radiotelemetry system (Dataquest ART^{TM} Bronze System, DSI, Harvard Bioscience Inc., St. Paul, MN, United States) comprised a pre-calibrated and silicone-coated TA11TA-F10

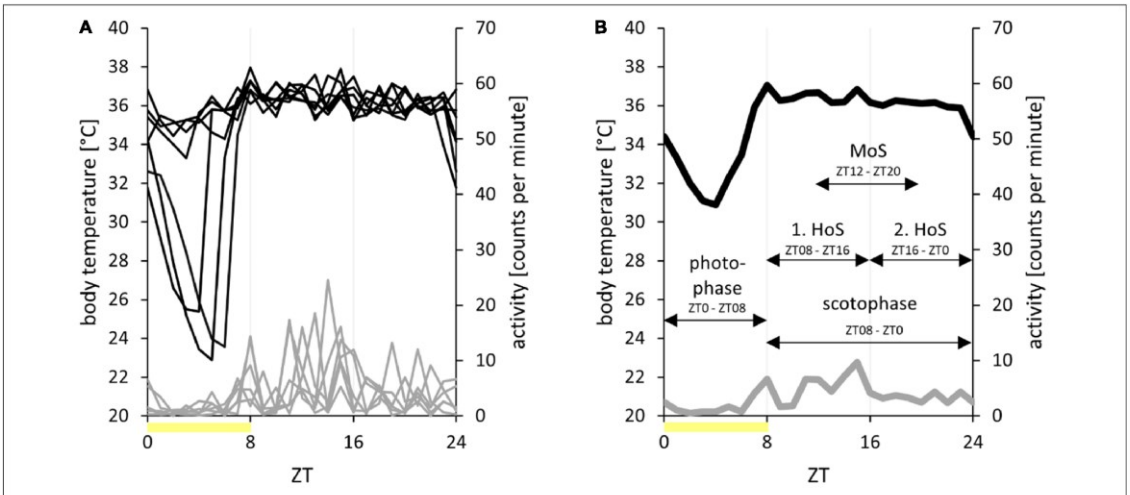

FIGURE 2 | Processing of radiotelemetry data II. Data of body temperature (in degree Celsius, *black*) and activity (in counts per minute, *gray*) of hamster EH02-27 over the course of 1 week in the short photoperiod (L/D, 8:16 h) with the photophases indicated as *yellow bars*. **(A)** Overlay. The data of each of the 7 days of the analysis week are overlaid for visualization on an *x*-axis from zeitgeber time 0 (ZT0) to ZT24. **(B)** Time frames. The data were averaged per ZT and week to visualize the body temperature and activity patterns of hamster EH02-27 over 1 week. In this study, the data were averaged per time frame and week (*arrows*). The time frames photophase, scotophase, first half of scotophase (*1. HoS*), second half of scotophase (*2. HoS*), and middle of scotophase (*MoS*) were used. Please note that the mean values per time frame and their standard deviations have been directly calculated from the raw dataset, on which the analysis of torpor parameters was also based.

radiofrequency transmitter (PhysioTel™, DSI, 1.1 cc volume, 1.6 g weight, 0.15°C measurement accuracy) implanted in the hamster's peritoneal cavity, a receiver plate (RPC-1, DSI) underneath the hamsters' home cage, a 20-channel Data Exchange Matrix (DEM, DSI), and a personal computer (Windows 7, 64-bit) outside the animal room. The raw data of core body temperature (in degree Celsius) and activity (counts per minute, cpm) were recorded in intervals of 3 min by the software "DataquestARTbronze" (2013). Body temperature was measured at the end of every 3-min interval. Activity was derived from the change of signal strength induced by the hamster, and therefore transmitter movement, relative to the receiver plate. This change was measured every 10 s and transformed by the system to cpm. At the end of every 3-min interval, an average activity value with the time-dependent unit cpm was recorded. An absolute activity could not be provided by the system.

Data Processing

Raw data processing and graphical representation were performed with Microsoft Excel (Microsoft Office 365, 2016), unless otherwise stated. While the activity dataset remained raw, the body temperature dataset was corrected for measurement errors by deleting physiologically impossible temperatures below ambient temperature or above 42°C as well as values with unphysiological fluctuations of more than 0.5°C per 3-min interval (Heldmaier and Ruf, 1992; **Figure 1A**). On these corrected data, the analyses of torpor parameters and the standard deviation of the mean body temperature were based. For analyses on a larger scale, data were averaged per hour (**Figure 1B**), week (**Figure 2A**), and time frame (**Figure 2B**). This allowed for comparisons between time frames within 1 week of analysis (approach 1) and the development of body temperature and activity in steps of 1 week over the course of adaptation to the short photoperiod (approach 2).

Time Frames

The total time frame accounted for the entire dataset of each analysis week. In SP, the photophase expands from ZT0 (including) to ZT08 (excluding), as shown in **Figures 1–3**. Accordingly, the scotophase expands from ZT08 to ZT0. For comparative analysis, the scotophase was split in the first half of scotophase from ZT08 to ZT16 and in the second half of scotophase from ZT16 to ZT0. Furthermore, the time frame middle of scotophase from ZT12 to ZT20 was used to exclude the potential interference of early torpor onsets and late torpor arousals (**Figure 2B**). In LP, the photophase expands from ZT0 to ZT16. Accordingly, the scotophase expands from ZT16 to ZT0. The time frames enabled a general description of the absolute locomotor activity extent during the hamsters' active and resting phases and, furthermore, the calculation of the activity ratios to compare the circadian patterns independent of the individual activity extent. For the photophase-to-scotophase activity ratio, values below 1 indicate a higher activity during scotophase and, therefore, nocturnality. The second-to-first half of scotophase activity ratio was calculated to further characterize the different activity phenotypes, whereby values below 1 indicate a higher activity during the first half of scotophase.

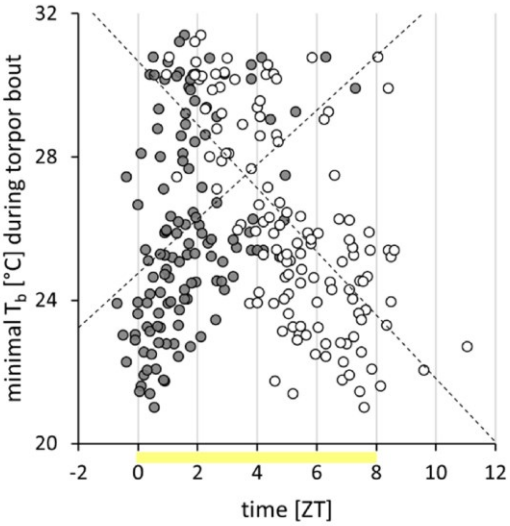

FIGURE 3 | Torpor characteristics of approach 1. Within the torpor analysis week, 127 torpor bouts, performed by 42 Djungarian hamsters, were examined. Of each bout, the torpor onset (*gray circles*) and the torpor offset (*white circles*) are shown. The minimal body temperature (T_b) during each torpor bout is positively correlated with its onset ($r = 0.385$, $p < 0.05$) and negatively correlated with its offset ($r = -0.628$, $p < 0.05$). Most bouts were performed within the photophase (*yellow*).

Statistics and Plotting

Data are given as the mean ± standard deviation of the mean, unless otherwise stated. Statistical tests were performed with SigmaPlot version 11 (Systat Software, San Jose, CA, United States). Data were tested for normality with the Shapiro–Wilk test. One-way repeated measures ANOVA with Holm–Sidak *post hoc* test was used for dependent, normally distributed data; Friedman repeated measures ANOVA with Tukey's *post hoc* test was used for dependent, non-normally distributed data. A two-tailed *t*-test was used for the comparison of two groups with independent, normally distributed data. Comparisons of more than two groups were done by one-way ANOVA with Holm–Sidak *post hoc* test for independent, normally distributed data and Kruskal–Wallis one-way ANOVA with Dunn's *post hoc* test for independent, non-normally distributed data. Two dependent datasets per animal were analyzed with the paired *t*-test for normally distributed data and with the Wilcoxon signed-rank test for non-normally distributed data.

Correlation of two parameters is shown in scatterplots. Pearson's product moment correlation was used to interpret normally distributed parameter correlations, with $p < 0.05$ as statistically significant. Statistically significant correlations are indicated by the *p*-value, the *r*, and the coefficient of determination R^2. Data distribution is shown in boxplots. The middle line represents the median, while the cross stands for the mean value. Each box extends from the 25th percentile to the 75th percentile. The whiskers depict the minimum and maximum values.

In the actograms, consecutive activities per hour were double plotted using the ActogramJ plugin for ImageJ (U.S. National Institutes of Health, Bethesda, MD, United States[1], 1997–2018). Labeling was done with Inkscape (1.0, ©2020, Inkscape Developers[2]) and Adobe® Photoshop CS2 (9.0, 1990–2005, Adobe Systems Incorporated, San Jose, CA, United States). Activities above the upper limit of 10 cpm are shown as 10 cpm. Since ZT0 was 1 h later in SP, an empty hour was inserted to align SP to LP for the actograms. The day of photoperiod change from LP to SP was excluded as photophase began according to the LP regime and ended according to the SP regime, resulting in an intermediate photophase length of 9 h.

RESULTS

Approach 1—Spontaneous Daily Torpor

For this approach, one representative SP week, SP15 ± 2 weeks, was chosen to analyze the adaptation and radiotelemetry parameters of 60 responders in relation to their individual torpor behavior. At least once during their individual data acquisition interval, 46 of the 60 animals expressed torpor, yet not necessarily during the week of analysis, while the remaining 14 animals were never observed in torpor.

In torpor-expressing hamsters ($n = 46$), the torpor incidence during the week of analysis had a median of 0.3 and ranged from 0.0 (no torpor, $n = 3$) to 1.0 (torpor every day, $n = 1$). Below 30°C reached 84 ± 33% of torpor bouts. Additionally, up to four torpor bout attempts were made per individual, with a median incidence of 0.1 for this cohort. The 46 animals showed either a torpor bout attempt or a torpor bout per definition on 55 ± 28% of the analyzed days.

Torpor Parameters

Within the week of analysis, the cohort expressed 127 torpor bouts, which were analyzed in detail. Torpor onset was at ZT1.6 ± 1.4 h and torpor offset at ZT5.3 ± 2.0 h (**Figure 3**). The torpor bouts had a duration of 218 ± 122 min. The minimal body temperature per bout was 26.0 ± 2.8°C. With an earlier torpor onset, a lower minimal body temperature ($r = 0.385$, $p < 0.05$; **Figure 3**) and a longer torpor bout duration ($r = -0.384$, $p < 0.05$) were reached, despite an earlier torpor offset ($r = 0.323$, $p < 0.05$). Nevertheless, a later torpor offset was generally associated with a longer duration ($r = 0.750$, $p < 0.05$) and a lower minimal body temperature ($r = -0.628$, $p < 0.05$; **Figure 3**).

To use the torpor parameters for phenotyping, the values were averaged for each of the 42 animals. Consequently, the cohort's torpor behavior was characterized by a torpor onset at 1.9 ± 1.4 h, a torpor offset at 5.4 ± 1.7 h, a torpor duration of 208 ± 101 min, and a minimal body temperature of 26.3 ± 2.4°C. Hamsters with an earlier mean torpor onset showed a lower standard deviation of their mean torpor onset (hamsters with at least two bouts,

[1]http://imagej.nih.gov/ij/

[2]http://inkscape.org/*developer/

$n = 35$, $r = 0.528$, $p < 0.05$) and a higher torpor incidence ($n = 42$, $r = -0.361$, $p < 0.05$).

The majority of torpor bouts had their on- and offsets within the photophase from ZT0 to ZT08 (**Figure 3**), but six torpor bouts started before ZT0 and ten ended after ZT08. Although some early torpor bouts already started during the second half of the preceding scotophase, and some very long or late torpor bouts reached into the first half of the following scotophase, torpor did not expand into the middle of the scotophase. The lowest body temperatures per hour and hamster recorded during the analysis week were 21.2°C during photophase, 22.9°C during the first half, and 30.7°C during the second half of scotophase, but 35.5°C during middle of scotophase.

Torpor Incidence Groups

After analysis of the torpor parameters, all 60 hamsters were assigned to four torpor incidence groups (**Figure 4**) to relate torpor behavior, adaptation, body temperature, and activity parameters. Hamsters of the group "never torpor" ($n = 14$) did not express torpor during their entire individual observation interval. Hamsters of the group "rarely torpor" ($n = 12$) were capable of torpor expression, but expressed no or one torpor bout during the week of analysis. Hamsters of the group "sometimes torpor" ($n = 22$) had a torpor incidence between 0.3 and 0.5, while those of the group "often torpor" ($n = 12$) had a torpor incidence of 0.5 or higher. Consequently, the median torpor incidence values were 0.1 in the group "rarely torpor", 0.3 in the group "sometimes torpor", and 0.7 in the group "often torpor" (**Table 1**). The torpor incidence groups differed in torpor onset, with ZT2.6 in hamsters of the group "rarely torpor", ZT2.0 in hamsters of the group "sometimes torpor", and ZT1.0 in hamsters of the group "often torpor".

The adaptation phenotype (**Table 2**) indicated that the "never torpor" group could be discriminated from the "often torpor" group by absolute body mass in SP12 and from all other torpor incidence groups by the relative body mass change in SP07 and SP12. Regarding no torpor and torpor expression only, "never torpor" hamsters showed a lower relative body mass change than did torpor-expressing hamsters after SP03 (**Figure 5A**).

Activity phenotyping per time frame showed that the "rarely torpor" group was more active than the "often torpor" group during scotophase, first half of scotophase, and middle of scotophase. Body temperature phenotyping per time frame revealed differences between the torpor incidence groups in all time frames (**Table 3**). Firstly, the "sometimes torpor" and "often torpor" groups had lower body temperatures than the "never torpor" and "rarely torpor" groups, even during the middle of scotophase. Secondly, the "sometimes torpor" and "often torpor" groups could be discriminated by the scotophase body temperature as well as by the standard deviation of the mean body temperature during the middle of scotophase. Thirdly, the groups "never torpor" and "rarely torpor" could be discriminated by the standard deviation of the mean body temperature during the middle of scotophase. The "never torpor" hamsters had higher mean body temperatures within all time frames than all "torpor" hamsters, also during the middle of scotophase [two-tailed t-test: $t_{(58)} = -4.026$, $p < 0.001$; "torpor": 36.0 ± 0.0°C SEM; "never torpor": 36.4 ± 0.1°C SEM)]. The lower the mean body temperature during the middle of scotophase, the smaller was its standard deviation in "torpor" hamsters, while this correlation was not given for the "never torpor" hamsters (**Figure 5B**).

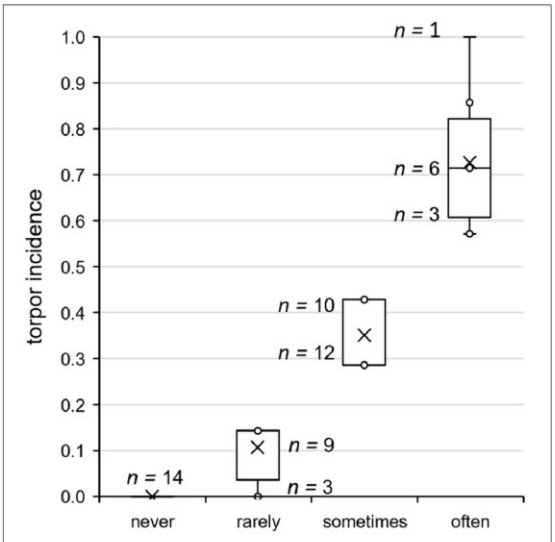

FIGURE 4 | Torpor incidence groups of approach 1. Grouping of all hamsters according to their individual torpor incidence shown in the week of analysis. From the distribution of the torpor incidence values of the hamsters expressing torpor, yet not necessarily during the week of analysis, three groups were derived for phenotyping. Taking the 25th percentile (torpor incidence of 0.2) and the 75th percentile (torpor incidence of 0.5) as thresholds, the animals were assigned to the groups "rarely torpor" (<25%, $n = 12$), "sometimes torpor" (25–75%, $n = 22$), and "often torpor" (>75%, $n = 12$). The torpor incidence varied between hamsters of the same group, as indicated with the sample sizes per torpor incidence value *next to the boxplots*. Responders that never expressed torpor during their individual implantation time accounted for the fourth group "never torpor" ($n = 14$).

Approach 2—Initial and Long-Term Effects of Short Photoperiod

Twenty-three percent of the hamsters which adapted to SP between 2018 and 2020 never expressed torpor. In approach 1, they could be discriminated from the torpor-expressing hamsters by the weaker body mass reduction and, thus, already during SP adaptation. Since 11 of the 60 hamsters had already been implanted before the beginning of SP, their body temperature and activity profiles were analyzed during the change from LP to SP and the following SP adaptation to identify potential additional predictors of torpor proneness early during adaptation. Due to the low sample size, comparisons of "torpor" hamsters ($n = 8$) and "never torpor" hamsters ($n = 3$) were statistically invalid. The values per parameter, time frame, experimental week, and individual are given in the supplementary tables (**Supplementary Tables 4–8**).

TABLE 1 | Phenotyping of the torpor incidence groups according to the torpor parameters of approach 1.

Torpor characteristics	Given values	Torpor incidence group				ANOVA		*Post hoc* test with $p < 0.050$
		Never torpor ($n = 14$)	Rarely torpor ($n = 12$)	Sometimes torpor ($n = 22$)	Often torpor ($n = 12$)	Test statistics	*p*-value	Comparison
Torpor per definition incidence	Median	–	**0.1**	**0.3**	**0.7**	$H_{(2)} = 40.0$	<0.001	Rarely *vs.* sometimes Rarely *vs.* often Sometimes *vs.* often
Torpor attempt incidence	Median	–	**0.0**	**0.2**	**0.1**	$H_{(2)} = 3.1$	0.215	–
Torpor onset (ZT)	Median	–	**2.6**	**2.0**	**1.0**	$H_{(2)} = 8.4$	0.015	Rarely *vs.* often Sometimes *vs.* often
Torpor offset (ZT)	Mean	–	**5.5**	**5.5**	**5.1**	$F_{(41,2)} = 0.2$	0.823	–
Torpor duration (min)	Mean	–	**174**	**200**	**246**	$F_{(41,2)} = 1.4$	0.259	–
Minimal torpor T_b (°C)	Mean	–	**27.2**	**26.5**	**25.4**	$F_{(41,2)} = 1.6$	0.219	–

*One week was analyzed. The grouping is based on the torpor per definition incidence (**Figure 4**). Each hamster's mean value per torpor parameter (onset, offset, duration, and minimal torpor body temperature) was included in the comparison. More details on the statistical tests are listed in **Supplementary Table 2**.*

TABLE 2 | Phenotyping of the torpor incidence groups according to the adaptation parameters of approach 1.

Adaptation parameters	Given values	Torpor incidence group				ANOVA		*Post hoc* test with $p = 0.050$
		Never torpor ($n = 14$)	Rarely torpor ($n = 12$)	Sometimes torpor ($n = 22$)	Often torpor ($n = 12$)	Test statistics	*p*-value	Comparison
Fur index in SP07	Median	**1.8**	**1.5**	**2.0**	**1.3**	$H_{(3)} = 3.6$	0.310	–
Fur index in SP12	Median	**3.3**	**3.0**	**3.3**	**3.3**	$H_{(3)} = 0.0$	0.998	–
Body mass in SP00 (g)	Mean	**35.0**	**35.9**	**37.2**	**35.3**	$F_{(56,3)} = 0.6$	0.615	–
Body mass in SP07 (g)	Mean	**30.5**	**28.9**	**30.4**	**28.4**	$F_{(56,3)} = 0.8$	0.475	–
Body mass in SP12 (g)	Mean	**29.9**	**27.3**	**28.2**	**25.5**	$F_{(56,3)} = 3.1$	0.035	Never *vs.* often
Body mass change in SP07 (%)	Mean	**–8.7**	**–19.3**	**–17.4**	**–19.2**	$F_{(56,3)} = 5.0$	0.004	Never *vs.* rarely Never *vs.* sometimes Never *vs.* often
Body mass change in SP12 (%)	Mean	**–10.7**	**–23.5**	**–23.3**	**–27.4**	$F_{(56,3)} = 12.5$	< 0.001	Never vs. rarely Never *vs.* sometimes Never *vs.* often

*Fur index, scored from 1 for a light brown summer fur to 6 for a dense white winter fur (Figala et al., 1973), and absolute body mass were assessed weekly over the course of adaptation to the short photoperiod. The relative body mass change was calculated in relation to SP00. Three weeks of interest were chosen, namely, SP00: start of adaptation; SP07: before torpor expression; and SP12: after first torpor bouts had been observed. More details on the statistical tests are listed in **Supplementary Table 2**.*

Body Temperature

To assess the initial effects of SP exposure, the cohort's body temperature measurements of the last week in LP and the first week in SP were compared (**Figure 6A**). In both LP and SP01, body temperature was significantly lower during the photophase than during the scotophase, while the reduction from LP to SP01 was only significant during the scotophase. The body temperature of the cohort further decreased over the course of SP adaptation (**Figure 6B**). The individual development of body temperature during the scoto- and photophases was diverse (**Figures 6C,D**). Hamster #06 was excluded from this and most other cohort models, as indicated in the figure legends. It expressed a torpor bout on the second day of SP, which is atypical or usually not noticed. It further developed a stereotypic jumping during photophase from SP04 to SP11.

First torpor bouts were expressed in SP07 (first torpor of hamster #03), SP08 (hamster #11), SP09 (hamsters #06 and #08), SP10 (hamsters #05 and #07), and SP11 (hamsters #09 and #10),

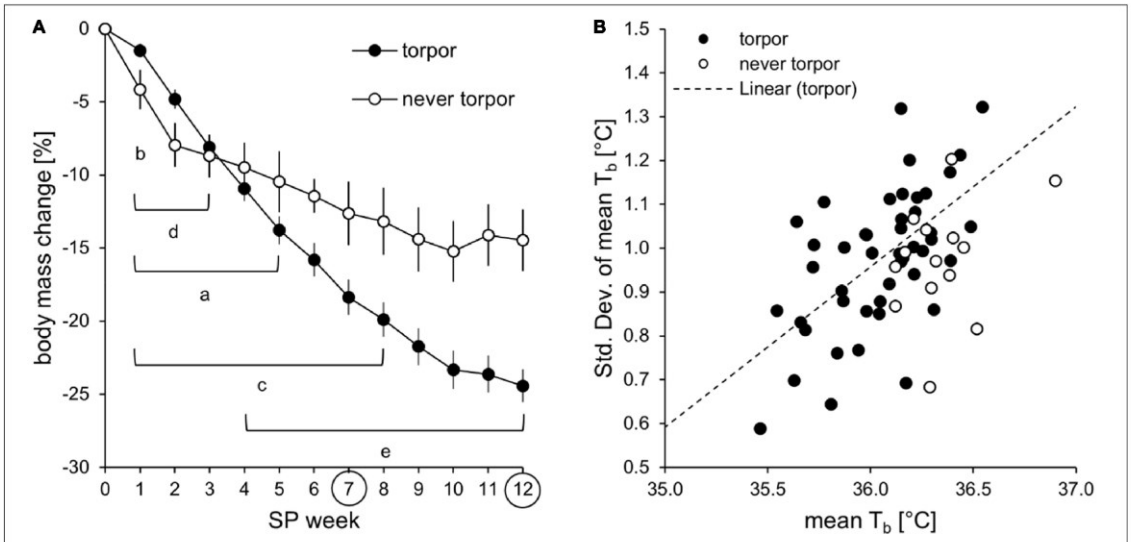

FIGURE 5 | Comparison of hamsters with and without torpor expression of approach 1. **(A)** Mean (±standard error) relative body mass change during adaptation to the short photoperiod [n_{torpor} = 46, $n_{never\ torpor}$ = 14]. Significant differences to SP07 of "torpor" (*a*) and "never torpor" (*b*) hamsters. Significant differences to SP12 of "torpor" (*c*) and "never torpor" (*d*) hamsters. Significant differences between "torpor" and "never torpor" hamsters (*e*) [two-way repeated measures ANOVA: $F_{(11,638)} = 10.124$, $p < 0.001$, with Holm–Sidak $p < 0.001$]. **(B)** Correlation of the mean body temperature and its standard deviation during the middle of scotophase. The higher the mean body temperature, the lower is its standard deviation in "torpor" hamsters ($n = 46$, with $R^2 = 0.3489$, $r = 0.591$, $p < 0.050$). This correlation could not be confirmed in "never torpor" hamsters.

with a median of 67 days of SP adaptation. The eight hamsters expressed between one and 12 torpor bouts until SP13, with a median of four. The absolute number of torpor bouts from SP08 to SP13 was positively correlated with the torpor incidence of SP13 ($n = 8$, $r = 0.948$, $p < 0.05$), the week of torpor analysis in approach 1. Three hamsters (#01, #02, and #12) did not express torpor until termination in SP14.

In this study, the delta body temperature was used as an indicator of the body temperature spectrum covered by the hamsters. It was calculated by subtracting the minimal body temperature per hour from the maximal body temperature per hour individually detected within a time frame per week. The cohort's scotophase delta was significantly lower in SP00 until SP05 when compared to SP12. Furthermore, it increased linearly in all 11 hamsters over the course of SP adaptation (**Figure 7A**). In contrast, the photophase delta was highly individual, especially when including torpor expression after SP07. Until SP13, the photophase delta rose to maximal 14.4°C, reflecting the difference between the coldest and the warmest hour of an animal within photophase and week (**Figure 7B**).

Activity

To assess the initial effects of SP exposure, the cohort's activity measurements of the last week in LP and the first week in SP were compared (**Figure 8A**). In the first week of SP, the cohort reduced its activity during scotophase, while its activity during the photophase remained constant. In both photoperiods, the hamsters were nocturnal, with a higher activity during scotophase.

According to observations and the radiotelemetry data, the activity levels strongly differed due to the hamsters' broad behavioral spectrum from calm to active. The highest activity per hour determined in each hamster's LP scotophase varied from 11 cpm in the calmest to 158 cpm in the most active hamster, while the variations during the LP photophase ranged from 6 to 60 cpm. In contrast, the highest activity per hour in SP01 varied from 12 to 101 cpm during the scotophase and from 5 to 26 cpm during the photophase.

Over the course of 13 weeks in SP, the scotophase activity was further reduced in general, while the photophase activity slightly increased (**Figure 8B**). However, the scoto- and photophase activities were differently modulated by the 11 hamsters (**Figures 8C,D**). Activity onset occurred sharply at the beginning of the scotophase, while activity faded over the course of the scotophase so that the offset was difficult to define (**Figure 9**). The hamsters adapted to the immediate change from LP to SP by expanding their activity gradually into the prolonged scotophase and shifted their activity peak to the new beginning of the scotophase. According to eye fitting using actograms, seven animals adapted their activity within the first SP week and two others during the second SP week, while adaptation occurred after 4 weeks in hamster #09 and after 8 weeks in the "never torpor" hamster #01.

The hamsters' nocturnality was additionally confirmed by a photophase-to-scotophase activity ratio calculated per

TABLE 3 | Phenotyping of the torpor incidence groups of approach 1 according to the activity and body temperature per time frame.

Parameters		Given values	Torpor incidence group				ANOVA		*Post hoc* test with $p = 0.050$
			Never torpor ($n = 14$)	Rarely torpor ($n = 12$)	Sometimes torpor ($n = 22$)	Often torpor ($n = 12$)	Test statistics	*p*-value	Comparison
Activity	Total (cpm)	Median	**4.0**	**4.8**	**4.4**	**2.9**	$H_{(3)} = 7.4$	0.060	–
	Photophase (cpm)	Median	**2.1**	**2.0**	**2.0**	**1.5**	$H_{(3)} = 3.4$	0.334	–
	Scotophase (cpm)	Median	**5.1**	**6.0**	**5.5**	**3.6**	$H_{(3)} = 9.2$	0.026	Rarely *vs*. often
	First half of scotophase (cpm)	Median	**5.8**	**8.0**	**6.9**	**3.9**	$H_{(3)} = 10.2$	0.017	Rarely *vs*. often
	Second. half of scotophase (cpm)	Median	**4.4**	**4.3**	**4.0**	**3.4**	$H_{(3)} = 4.1$	0.248	–
	Middle of scotophase (cpm)	Median	**4.9**	**6.0**	**5.5**	**3.7**	$H_{(3)} = 8.4$	0.039	Rarely *vs*. often
	Std. Dev. of middle of scotophase (cpm)	Median	**10.3**	**13.0**	**11.7**	**9.5**	$H_{(3)} = 4.8$	0.189	–
	Photophase-to-scotophase ratio	Median	**0.4**	**0.4**	**0.4**	**0.5**	$H_{(3)} = 0.3$	0.951	–
	Second-to-first half of scotophase ratio	Median	**0.7**	**0.5**	**0.7**	**0.8**	$H_{(3)} = 6.8$	0.078	–
Body temperature	Total (°C)	Median	**36.1**	**35.8**	**35.4**	**34.6**	$H_{(3)} = 47.8$	<0.001	Never *vs*. sometimes
									Never *vs*. often
									Rarely *vs*. sometimes
									Rarely *vs*. often
	Photophase (°C)	Median	**35.7**	**35.1**	**34.3**	**32.1**	$H_{(3)} = 47.0$	< 0.001	Never *vs*. sometimes
									Never *vs*. often
									Rarely *vs*. sometimes
									Rarely *vs*. often
	Scotophase (°C)	Mean	**36.4**	**36.2**	**36.0**	**35.8**	$F_{(56,3)} = 18.5$	<0.001	Never *vs*. sometimes
									Never *vs*. often
									Rarely *vs*. sometimes
									Rarely *vs*. often
									Sometimes *vs*. often
	First half of scotophase (°C)	Median	**36.5**	**36.4**	**36.3**	**35.9**	$H_{(3)} = 27.7$	<0.001	Never *vs*. sometimes
									Never *vs*. often
									Rarely *vs*. often
	Second half of scotophase (°C)	Median	**36.2**	**36.0**	**35.9**	**35.6**	$H_{(3)} = 27.5$	<0.001	Never *vs*. sometimes
									Never *vs*. often
	Middle of scotophase (°C)	Mean	**36.3**	**36.3**	**36.0**	**35.9**	$F_{(56,3)} = 13.4$	<0.001	Never *vs*. sometimes
									Never *vs*. often
									Rarely *vs*. sometimes
									Rarely *vs*. often
	Standard deviation of middle of scotophase (°C)	Mean	**0.97**	**1.1**	**0.98**	**0.84**	$F_{(56,3)} = 7.8$	<0.001	Never *vs*. rarely
									Never *vs*. often
									Rarely *vs*. often
									Sometimes *vs*. often

Data of one analysis week were used. More details on the statistical test results are listed in ***Supplementary Table 3****. The lower the photophase-to-scotophase activity ratio, the higher the degree of nocturnality. The lower the second-to-first half of scotophase activity ratio, the higher the activity during the first half of scotophase.*

hamster and week (**Figure 10**). Ratios below 1 indicate a higher activity during scotophase and, therefore, nocturnality. Nocturnality of the cohort was most pronounced in LP and became weaker until SP05 (the ratio increased from about 0.2 to 0.5). From SP05, the ratio remained at about 0.5, indicating that the photophase activity was half that of the scotophase activity. The hyperactivity hamster #06 expressed during photophase after SP04 was reflected by ratios higher than 1, indicating diurnality (**Figure 10**, insert).

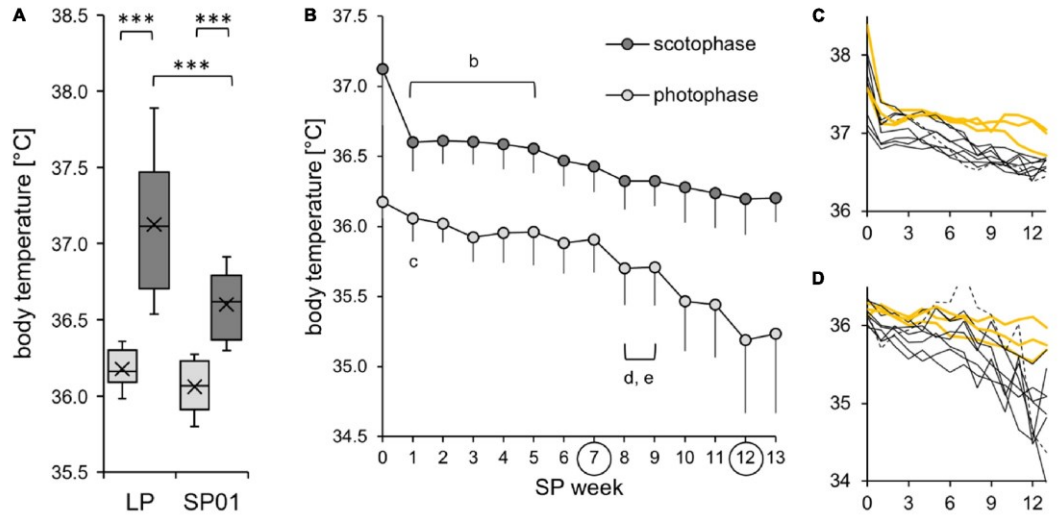

FIGURE 6 | Body temperature during the short photoperiod adaptation of approach 2. The exact values per hamster can be found in **Supplementary Table 4**. **(A)** The cohort's initial reduction of body temperature after the change of the light regime (n = 10). Comparison of body temperature during photophase (*light gray*) and scotophase (*dark gray*) of the last week of the long photoperiod (*LP*) and the first week of the short photoperiod (*SP01*). According to a two-way repeated measures ANOVA, body temperature was affected by both time frame [$F_{(1,9)}$ = 62.256, $p < 0.001$, power = 1.0] and light regime [$F_{(1,9)}$ = 83.125, $p < 0.001$, power = 1.0]. In addition, there was an interaction between the effects of time frame and light regime [$F_{(1,9)}$ = 15.373, p = 0.004, power = 0.9). *Post hoc* Holm–Sidak tests confirmed that body temperature was significantly higher during the scotophase in both LP and SP01 (***$p < 0.001$). Furthermore, body temperature during the scotophase (***$p < 0.001$) was significantly higher in LP than that in SP01. Hamster #06 was excluded because it performed a torpor bout on the second day of SP, which is atypical or usually not noticed. **(B)** The cohort's further reduction of body temperature (n = 10). With focus on the weeks from SP01 to SP07 without torpor expression, body temperature was reduced over the course of SP adaptation. Significant differences to the SP07 of scotophase (*b*) [one-way repeated measures ANOVA: $F_{(6,54)}$ = 7.599, $p < 0.001$] as well as of photophase (*c*) [one-way repeated measures ANOVA: $F_{(6,54)}$ = 4.851, $p < 0.001$], both confirmed with Holm–Sidak $p < 0.001$. With focus on the weeks from SP08 to SP12 including torpor bouts, body temperature was further decreased. Significant differences to the SP12 for scotophase (*d*) [one-way repeated measures ANOVA: $F_{(5,45)}$ = 4.978, p = 0.001, with Holm–Sidak p = 0.002] as well as for photophase (*e*) [Friedman repeated measures ANOVA: $\chi^2_{(5)}$ = 30.114, $p < 0.001$, with Tukey's test $p < 0.05$]. Hyperactive hamster #06 was excluded since a stereotypic jumping during photophase was also reflected in the body temperature. **(C,D)** Individual reduction of body temperature during scotophase **(C)** and photophase **(D)** for each of the 11 hamsters. Body temperature (in degree Celsius) is shown on the *y*-axis, the SP week on the *x*-axis, with hamster #06 as *dotted line*, the three "never torpor" hamsters as *yellow lines*, and all others as *thin black lines*.

The cohort maintained a higher activity in the first than in the second half of scotophase, with an average second-to-first half of scotophase activity ratio smaller than 1, namely, 0.7 ± 0.3 in SP01 and 0.6 ± 0.2 in later weeks. Exceptions were a ratio of 1.7 in hamster #09 during SP01 and a ratio of 1.3 in hamster #07 during SP09, as they were more active in the second half of the scotophase. The extremely slow activity adaptation of hamster #01 was reflected by a ratio decline from 8.3 in SP01 to 0.7 in SP13, with ratios smaller than 1 after SP08.

Body Mass and Fur

All hamsters reduced their body mass during SP adaptation (**Figure 11A**). The cohort had an initial body mass of 32.7 ± 5.2 g, which was reduced by -19 ± 8% to 26.5 ± 4.3 g in SP07. "Never torpor" hamsters seem to have a less drastic reduction of body mass, as already shown in approach 1 (**Figure 5A**). All hamsters changed their light brown summer fur to a dense white winter fur over the course of SP adaptation (**Figure 11B**). The first changes became visible in SP04 in three of 11 animals. Hamster #08 started to change its fur in SP10, when most other animals already finished their fur change.

DISCUSSION

In the present study, the high variability of the adaptation parameters and torpor use in Djungarian hamsters was confirmed for all the observed parameters; however, the two analytic approaches for a large and detailed sample set also revealed new aspects. Overall, the hamster colony at Ulm University resembles the animals in early reports after domestication (Figala et al., 1973; Ross, 1998), yet with a weaker adaptation response. This likely results from the high ambient temperature of 20°C, corresponding to the lower limit of the hamsters' thermoneutral zone when SP-adapted (Heldmaier and Steinlechner, 1981a). Although the present animals have a domestication history of 50 years, outbreeding could preserve their circadian and seasonal phenotype, i.e., nocturnality as well as a body mass reduction

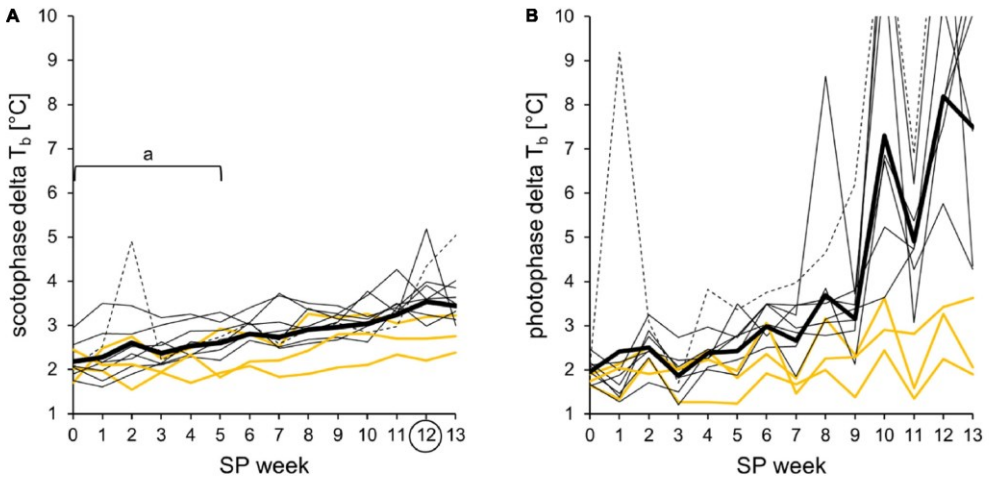

FIGURE 7 | Delta body temperature during the short photoperiod adaptation of approach 2. The difference between the highest value per hour and the lowest value per hour, detected within a time frame, is shown for each animal and week. Hamster #06 is represented as *dotted line*, the three "never torpor" hamsters as *yellow lines*, all others as *thin black lines*, and the cohort's mean delta body temperature as *thick black line*. The exact values per hamster can be found in **Supplementary Table 5**. **(A)** Delta body temperature of scotophase. The values per individual were averaged as delta of the cohort (n = 11, *thick line*), which showed a linear development (from SP00 to SP13: R^2 = 0.936, r = 0.967, $p < 0.05$). For the cohort, significant differences to SP12 are indicated with "*a*" [Friedman repeated measures ANOVA: $\chi^2_{(13)}$ = 93.566, $p < 0.001$, with Tukey's test $p < 0.05$]. **(B)** Delta body temperature of photophase. Spontaneous daily torpor, irregularly expressed by hamster #06 in SP01 and regularly expressed by eight of the 11 hamsters after SP07, caused high delta body temperatures during photophase.

of 20%, a fur index between 3 and 5, and torpor expression in most animals.

Torpor

The expression of spontaneous daily torpor in Djungarian hamsters has been shown to be under strict circadian control (Ruf et al., 1989; Ruby and Zucker, 1992). The analyses of the present study, however, indicate a rather flexible timing of torpor during photophase (**Figure 3** and **Table 1**). The 127 torpor bouts analyzed had their onset at ZT1.6 ± 1.4 h. It is important to notice that the reduction of the metabolic rate below the resting metabolic rate during torpor entrance precedes the reduction of body temperature below 32°C by almost an hour (Ruf and Heldmaier, 2000; Heldmaier et al., 2004). Consequently, all torpor onsets determined by body temperature measurements before ZT01 already occurred before the end of the scotophase and thus without light as a proximate induction stimulus.

The 46 torpor-expressing hamsters analyzed in approach 1 had shown at least one torpor bout within their individual observation interval. For reasons of comparability, the approach analyzed one representative SP week during the torpor period, resulting in a median torpor incidence of 0.3 with some hamsters that did not show torpor in this specific week. The respective torpor parameters were analyzed for single torpor bouts irrespective of animal (n = 127) and means per animal (n = 42). Both analyses revealed useful correlations for future interpretations of individual torpor behavior. Increasing the torpor incidence resulted in a higher probability of early and therefore deeper and longer bouts with an early torpor offset, and *vice versa*. Interestingly, torpor onset and its standard deviation correlated positively in the cohort, indicating a lower variability of early torpor bouts and an increasing degree of synchronization to ZT0 with increasing torpor incidence.

Torpor bouts that start early may favor energy saving because they resulted in lower minimal body temperatures per bout and longer torpor bouts in the present study (see also Ruf and Heldmaier, 1992). The hypothermic body temperature and the reduced activity at the beginning of the scotophase additionally indicate post-torpor effects on the hamsters' scotophase behavior (**Table 3**). Earlier studies have shown that the hamsters' circadian rhythm diminishes in SP, whereby torpor might impair sleep during the resting phase (Deboer et al., 2000; Deboer and Tobler, 2003; Scherbarth and Steinlechner, 2008). Time might get lost for feeding, and this energy deficit might directly demand for the next even deeper and longer torpor bouts. This is supported by the observations of a low scotophase activity coinciding with a low scotophase body temperature (**Table 3**), consequently a smaller standard deviation of body temperature (**Figure 5B**), and a higher torpor incidence with early, deep, and long torpor bouts (**Table 1** and **Figure 3**).

Furthermore, the present study revealed a remarkable incidence of torpor bout attempts in torpor-expressing hamsters (**Table 1**) never reported in the literature. They started at the same time and in the same shape as torpor bouts, but were interrupted at about 33°C (**Figure 1**). It is unclear whether torpor bouts were interrupted by yet undefined external disturbances or due to internal physiological factors. So far, the energy-saving potential of torpor bout attempts remains unknown, but should

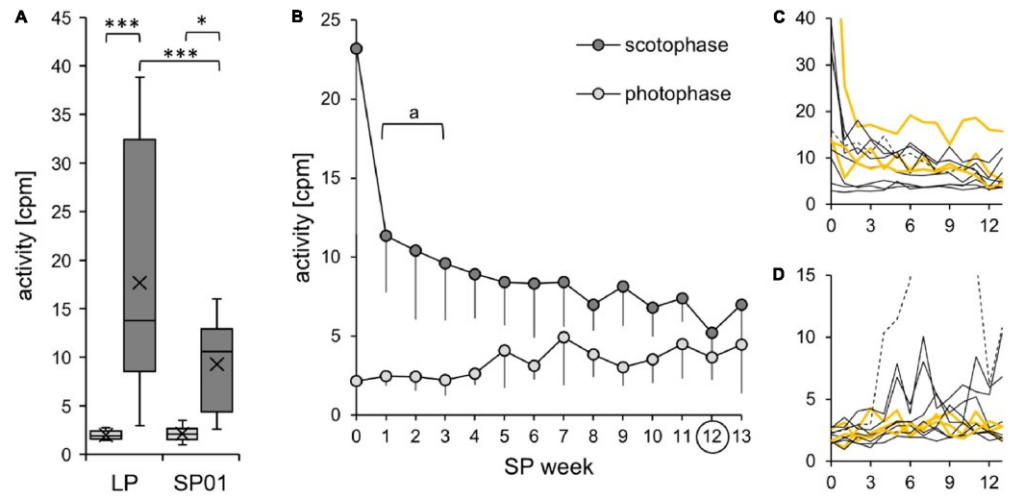

FIGURE 8 | Activity during the short photoperiod adaptation of approach 2. The exact values per hamster can be found in **Supplementary Table 6**. **(A)** The cohort's initial adaptation of activity after the change of the light regime ($n = 10$). Comparison of activity during photophase (*light gray*) and scotophase (*dark gray*) of the last week of the long photoperiod (*LP*) and the first week of the short photoperiod (*SP01*). According to the two-way repeated measures ANOVA, the activity was affected by both time frame [$F_{(1,9)} = 21.155$, $p = 0.001$, power = 0.984] and light regime [$F_{(1,9)} = 7.689$, $p = 0.022$, power = 0.637]. In addition, there was an interaction between the effects of time frame and light regime [$F_{(1,9)} = 7.815$, $p = 0.021$, power = 0.645]. *Post hoc* Holm–Sidak tests confirmed that the activity was significantly higher in LP scotophase (***$p < 0.001$) and in SP01 (*$p < 0.026$) compared to that in photophase. Furthermore, scotophase activity was higher in LP than that in SP01 (***$p < 0.001$), yet with a low power. Hamster #02 was excluded from the cohort's model since it had an outlying scotophase activity level in LP (beyond the three times interquartile distance threshold of the cohort), with a drastic initial decrease from 79 cpm during LP scotophase to 25 cpm during SP01 scotophase. **(B)** Further activity development of the cohort ($n = 6$). When comparing the adaptation period from SP01 to SP12, the scotophase activity was reduced. Significant differences to SP12 are indicated with "*a*" [one-way repeated measures ANOVA: $F_{(12,60)} = 4.750$, $p < 0.001$, with Holm–Sidak $p < 0.001$]. The photophase activity slightly rose, yet with a significant difference from SP04 to SP08 only [Friedman repeated measures ANOVA: $\chi^2_{(13)} = 36.229$, $p < 0.001$, with Tukey's test $p < 0.05$]. Excluded were hamster #01, with high LP activity and an extremely slow activity adaptation to SP; hamster #02, with outlying LP activity; hamster #06, with stereotypic jumping behavior in the cage corners during photophase from SP04 to SP11; and the hamsters #10 and #11, which were extremely calm and did not modulate initial activity. **(C,D)** Individual reduction of body temperature during scotophase **(C)** and photophase **(D)** for each of the 11 hamsters. Activity (in counts per minute) is displayed on the *y*-axis, the SP week on the *x*-axis with hamster #06 as *dotted line*, the three "never torpor" hamsters as *yellow lines*, and all others as *thin black lines*.

be examined *via* metabolic rate measurements in conditions carefully controlled for external disturbance factors as they might also reveal new insights into the other functions of torpor (Geiser and Brigham, 2012).

Rare reports of torpor expression without SP adaptation or food restriction exist (Steinlechner et al., 1986). Hamster #06 expressed an irregular torpor bout on the second SP day with an onset at ZT23, which accounts for the ZT0 of LP. Like the other hamsters of the cohort, hamster #06 started to express torpor bouts regularly in SP09 and had a torpor incidence of 0.7 ("often torpor") in SP13.

The torpor analysis of this study is not free of bias. Data analysis started and ended at ZT0 (beginning of photophase). While individual torpor incidence included all recorded torpor bouts per hamster, torpor bouts starting before ZT0 on the first day of the analysis week could not be analyzed in detail. An alternative data analysis starting and ending at ZT08 (beginning of scotophase) would have resulted in a much higher number of incomplete torpor bouts, as torpor offset after ZT08 was more common than torpor onset before ZT0. Furthermore, the present results show that torpor affected the second half of scotophase prior to torpor as well as the first half of scotophase after torpor. Consequently, the choice of the start and end of an observation interval must be considered thoroughly regarding aims of future studies.

Sampling Paradigm

The phenotyping of the torpor incidence groups was also used to reassess previous organ sampling schemes (Herwig et al., 2007; Bank et al., 2017; Cubuk et al., 2017a,b). In these sampling paradigms, hypothermic (HT) hamsters were sampled at torpor onset (ZT01), deep torpor (ZT04), torpor offset (ZT07), and after torpor (ZT16), along with time-matched normothermic (NT) hamsters. As there are high inter-individual variabilities of the torpor incidence, onset, depth, and duration within a cohort, not every hamster can be sampled for each group, which impedes a random assignment beforehand. Assuming that the individual torpor timing and torpor incidence are an integrative part of the hamster's long-term adaptational response, which is determined by a set of hitherto unknown genetic and environmental factors, the data might reflect not only acute effects but also prerequisites of torpor behavior. Consequently, the individual torpor behavior

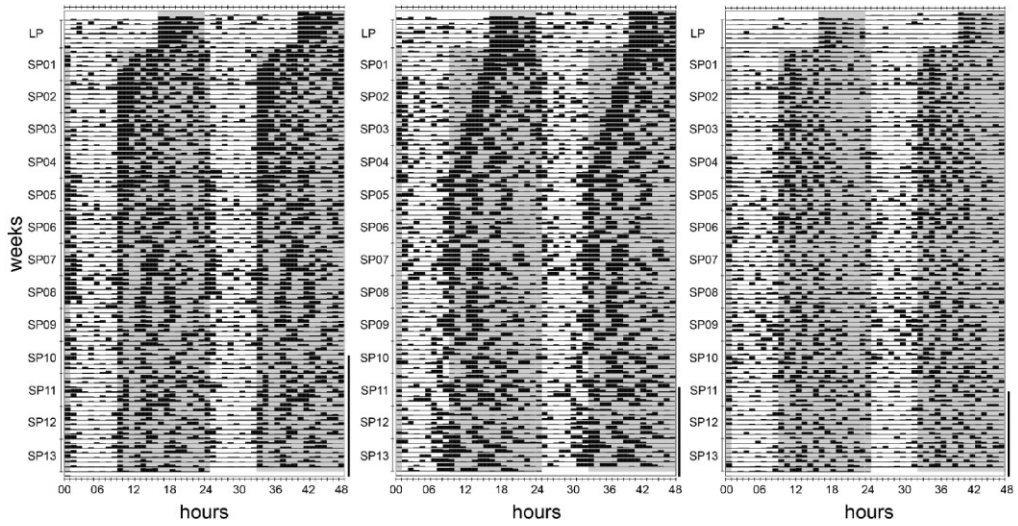

FIGURE 9 | Actograms of three individuals of approach 2 during 1 week in the long photoperiod and adaptation to the short photoperiod. *Black bars* indicate the activity performed within an hour, while values from 0 to 10 cpm are displayed. The long photoperiod (LP) and short photoperiod (SP) scotophases are indicated with *gray areas*. The days following the first torpor bout are marked with a *vertical line on the right side* of each actogram. All 11 hamsters adapted gradually to the immediate change from LP to SP, however at different paces. The *left actogram* (hamster #07) serves as an example for the majority of hamsters that showed a fast adaptation within days. The *middle actogram* (hamster #09) represents one of two hamsters with a gradual adaptation within weeks. The *right actogram* represents one of two hamsters showing a fast adaptation, but a very low activity level that impeded the analysis of temporal activity organization (hamster #10).

must be determined beforehand to achieve an equal distribution among sampling groups.

The majority of torpor-expressing hamsters (22 out of 46, 48%) showed torpor sometimes (incidence between 0.3 and 0.5; **Figure 4**) and fit best for all the sampling groups and time points (**Table 1**). However, torpor attempt incidence is highest in these hamsters (**Table 2**). A torpor bout attempt would not allow sampling for the particular day since the hamster was neither in torpor per definition nor constantly normothermic (**Figure 1A**). Hamsters never or rarely expressing torpor are indeed likely to be sampled as normothermic controls. Yet, given their flexible torpor timing, they are also adequate for sampling in hypothermia at ZT01 and ZT07. Hamsters with a high torpor incidence are more likely to be sampled for the hypothermic sampling group, but are not always adequate for sampling at ZT01 and ZT07 since they tended to be almost in deep torpor at ZT01 and finished the torpor bout before ZT07 (**Figure 3**). Thus, it cannot be assumed that hamsters often expressing torpor are all sampled for the HT group and those that express torpor rarely are all sampled in the NT group.

In future studies, the torpor behavior should be assessed in detail during 1 week of radiotelemetry tracking before sampling. Respective conclusions can be drawn to plan the assignment of each hamster to a certain sampling group in the following week since a stable torpor behavior from one to the next week was assumed due to the positive correlation between the absolute number of torpor bouts until SP12 and the torpor incidence in SP13 of approach 2.

However, this study also indicates restrictions of the rigid yet adequate sampling paradigm. The described flexibility in torpor incidence, timing of torpor, and course of body temperature during a torpor bout is respected in the paradigm as well as possible. An expansion of the sampling time points, from, e.g., ZT01 to ZT0–ZT02, would be eligible for studies on hypo- and normothermia alone, but inconvenient for studies on the circadian rhythm of hypo- and normothermic hamsters. Adapting the 32°C torpor definition threshold is impeded by both torpor bout attempts, which might be misinterpreted as torpor bouts, and the high minimal body temperatures of hamsters rarely expressing torpor. In relation to this, it should be mentioned that the torpor definition threshold of the present and many earlier studies (32°C for at least 30 min) is under constant debate (Boyles et al., 2011; Brigham et al., 2011) and might be refined by including metabolic rate measurements (Diedrich et al., 2015).

Never Torpor

The present study enables a better identification of responders without torpor expression. In approach 1, 14 "never torpor" hamsters out of a cohort with 60 individuals responded more weakly to SP in terms of body mass reduction (**Figure 5A** and **Table 2**). A high mean body temperature with a low standard deviation during the middle of scotophase allows discriminating "never torpor" hamsters not only from "torpor" hamsters but also from "rarely torpor" hamsters, with no to one torpor bout within the analysis week (**Figure 5B** and **Table 3**). Yet, due to the

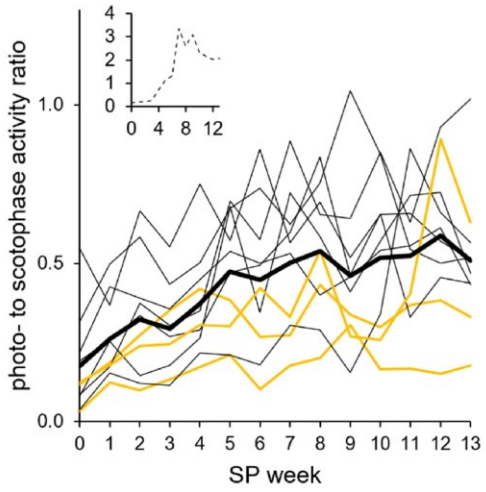

FIGURE 10 | Photophase-to-scotophase activity ratio during the short photoperiod adaptation of approach 2. For each animal and week, the photophase-to-scotophase activity ratio was calculated to identify nocturnality (ratio < 1) and diurnality (ratio > 1). Individual ratios (the three "never torpor" hamsters as *yellow lines* and all others as *thin black lines*; *inset*: graph of hyperactive hamster #06) were averaged for the cohort's ratio (*thick line*). The cohort's ratio (n = 10, without hamster #06) showed a positive linear correlation with progressing adaptation to the short photoperiod (SP) (R^2 = 0.8144, r = 0.902, $p < 0.05$). Significant differences to SP07 before torpor expression were found in SP00 and SP01, while differences to SP12 occurred in SP00, SP01, and SP03 [Friedman repeated measures ANOVA: $\chi^2_{(13)}$ = 68.811, $p < 0.001$, with Tukey's test $p < 0.05$]. The exact values per hamster can be found in **Supplementary Table 7**.

small sample size of the early implanted hamsters of approach 2 with three "never torpor" hamsters out of 11, this study cannot reveal at which time point of adaptation these differences became significant. However, an identification of the "never torpor" hamsters 2 weeks after implantation is not sufficient to reduce the number of animals in an experiment or the number of invasive transmitter implantations.

In approach 2, "never torpor" hamsters appeared to respond more weakly in all the observed parameters, suggesting a different metabolic programming of hamsters never expressing torpor at given circumstances (Cubuk et al., 2016; Diedrich et al., 2020). The most promising indicators of "never torpor" hamsters might be a higher body temperature during scotophase over the entire course of SP adaptation (**Figure 6C**) and a smaller delta body temperature and, therefore, variation during both scoto- and photophases (**Figure 7**). Indirect calorimetry could be used as a non-invasive alternative to extrapolate from individual fluctuations of metabolic rate to those of body temperature and, thus, torpor or no torpor expression. Body temperature and the metabolic rate correlate (Heldmaier and Ruf, 1992), and our own preliminary measurements in SP-adapted hamsters regarding the middle of scotophase also revealed a positive correlation between the standard deviation of the mean body temperature and the standard deviation of the mean metabolic rate (n = 7, R^2 = 0.74, r = 0.86, p = 0.006). Furthermore, non-invasive infrared cameras with tracking software would enable more attention on the peculiarities regarding the activity levels and activity patterns of "never torpor" hamsters, e.g., a high scotophase activity in LP (hamster #02), a very slow activity adaptation to SP (hamster #01), as well as a photophase-to-scotophase activity ratio below the cohort's mean, suggesting a more pronounced nocturnality in "never torpor" hamsters (**Figure 10**).

Next Torpor

Besides the early identification of torpor-expressing responders, the acute prediction of the next torpor bout in individual hamsters would be of interest to improve planning of sampling. While a study on marsupial sugar gliders has suggested reductions of activity and body temperature as acute predictors of torpor (Christian and Geiser, 2007), efforts to use radiotelemetry data have been hitherto without success. A relation between the activity pattern and the torpor behavior was not found (**Figures 1**, **2**, 9), but the activity ratios on, e.g., a daily instead of a weekly basis, a refined correlation analysis between activity and body temperature, and the standard deviations of the mean values seem to be promising (**Figures 5**, **10**, 11). The most reliable parameter for acute torpor prediction has been and still is the previous torpor incidence, which seems to be rather stable within an individual.

Adaptation to Short Photoperiod

Djungarian hamsters should be more active in LP than in SP since they expect mating and the intense care for their litters. The resulting high energy demand requires a high foraging activity, which can be reduced during the early stages of SP adaptation as a function of decreasing food intake, body mass, and reproductive activity (Ruf and Heldmaier, 2000). Indeed, a high activity and body temperature in LP and lower values when SP-adapted have been reported (Hamann, 1987; Prendergast et al., 2013) and were confirmed in this study. While body temperature was lower in SP during all time frames (**Figure 6**), activity was similar in both LP and SP photophase and differed only in scotophase (**Figure 8**).

The transition of the activity and body temperature patterns from LP to SP has not yet been described for hamsters kept in artificial photoperiods. In this study, the hamsters were subjected to an abrupt light shift from LP to SP, whereby the photophase began 1 h later and ended 7 h earlier. This manner of transition has been used for several hamster cohorts and experiments at Ulm University to allow for the described sampling paradigm when SP-adapted. Consequently, the responses shown in this study may have reflected this specific circadian phase entrainment to the photic *zeitgeber*. Regardless of the transition pattern, the potential influence of a certain shift on the hamster's individual adaptation and torpor capability must be considered. A fast activity adaptation was previously shown for diverse complex light regime changes, yet with high variations within the cohort including individuals with a low or no adaptation performance (Gorman and Elliott, 2004). Most hamsters were able to re-entrain to a ZT0 shift by 5 h (16:8 h) within 14 days, while some showed a free-running activity pattern

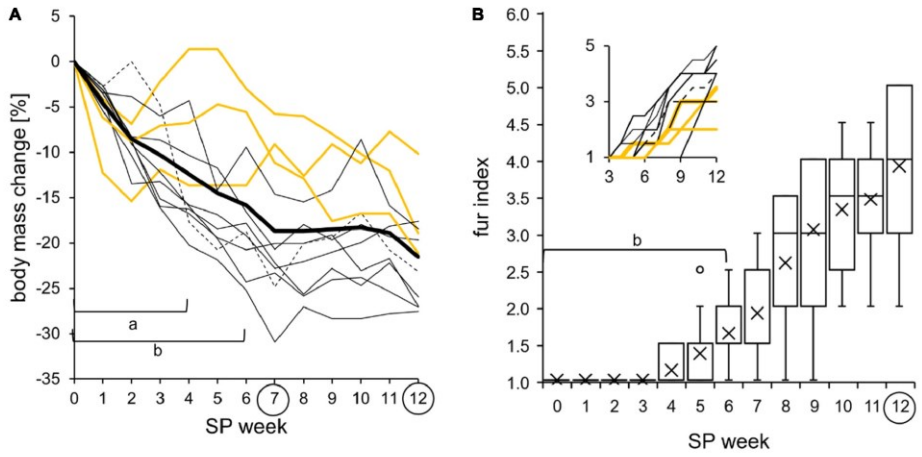

FIGURE 11 | Body mass change and molt into a white winter fur during the short photoperiod adaptation of approach 2 (n = 11). The exact values per hamster can be found in **Supplementary Table 8**. **(A)** Relative body mass change with the long photoperiod (LP) as baseline. The cohort's significant differences of the relative body mass change (*thick line*) to SP07 are indicated with "*a*" e.g., to SP12 with "*b*" [one-way repeated measures ANOVA: $F_{(12,120)} = 28.777$, $p < 0.001$, with Holm–Sidak $p < 0.001$]. All hamsters changed their body mass during the short photoperiod (SP) adaptation (hamster #06 as *dotted line*, the three "never torpor" hamsters as *yellow lines*, and all others as *thin black lines*). **(B)** Fur index from 1 for summer fur to 6 for winter fur. The cohort's significant differences of fur index (*boxplots*) to SP12 are indicated with "*b*" [Friedman repeated measures ANOVA: $\chi^2_{(12)} = 122.375$, $p < 0.001$, with Tukey's test $p < 0.05$]. All hamsters increased their fur index. *Inset*: graph with color code of graph **(A)**.

or even arrhythmia (Barakat et al., 2004, 2005). In the present study, the majority of hamsters showed a fast response to the new light regime by an immediate synchronization as well as reductions of activity and body temperature during the first SP week (**Figures 6A**, 8A). In contrast, the body mass and fur index, two parameters strongly influencing thermoregulation, remained initially unchanged (**Figure 11**).

Activity requires an increase in the metabolic rate, which produces heat and increases body temperature. Thus, the immediate reduction of the scotophase body temperature after the change from LP to SP was largely attributable to the immediate decrease in scotophase activity, although the velocity of this change was rather impressive. As activity recordings have been shown to largely reflect feeding bouts (Ruf and Heldmaier, 1993), the activity decrease observed in this study might have resulted from a decreased drive to feed in order to initiate body mass reduction during SP adaptation (Knopper and Boily, 2000). Earlier studies have already measured lower scoto- and photophase body temperatures in SP- than in LP-adapted Djungarian hamsters (Heldmaier and Steinlechner, 1981a; Korhonen et al., 2008). The present study, however, showed for the first time that this decrease in body temperature already occurs at the very beginning of the SP adaptation and further proceeds during the adaptation process (**Figure 6**). The hamsters appeared to tolerate the rather acute body temperature reduction and additionally showed an increasing difference between the maximum and minimum body temperatures prior to the beginning of torpor expression, surprisingly not only during photophase but also during scotophase (**Figure 7**). This observation might be a first indication for an SP-induced early change in body temperature set point, which is gradually adjusted and integrated in the complex morphological and physiological adaptation processes until the beginning of the torpor period. Although this study cannot provide sufficient information on the mechanisms behind the body temperature adjustments, it can be assumed that they contribute to the overall energy-saving purpose of the Djungarian hamster's adaptative syndrome (Heldmaier and Lynch, 1986).

The high variability in adaptation is considered to be natural and not indicative of the negative effects of domestication and genetic bottlenecks (Figala et al., 1973), as a hamster population should benefit from a certain degree of individual flexibility and variation to cope with acute and unpredictable changes in environmental conditions (Ruf et al., 1991, 1993). Nevertheless, since the Siberian winter is usually long and harsh, nature should have selected for hamsters with a fast and strong adaptation in response to the decreasing photoperiod length, followed by flexible torpor use as anticipation of acute energetic challenges, which are not given in laboratory conditions (Diedrich et al., 2015, 2020).

Nocturnality

According to the developer, the DSI activity data indicate no, low, or high activity per 3-min recording interval. The method developed for this study made the activity data accessible in more detail by using larger data bins, namely, time frames per week, which leveled natural and technical outliers, while a sufficient time increment was maintained for both long- and short-term observations (**Figures 1**, **2**). Nevertheless, the absolute activity

data, recorded and analyzed in cpm, are based on the signal strength changes, which might slightly vary with position and speed the transmitter moving over its receiver. The activity mean values of several animals must be interpreted with caution (**Table 3** and **Figure 8**), while the introduced activity ratios are a promising tool to characterize activity in relative terms with each animal as its own control (**Table 3** and **Figure 10**).

For the present study, using both absolute and relative activity data complemented and verified each other. A higher activity during scotophase than during photophase has been described for rodents in general and has incidentally been shown for Djungarian hamsters (Wynne-Edwards et al., 1999; Refinetti, 2006; Weinert et al., 2009), which could be confirmed in the present study (**Figures 8–10**, **Table 3**, and **Supplementary Table 6**). Previously, different circadian phenotypes have been described, ranging from wild type over delayed onset and arrhythmic to non-responder (Margraf et al., 1991; Gorman and Zucker, 1997; Schöttner et al., 2011). In the present study, all hamsters were nocturnal, with higher absolute activity values during the scotophase and a photophase-to-scotophase activity ratio below 1, while hamster #06's hyperactivity during the photophase was reflected by photophase-to-scotophase activity ratios higher than 1, proving diurnality. Unlike the other hamsters of the cohort, the calm sibling hamsters #10 and #11, did not decrease their activity over the course of SP adaptation, probably because they could not fall below the basal activity level. Their nocturnality was difficult to detect due to the irregular and shallow activity bouts, but was proven with the photophase-to-scotophase activity ratio.

The activity ratios for the smaller time frames enable a more subtle discrimination of the circadian phenotypes, e.g., the second-to-first half of scotophase activity ratio. In most hamsters, activity started and peaked at the beginning of the scotophase, declined over the course of the scotophase, and had already faded at the beginning of the photophase without clear-cut ending, which could be proven by second-to-first half of scotophase activity ratios smaller 1. SP caused a shift of the hamsters' activity phase and its peak toward the new beginning of scotophase, which was visualized by actograms and reflected by both activity ratios. This pace enabled defining one slow (hamster #09) and one very slow (hamster #01, "never torpor") activity responder. During progressing SP adaptation, the actograms of this study suggest increasing flexibility of the daily activity–rest rhythm. This was supported by a decreasing degree of nocturnality, indicated by an increasing photophase-to-scotophase activity ratio. The activity ratios used in this study had no significant influence on and were not influenced by the torpor incidence.

CONCLUSION

The incidence, timing, and traits of spontaneous daily torpor show low intra- but high inter-individual variabilities over the torpor period in Djungarian hamsters. Therefore, a detailed body temperature analysis of one representative SP week after complete adaptation might contribute to a refinement of the organ sampling schemes realized in the following week. Hamsters with different torpor incidences, and therefore phenotypes, could then be assigned more equally to different sampling groups regarding metabolic state (hypothermic *vs.* normothermic) at a defined time (torpor entry, deep torpor, and arousal). This standardization will further improve the outcomes of molecular analyses of the torpor regulatory pathways.

Hamsters that never expressed torpor had a low body mass reduction and could be discriminated from torpor-expressing hamsters by high mean body temperatures with low fluctuations in the middle of the scotophase. Moreover, weak or slow SP adaptations of body temperature, activity body mass, and fur index were found. However, an early estimation of the subsequent torpor behavior, and therefore a reduction of animals subjected to implantation, remains difficult because of the high variability of the SP adaptation pace and extent within a hamster cohort. Non-invasive alternative methods like infrared cameras with tracking software to assess activity or indirect calorimetry for metabolic rate measurements should be considered to analyze hamsters' adaptation and torpor phenotypes before transmitter implantation.

As an immediate response to an abrupt change from LP to SP, scotophase activity and the body temperature decreased in the hamsters, indicating profound physiological changes at the very beginning of adaptation. This underpins the importance of a careful control of the experimental photoperiod regimes and suggests focusing more on the initial metabolic profiles of SP adaptation.

The adaptation parameters gradually changed, even weeks before the anticipated beginning of the energy-demanding winter. This preparatory period allows a fine-tuning of parameters since they start and develop with high variability. The individually fine-tuned set point of body temperature might have a central meaning for torpor integration into the overall energy balance of SP-adapted hamsters.

DATA AVAILABILITY STATEMENT

The raw data supporting the conclusions of this article will be made available by the authors, without undue reservation.

ETHICS STATEMENT

The animal study was reviewed and approved by Regierungspräsidium Tübingen, Germany (1411).

AUTHOR CONTRIBUTIONS

All the authors conceived the project, interpreted the data, and agreed to be accountable for the content of the work. EH and VD performed the experiments and analyzed the data. EH wrote the manuscript, which was carefully revised by all authors.

FUNDING

EH was funded by a grant from the German Research Foundation to AH (HE 6383/2).

ACKNOWLEDGMENTS

We thank Sabine Schmidt and Elisabeth Picca for animal breeding and care as well as Insa Krey and Alexandra Hentrich for their contribution to the method development. We also thank the reviewers for their valuable comments.

SUPPLEMENTARY MATERIAL

The Supplementary Material for this article can be found online at: https://www.frontiersin.org/articles/10.3389/fphys.2021.626779/full#supplementary-material

Supplementary Table 1 | Background information about the hamsters of this study. The hamsters' ID comprises the cohorts' name and a running number. Besides males (m) and females (f), the torpor incidence group is indicated by a raster, from "often torpor" in the first block over "sometimes torpor" and "rarely torpor" to "never torpor" in the last block. The transmitter runtime is given in weeks. The 11 animals of cohort EH04 were implanted already in LP and used in both approaches, while those of the cohorts EH02 and EH03 were implanted when adapted to SP and used in approach 1 only.

Supplementary Table 2 | Additional statistics of analysis of approach 1 regarding torpor characteristics and adaptation parameters of the analysis week per torpor incidence group (**Tables 1**, **2**).

Supplementary Table 3 | Additional statistics of the radiotelemetry analysis of approach 1 regarding pattern of activity and body temperature of one experimental week per torpor incidence group (**Table 3**).

Supplementary Table 4 | Body temperature values per time frame, week in long photoperiod (LP) and short photoperiod (SP) as well as individual of approach 2. Yellow marked hamsters did not express spontaneous daily torpor. Sparklines in the last column indicate the individual change, with the hamster's highest value as 100% and its lowest as 0%.

Supplementary Table 5 | Delta body temperature values per time frame, week in long photoperiod (LP) and short photoperiod (SP) as well as individual of approach 2. Yellow marked hamsters did not express spontaneous daily torpor. Sparklines in the last column indicate the individual change, with the hamster's highest value as 100% and its lowest as 0%.

Supplementary Table 6 | Activity values per time frame, week in long photoperiod (LP) and short photoperiod (SP) as well as individual of approach 2. Yellow marked hamsters did not express spontaneous daily torpor. Sparklines in the last column indicate the individual change, with the hamster's highest value as 100% and its lowest as 0%.

Supplementary Table 7 | Activity ratio values per time frame, week in long photoperiod (LP) and short photoperiod (SP) as well as individual of approach 2. Yellow marked hamsters did not express spontaneous daily torpor. Red color marks ratios above 1.0 indicating diurnal activity patterns (upper part) or higher activity during the second half of the scotophase (lower part). Sparklines in the last column indicate the individual change, with the hamster's highest value as 100% and its lowest as 0%. Second to first half of scotophase ratio was not raised for LP with a scotophase of eight hours.

Supplementary Table 8 | Adaptation parameter values per week in long photoperiod (LP) and short photoperiod (SP) as well as individual of approach 2. Yellow marked hamsters did not express spontaneous daily torpor. Sparklines in the last column indicate the individual change, with the hamster's highest value as 100% and its lowest as 0%.

REFERENCES

Bank, J. H. H., Cubuk, C., Wilson, D., Rijntjes, E., Kemmling, J., Markowsky, H., et al. (2017). Gene expression analysis and microdialysis suggest hypothalamic triiodothyronine (T3) gates daily torpor in Djungarian hamsters (*Phodopus sungorus*). *J. Comp. Physiol. B Biochem. Syst. Environ. Physiol.* 187, 857–868. doi: 10.1007/s00360-017-1086-1085

Bank, J. H. H., Kemmling, J., Rijntjes, E., Wirth, E. K., and Herwig, A. (2015). Thyroid hormone status affects expression of daily torpor and gene transcription in Djungarian hamsters (*Phodopus sungorus*). *Horm. Behav.* 75, 120–129. doi: 10.1016/j.yhbeh.2015.09.006

Barakat, M. T., O'Hara, B. F., Cao, V. H., Heller, H. C., and Ruby, N. F. (2005). Light induces c- fos and per1 expression in the suprachiasmatic nucleus of arrhythmic hamsters. *Am. J. Physiol. Integr. Comp. Physiol.* 289, R1381–R1386. doi: 10.1152/ajpregu.00695.2004

Barakat, M. T., O'Hara, B. F., Cao, V. H., Larkin, J. E., Heller, H. C., and Ruby, N. F. (2004). Light pulses do not induce c-fos or per1 in the SCN of hamsters that fail to reentrain to the photocycle. *J. Biol. Rhythms* 19, 287–297. doi: 10.1177/0748730404266771

Boyles, J. G., Smit, B., and McKechnie, A. E. (2011). Does use of the torpor cut-off method to analyze variation in body temperature cause more problems than it solves? *J. Therm. Biol.* 36, 373–375. doi: 10.1016/j.jtherbio.2011.07.007

Brigham, R. M., Willis, C. K. R., Geiser, F., and Mzilikazi, N. (2011). Baby in the bathwater: should we abandon the use of body temperature thresholds to quantify expression of torpor? *J. Therm. Biol.* 36, 376–379. doi: 10.1016/j.jtherbio.2011.08.001

Choukèr, A., Bereiter-Hahn, J., Singer, D., and Heldmaier, G. (2019). Hibernating astronauts — science or fiction? *Eur. J. Physiol.* 471, 819–828. doi: 10.1007/s00424-018-2244-2247

Christian, N., and Geiser, F. (2007). To use or not to use torpor? activity and body temperature as predictors. *Naturwissenschaften* 94, 483–487. doi: 10.1007/s00114-007-0215-215

Cubuk, C., Bank, J. H. H., and Herwig, A. (2016). The chemistry of cold: mechanisms of torpor regulation in the siberian hamster. *Physiology* 31, 51–59. doi: 10.1152/physiol.00028.2015

Cubuk, C., Kemmling, J., Fabrizius, A., and Herwig, A. (2017a). Transcriptome analysis of hypothalamic gene expression during daily torpor in Djungarian hamsters (*Phodopus sungorus*). *Front. Neurosci.* 11:122. doi: 10.3389/fnins.2017.00122

Cubuk, C., Markowsky, H., and Herwig, A. (2017b). Hypothalamic control systems show differential gene expression during spontaneous daily torpor and fasting-induced torpor in the Djungarian hamster (*Phodopus sungorus*). *PLoS One* 12:e0186299. doi: 10.1371/journal.pone.0186299

Dave, K. R., Christian, S. L., Perez-Pinzon, M. A., and Drew, K. L. (2012). Neuroprotection: lessons from hibernators. *Comp. Biochem. Physiol. - B Biochem. Mol. Biol.* 162, 1–9. doi: 10.1016/j.cbpb.2012.01.008

Deboer, T., and Tobler, I. (2003). Sleep regulation in the Djungarian hamster: comparison of the dynamics leading to the slow-wave activity increase after sleep deprivation and daily torpor. *Sleep* 26, 567–572. doi: 10.1093/sleep/26.5.567

Deboer, T., Vyazovskiy, V. V., and Tobler, I. (2000). Long photoperiod restores the 24-h rhythm of sleep and EEG slow-wave activity in the Djungarian hamster (*Phodopus sungorus*). *J. Biol. Rhythms* 15, 429–436. doi: 10.1177/074873040001500508

Diedrich, V., Haugg, E., Dreier, C., and Herwig, A. (2020). What can seasonal models teach us about energy balance? *J. Endocrinol.* 244, R17–R32.

Diedrich, V., Kumstel, S., and Steinlechner, S. (2015). Spontaneous daily torpor and fasting-induced torpor in Djungarian hamsters are characterized by distinct patterns of metabolic rate. *J. Comp. Physiol. B Biochem. Syst. Environ. Physiol.* 185, 355–366. doi: 10.1007/s00360-014-0882-884

Figala, J., Hoffmann, K., and Goldau, G. (1973). Zur jahresperiodik beim dsungarischen zwerghamster *Phodopus sungorus* pallas. *Oecologia* 12, 89–118. doi: 10.1007/BF00345511

Geiser, F. (2008). Ontogeny and phylogeny of endothermy and torpor in mammals and birds. *Comp. Biochem. Physiol. - A Mol. Integr. Physiol.* 150, 176–180. doi: 10.1016/j.cbpa.2007.02.041

Geiser, F., and Brigham, R. M. (2012). "The other functions of torpor," in *Living in a Seasonal World*, eds T. Ruf, C. Bieber, W. Arnold, and E. Millesi (Berlin: Springer).

Gorman, M. R., and Elliott, J. A. (2004). Dim nocturnal illumination alters coupling of circadian pacemakers in *Siberian hamsters*, *Phodopus sungorus*. *J. Comp. Physiol.* 190, 631–639. doi: 10.1007/s00359-004-0522-527

Gorman, M. R., and Zucker, I. (1997). Environmental induction of photononresponsiveness in the *Siberian hamster*, *Phodopus sungorus*. *Am. J. Physiol. - Regul. Integr. Comp. Physiol.* 272, 887–895. doi: 10.1152/ajpregu.1997.272.3.r887

Hamann, U. (1987). Zu Aktivität und verhalten von drei Taxa der zwerghamster der gattung phodopus miller, 1910. *Mamm. Biol.* 52, 65–76.

Heldmaier, G., and Lynch, G. R. (1986). Pineal involvement in thermoregulation and acclimatization. *Pineal Res. Rev.* 4, 97–139.

Heldmaier, G., Ortmann, S., and Elvert, R. (2004). Natural hypometabolism during hibernation and daily torpor in mammals. *Respir. Physiol. Neurobiol.* 141, 317–329. doi: 10.1016/j.resp.2004.03.014

Heldmaier, G., and Ruf, T. (1992). Body temperature and metabolic rate during natural hypothermia in endotherms. *J. Comp. Physiol. B* 162, 696–706. doi: 10.1007/BF00301619

Heldmaier, G., and Steinlechner, S. (1981a). Seasonal control of energy requirements for thermoregulation in the Djungarian hamster (*Phodopus sungorus*), living in natural photoperiod. *J. Comp. Physiol. B Biochem. Syst. Environ. Physiol.* 142, 429–437. doi: 10.1007/BF00688972

Heldmaier, G., and Steinlechner, S. (1981b). Seasonal pattern and energetics of short daily torpor in the Djungarian hamster, *Phodopus sungorus*. *Oecologia* 48, 265–270. doi: 10.1007/BF00347975

Herwig, A., Ivanova, E. A., Lydon, H., Barrett, P., Steinlechner, S., and Loudon, A. S. I. (2007). Histamine H3 receptor and orexin a expression during daily torpor in the Djungarian hamster (*Phodopus sungorus*). *J. Neuroendocrinol.* 19, 1001–1007. doi: 10.1111/j.1365-2826.2007.01620.x

Hoffmann, K. (1982). "The critical photoperiod in the djungarian hamster *Phodopus sungorus*," in *Vertebrate Circadian Systems. Proceedings in Life Sciences*, eds J. Aschoff, S. Daan, and G. A. Groos (Berlin: Springer).

Jastroch, M., Giroud, S., Barrett, P., Geiser, F., Heldmaier, G., and Herwig, A. (2016). Seasonal control of mammalian energy balance: recent advances in the understanding of daily torpor and hibernation. *J. Neuroendocrinol.* 28, 1–10. doi: 10.1111/jne.12437

Jones, J. S., Fileccia, E. L., Murphy, M., Fowler, M. J., King, M. V., Shortall, S. E., et al. (2014). Cathinone increases body temperature, enhances locomotor activity, and induces striatal c-fos expression in the *Siberian hamster*. *Neurosci. Lett.* 559, 34–38. doi: 10.1016/j.neulet.2013.11.032

Kirsch, R., Ouarour, A., and Pévet, P. (1991). Daily torpor in the Djungarian hamster (*Phodopus sungorus*): photoperiodic regulation, characteristics and circadian organization. *J. Comp. Physiol. A* 168, 121–128. doi: 10.1007/BF00217110

Knopper, L. D., and Boily, P. (2000). The energy budget of captive siberian hamsters, *Phodopus sungorus*, exposed to photoperiod changes: mass loss is caused by a voluntary decrease in food intake. *Physiol. Biochem. Zool.* 73, 517–522. doi: 10.1086/317730

Korhonen, T., Mustonen, A.-M., Nieminen, P., and Saarela, S. (2008). Effects of cold exposure, exogenous melatonin and short-day treatment on the weight-regulation and body temperature of the *Siberian Hamster* (*Phodopus sungorus*). *Regul. Pept.* 149, 60–66. doi: 10.1016/j.regpep.2007.09.033

Margraf, R. R., Zlomanczuk, P., Liskin, L. A., and Lynch, G. R. (1991). Circadian differences in neuronal activity of the suprachiasmatic nucleus in brain slices prepared from photo-responsive and photo-non-responsive *Djungarian hamsters*. *Brain Res.* 544, 42–48. doi: 10.1016/0006-8993(91)90883-W

Paul, M. J., Freeman, D. A., Jin, H. P., and Dark, J. (2005). Neuropeptide Y induces torpor-like hypothermia in *Siberian hamsters*. *Brain Res.* 1055, 83–92. doi: 10.1016/j.brainres.2005.06.090

Paul, M. J., Kauffman, A. S., and Zucker, I. (2004). Feeding schedule controls circadian timing of daily torpor in SCN-ablated *Siberian hamsters*. *J. Biol. Rhythms* 19, 226–237. doi: 10.1177/0748730404264337

Piscitiello, E., Herwig, A., Haugg, E., Schröder, B., Breves, G., Steinlechner, S., et al. (2021). Acclimation of intestinal morphology and function in Djungarian hamsters (*Phodopus sungorus*) related to seasonal and acute energy balance. *J. Exp. Biol.* 224:jeb232876. doi: 10.1242/jeb.232876

Prendergast, B. J., Cable, E. J., Cisse, Y. M., Stevenson, T. J., and Zucker, I. (2013). Pineal and gonadal influences on ultradian locomotor rhythms of male *Siberian hamsters*. *Horm. Behav.* 63, 54–64. doi: 10.1016/j.yhbeh.2012.11.001

Przybylska, A. S., Wojciechowski, M. S., and Jefimow, M. (2019). Photoresponsiveness affects life history traits but not oxidative status in a seasonal rodent. *Front. Zool.* 16:11. doi: 10.1186/s12983-019-0311-3

Refinetti, R. (2006). Variability of diurnality in laboratory rodents. *J. Comp. Physiol. A Neuroethol. Sensory Neural Behav. Physiol.* 192, 701–714. doi: 10.1007/s00359-006-0093-x

Ross, P. D. (1998). Phodopus sungorus. *Mamm. Species* 595, 1–9. doi: 10.2307/3504390

Ruby, N. F., and Zucker, I. (1992). Daily torpor in the absence of the suprachiasmatic nucleus in *Siberian hamsters*. *Am. J. Physiol.* 263, R353–R362. doi: 10.1152/ajpregu.1992.263.2.R353

Ruf, T., and Heldmaier, G. (1992). The impact of daily torpor on energy requirements in the *Djungarian hamster*. *Phodopus sungorus*. *Physiol. Zool.* 65, 994–1010. doi: 10.2307/30158554

Ruf, T., and Heldmaier, G. (1993). "Individual energetic strategies in winter-adapted *Djungarian hamsters*: the relation between daily torpor, locomotion, and food consumption," in *Life in the Cold*, ed. C. Carey (Boca Raton, FL: CRC Press), 99–107.

Ruf, T., and Heldmaier, G. (2000). "*Djungarian hamsters* — Small graminivores with daily torpor," in *Activity Patterns in Small Mammals. Ecological Studies (Analysis and Synthesis)*, 141, eds S. Halle and N. C. Stenseth (Berlin: Springer), 217–234. doi: 10.1007/978-3-642-18264-8_14

Ruf, T., Klingenspor, M., Preis, H., and Heldmaier, G. (1991). Daily torpor in the Djungarian hamster (*Phodopus sungorus*): interactions with food intake, activity, and social behaviour. *J. Comp. Physiol. B* 160, 609–615.

Ruf, T., Steinlechner, S., and Heldmaier, G. (1989). "Rhythmicity of body temperature and torpor in the *Djungarian hamster*, *Phodopus sungorus*," in *Proceedings of the Living in the Cold: 2nd International Symposium*, eds A. Malan and B. Canguilhem (Le Hohwald: Colloques INSERM/John Libbey Eurotext Ldt), 53–61.

Ruf, T., Stieglitz, A., Steinlechner, S., Blank, J. L., and Heldmaier, G. (1993). Cold exposure and food restriction facilitate physiological responses to short photoperiod in Djungarian hamsters (*Phodopus sungorus*). *J. Exp. Zool.* 267, 104–112. doi: 10.1002/jez.1402670203

Scherbarth, F., and Steinlechner, S. (2008). The annual activity pattern of Djungarian hamsters (*Phodopus sungorus*) is affected by wheel-running activity. *Chronobiol. Int.* 25, 905–922. doi: 10.1080/07420520802544514

Scherbarth, F., and Steinlechner, S. (2010). Endocrine mechanisms of seasonal adaptation in small mammals: from early results to present understanding. *J. Comp. Physiol. B Biochem. Syst. Environ. Physiol.* 180, 935–952. doi: 10.1007/s00360-010-0498-492

Schöttner, K., Waterhouse, J., and Weinert, D. (2011). The circadian body temperature rhythm of Djungarian Hamsters (*Phodopus sungorus*) revealing different circadian phenotypes. *Physiol. Behav.* 103, 352–358. doi: 10.1016/j.physbeh.2011.02.019

Scribner, S. J., and Wynne-Edwards, K. E. (1994). Disruption of body temperature and behavior rhythms during reproduction in dwarf hamsters (*Phodopus*). *Physiol. Behav.* 55, 361–369. doi: 10.1016/0031-9384(94)90147-90143

Steinlechner, S., Heldmaier, G., Weber, C., and Ruf, T. (1986). "Role of photoperiod: pineal gland interaction in torpor control," in *Living in the Cold: Physiological and Biochemical Adaptions*, eds H. C. Heller, L. C. H. Wang, and X. Musacchia (New York, NY: Elsevier Science Publishing Co., Inc.), 301–307.

Weinert, D., Schöttner, K., Surov, A. V., Fritzsche, P., Feoktistova, N. Y., Ushakova, M. V., et al. (2009). Circadian activity rhythms of dwarf hamsters (*Phodopus spp.*) under laboratory and semi-natural conditions. *Russ. J. Theriol.* 8, 47–58. doi: 10.15298/rusjtheriol.08.1.05

Wynne-Edwards, K. E., Surov, A. V., and Telitzina, A. Y. (1999). Differences in endogenous activity within the genus *Phodopus*. *J. Mammal.* 80, 855–865. doi: 10.2307/1383254

Conflict of Interest: The authors declare that the research was conducted in the absence of any commercial or financial relationships that could be construed as a potential conflict of interest.

Copyright © 2021 Haugg, Herwig and Diedrich. This is an open-access article distributed under the terms of the Creative Commons Attribution License (CC BY). The use, distribution or reproduction in other forums is permitted, provided the original author(s) and the copyright owner(s) are credited and that the original publication in this journal is cited, in accordance with accepted academic practice. No use, distribution or reproduction is permitted which does not comply with these terms.

2.2 Supplementary Material



Supplementary Materials

Haugg E, Herwig A and Diedrich V (2021) Body Temperature and Activity Adaptation of Short Photoperiod-Exposed Djungarian Hamsters (Phodopus sungorus): Timing, Traits, and Torpor. Front. Physiol. 12:626779.

doi: 10.3389/fphys.2021.626779

Correspondence to: elena.haugg@uni-ulm.de

This file includes:

Supplementary Table 1: Background information about the hamsters (both approaches)

Supplementary Table 2: Additional statistics of torpor characteristics and adaptation parameters (approach 1)

Supplementary Table 3: Additional statistics of the radiotelemetry analysis (approach 1)

Supplementary Table 4: Body temperature values (approach 2)

Supplementary Table 5: Delta body temperature values (approach 2)

Supplementary Table 6: Activity values (approach 2)

Supplementary Table 7: Activity ratio values (approach 2)

Supplementary Table 8: Adaptation parameter values (approach 2)

Supplementary materials **Hamster temperature and activity adaptation**

SUPPLEMENTS

Supplementary Table 1: Background information about the hamsters of this study. The hamsters' ID comprises the cohorts' name and a running number. Besides males (m) and females (f), the torpor incidence group is indicated by a raster, from "often" torpor in the first block over "sometimes" and "rarely" to "never" torpor in the last block. The transmitter runtime is given in weeks. The eleven animals of cohort EH04 were implanted already in LP and used in both approaches, while those of the cohorts EH02 and EH03 were implanted when adapted to SP and used in approach 1 only.

cohort											
key data			torpor	age [weeks] at				duration [weeks] in SP at			transmitter
portion	#		incidence	SP	surgery	analysis	sacrifice	surgery	analysis	sacrifice	runtime
males	41	mean	0.4	16.1	26.4	30.8	32.5	10.3	14.7	16.4	6.1
females	19	Std. Dev.	0.2	2.9	7.2	3.6	3.6	6.3	2.1	2.4	5.0
torpor	46	min	0.0	10.1	11.1	25.6	26.7	-2.6	11.9	12.9	2.0
never torpor	14	max	1.0	23.3	36.4	39.4	40.4	17.0	22.7	23.7	17.0
EH02	27	median	0.3	15.9	27.9	30.2	32.4	12.9	14.9	16.1	3.8
EH03	22	1. quartile	0.2	14.0	26.0	28.0	29.4	10.8	12.8	14.3	2.9
EH04	11	3. quartile	0.5	17.5	30.3	33.1	35.2	13.9	15.9	17.9	6.5

individuals											
key data		torpor incidence		age [weeks] at				duration [weeks] in SP at			transmitter
ID	gender	group	value	SP	surgery	analysis	sacrifice	surgery	analysis	sacrifice	runtime
EH02-45	f	often	1.0	10.1	24.4	27.4	28.4	14.3	17.3	18.3	4.0
EH02-14	f	often	0.9	14.1	27.1	29.0	30.0	13.0	14.9	15.9	2.9
EH03-26	m	often	0.9	18.3	29.4	31.1	32.1	11.1	12.9	13.9	2.7
EH02-03	m	often	0.7	19.7	32.9	34.7	35.7	13.1	15.0	16.0	2.9
EH02-12	f	often	0.7	14.1	31.1	36.9	37.9	17.0	22.7	23.7	6.7
EH03-10	m	often	0.7	19.4	29.7	36.3	37.3	10.3	16.9	17.9	7.6
EH03-19	m	often	0.7	15.7	29.6	33.1	34.1	13.9	17.4	18.4	4.6
EH03-27	m	often	0.7	18.3	29.3	33.6	35.1	11.0	15.3	16.9	5.9
EH04-06	f	often	0.7	15.9	13.4	28.0	29.9	-2.4	12.1	14.0	16.4
EH02-16	m	often	0.6	13.4	28.1	30.3	31.3	14.7	16.9	17.9	3.1
EH03-05	m	often	0.6	21.1	35.1	36.4	37.4	14.0	15.3	16.3	2.3
EH04-10	m	often	0.6	14.0	11.7	26.1	28.3	-2.3	12.1	14.3	16.6
EH02-02	m	sometimes	0.4	23.3	36.3	38.1	39.1	13.0	14.9	15.9	2.9
EH02-04	m	sometimes	0.4	12.1	26.4	27.9	28.9	14.3	15.7	16.7	2.4
EH02-28	f	sometimes	0.4	16.9	30.0	31.7	32.7	13.1	14.9	15.9	2.7
EH02-35	m	sometimes	0.4	19.7	32.9	34.4	35.4	13.1	14.7	15.7	2.6
EH03-02	f	sometimes	0.4	22.4	33.6	39.4	40.4	11.1	17.0	18.0	6.9
EH03-13	m	sometimes	0.4	16.0	26.0	27.9	28.9	10.0	11.9	12.9	2.9
EH03-20	f	sometimes	0.4	15.7	26.7	31.1	32.1	11.0	15.4	16.4	5.4
EH03-30	m	sometimes	0.4	15.9	27.0	28.1	29.1	11.1	12.3	13.3	2.1
EH03-33	m	sometimes	0.4	15.6	27.4	28.6	29.6	11.9	13.0	14.0	2.1
EH04-03	m	sometimes	0.4	15.6	13.0	27.7	30.0	-2.6	12.1	14.4	17.0
EH02-01	m	sometimes	0.3	12.1	26.3	28.6	29.6	14.1	16.4	17.4	3.3
EH02-06	f	sometimes	0.3	11.9	24.7	26.9	27.9	12.9	15.0	16.0	3.1
EH02-07	m	sometimes	0.3	11.9	24.7	26.6	27.6	12.9	14.7	15.7	2.9
EH02-09	m	sometimes	0.3	13.6	27.4	28.4	29.4	13.9	14.9	15.9	2.0
EH02-17	m	sometimes	0.3	17.7	30.6	32.6	33.6	12.9	14.9	15.9	3.0
EH02-18	f	sometimes	0.3	16.4	29.4	31.3	32.3	13.0	14.9	15.9	2.9
EH02-39	f	sometimes	0.3	16.1	29.3	30.3	31.3	13.1	14.1	15.1	2.0
EH03-01	m	sometimes	0.3	22.7	33.0	35.3	36.3	10.3	12.6	13.6	3.3
EH03-08	m	sometimes	0.3	19.4	29.4	31.7	32.7	10.0	12.3	13.3	3.3
EH03-11	m	sometimes	0.3	17.4	31.1	33.1	34.1	13.7	15.7	16.7	3.0
EH03-36	f	sometimes	0.3	15.6	27.7	28.9	29.9	12.1	13.3	14.3	2.1
EH03-38	m	sometimes	0.3	13.6	25.9	27.0	28.0	12.3	13.4	14.4	2.1
EH02-05	m	rarely	0.1	16.9	30.7	33.3	34.3	13.9	16.4	17.4	3.6
EH02-10	m	rarely	0.1	18.9	33.6	35.0	36.0	14.7	16.1	17.1	2.4
EH02-20	f	rarely	0.1	13.6	27.4	28.9	29.9	13.9	15.3	16.3	2.4
EH02-25	m	rarely	0.1	17.1	30.3	32.4	33.4	13.1	15.3	16.3	3.1
EH02-30	m	rarely	0.1	20.9	35.9	38.0	39.0	15.0	17.1	18.1	3.1
EH03-32	m	rarely	0.1	15.9	27.7	31.1	32.1	11.9	15.3	16.3	4.4
EH04-07	m	rarely	0.1	14.9	12.4	27.0	28.4	-2.4	12.1	13.6	16.0
EH04-08	m	rarely	0.1	14.9	12.4	27.0	29.1	-2.4	12.1	14.3	16.7
EH04-09	f	rarely	0.1	14.9	12.6	27.0	28.4	-2.3	12.1	13.6	15.9
EH02-37	m	rarely	0.0	20.9	35.9	38.6	39.6	15.0	17.7	18.7	3.7
EH04-05	m	rarely	0.0	15.9	13.4	28.0	30.3	-2.4	12.1	14.4	16.9
EH04-11	f	rarely	0.0	13.4	11.1	25.6	26.7	-2.3	12.1	13.3	15.6
EH02-08	f	never	-	11.9	26.7	27.9	32.6	14.9	16.0	20.7	5.9
EH02-15	m	never	-	13.7	28.4	29.6	34.0	14.7	15.9	20.3	5.6
EH02-24	f	never	-	13.7	30.1	31.3	34.0	16.4	17.6	20.3	3.9
EH02-26	f	never	-	13.7	30.4	31.6	34.4	16.7	17.9	20.7	4.0
EH02-27	m	never	-	19.7	36.4	37.6	40.4	16.7	17.9	20.7	4.0
EH03-12	m	never	-	16.0	29.0	30.1	35.9	13.0	14.1	19.9	6.9
EH03-14	m	never	-	16.0	29.9	31.0	36.3	13.9	15.0	20.3	6.4
EH03-17	m	never	-	15.7	29.6	30.7	35.6	13.9	15.0	19.9	6.0
EH03-31	m	never	-	15.9	27.7	28.9	33.0	11.9	13.0	17.1	5.3
EH03-34	m	never	-	15.6	27.7	28.9	32.7	12.1	13.3	17.1	5.0
EH03-35	m	never	-	15.6	27.7	28.9	32.7	12.1	13.3	17.1	5.0
EH04-01	m	never	-	16.0	13.4	28.1	29.3	-2.6	12.1	13.3	15.9
EH04-02	f	never	-	16.0	13.4	28.1	29.3	-2.6	12.1	13.3	15.9
EH04-12	f	never	-	14.0	11.7	26.1	27.4	-2.3	12.1	13.4	15.7

Supplementary Table 2: Additional statistics of analysis of approach 1 regarding torpor characteristics and adaptation parameters of the analysis week per torpor incidence group (Tables 1 and 2).

	parameter	normality test	equal variance test	*post-hoc*- test		Dunn's	Holm-Sidak
		p-value	p-value	comparison	p-value	Q-value	t-value
torpor	torpor per definition incidence	< 0.050	-	rarely vs. sometimes rarely vs. often sometimes vs. often	<0.050 <0.050 <0.050	3.5 6.2 3.5	- - -
	torpor attempt incidence	< 0.050	-	-	-	-	-
	torpor onset [ZT]	< 0.050	-	rarely vs. often sometimes vs. often	<0.050 <0.050	2.5 2.5	- -
	torpor offset [ZT]	0.277	0.21	-	-	-	-
	torpor duration [minutes]	0.117	0.993	-	-	-	-
	minimal torpor Tb [°C]	0.296	0.336	-	-	-	-
adaptation	fur index in SP07	-	-	-	-	-	-
	fur index in SP12	-	-	-	-	-	-
	body mass in SP00 [g]	0.110	0.675	-	-	-	-
	body mass in SP07 [g]	0.169	0.615	-	-	-	-
	body mass in SP12 [g]	0.232	0.332	never vs. often	0.005	-	2.9
	body mass change in SP07 [%]	0.925	0.483	never vs. rarely never vs. sometimes never vs. often	0.002 0.002 0.003	- - -	3.2 3.2 3.1
	body mass change in SP12 [%]	0.240	0.663	never vs. rarely never vs. sometimes never vs. often	<0.001 <0.001 <0.001	- - -	4.3 4.8 5.6

Supplementary materials **Hamster temperature and activity adaptation**

Supplementary Table 3: Additional statistics of the radiotelemetry analysis of approach 1 regarding pattern of activity and body temperature of one experimental week per torpor incidence group (Table 3).

	parameter	normality test	equal variance test	*post-hoc*- test		Dunn's	Holm-Sidak
		p-value	p-value	comparison	p-value	Q-value	t-value
activity	total [cpm]	< 0.050	-	-	-	-	-
	photophase [cpm]	< 0.050	-	-	-	-	-
	scotophase [cpm]	< 0.050	-	rarely vs. often	< 0.050	2.8	-
	first half of scotophase [cpm]	< 0.050	-	rarely vs. often	< 0.050	3.0	
	second half of scotophase [cpm]	< 0.050	-	-	-	-	-
	middle of scotophase [cpm]	< 0.050	-	rarely vs. often	< 0.050	2.8	-
	Std. Dev. of middle of scotophase [cpm]	< 0.050	-	-	-	-	-
	photo- to scotophase ratio	< 0.050	-	-	-	-	-
	second to first half of scotophase ratio	< 0.050	-	-	-	-	-
body temperature	total [°C]	< 0.050	-	never vs. sometimes	< 0.050	5.1	-
				never vs. often	< 0.050	6.3	-
				rarely vs. sometimes	< 0.050	2.7	-
				rarely vs. often	< 0.050	4.1	-
	photophase [°C]	< 0.050	-	never vs. sometimes	< 0.050	5.1	-
				never vs. often	< 0.050	6.2	-
				rarely vs. sometimes	< 0.050	2.7	-
				rarely vs. often	< 0.050	4.1	-
	scotophase [°C]	0.117	0.273	never vs. sometimes	< 0.001	-	4.9
				never vs. often	< 0.001	-	7.0
				rarely vs. sometimes	0.016	-	2.5
				rarely vs. often	< 0.001	-	4.9
				sometimes vs. often	0.004	-	3.0
	1. half of scotophase [°C]	< 0.050	-	never vs. sometimes	< 0.050	3.1	-
				never vs. often	< 0.050	4.8	-
				rarely vs. often	< 0.050	3.9	-
	2. half of scotophase [°C]	0.472	< 0.050	never vs. sometimes	< 0.050	3.9	-
				never vs. often	< 0.050	5.0	-
	middle of scotophase [°C]	0.818	0.488	never vs. sometimes	< 0.001	-	4.2
				never vs. often	< 0.001	-	5.7
				rarely vs. sometimes	0.006	-	2.8
				rarely vs. often	< 0.001	-	4.5
	Std. Dev. of middle of scotophase [°C]	0.135	0.659	never vs. rarely	0.021	-	2.4
				never vs. often	0.011	-	2.6
				rarely vs. often	< 0.001	-	4.8
				sometimes vs. often	0.003	-	3.1

Hamster temperature and activity adaptation

Supplementary Table 4: Body temperature values per time frame, week in long photoperiod (LP) and short photoperiod (SP) as well as individual of approach 2. Yellow marked hamsters did not express spontaneous daily torpor. Sparklines in the last column indicate the individual change, with the hamster's highest value as 100% and its lowest as 0%.

	body temperature [°C], total													
	LP	SP01	SP02	SP03	SP04	SP05	SP06	SP07	SP08	SP09	SP10	SP11	SP12	SP13
#01	36.4	36.5	36.5	36.5	36.6	36.5	36.5	36.5	36.4	36.5	36.4	36.4	36.5	36.3
#02	36.8	36.7	36.6	36.5	36.6	36.5	36.4	36.4	36.4	36.3	36.4	36.4	36.3	36.3
#03	36.3	36.2	36.2	36.2	36.2	36.3	36.2	36.1	35.9	36.1	35.9	36.0	35.8	35.7
#05	36.6	36.5	36.6	36.5	36.6	36.5	36.4	36.3	36.1	36.0	35.8	35.6	35.6	35.9
#06	36.5	36.3	36.4	36.5	36.4	36.4	36.3	36.3	36.1	36.1	35.9	36.1	35.5	35.4
#07	36.4	36.3	36.5	36.4	36.5	36.4	36.3	36.4	36.0	36.0	35.9	35.9	35.7	35.8
#08	36.5	36.3	36.3	36.2	36.1	36.1	35.9	35.9	35.9	35.8	35.6	35.9	35.5	35.6
#09	36.7	36.7	36.6	36.5	36.4	36.4	36.3	36.4	36.2	36.2	36.0	36.0	35.8	36.0
#10	36.3	36.2	36.3	36.3	36.3	36.1	36.1	36.2	36.0	36.2	36.0	35.7	35.6	35.4
#11	36.3	36.1	36.2	36.1	36.0	36.1	36.1	36.0	35.9	35.8	35.8	35.7	35.8	35.7
#12	36.5	36.6	36.5	36.5	36.5	36.6	36.5	36.5	36.3	36.3	36.3	36.1	36.1	36.1
	body temperature [°C], scotophase													
	LP	SP01	SP02	SP03	SP04	SP05	SP06	SP07	SP08	SP09	SP10	SP11	SP12	SP13
#01	37.1	36.6	36.6	36.7	36.7	36.7	36.7	36.7	36.6	36.6	36.7	36.6	36.7	36.5
#02	37.9	36.9	36.8	36.8	36.8	36.7	36.7	36.6	36.7	36.5	36.7	36.7	36.7	36.5
#03	36.7	36.4	36.4	36.4	36.4	36.5	36.4	36.3	36.2	36.3	36.3	36.2	36.2	36.1
#05	37.2	36.7	36.8	36.7	36.8	36.7	36.6	36.5	36.3	36.1	36.1	36.1	36.1	36.1
#06	37.1	36.6	36.7	36.7	36.6	36.4	36.3	36.1	36.0	36.1	36.1	36.1	35.9	35.9
#07	37.1	36.6	36.7	36.7	36.7	36.7	36.6	36.5	36.2	36.3	36.1	36.2	36.1	36.2
#08	37.5	36.5	36.5	36.6	36.4	36.3	36.2	36.1	36.1	36.1	36.0	36.0	35.9	36.1
#09	37.5	36.9	36.8	36.7	36.6	36.5	36.4	36.4	36.3	36.4	36.1	36.2	35.9	36.2
#10	36.6	36.4	36.4	36.4	36.4	36.3	36.2	36.3	36.2	36.2	36.1	36.0	36.0	36.1
#11	36.5	36.3	36.4	36.3	36.3	36.3	36.3	36.2	36.1	36.1	36.1	36.0	36.1	36.0
#12	37.1	36.8	36.6	36.7	36.7	36.8	36.6	36.6	36.5	36.5	36.5	36.4	36.3	36.2
	body temperature [°C], photophase													
	LP	SP01	SP02	SP03	SP04	SP05	SP06	SP07	SP08	SP09	SP10	SP11	SP12	SP13
#01	36.1	36.3	36.2	36.1	36.2	36.1	36.1	36.1	36.1	36.1	36.0	36.1	36.1	36.0
#02	36.3	36.2	36.1	36.0	36.1	36.0	35.9	35.8	35.8	35.8	35.7	35.6	35.5	35.7
#03	36.1	36.0	35.9	35.8	35.8	35.9	35.7	35.7	35.2	35.6	35.1	35.5	35.0	34.9
#05	36.4	36.1	36.2	36.0	36.2	36.2	36.1	36.1	35.8	35.7	35.1	34.7	34.5	35.4
#06	36.2	35.7	35.9	35.9	36.0	36.3	36.3	36.7	36.2	36.1	35.7	36.0	34.6	34.4
#07	36.0	35.8	36.0	35.9	35.9	35.9	35.8	36.1	35.7	35.5	35.3	35.2	35.0	35.1
#08	36.0	35.9	35.7	35.6	35.7	35.5	35.4	35.5	35.4	35.3	34.9	35.6	34.5	34.8
#09	36.3	36.3	36.1	36.1	35.9	36.2	36.1	36.2	36.0	35.8	35.7	35.6	35.5	35.7
#10	36.2	36.0	36.0	36.0	36.0	35.9	35.9	35.9	35.7	36.1	35.7	35.3	34.7	34.0
#11	36.1	35.8	35.9	35.7	35.5	35.6	35.7	35.6	35.5	35.3	35.2	35.1	35.2	35.1
#12	36.2	36.2	36.1	36.1	36.2	36.2	36.2	36.1	36.0	35.9	35.9	35.7	35.8	35.7

Supplementary materials **Hamster temperature and activity adaptation**

Supplementary Table 5: Delta body temperature values per time frame, week in long photoperiod (LP) and short photoperiod (SP) as well as individual of approach 2. Yellow marked hamsters did not express spontaneous daily torpor. Sparklines in the last column indicate the individual change, with the hamster's highest value as 100% and its lowest as 0%.

	delta body temperature [°C], scotophase													
	LP	SP01	SP02	SP03	SP04	SP05	SP06	SP07	SP08	SP09	SP10	SP11	SP12	SP13
#01	2.0	2.0	1.5	1.9	1.7	1.9	2.1	1.8	1.9	2.1	2.1	2.3	2.2	2.4
#02	1.7	2.5	2.7	2.3	2.5	2.9	2.8	2.5	3.3	3.2	3.3	3.1	3.2	3.2
#03	2.1	1.7	2.1	2.1	2.3	2.2	2.7	2.5	2.7	2.7	2.6	3.4	3.2	3.1
#05	2.1	2.0	2.4	2.1	2.4	2.4	2.8	2.7	3.4	3.1	3.1	3.5	3.0	3.3
#06	2.1	2.5	4.9	2.2	2.5	2.7	3.0	2.6	2.9	3.1	2.8	3.0	4.3	5.0
#07	2.4	2.2	2.2	2.6	2.3	2.7	2.8	2.9	3.0	3.2	3.1	3.5	3.6	3.6
#08	2.9	3.5	3.4	3.2	3.3	3.1	3.4	3.7	3.5	3.4	3.2	3.4	4.0	3.8
#09	2.6	2.8	2.8	3.0	3.2	3.3	3.0	3.1	2.9	3.1	3.8	3.3	3.9	3.5
#10	1.8	1.6	1.9	2.1	2.6	2.6	3.1	2.5	2.6	2.7	3.0	3.2	5.2	3.0
#11	1.9	2.2	2.5	2.5	2.9	2.9	3.1	3.7	3.4	3.3	3.7	4.3	3.6	4.0
#12	2.5	2.1	2.1	1.9	2.3	1.8	2.2	2.2	2.4	2.8	2.8	2.7	2.7	2.8
	delta body temperature [°C], photophase													
	LP	SP01	SP02	SP03	SP04	SP05	SP06	SP07	SP08	SP09	SP10	SP11	SP12	SP13
#01	1.6	1.3	2.2	1.3	1.3	1.2	1.9	1.7	2.0	1.4	2.4	1.3	2.2	1.9
#02	1.9	2.1	2.5	2.0	2.4	1.8	2.4	1.8	3.2	2.3	3.6	1.6	3.3	2.1
#03	2.1	2.2	2.4	2.2	2.3	2.8	3.5	3.2	8.6	3.7	11.1	3.1	8.1	10.0
#05	1.7	1.3	1.7	1.5	2.4	2.8	3.0	2.8	2.8	2.9	13.2	12.9	14.0	4.3
#06	2.1	9.2	3.1	1.7	3.8	3.4	3.8	4.0	4.6	6.2	12.5	6.9	14.2	14.4
#07	2.0	1.5	2.3	1.2	2.1	2.2	2.5	2.5	3.8	2.1	6.9	5.4	7.5	10.7
#08	2.2	1.7	2.8	2.1	2.5	2.4	3.5	3.5	3.6	3.5	12.2	6.2	13.2	12.5
#09	2.1	1.4	2.9	2.0	2.2	3.5	2.8	3.5	3.5	3.8	5.2	4.7	10.3	7.4
#10	1.6	1.9	2.4	1.8	2.0	1.9	3.0	1.9	3.1	3.4	3.6	4.7	8.0	11.2
#11	2.5	2.0	3.2	2.7	3.0	2.7	3.5	2.9	3.1	3.1	6.7	4.3	5.8	4.3
#12	1.7	2.0	1.9	2.0	2.2	2.0	3.1	1.5	2.3	2.3	2.9	2.8	3.4	3.6

Hamster temperature and activity adaptation

Supplementary Table 6: Activity values per time frame, week in long photoperiod (LP) and short photoperiod (SP) as well as individual of approach 2. Yellow marked hamsters did not express spontaneous daily torpor. Sparklines in the last column indicate the individual change, with the hamster's highest value as 100% and its lowest as 0%.

	activity [cpm], total													
	LP	SP01	SP02	SP03	SP04	SP05	SP06	SP07	SP08	SP09	SP10	SP11	SP12	SP13
#01	6	4	7	9	6	9	6	8	6	7	6	9	5	4
#02	28	18	12	12	12	11	13	13	13	10	13	13	12	11
#03	5	4	3	3	3	3	3	3	3	4	3	5	3	3
#05	13	10	13	10	9	9	10	10	8	8	7	7	3	6
#06	7	9	10	8	13	11	12	16	12	12	12	11	4	7
#07	5	8	7	6	6	6	5	5	6	6	4	5	4	4
#08	14	8	9	7	7	8	9	8	7	9	7	9	8	10
#09	13	12	9	11	9	10	6	11	6	7	7	8	6	10
#10	2	3	3	4	4	4	4	3	3	4	4	4	3	3
#11	2	2	3	2	3	4	3	3	4	3	3	3	4	3
#12	6	9	7	6	6	5	6	6	6	6	5	5	3	4
	activity [cpm], scotophase													
	LP	SP01	SP02	SP03	SP04	SP05	SP06	SP07	SP08	SP09	SP10	SP11	SP12	SP13
#01	14	6	10	12	8	11	7	10	7	9	7	11	7	5
#02	79	25	17	17	16	15	19	18	18	13	18	19	16	16
#03	10	5	4	4	3	4	4	4	4	4	4	5	4	4
#05	33	14	18	14	12	10	13	11	9	10	8	7	4	7
#06	16	13	13	11	15	10	11	9	8	7	8	8	3	5
#07	12	10	9	8	8	7	6	6	7	7	5	7	5	5
#08	39	11	12	10	10	11	13	11	9	12	9	10	9	12
#09	32	16	11	14	11	11	7	11	7	8	7	9	6	10
#10	5	4	4	5	5	5	4	4	4	4	4	4	3	4
#11	3	3	3	3	3	5	3	4	4	4	3	3	4	4
#12	13	12	9	8	8	7	7	8	7	8	7	6	4	4
	activity [cpm], photophase													
	LP	SP01	SP02	SP03	SP04	SP05	SP06	SP07	SP08	SP09	SP10	SP11	SP12	SP13
#01	2	1	3	4	3	4	2	3	3	3	2	4	3	2
#02	3	3	2	2	3	3	2	3	4	4	3	3	2	3
#03	2	2	1	1	2	2	2	2	2	2	2	3	2	2
#05	3	4	3	3	3	7	5	8	5	4	5	5	3	3
#06	2	3	3	3	10	11	15	31	20	21	19	16	6	11
#07	2	3	3	2	2	3	3	4	6	3	3	2	2	2
#08	1	2	1	1	2	2	2	3	2	2	3	8	6	7
#09	3	3	4	4	4	8	4	10	4	5	6	6	5	10
#10	1	2	2	2	3	3	3	2	3	5	4	2	2	2
#11	2	1	2	2	2	3	3	2	3	2	2	2	2	2
#12	2	2	2	2	3	2	3	3	4	2	2	2	3	3

Supplementary materials **Hamster temperature and activity adaptation**

Supplementary Table 7: Activity ratio values per time frame, week in long photoperiod (LP) and short photoperiod (SP) as well as individual of approach 2. Yellow marked hamsters did not express spontaneous daily torpor. Red color marks ratios above 1.0 indicating diurnal activity patterns (upper part) or higher activity during the second half of the scotophase (lower part). Sparklines in the last column indicate the individual change, with the hamster's highest value as 100% and its lowest as 0%. Second to first half of scotophase ratio was not raised for LP with a scotophase of eight hours.

	photo- to scotophase activity ratio														
	LP	SP01	SP02	SP03	SP04	SP05	SP06	SP07	SP08	SP09	SP10	SP11	SP12	SP13	
#01	0.1	0.2	0.3	0.4	0.4	0.4	0.3	0.3	0.4	0.3	0.3	0.4	0.4	0.3	
#02	0.0	0.1	0.1	0.1	0.2	0.2	0.1	0.2	0.2	0.3	0.2	0.2	0.2	0.2	
#03	0.2	0.4	0.4	0.4	0.4	0.5	0.5	0.5	0.4	0.5	0.5	0.6	0.6	0.4	
#05	0.1	0.3	0.1	0.2	0.3	0.7	0.3	0.7	0.6	0.4	0.6	0.7	0.7	0.5	
#06	0.1	0.2	0.2	0.3	0.7	1.1	1.3	3.4	2.6	3.1	2.3	2.2	2.0	2.1	
#07	0.2	0.3	0.3	0.3	0.3	0.5	0.5	0.6	0.8	0.5	0.7	0.3	0.5	0.4	
#08	0.0	0.2	0.1	0.1	0.2	0.2	0.2	0.3	0.3	0.2	0.3	0.9	0.7	0.6	
#09	0.1	0.2	0.4	0.3	0.3	0.7	0.6	0.9	0.7	0.6	0.9	0.6	0.9	1.0	
#10	0.3	0.5	0.6	0.4	0.5	0.7	0.7	0.6	0.8	1.0	0.8	0.5	0.5	0.5	
#11	0.5	0.4	0.7	0.6	0.7	0.6	0.9	0.6	0.7	0.5	0.7	0.7	0.6	0.5	
#12	0.1	0.2	0.2	0.2	0.3	0.3	0.4	0.3	0.5	0.3	0.3	0.4	0.9	0.6	
	second to first half of scotophase ratio														
	LP	SP01	SP02	SP03	SP04	SP05	SP06	SP07	SP08	SP09	SP10	SP11	SP12	SP13	
#01		8.3	5.3	2.4	2.5	2.1	1.6	1.1	0.9	0.7	0.8	0.7	0.5	0.7	
#02		0.7	0.4	0.4	0.4	0.5	0.3	0.2	0.5	0.7	0.4	0.5	0.6	0.5	
#03		0.9	0.5	0.6	0.5	0.6	0.5	0.7	0.6	0.7	0.9	0.7	0.7	1.0	
#05		0.5	0.2	0.5	0.5	0.8	0.7	0.5	0.6	0.6	0.5	0.9	0.5	0.4	
#06		0.5	0.4	0.3	0.5	0.4	0.4	0.5	0.3	0.5	0.3	0.5	0.6	0.5	
#07		0.7	0.4	0.4	0.4	0.7	0.8	0.6	0.9	1.3	0.9	0.8	0.7	1.0	
#08		0.6	0.7	0.6	0.6	0.8	0.5	0.8	0.5	0.3	0.6	0.7	0.8	0.6	
#09		1.7	0.8	0.4	0.5	0.5	0.3	0.3	0.4	0.3	0.7	0.6	0.4	0.3	
#10		0.6	0.5	0.5	0.5	0.6	0.6	0.6	0.6	0.7	0.7	0.9	0.6	0.8	
#11		0.7	0.8	0.8	0.7	0.8	1.0	0.9	0.5	0.6	0.5	0.5	0.4	0.5	
#12		0.6	0.5	0.4	0.4	0.6	0.4	0.6	0.6	0.7	0.8	0.6	0.5	0.8	

Supplementary Table 8: Adaptation parameter values per week in long photoperiod (LP) and short photoperiod (SP) as well as individual of approach 2. Yellow marked hamsters did not express spontaneous daily torpor. Sparklines in the last column indicate the individual change, with the hamster's highest value as 100% and its lowest as 0%.

	BM [g]	body mass change [%]												
	LP	SP01	SP02	SP03	SP04	SP05	SP06	SP07	SP08	SP09	SP10	SP11	SP12	terminal
#01	36.5	-4.1	-6.8	-2.2	1.4	1.4	-3.0	-5.8	-6.0	-7.9	-10.1	-12.1	-18.9	-19.2
#02	28.6	-12.2	-15.4	-11.9	-13.6	-13.6	-13.6	-9.1	-12.6	-9.1	-11.2	-7.7	-10.1	-11.5
#03	38.6	-4.1	-13.5	-13.2	-15.8	-16.8	-19.2	-22.8	-22.0	-21.0	-19.9	-18.1	-17.6	-16.1
#05	38.5	-5.5	-10.4	-16.1	-20.3	-21.8	-25.2	-30.9	-27.0	-28.3	-28.3	-27.8	-27.5	-28.8
#06	29.4	-2.7	0.0	-4.8	-17.7	-20.7	-18.7	-24.8	-20.1	-19.4	-16.7	-20.7	-23.1	-20.7
#07	39.5	-3.5	-9.1	-12.2	-15.9	-19.5	-24.3	-23.3	-25.8	-24.1	-23.8	-25.3	-27.1	-26.6
#08	23.3	-3.4	-3.9	-6.0	-4.3	-14.2	-9.4	-14.6	-15.5	-14.2	-8.6	-15.9	-18.5	-16.3
#09	30.4	-2.6	-8.9	-15.1	-16.8	-19.4	-20.7	-20.1	-20.1	-19.1	-23.0	-21.7	-27.0	-23.0
#10	32.0	-3.1	-8.8	-15.9	-16.3	-18.4	-17.8	-22.2	-25.6	-22.8	-24.7	-22.2	-25.9	-24.4
#11	29.0	-3.1	-8.3	-8.6	-10.3	-11.7	-16.6	-20.7	-17.9	-19.7	-17.9	-19.3	-19.7	-19.3
#12	34.1	-6.2	-8.8	-7.0	-6.7	-4.7	-5.6	-11.1	-12.9	-17.6	-16.7	-16.7	-21.1	-20.2
	fur index (1 - "summer" to 6 - "winter" fur)													
	LP	SP01	SP02	SP03	SP04	SP05	SP06	SP07	SP08	SP09	SP10	SP11	SP12	terminal
#01	1.0	1.0	1.0	1.0	1.0	1.5	1.5	1.5	1.5	2.0	2.5	3.0	3.0	3.0
#02	1.0	1.0	1.0	1.0	1.0	1.5	1.5	1.5	2.0	3.0	3.0	3.0	3.5	3.5
#03	1.0	1.0	1.0	1.0	1.5	2.5	2.5	3.0	3.5	4.0	4.0	4.0	4.0	4.0
#05	1.0	1.0	1.0	1.0	1.0	1.0	1.5	1.5	2.0	3.0	3.0	3.0	4.0	4.0
#06	1.0	1.0	1.0	1.0	1.0	1.0	1.5	2.0	3.0	3.0	3.5	3.5	4.0	4.0
#07	1.0	1.0	1.0	1.0	1.0	1.0	2.0	2.0	3.5	4.0	4.0	4.0	5.0	5.0
#08	1.0	1.0	1.0	1.0	1.0	1.0	1.0	1.0	1.0	1.0	2.0	3.0	3.0	3.0
#09	1.0	1.0	1.0	1.0	1.0	1.0	1.5	1.5	3.0	3.5	4.0	4.0	4.5	5.0
#10	1.0	1.0	1.0	1.0	1.5	2.0	2.0	2.5	3.5	4.0	4.0	4.0	5.0	5.0
#11	1.0	1.0	1.0	1.0	1.5	1.5	2.0	3.0	3.5	4.0	4.5	4.5	5.0	5.0
#12	1.0	1.0	1.0	1.0	1.0	1.0	1.0	1.5	2.0	2.0	2.0	2.0	2.0	2.0

Chapter 3

Comparative Transcriptomics of the Djungarian Hamster Hypothalamus during Short Photoperiod Acclimation and Spontaneous Torpor

Published as original research article on 11 December 2021 in FEBS Open Bio, doi: 10.1002/2211-5463.13350

Authors: Elena Haugg, Janus Borner, Victoria Diedrich, Annika Herwig

Edited by: Miguel De la Rosa, University of Seville, Spain

Copyright © 2021 The Authors. FEBS Open Bio published by John Wiley & Sons Ltd on behalf of Federation of European Biochemical Societies. This is an open access article under the terms of the Creative Commons Attribution License (CC BY 4.0, https://creativecommons.org/licenses/by/4.0/), which permits use, distribution and reproduction in any medium, provided the original work is properly cited.

3.1 Main Document

Check for updates

FEBS openbio

FEBS PRESS science publishing by scientists

Comparative transcriptomics of the Djungarian hamster hypothalamus during short photoperiod acclimation and spontaneous torpor

Elena Haugg[1], Janus Borner[2,3], Victoria Diedrich[1] and Annika Herwig[1]

1 Institute of Neurobiology, Ulm University, Germany
2 Institute of Evolutionary Ecology and Conservation Genomics, Ulm University, Germany
3 Sackler Institute for Comparative Genomics, American Museum of Natural History, New York, NY, USA

Keywords
RNA-Seq; gene expression; metabolism; hypothermia; Siberian hamster; *Phodopus sungorus*

Correspondence
E. Haugg, Institute of Neurobiology, Ulm University, Albert-Einstein-Allee 11, 89081 Ulm, Germany
E-mail: elena.haugg@uni-ulm.de

(Received 12 July 2021, revised 30 November 2021, accepted 10 December 2021)

doi:10.1002/2211-5463.13350

The energy-saving strategy of Djungarian hamsters (*Phodopus sungorus*, Cricetidae) to overcome harsh environmental conditions comprises of behavioral, morphological, and physiological adjustments, including spontaneous daily torpor, a metabolic downstate. These acclimatizations are triggered by short photoperiod and orchestrated by the hypothalamus. Key mechanisms of long-term photoperiodic acclimatizations have partly been described, but specific mechanisms that acutely control torpor remain incomplete. Here, we performed comparative transcriptome analysis on hypothalamus of normometabolic hamsters in their summer- and winter-like state to enable us to identify changes in gene expression during photoperiodic acclimations. Comparing nontorpid and torpid hamsters may also be able to pin down mechanisms relevant for torpor control. A *de novo* assembled transcriptome of the hypothalamus was generated from hamsters acclimated to long photoperiod or to short photoperiod. The hamsters were sampled either during long photoperiod normothermia, short photoperiod normothermia, or short photoperiod-induced spontaneous torpor with a body temperature of 24.6 ± 1.0 °C, or. The mRNA-seq analysis revealed that 32 and 759 genes were differentially expressed during photoperiod or torpor, respectively. Biological processes were not enriched during photoperiodic acclimatization but were during torpor, where transcriptional and metabolic processes were reinforced. Most extremely regulated genes (those genes with $|\log2(FC)| > 2.0$ and padj < 0.05 of a pairwise group comparison) underpinned the role of known key players in photoperiodic comparison, but these genes exhibit adaptive and protective adjustments during torpor. Targeted analyses of genes from potentially involved hypothalamic systems identified gene regulation of previously described torpor-relevant systems and a potential involvement of glucose transport.

Djungarian hamsters (*Phodopus sungorus*, Cricetidae) are photoperiodic mammals [1,2]. In summer or summer-like long photoperiod (LP; e.g., 16:8 light:darkness), they have a high body mass, body temperature, and activity level. They are reproductively active and camouflaged to their environment by a light

Abbreviations
HT, hypothermia; log2(FC), logarithm of fold change to the base 2; LP, summer-like long photoperiod; NT, normothermia; padj, adjusted ?*P*-value; SP, winter-like short photoperiod; Tb, core body temperature; ZT, *Zeitgeber-time*.

FEBS Open Bio (2021) © 2021 The Authors. *FEBS Open Bio* published by John Wiley & Sons Ltd on behalf of Federation of European Biochemical Societies.
This is an open access article under the terms of the Creative Commons Attribution License, which permits use, distribution and reproduction in any medium, provided the original work is properly cited.

brown fur. As soon as photophase decreases below 13 h of light per day during autumn in the field [3], or after a transfer to winter-like short photoperiod in captivity (SP; e.g., 8:16 light:darkness), the hamsters reduce body temperature, activity during scotophase, food intake, and body mass. They recede their gonads and stop to reproduce. They grow a dense white winter fur which improves insulation capacity [4–6]. The manifestation of these acclimation parameters is highly individual and therefore variable within a cohort [6].

After about ten weeks of short photoperiod exposure, the individual acclimation reaches a certain threshold. 75% of hamsters start to express spontaneous daily torpor, even at 20 °C ambient temperature with food and water *ad libitum* [6]. Torpor is characterized by a precisely regulated natural reduction of metabolism resulting in a body temperature decrease below normothermic values, so-called hypothermia [7], for several hours during photophase [8]. On average, torpor is expressed on two days of a representative week. However, torpor behavior is highly individual [6].

Morphological, behavioral, and physiological acclimatizations to environmental cues such as day length are elements of a complex energy-saving strategy that is orchestrated within the hypothalamus by the photoperiodic neuroendocrine system including the suprachiasmatic nucleus, the endogenous mammalian photic, and circadian pacemaker [9–11]. The underlying regulatory mechanisms of photoperiod-controlled adjustments of body mass and reproduction in *Phodopus* have been extensively studied and were recently reviewed [12]. They involve gene expression changes in the thyroid system via the *Pars tuberalis* of the pituitary gland, in energy metabolism, mediated by glucose-sensitive tanycytes lining the third ventricle, and in the signaling of hypothalamic neurons sensitive, for example, *POMC, NPY, AGRP,* and *CARTPT,* which drive orexigenic and anorexigenic physiological responses [13,14]. Since the expression of torpor is dependent on signaling of various hormonal systems changing with photoperiodic as well as nutritional state and circadian rhythm, it can be assumed that the hypothalamus is also involved in its proximate control. Although several hypothalamic systems are likely to regulate torpor, gene expression studies using either whole transcriptome approaches or targeted gene expression analyses could not yet nail down specific mechanisms [15,16].

In a previous NGS approach, we tried to identify signaling mechanisms within the hamsters' hypothalamus during torpor entrance [17]. However, the data revealed general molecular adjustments likely maintaining functional integrity, rather than signaling mechanisms. It is unclear which thresholds are applicable to pin down physiologically relevant genes. In general, transcriptome analyses in a nonmodel organism such as the Djungarian hamster are challenging given the lack of both an annotated reference genome and standardized, adequate bioinformatical as well as statistical pipelines [17,18]. In the present study, we used the hamsters as physiology-based model organism for seasonal acclimation and torpor research, in which some of the underlying hypothalamic signaling mechanisms have already been disentangled. We sequenced hypothalami of summer-like long photoperiod- and winter-like short photoperiod-acclimated hamsters in their normothermic state, as well as of short photoperiod-acclimated hamsters during torpor. With this data set, we tried to define parameters allowing us to confirm already known gene expression changes in a photoperiodic context. We assumed that the applied methods would also identify genes that are likely to have biological relevance in hypothalamic torpor control. Despite enrichment analyses and most extremely regulated genes, we specifically screened for indicator genes that were preselected from hypothalamic systems potentially involved in torpor control, such as the circadian system, thyroid system, growth axis, and metabolic energy balance. [12]

Materials and methods

Breeding and housing

Twelve Djungarian hamsters *(Phodopus sungorus)* were bred in 2019 according to an outbred crossing scheme in the indoor breeding colony at the Institute of Neurobiology (Ulm University, Germany) in accordance with the local ethics committee (35/9185.46-3). Ambient temperature was maintained at 20 ± 1 °C. Artificial light (150 lux) was provided 16 h per day in summer-like long photoperiod (LP). Additional constant red light (< 5 lux) enabled animal handling during the scotophase. Tap water and food (Altromin hamster breeding diet 7014, Lage, Germany) were provided *ad libitum*, supplemented by cucumber, oat flakes, and sunflower seeds once a week. Adult hamsters were single housed in Makrolon Type III cages (26.5 × 42.5 × 18.0 cm) with wooden bedding and tissue as nesting material.

Radiotelemetry

To assess spontaneous torpor expression, the core body temperature (Tb) was monitored in real time in a resolution of 3 min using a radiotelemetry system with DataQuest™ ARTBRONZE software (DSI—Data Sciences International, Harvard Bioscience Inc., St. Paul, MN, USA). A receiver board (RPC1) was positioned under each individual home cage. A transmitter (model TA-11TA-F10, silicone-coated, 1.1 cc volume, 1.6 g weight, 0.15 °C accuracy) was implanted intraperitoneally under isoflurane anesthesia

FEBS Open Bio (2021) © 2021 The Authors. *FEBS Open Bio* published by John Wiley & Sons Ltd on behalf of Federation of European Biochemical Societies.

(2.5% and 1 mL·min^{-1} for induction, 0.75 to 2.0% and 0.4 mL·min^{-1} for maintenance) and carprofen analgesia (5 mg·kg^{-1} i.p. Rimadyl®, Zoetis Deutschland GmbH, Berlin). Recovery from surgery was supported by additional oat flakes, sunflower seeds, cucumber, and nesting material. Body mass, fur care, posture, and behavior were monitored daily for about seven days until recovery. Experimental and surgical procedures were approved by the Regierungspräsidium Tübingen, Germany (1411). Radiotelemetry data of hamsters were analyzed previously [6].

Key data of hamsters

Four of the twelve hamsters remained in LP, had an initial body mass of 33 ± 4 g, and were not implanted with DSI transmitters. They were sacrificed with a body mass of 34 ± 4 g at an age of 30 ± 1 weeks. Eight of the twelve hamsters were transferred to winter-like short photoperiod (SP) with 8 h of light per day at an age of 17 ± 3 weeks, were implanted with DSI transmitters at an age of 29 ± 2 weeks, and sacrificed two to eight weeks later at an age of 33 ± 4 weeks. During the 16 ± 2 weeks of SP acclimation, they reduced their body mass by 21 ± 13% to 27 ± 2 g. Background information on each hamster is provided (Table S1).

Sampling scheme

All twelve hamsters were sacrificed 4 h after the beginning of the photophase at approximately ZT04 (Fig. 1) in three sampling groups: either SP-hypothermic at the nadir of torpor (SP-HT, n = 4, three males, one female, Tb = 24.6 ± 1.0 °C), SP-normothermic (SP-NT, n = 4, two males, two females, Tb = 35.3 ± 0.3 °C), or LP-normothermic (LP-NT, n = 4, two males, two females, not implanted). Before sampling, all SP-acclimated hamsters had expressed at least one torpor bout (Table S1). Spontaneous daily torpor was defined as a core body temperature below 32 °C for at least 30 min [16,19,20]. The body temperature patterns of the last day and the day before are provided (Fig. S1). All hamsters were sacrificed with carbon dioxide. The circulatory system was perfused transcardially with 0.1 M sterile PBS (pH = 7.42). To reduce the number of laboratory animals, the hamsters were dedicated to several studies on other organs taken after decapitation (unpublished data).

Dissection of hypothalamus

The brain was quickly removed, shock frozen on dry ice, and stored at −80 °C. For further processing, the brains were trimmed in a cryochamber of −17 °C with a razor blade. The hypothalamus was clearly visible as a central elevation on the ventral side of the brain expanding from Bregma 0.38 mm to −2.80 mm (according to the mouse brain atlas [21]). The hypothalamus was first trimmed to a tissue cuboid cutting from ventral to dorsal. To remove the thalamus and the cortex, brains were cut from anterior to posterior directly on the anterior part of the anterior commissure, visible as most ventral bilateral white matter. Edges of the tissue cuboid were removed cutting from ventral to dorsal to resemble the cylindric shape of the hypothalamus.

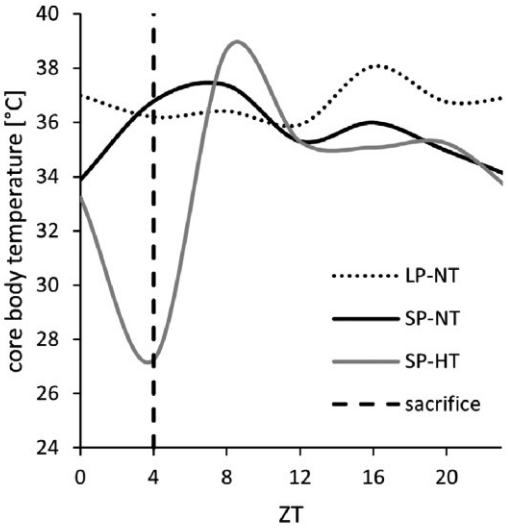

Fig. 1. Exemplary core body temperature patterns. Raw data measured in intervals of 3 min were processed to mean body temperature per hour and displayed in intervals of 4 h. The hamsters of this study were sacrificed around ZT04 (vertical line). Individual core body temperature patterns of SP-acclimated hamsters are attached in Fig. S1. LP-acclimated hamsters of this study were not implanted. Plotted data were derived from another studies' hamster which was monitored in LP as well as SP with food and water *ad libitum* at 20 °C ambient temperature [6].

Purification of total RNA, isolation, and sequencing of mRNA

Hypothalamic tissue was homogenized in 100 µL buffer RLT with beta-ME using prefilled 2-mL beadbug tubes containing Zirconium beads (Biozym Scientific GmbH, Oldendorff, Germany) on a microtube homogenizer (D1030-E, Benchmark Scientific Inc., Sayreville, NJ, USA). Purification of total RNA was performed using the RNeasy Midi Kit (Qiagen GmbH, Hilden, Germany). The concentration of total RNA ranged between 15 and 86 ng·µL^{-1} (56 ± 23 ng·µL^{-1}; NanoDrop 2000 spectrophotometer, Thermo Fisher Scientific GmbH, Dreieich, Germany). For further processing, the samples were sent to StarSEQ GmbH, Mainz, Germany. The RNA integrity number (RIN) varied between 7.8 and 9.5 (8.5 ± 0.5). The rRNA

FEBS Open Bio (2021) © 2021 The Authors. *FEBS Open Bio* published by John Wiley & Sons Ltd on behalf of Federation of European Biochemical Societies.

ratio [28 s/18 s] varied between 1.4 and 1.8 (1.7 ± 0.1). The mRNA was isolated and the library prepared (NEBNext® Ultra™ II directional, dual index RNA). RNA-Seq was performed in 2020 on an Illumina NextSeq 500 (1 lane, 50 mio paired end reads, 2 × 25 mio reads, 2 × 150 nt, 7.5 gb).

Bioinformatics

Bioinformatics were performed on the bwForCluster NEMO of the Baden-Württemberg High Performance Computing (bwHPC) project. After quality control of each fastq file using FastQC 0.11.9 [22], on average, 32,717,097 read pairs per sample (Table S2) were processed in several steps. Data of each sample were prepared with trim-galore 0.6.6 [23]. In total, 392,605,160 read pairs from all samples were pooled to generate a single *de novo* transcriptome assembly containing 868,657 transcripts using Trinity 2.8.5 [24,25]. The transcripts were mapped against the reference proteome of *Mus musculus* (GRCm39, Annotation Release 109) using blastx 2.5.0+ with an e-value < 1E-5 [26,27]. In total, 171,923 transcripts of the hamster assembly were successfully mapped against the reference. A reduced assembly containing only transcripts with a hit against a mouse protein was generated using 'extract_hits_from_fasta.rb'. A transcript-to-GeneID dictionary was generated based on the best hit to the mouse proteome by using 'hits_to_genemap.rb'. The reads from each sample were then mapped back to the reduced assembly using bowtie 1.3.0 [28]. The non-normalized differential gene expression was calculated for each sample using rsem 1.3.1 [29].

Data depositories and supplied scripts

The raw Illumina data have been deposited at the NCBI Sequence Read Archive under SRA Study accession number SRP326941 within the Bioproject PRJNA743775. Both, the original and the processed *de novo* assembly and the non-normalized gene expression have been deposited in NCBI's Gene Expression Omnibus [30]. These data are accessible through GEO Series accession number GSE179663 (https://www.ncbi.nlm.nih.gov/geo/query/acc.cgi?acc=GSE179663). An overview of accession numbers within SRA and GEO is attached as Table S2. The data processing pipeline from raw Illumina data to non-normalized gene expression are attached as Doc S2. Both ruby-scripts were uploaded to SourceForge (https://sourceforge.net/projects/prepare-transcript-to-gene-map/). The R-script with R-session info is attached as Doc S3.

Statistics

Statistics and principal component analysis were performed in RStudio 3.5.2 [31,32] using DESeq2 [33–35]. Data were normalized across all samples of a pairwise group comparison to level methodical bias. In this study, two pairwise group comparisons were conducted: NT: SP vs LP to reveal photoperiod-driven differential gene expression of normothermic Djungarian hamsters, and SP: HT vs NT to detect torpor-driven differential gene expression of SP-acclimated Djungarian hamsters. Processing and graphical representation of normalized data was performed with Microsoft Excel (Office 365, 2016).

Data interpretation

Data analysis was based on the numerical GeneID. One GeneID includes all isoforms, precursors, and preproproteins. Per gene present with at least ten counts in a pairwise group comparison, the averaged count per group was compared with the averaged count of the other group, resulting in the gene's fold change, provided as log2(FC), and the significance of this fold change (adjusted *P*-value, padj). A negative fold change indicates a downregulated gene, a positive fold change an upregulated gene. A log2(FC) of −1 indicates half the expression in the first-named compared with the second-named group of a pairwise comparison, while a log2(FC) of 1 indicates a doubled expression, a log2(FC) of 2 a quadrupled expression, etc.

Gene expression profiling

Several analyses were used in this study to pin down the most relevant data. The principal component analysis (Fig. 2) visualizes the distance between each sample of this study by their respective overall gene expression. The volcano plots for each pairwise group comparison (Fig. 3) visualize each genes' fold change dependent on its significance. In this study, differentially expressed genes were defined as statistically significant with a padj < 0.05 and any fold change. Highly statistically significant differentially expressed genes were stated as padj < 0.001.

GO enrichment analysis

A GO enrichment analysis for each pairwise group comparison was performed to identify biological processes that are under regulation. The differentially expressed genes with padj < 0.05 were tested. All present genes with any padj-value served as background to create the baseline of expectable regulation of biological processes. Data were analyzed using the PANTHER Overrepresentation Test (Released 20210224) based on the GO Ontology database (https://doi.org/10.5281/zenodo.4495804 Released 20210201), with Fisher's exact as test type and false discovery rate correction. (PANTHER-tool via http://geneontology.org/) [36–38]. The genes' fold change was irrelevant for this test.

FEBS Open Bio (2021) © 2021 The Authors. *FEBS Open Bio* published by John Wiley & Sons Ltd on behalf of Federation of European Biochemical Societies.

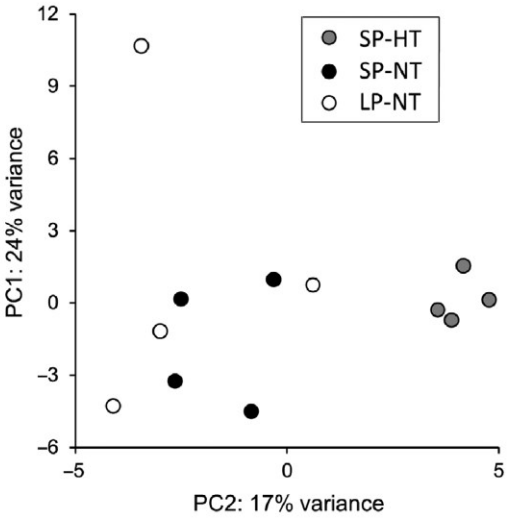

Fig. 2. Principal component analysis. Differences in gene expression profiles of samples and sampling groups in the first two dimensions. The closer two dots, the more similar the gene expression profiles of two samples.

Most extremely regulated genes

In addition to the threshold of significance, padj < 0.05, a threshold for the fold change, |log2(FC)| > 2, was applied to detect the most extremely regulated genes in the pairwise group comparisons.

Indicator genes

As reviewed earlier, several hypothalamic systems including the circadian clock system, thyroid system, growth axis, and energy metabolism are of relevance in photoperiodic acclimation and/or orchestration of torpor [12]. Here, we specifically screened for differential expression of genes relevant to these systems in each pairwise group comparison. Immediate early genes of the Fos/Jun family were screened as representatives of transcriptional activity [39–41]. Our list of preselected indicator genes was extended to additional gene products and their receptors according to their annotation of biological function in the systems of interest according to AmiGO 2 (http://amigo.geneontology.org/amigo/search/annotation, 17.09.2021) and search in the UniProt knowledge base (https://www.uniprot.org/), again using *Mus musculus* as reference. The 68 preselected indicator genes are introduced in Table 1.

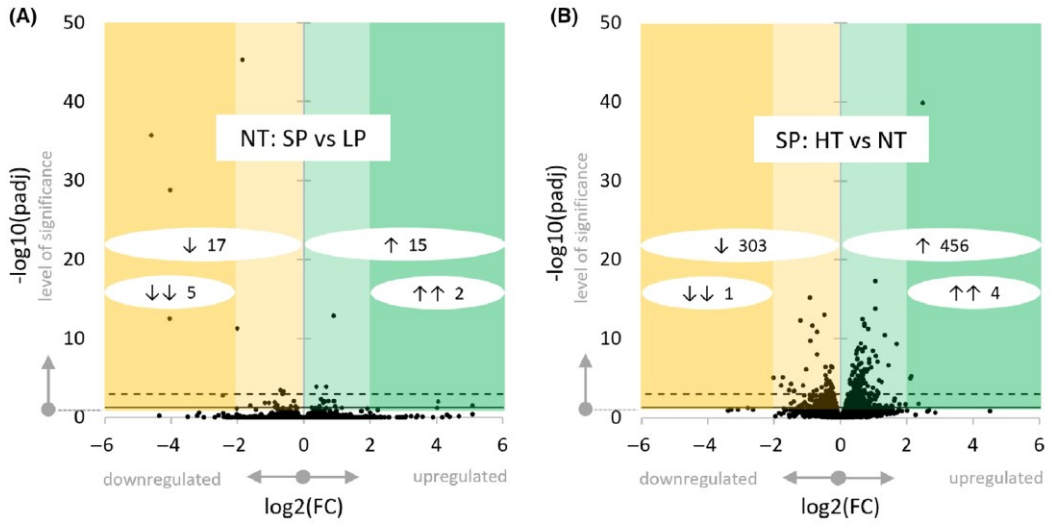

Fig. 3. Volcano plots. Differential gene expression for the NT: SP vs LP comparison (A) and the SP: HT vs NT comparison (B). All mapped genes (dots) are represented by fold change (x-axis) in dependence on significance (y-axis). Differentially expressed genes are shown in the colored areas above the horizontal significance threshold (black line, −log10(0.05) = 1.3). Genes indicated with padj < 0.001 throughout this study are shown above the dotted line (−log10(0.001) = 3.0). The numbers of regulated genes per area are indicated (white circles expanding over the fold change values covered, with ↓↓ extremely downregulated in dark yellow area, ↓ downregulated in yellow area, ↑ upregulated in green area, ↑↑ extremely upregulated in dark green area).

FEBS Open Bio (2021) © 2021 The Authors. *FEBS Open Bio* published by John Wiley & Sons Ltd on behalf of Federation of European Biochemical Societies.

Table 1. The 68 preselected indicator genes. Genes of several key systems with potential regulatory function in torpor expression and photoperiodic status were screened for differential gene expression.

System	#	Gene	Gene product
Transcription	1 + 2	*Fos* + *Fosb*	Proto-oncogene c-fos + protein fosb
	3 + 4 + 5	*Jun* + *Junb* + *Jund*	Transcription factor ap-1 / c-jun + jun-b + jun-d
	6 + 7	*c-Jun1* + *c-Jun3*	c-jun-amino-terminal kinase-interacting protein 1 + 3
Clock	8	*Avp*	Vasopressin-neurophysin 2-copeptin
	9	*Avpr1a*	Vasopressin v1a receptor
	10 + 11	*Bmal1* + *Bmal2*	Brain and muscle arnt-like 1 + 2
	12	*Bhlhe40*	Class e basic helix-loop-helix protein 40
	13	*Clock*	Circadian locomoter output cycles protein kaput
	14 + 15	*Cry1* + *Cry2*	Cryptochrome 1 + 2
	16	*Gpr50*	Melatonin-related receptor
	17	*Id2*	DNA-binding protein inhibitor id-2
	18	*Mta1*	Metastasis-associated protein mta1
	19 + 20	*Mtnr1a* + *Mtnr1b*	Melatonin receptor type 1a + 1b
	21 + 22 + 23	*Per1* + *Per2* + *Per3*	Period circadian protein homolog 1 + 2 + 3
	24	*Pml*	Protein pml
	25	*Ppp1cc*	Serine/threonine–protein phosphatase
	26	*Timeless*	Protein timeless homolog
	27	*Vip*	Vasoactive intestinal peptide
Thyroid	28 + 29	*Dio1* + *Dio2*	Iodothyronine deiodinase type i + ii
	30	*Dio3*	Thyroxine 5-deiodinase
	31	*Mct8*	Monocarboxylate transporter 8
	32 + 33	*Thra* + *Thrb*	Thyroid hormone receptor alpha + beta
	34	*Trh*	Pro-thyrotropin-releasing hormone
	35 + 36	*Trhr* + *Trhr2*	Thyrotropin-releasing hormone receptor 1 + 2
	37	*Tshr*	Thyrotropin receptor
	38	*Txnip*	Thioredoxin-interacting protein
Growth	39	*GH*	Somatotropin / growth hormone
	40	*Sst*	Somatostatin
	41 - 45	*Sstr1 - Sstr5*	Somatostatin receptor type 1 - 5
Metabolism	46 + 47	*Tas1r3* + *Tas1r2*	Taste receptor type 1 member 3 + 2
	48	*Glut1*	Glucose transporter member 1
	49 - 52	*Glut3 - 6*	Glucose transporter member 3 - 6
	53	*P2ry1*	P2y purinoceptor 1
	54	*Fgfr1*	Fibroblast growth factor receptor 1
	55	*Insr*	Insulin receptor
	56	*Lepr*	Leptin receptor
	57	*Agrp*	Agouti-related protein
	58	*Cartpt*	Cocaine- and amphetamine-regulated transcript protein
	59	*Pomc*	Pro-opiomelanocortin
	60 + 61	*Mc3r* + *Mc4r*	Melanocortin receptor 3 + 4
	62	*Npy*	Pro-neuropeptide y
	63 + 64	*Npy1r* + *Npy2r*	Neuropeptide y receptor type 1 + 2
	65	*Qrfp*	Orexigenic neuropeptide qrfp
	66	*Qrfpr*	Pyroglutamylated rf-amide peptide receptor
	67	*Ncam1*	Neural cell adhesion molecule 1
	68	*Vim*	Vimentin, cytosceleton of glial cells

Results

To validate known mechanisms of photoperiodic acclimation and to generate hypotheses of underlying mechanisms of spontaneous torpor control, this study analyzed hypothalamic mRNA-Seq data gained from LP-acclimated normothermic, SP-acclimated normothermic, and SP-acclimated hypothermic Djungarian hamsters.

Gene expression profiles

The *de novo* transcriptome assembly with 392,605,160 read pairs (Table S2) gained from 12 hypothalamic

FEBS Open Bio (2021) © 2021 The Authors. *FEBS Open Bio* published by John Wiley & Sons Ltd on behalf of Federation of European Biochemical Societies.

samples had on average 32,717,097 read pairs per sample. 171,923 transcripts of 868,657 transcripts in total were successfully mapped against more than 16.000 annotated genes of the reference *Mus musculus*.

A principal component analysis was conducted to describe the distance of each samples' overall gene expression profile (Fig. 2). Samples were tightly clustered within the hypothermic SP-acclimated group, less clustered within the normothermic SP-acclimated group, and most diverse within the normothermic LP-acclimated group. In the first dimension, the samples of the normothermic SP-acclimated group scattered less than the samples of the normothermic LP-acclimated group. In the second dimension, the gene expression profiles of the hypothermic group differed from the two normothermic groups, regardless of the photoperiodic acclimation.

The three sampling groups were used in two pairwise group comparisons: NT: SP vs LP to describe transcriptomic differences driven by photoperiod and SP: HT vs NT to unravel torpor-driven differential gene expression. In the photoperiodic comparison (NT: SP vs LP), 32 of 16,199 genes (0.2%) reached the level of significance, whereas 759 of 16,195 genes, (4.7%) were significantly regulated during torpor (SP: HT vs NT).

The graphical representation of differential gene expression revealed few regulated genes with high fold changes between photoperiods (NT: SP vs LP; Fig. 3A) and many regulated genes with a mainly moderate fold change during torpor (SP: HT vs NT; Fig. 3B). While 15 genes were upregulated and 17 genes downregulated between photoperiods, the data show a torpor-driven upregulation of 456 and downregulation of 303 genes within the hypothalamus.

GO enrichment analysis

The photoperiodic comparison (NT: SP vs LP) revealed no enriched biological processes. During torpor (SP: HT vs NT), transcriptional, biosynthetic, cellular, and metabolic processes were enriched (Table 2). Listed are GO terms of those biological processes found to be regulated by less or more genes with padj < 0.05 than expected using all present genes as background.

Most extremely regulated genes

Within the predefined thresholds padj < 0.05 and |log2 (FC)| > 2.0 (Table 3), seven genes were regulated by

Table 2. GO enrichment analysis. Data basis is the SP: HT vs NT comparison. Regulated genes with padj < 0.05 were tested, while all present genes were used as background. Listed are GO terms of those biological processes found to be regulated by less or more genes than expected using a false discovery rate (FDR) < 0.05.

	Reference		Test				
Go biological process complete	GO term	Hits		Expected	Fold enrich	Raw *P*-value	FDR
Total		15604	748	-	-	-	-
Regulation of gene expression	GO:0010468	3855	258	185	1.4	6.42E-09	3.30E-05
Regulation of nucleic acid-templated transcription	GO:1903506	2698	192	129	1.5	2.50E-08	4.80E-05
Regulation of transcription dna-templated	GO:0006355	2694	192	129	1.5	1.87E-08	4.12E-05
Regulation of transcription by rna polymerase ii	GO:0006357	2054	140	98	1.4	2.87E-05	2.46E-02
Regulation of biosynthetic process	GO:0009889	3364	223	161	1.4	2.90E-07	3.44E-04
Regulation of rna biosynthetic process	GO:2001141	2701	192	129	1.5	2.53E-08	4.33E-05
Regulation of macromolecule biosynthetic process	GO:0010556	3149	218	151	1.4	1.40E-08	4.31E-05
Regulation of cellular biosynthetic process	GO:0031326	3293	220	158	1.4	1.85E-07	2.59E-04
Regulation of cellular macromolecule biosynthetic process	GO:2000112	3115	216	149	1.5	1.60E-08	4.12E-05
Regulation of cellular process	GO:0050794	8801	486	422	1.2	3.25E-06	3.13E-03
Regulation of cellular metabolic process	GO:0031323	4981	304	239	1.3	9.95E-07	1.02E-03
Cellular macromolecule metabolic process	GO:0044260	3655	225	175	1.3	4.98E-05	4.04E-02
Negative regulation of macromolecule metabolic process	GO:0010605	2333	156	112	1.4	2.33E-05	2.11E-02
Regulation of macromolecule metabolic process	GO:0060255	5077	320	243	1.3	1.14E-08	4.37E-05
Regulation of metabolic process	GO:0019222	5534	336	265	1.3	2.41E-07	3.09E-04
Regulation of nitrogen compound metabolic process	GO:0051171	4615	290	221	1.3	1.59E-07	2.44E-04
Regulation of nucleobase-containing compound metabolic process	GO:0019219	3168	222	152	1.5	2.93E-09	2.26E-05
Regulation of primary metabolic process	GO:0080090	4781	297	229	1.3	3.20E-07	3.52E-04
Regulation of rna metabolic process	GO:0051252	2936	211	141	1.5	1.33E-09	2.05E-05

FEBS Open Bio (2021) © 2021 The Authors. *FEBS Open Bio* published by John Wiley & Sons Ltd on behalf of Federation of European Biochemical Societies.

photoperiod (NT: SP vs LP) and five by torpor (SP: HT vs NT). In SP-normothermia compared to LP-normothermia (NT: SP vs LP), thyroxine 5-deiodinase (*Dio3*) and chondroitin sulfate proteoglycan 4B (*Cspg4b*) were upregulated, while five genes were downregulated, namely lecithin retinol acyltransferase (*Lrat*), anaphase-promoting complex subunit CDC26 (*Cdc26*), pro-FMRFamide-related neuropeptide VF (*Npvf*), thyrotropin subunit beta (*Tshb*), and glycoprotein hormones alpha chain (*Cga*). Four genes were upregulated in SP-hypothermia compared with SP-normothermia (SP: HT vs NT), namely RNA-binding protein 3-like (*Rbm3-ps*), grainyhead-like protein 2 homolog (*Grhl2*), adipolin (*C1qtnf12*), and short coiled-coil protein-like (*Gm16500*), while egl nine homolog 1 (*Egln1*) was downregulated.

Indicator genes

Among the indicator genes, thyroxine 5-deiodinase (*Dio3*) and period circadian protein homolog (*Per3*) were upregulated in SP-normothermia compared with LP-normothermia (NT: SP vs LP), while pro-opiomelanocortin (*Pomc*) and melatonin-related receptor (*Gpr50*) were downregulated. With a −log10(-padj) of 45.3, *Gpr50* had the highest significance among all other regulated genes of this study. In SP-hypothermia compared with SP-normothermia (SP: HT vs NT), somatostatin receptor type 1 (*Sstr1*), glucose transporter member 3 (*Slc2a3* / *Glut3*), and protein PML (*Pml*) were upregulated, whereas transcription factor AP-1 (*Jun*), c-Jun-amino-terminal kinase-interacting protein 1 (*Mapk8ip1* / *c-Jun1*), class E basic helix-loop-helix protein 40 (*Bhlhe40*), and serine/threonine–protein phosphatase PP1-gamma catalytic subunit (*Ppp1cc*) were downregulated.

Some indicator genes were not present in the hypothalamic mRNA-Seq data of the Djungarian hamster, namely melatonin receptor type 1B (*Mtnr1b*), and taste receptor type 1 member 2 (*Tas1r2*). Somatotropin / growth hormone (*GH*) had outlying values in NT: SP vs LP and was not present in SP: HT vs NT. All 68 predefined indicator genes are listed (Table 1). The significantly regulated indicator genes are presented (Table 4). The results of all indicator genes are provided in the supplementary material (Table S3).

Table 3. Most extremely regulated genes. All genes with padj < 0.05 and |log2(FC)| > 2.0 for both pairwise group comparisons are listed. A negative log2(FC) indicates downregulation, a positive log2(FC) upregulation relative to the respective baseline (LP-NT for photoperiodic comparison and SP-NT for torpor comparison).

	padj	log2(FC)	Gene	Gene product
NT: SP vs LP	0.038	5.1	*Dio3*	Thyroxine 5-deiodinase
	0.010	4.1	*Cspg4b*	Chondroitin sulfate proteoglycan 4B
	< 0.001	−2.0	*Lrat*	Lecithin retinol acyltransferase
	0.002	−2.4	*Cdc26*	Anaphase-promoting complex subunit CDC26
	< 0.001	−4.0	*Npvf*	Pro-fmrfamide-related neuropeptide VF
	< 0.001	−4.0	*Tshb*	Thyrotropin subunit beta
	< 0.001	−4.6	*Cga*	Glycoprotein hormones alpha chain
SP: HT vs NT	< 0.001	2.5	*Rbm3-ps*	RNA-binding protein 3-like
	0.018	2.4	*Grhl2*	Grainyhead-like protein 2 homolog
	< 0.001	2.1	*C1qtnf12*	Adipolin
	< 0.001	2.1	*Gm16500*	Short coiled-coil protein-like
	< 0.001	−2.0	*Egln1*	Egl nine homolog 1

Table 4. Regulated indicator genes. Indicator genes with padj < 0.05 for each pairwise group comparison. The results of all 68 preselected indicator genes, as introduced in Table 1, are provided in Table S3. A negative log2(FC) indicates downregulation, a positive log2(FC) upregulation relative to the respective baseline (LP-NT for photoperiodic comparison and SP-NT for torpor comparison).

	padj	log2(FC)	Gene	Gene product
NT: SP vs LP	0.038	5.1	*Dio3*	Thyroxine 5-deiodinase
	< 0.001	0.7	*Per3*	Period circadian protein homolog 3
	0.015	−1.0	*Pomc*	Pro-opiomelanocortin
	< 0.001	−1.8	*Gpr50*	Melatonin-related receptor
SP: HT vs NT	0.013	0.3	*Sstr1*	Somatostatin receptor type 1
	0.043	0.2	*Glut3*	Glucose transporter member 3
	0.008	0.5	*Pml*	Protein PML
	< 0.001	−0.4	*Jun*	Transcription factor AP-1 / c-Jun
	0.041	−0.2	*c-Jun1*	c-Jun-amino-terminal kinase-interacting protein 1
	< 0.001	−0.5	*Bhlhe40*	Class E basic helix-loop-helix protein 40
	0.048	−0.1	*Ppp1cc*	Serine/threonine–protein phosphatase

FEBS Open Bio (2021) © 2021 The Authors. *FEBS Open Bio* published by John Wiley & Sons Ltd on behalf of Federation of European Biochemical Societies.

Discussion

Seasonal acclimatizations of Djungarian hamsters including the use of spontaneous torpor have been intensely studied. Key hypothalamic mechanisms of long-term acclimatizations in body mass and reproduction have been described. However, the proximate hypothalamic control of torpor episodes has remained rather unclear. Here, we analyzed hypothalamic transcriptomes of LP- and SP-acclimated normothermic as well as SP-acclimated torpid Djungarian hamsters to confirm existing knowledge from a photoperiodic context. We were assuming that the applied methods would also pin down relevant genes involved in torpor control.

Our approaches could well validate existing knowledge of photoperiodic gene expression changes in the hypothalamus, using a combination of indicator genes and those with most extreme regulation. Enrichment analyses failed to reveal enriched pathways due to short photoperiod exposure, suggesting that few very distinct changes maintain the photoperiodic response. During torpor however, many biological processes were enriched. This is likely reflecting mechanisms of the brain to compensate for the severely suppressed metabolism and decreased body temperature to maintain functional integrity. These supposedly adaptive mechanisms were also reflected in the most extremely regulated genes. Within the more hypothesis-driven analysis of indicator genes, we found few differentially expressed genes with regulatory potential. Hence, although our applied methods are well able to detect gene expression changes relevant to regulate photoperiodic acclimation, distinct regulatory mechanisms might be overridden by vital overall adaptive mechanisms during torpor and are thus more difficult to pin down.

Effects of the body temperature difference between sampling groups

Overall, our analyses revealed a substantially lower number of genes regulated by photoperiod (32) than by torpor (759). There is evidence that the difference between the terminal body temperatures of two sampling groups affects the number of regulated genes.

In the present study, 32 genes were regulated by photoperiod using SP-acclimated hamsters which had expressed at least one torpor bout after sixteen weeks of acclimation (NT: SP vs LP). A previous study by Bao et al. also found 32 genes regulated by photoperiod using hamsters after eight weeks of acclimation to a 10:14 light:darkness SP-light regime [18], hence probably prior to torpor manifestation. In thirteen-lined ground squirrels that are obligate and seasonal hibernators with deep, multi-day torpor bouts, far more pronounced seasonal differences in gene expression were described (1206 genes in the summer vs. interbout normothermia comparison). These differences might result from species-specific differences in control mechanisms that might be more pronounced and hardwired in an obligate seasonal hibernator as opposed to a photoperiodic daily heterotherm [42].

Our present study showed 759 genes to be regulated during torpor at ZT04 (456 up, 303 down, proportion 6 : 4) with a body temperature difference of 10 °C (SP: HT vs NT). A previous study by Cubuk et al. [17] revealed 284 regulated genes during torpor entrance at ZT01 (181 up, 103 down, proportion 6 : 4) with a body temperature difference of about 6 °C [17]. It is reasonable to assume that the severe depression of metabolic rate, resulting in low body temperatures and thus high body temperature differences between the torpid and the nontorpid group (Fig. 1), leads to more severe gene expression changes as opposed to purely photoperiodic changes in metabolically active and normothermic animals (Fig. 2, Fig. 3). In thirteen-lined ground squirrels, comparable relationships between body temperature and number of differentially expressed genes were found during the hibernation season. Within the same seasonal state, only few hypothalamic genes were regulated between sampling groups with a small body temperature difference, whereas many genes were regulated between sampling groups with a large body temperature difference [42].

Direction of regulation and transcriptional activity

Especially in small endotherms, a metabolic downstate comes along with low body temperatures. Probable side effects are a slowed down transcription as well as post-transcriptional effects, such as prolongation of mRNA half-life or altered translation [43,44]. However, the proportion between up- and downregulated genes is high. In Djungarian hamster, the proportion is 6 : 4 in both torpor entry compared with SP-normothermia [17] and deep torpor compared with SP-normothermia (Fig. 3). In thirteen-lined ground squirrel, the proportion is 6 : 4 in torpor entrance vs. interbout normothermia and 7 : 3 in torpor arousal vs. interbout normothermia [42]. These proportions indicate that metabolic downstates are rather actively regulated in the hypothalamus than simply caused by slowed down transcription in the torpid sampling group.

However, the immediate early genes *c-Jun1* and *Jun* were downregulated during torpor, which is consistent

FEBS Open Bio (2021) © 2021 The Authors. *FEBS Open Bio* published by John Wiley & Sons Ltd on behalf of Federation of European Biochemical Societies.

with hypothalamic gene expression data from Djungarian hamster and hibernating golden-mantled ground squirrel [39,45]. No members of the Fos family were regulated in this study. Although a member of the Jun family dimerizes with a member of the Fos family to become transcriptionally active, a downregulation of one family might already suggest an overall transcriptional downregulation. Yet, this interpretation might be too simple, given the lack of anatomical precision in a whole hypothalamus approach, which cannot differentiate nucleus-specific activation or deactivation of immediate early genes. Furthermore, mRNA of transcriptional factors has reasonably a shorter half-life than mRNA of genes related to metabolism and structure [46].

GO enrichment analyses

The GO enrichment analysis did not identify enriched processes in the photoperiodic comparison (NT: SP vs LP), but revealed enriched transcriptional, biosynthetic, cellular, and metabolic processes during torpor (SP: HT vs NT; Table 2). These findings indicate that photoperiodic acclimations are rather driven by very distinct mechanisms that are not picked up by this general method in a whole hypothalamus transcriptome approach. During torpor however, severe remodeling of many major processes comes to the fore, likely reflecting general adaptive and protective mechanisms of the brain to the metabolic depression and low body temperature. These dominant changes are likely to override distinct control signals. This picture might be underlined by the fact that the small number of genes regulated by photoperiod showed high fold changes, whereas most of the large number of genes regulated in torpor showed moderate fold changes (Fig. 3). Furthermore, highly specialized, essential genes probably not investigated in detail are annotated to few or even no biological processes. In the GO enrichment analysis, they are methodologically suppressed by genes involved in general and therefore well-studied functions, which are annotated to various biological processes. Besides this, the GO enrichment analysis does not respect a regulated genes' biological relevance in terms of fold change and padj-values.

Most extremely regulated genes

In this study, most extremely regulated genes were defined as genes with padj < 0.05 and $|\log2(FC)| > 2.0$. These strict parameters were chosen because they were able to pick up the known key players of physiologically relevant gene expression changes in the photoperiodic comparison. Applying the same thresholds in the torpor comparison, we identified genes that appear to rather reflect adaptive mechanisms of the brain.

Comparison SP-NT vs. LP-NT

Comparison between photoperiods revealed seven most extremely regulated genes. In SP, *Dio3* was among the upregulated genes. *Dio3* is a T3 catabolic enzyme, converting the bioactive hormone into inactive or less active derivates. Upregulation in SP is consistent with previous data, demonstrating that *Dio3*-dependent reduction of hypothalamic T3 availability is a crucial driver of SP-acclimation in Djungarian hamsters [47–51].

Tshb, encoding for the thyrotropin beta subunit, was downregulated in normothermic SP-acclimated hamsters. Downregulation of *Tshb* in *Pars tuberalis* has previously been identified as crucial interface of melatonin signaling and hypothalamic gene expression in many species [52–54]. In birds and mammals, thyrotropin interconnects the circadian clock with the thyroid system and indirectly controls reproduction and the molt circle [55–58].

Cga had, with a log2(FC) of −4.6, the most extreme (down)regulation during SP-acclimation (Fig. 3A). *Cga* contributes as glycoprotein hormones alpha chain with the hormone-specific beta subunits TSHB, LHB, and FSHB to the formation of the hypothalamic hormones thyrotropin, lutropin, and follitropin, respectively [59].

Lrat, the lecithin retinol acetyltransferase, was downregulated in SP-acclimated hamsters. This enzyme is important for vision. It does not only play a role in the retina, but also play a role in other tissues to metabolize vitamin A [60,61]. In the photoperiodic context, retinoic acid-signaling genes were reported to be differentially regulated within the hypothalamus and may play a role in body mass regulation and energy metabolism [62,63].

Npvf was downregulated in SP. *Npvf* encodes RFamide-related peptides (*Rfrp*), such as kisspeptin and *Qrfp*. Kisspeptin plays a role in the photoperiodic control of reproduction, while *Qrfp* is relevant for hypometabolism in mice [5,64,65]. *Npvf* was previously found to be downregulated in hypothalamus during early SP acclimation (SP08) [18].

The other most extremely regulated genes were not directly linked to photoperiodic acclimation. The uncharacterized protein LOC408066, also known as chondroitin sulfate proteoglycan 4B at locus *Cspg4b* and upregulated in SP-acclimated hamsters, is related

FEBS Open Bio (2021) © 2021 The Authors. *FEBS Open Bio* published by John Wiley & Sons Ltd on behalf of Federation of European Biochemical Societies.

to diverse topics in several fields. As structural macromolecules of connective tissues' extracellular matrix, *Cspg4b* might be related to brain plasticity. *Cdc26*, downregulated in SP-acclimated hamsters, has been studied in Chinese hamster ovary cells only, but might contribute as part of the anaphase-promoting complex to brain structure and metabolism [66].

Comparison SP-HT vs. SP-NT

Using the same thresholds, we picked up five regulated genes during torpor that appear to reflect adaptive mechanisms. During torpor, the cold-shock protein *Rbm3* was upregulated. Studies on natural and enforced hypothermia in the hibernating 13-line ground squirrels and in cooled mice suggest that *Rbm3* and other cold-inducible RNA-binding proteins within the brain might enable RNA stability and protein synthesis at low body temperatures, which is important for synaptic regeneration and therefore structural plasticity [67–69].

Egln1 was downregulated during torpor. Although its biological relevance is still unclear, it has been linked to ischemia and hypoxia in mouse and human due to, for example, its suppression of hypoxia-inducible factor 1α (HIF-1α) [70–72]. The importance of avoiding blood clotting and tolerating low oxygen content in the context of torpor and hibernation has been previously discussed [73,74].

The genes upregulated during torpor have not been in focus of torpor research so far. Adipolin has been studied regarding diabetes, obesity, and cardiovascular diseases such as ischemia. It increases insulin sensibility and favors glucose tolerance and uptake, which might play a role for energy gain and storage in the torpid hypothalamus [75]. *Grhl2* appears to play a role in hearing loss. The expression of *Grhl2* and HIF-1α was linked [76]. At this point, no information is available on the function of *Gm16500*, also known as predicted gene 16500 or short coiled-coil protein-like.

Overall, the most regulated genes during torpor also reflect major structural changes, rather than distinct signaling mechanisms. This was already concluded from our previous study, which analyzed gene expression during torpor entrance, although time point of sampling, bioinformatic approach, reference organism, and consequently the actual regulated genes were different [17].

Indicator genes

In a more targeted approach to identify mechanisms involved in torpor control, we specifically screened a number of indicator genes from potentially relevant hypothalamic systems (Table 1) as reviewed earlier [12]. These genes were chosen based on existing knowledge from physiological data regarding single gene products, their receptors, or annotation to a particular system of interest such as the circadian clock system, thyroid system, growth axis, and energy metabolism. Only few of the 68 indicator genes were found significantly regulated in either group comparison. It is possible that only single components of a given system are altered and thereby change their output. Moreover, relevant genes in the brain often occur in a nucleus-specific way and expression changes might disappear when sequencing the whole hypothalamus. Furthermore, each gene product has naturally several functions in diverse systems, whereas current knowledge is incomplete.

Comparison SP-NT vs. LP-NT

Four of 68 indicator genes were differentially regulated by photoperiod (Table 4). Among those genes, we found *Dio3* to be upregulated with an extremely high log2(FC) of 5.1 (see paragraph 'Most extremely regulated genes'). By contrast, *Per3* was upregulated with high significance in SP-normothermia. *Per3* is a photoinducible clock gene oscillating with circadian rhythm [77,78]. Since we only assessed gene expression data at one circadian time point (ZT04), we are unable to draw conclusions about the clockwork here. Differential gene expression might reflect photoperiod-specific clockwork changes. *Pomc* was downregulated in SP-acclimated hamsters' hypothalamus, which is consistent with earlier studies on the hamsters' energy homeostasis. *Pomc* might be involved in controlling the photoperiodic body mass acclimation of Djungarian hamsters [79,80].

The gene with the most extreme significance of this study was *Gpr50*, downregulated in SP-acclimated hamsters. This photoperiodic downregulation of *Gpr50* has previously been demonstrated [50,51,81]. Besides its role in photoperiodic acclimations, studies on mice indicate that lack of *Gpr50* augments fasting-induced torpor and suppresses leptin responsiveness as well as thyrotropin-release hormone [82]. Thus, a photoperiodically reduced expression of *Gpr50* might be a torpor-permissive factor, although the gene is not regulated during individual torpor bouts. Furthermore, *Gpr50* seems to play a major role in overall energy metabolism, as knockout mice had a higher food intake, a higher locomotor activity, and higher basal metabolic rate, yet a lower body mass and fat mass [83]. *Gpr50* is likely to be located on the X-chromosome. Although

FEBS Open Bio (2021) © 2021 The Authors. *FEBS Open Bio* published by John Wiley & Sons Ltd on behalf of Federation of European Biochemical Societies.

irrelevant for this NT: SP vs LP comparison with two males and two females in each group, the location of a gene on sex chromosomes might play a role for the interpretation of the results of the other comparison. In SP: HT vs NT, three males and one male sampled in torpor were used to compare their gene expression with those of two males and two females sampled on a torpor-free day.

Comparison SP-HT vs. SP-NT

Seven of 68 indicator genes were differentially expressed during torpor (Table 4). The somatostatin receptor *Sstr1* was upregulated. It has previously been demonstrated that the GH axis is regulated by photoperiod and involved in torpor control [84]. Downregulation of the axis by a somatostatin receptor 1 agonist has been demonstrated to reinforce torpor behavior. Upregulation of GH axis components during torpor in our current data might either result from the pulsatile nature of this system or represent highly dynamic regulation over the different torpor phases. The GH axis should be investigated during torpor in more detail, since this system seems to play a major role not only in the Djungarian hamster but also in hibernators as the European hamster [85].

Glut3, the most important glucose and galactose transporter in the brain, was upregulated during torpor. This might be related to an enhanced hexose transport to the brain. Plasma glucose levels are reduced during torpor, while hypoglycemia seems to be rather a consequence than a requisite for torpor [86,87]. Either more glucose transporters ensure sufficient glucose availability to the brain despite low glucose levels, or the low plasma glucose levels are caused by an enhanced glucose consumption of the brain during torpor and in preparation for torpor arousal, mediated by more glucose transporters. Both mechanisms might help to maintain functionality of the brain during torpor, which is an energy-saving mechanism integrated in the overall short photoperiod-adjusted energy balance, yet energy-consuming during certain stages of torpor orchestration [88]. Besides possible roles of the upregulation of a glucose transporter in the hypothalamus, the known photoperiodic changes in the glucose metabolism of tanycytes were reviewed elsewhere [89]. Furthermore, *Glut3* expression can be mediated by HIF-1α [90,91], which again links glucose metabolism with ischemia and hypoxia.

Although uninvestigated in the Djungarian hamster so far, *Pml* is annotated to the mouse' circadian clock. A loss of *Pml* causes a downregulation of *Per2, Per1, Cry1, Bmal1,* and *Npas2* expression in the mouse' suprachiasmatic nucleus [92]. Its upregulation in torpor is hard to interpret because of a hardly regulated clock on hypothalamic resolution and various other functions of *Pml*, like in the Tgf-beta signaling pathway [93].

Besides a downregulation of the immediate early genes *Jun* and *c-Jun1* (see paragraph 'Direction of regulation and transcriptional activity'), *Bhlhe40* and *Ppp1cc* were downregulated in torpor as well, both with proven functions in the mouse' circadian clock with unclear consequences. *Bhlhe40* regulates the phase of several clock genes, perhaps in a novel feedback loop different from the positive regulator *CLOCK*/*BMAL* and the negative regulator *PER*/*CRY* [94,95]. *Ppp1cc* is an enzyme with countless substrates, which plays a role in as much biological processes including energy metabolism of cells [96] and regulation of time period [97].

Some indicator genes were annotated in the reference *Mus musculus* but were absent in this study's data on hypothalamic mRNA expressed by the Djungarian hamster (Table S3). This might either result from sequence divergence between the two species in combination with the application of a similarity threshold, or from absence of the gene in the hypothalamus of *Phodopus sungorus*. Phylogenetic relations within the Rodentia, genetic distances between species, and heterozygosity between subpopulations are under constant research, facing genetic bottlenecks, and inbreed of laboratory animals [98–100].

The lack of functional *Mtnr1b* in the Djungarian hamster has been previously described, underlining the functionality of our data approach [101]. To our knowledge, the absence of the sweet taste receptor *Tas1r2* in its hypothalamus has not been described so far. Interestingly, *Tas1r2* null mice do have more glucose nonresponsive tanycytes, while a respectable number of glucosensitive tanycytes use other, hitherto unknown, mechanisms for glucose-sensing [102]. The Djungarian hamster can compensate the lack of *Tas1r2* with *Tas1r3* and other mechanisms, since it is able to time not only spontaneous torpor to photophase, but also fasting-induced torpor to a known feeding schedule [103].

Conclusion

Taken together, our approach was able to validate existing knowledge about hypothalamic key players of photoperiodic control. For example, analysis of both, most extremely regulated and predefined indicator genes, confirmed a downregulation of *Dio3* expression during short photoperiod adaptation of Djungarian

FEBS Open Bio (2021) © 2021 The Authors. *FEBS Open Bio* published by John Wiley & Sons Ltd on behalf of Federation of European Biochemical Societies.

hamsters. Less distinct results were found when applying the same parameters to pin down torpor control mechanisms. Considering both, most extremely regulated and indicator genes, only the regulation of *Egln1* and *Glut3* stood out immediately, since both genes and gene products can be related by the transcriptional complex HIF. Interestingly, the short-term factor torpor led to a substantially higher number of significantly regulated genes compared with the long-term factor season, whereby the majority of torpor-related changes could be attributed to remodeling processes, likely reflecting general adaptive and protective mechanisms of the brain to the metabolic depression and low body temperature. The enrichment of these transcriptional, biosynthetic, cellular, and metabolic processes emphasizes that metabolic downstates are actively regulated and not simply caused by slowed down transcription. The torpor-related gene expression analysis produced less distinct results but has generated valuable data to generate new hypotheses about proximate hypothalamic regulation of individual torpor episodes. More targeted approaches allowing nucleus or even cell-specific analyses of mechanisms might help to further narrow down respective physiological mechanisms. This study provides a basis for future research in biomolecular and neuroendocrine studies on spontaneous torpor. It contributes a valuable, open-source data set for future screening of further genes of interest.

Acknowledgments

We thank Dr. Carola Dreier, Prof. Dr. Anita Marchfelder, Elisabeth Picca, and Sabine Schmidt for technical content support. EH was funded by a grant from the German Research Foundation to AH [HE 6382/2-1]. The bioinformatics was performed on the computational resource bwForCluster NEMO. The authors acknowledge support by the state of Baden-Württemberg through bwHPC and the German Research Foundation (DFG) through grant no INST 39/963-1 FUGG (bwForCluster NEMO). We thank the anonymous reviewers for their valuable comments.

Conflict of interest

The authors declare that the research was conducted in the absence of any commercial or financial relationships that could be construed as a potential conflict of interest.

Author contributions

All authors conceived the project. EH performed the animal work. EH and VD performed surgery and sacrifice. JB developed the bioinformatical pipeline. EH performed the bioinformatics, statistics, and analyses under supervision of JB. EH, VD, and AH interpreted the data. EH wrote the manuscript, which was carefully revised by all authors. All authors agree to be accountable for the content of the work.

Data accessibility

The data that support the findings of this study are openly available in NCBI's Gene Expression Omnibus and are accessible through GEO Series accession number GSE179663 (https://www.ncbi.nlm.nih.gov/geo/query/acc.cgi?acc=GSE179663). An overview of accession numbers within SRA and GEO is attached as Table S2. The data processing pipeline from raw Illumina data to non-normalized gene expression is attached as Doc S2. Both ruby-scripts were uploaded to SourceForge (https://sourceforge.net/projects/prepare-transcript-to-gene-map/). The R-script with R-session info is attached as Doc S3.

References

1 Figala J, Hoffmann K, Goldau G. Zur Jahresperiodik beim Dsungarischen Zwerghamster *Phodopus sungorus* Pallas. *Oecologia*. 1973;**12**:89–118.
2 Steinlechner S. Endokrine Mechanismen bei der jahreszeitlichen Klimaanpassung Fallstudie : Jahreszeitliche Anpassungen. In: Hirzel S, editor. *Endokrinologie IV: Vorträge im Rahmen des Projekts "Zeitstrukturen endokriner Systeme". Abhandlungen der Sächsischen Akademie der Wissenschaften zu Leipzig. Mathematisch-naturwissenschaftliche Klasse*. Stuttgart, Germany: E. Peschke; 2009. p. 99–112.
3 Hoffmann K. The critical photoperiod in the Djungarian hamster Phodopus sungorus. In *Vertebrate circadian systems* (Aschoff J, Daan S, Groos G, eds), Berlin: Springer; 1982. pp. 297–304.
4 Cubuk C, Bank JHH, Herwig A. The chemistry of cold: mechanisms of torpor regulation in the siberian hamster. *Physiology*. 2016;**31**:51–9.
5 Scherbarth F, Steinlechner S. Endocrine mechanisms of seasonal adaptation in small mammals: From early results to present understanding. *J Comp Physiol B Biochem Syst Environ Physiol*. 2010;**180**:935–52.
6 Haugg E, Herwig A, Diedrich V. Body temperature and activity adaptation of short photoperiod-exposed djungarian hamsters (*Phodopus sungorus*). Timing, Traits, and Torpor. *Front Physiol*. 2021;**12**.
7 Blatteis C, Boulant J, Cabanac M, Cannon B, Feedman R, Gordon CJ, et al. Glossary of terms for thermal physiology. *Jpn J Physiol*. 2001;**51**:245–80.

FEBS Open Bio (2021) © 2021 The Authors. *FEBS Open Bio* published by John Wiley & Sons Ltd on behalf of Federation of European Biochemical Societies.

8 Heldmaier G, Steinlechner S. Seasonal pattern and energetics of short daily torpor in the Djungarian hamster, *Phodopus sungorus*. *Oecologia*. 1981;**48**:265–70.
9 Cedernaes J, Waldeck N, Bass J. Neurogenetic basis for circadian regulation of metabolism by the hypothalamus. *Genes Dev*. 2019;**33**:1136–58.
10 Morgan PJ, Ross AW, Mercer JG, Barrett P. Photoperiodic programming of body weight through the neuroendocrine hypothalamus. *J Endocrinol*. 2003;**177**:27–34.
11 van Esseveldt LKE, Lehman MN, Boer GJ. The suprachiasmatic nucleus and the circadian time-keeping system revisited. *Brain Res Rev*. 2000;**33**:34–77.
12 Diedrich V, Haugg E, Dreier C, Herwig A. What can seasonal models teach us about energy balance ? *J Endocrinol*. 2020;**244**:R17–32.
13 Ebling FJP, Lewis JE. Tanycytes and hypothalamic control of energy metabolism. *Glia*. 2018;**66**:1176–84.
14 Helfer G, Barrett P, Morgan PJ. A unifying hypothesis for control of body weight and reproduction in seasonally breeding mammals. *J Neuroendocrinol*. 2019;**31**:1–12.
15 Crawford FIJ, Hodgkinson CL, Ivanova EA, Logunova LB, Evans GJ, Steinlechner S, et al. Influence of torpor on cardiac expression of genes involved in the circadian clock and protein turnover in the Siberian hamster *(Phodopus sungorus)*. *Physiol Genomics*. 2007;**31**:521–30.
16 Cubuk C, Markowsky H, Herwig A. Hypothalamic control systems show differential gene expression during spontaneous daily torpor and fasting-induced torpor in the Djungarian hamster *(Phodopus sungorus)*. *PLoS One*. 2017;**12**:e0186299.
17 Cubuk C, Kemmling J, Fabrizius A, Herwig A. Transcriptome analysis of hypothalamic gene expression during daily torpor in Djungarian hamsters *(Phodopus sungorus)*. *Front Neurosci*. 2017;**11**:122.
18 Bao R, Onishi KG, Tolla E, Ebling FJP, Lewis JE, Anderson RL, et al. Genome sequencing and transcriptome analyses of the Siberian hamster hypothalamus identify mechanisms for seasonal energy balance. *Proc Natl Acad Sci*. 2019;**116**:13116–21.
19 Paul MJ, Freeman DA, Jin HP, Dark J. Neuropeptide Y induces torpor-like hypothermia in Siberian hamsters. *Brain Res*. 2005;**1055**:83–92.
20 Diedrich V, Kumstel S, Steinlechner S. Spontaneous daily torpor and fasting-induced torpor in Djungarian hamsters are characterized by distinct patterns of metabolic rate. *J Comp Physiol B Biochem Syst Environ Physiol*. 2015;**185**:355–66.
21 Franklin K, Paxinos G. *The mouse brain in stereotaxic coordinates*, 3rd edn. Elsevier; 2008.
22 Andrews S. FastQC: A Quality Control Tool for High Throughput Sequence Data. 2010. https://www.bioinformatics.babraham.ac.uk/projects/fastqc/
23 Krueger F. TrimGalore. 2020; https://github.com/FelixKrueger/TrimGalore
24 Grabherr MG, Haas BJ, Yassour M, Levin JZ, Thompson DA, Amit I, et al. Trinity: reconstructing a full-length transcriptome without a genome from RNA-Seq data. *Nat Biotechnol*. 2013;**29**:644–52.
25 Haas BJ, Papanicolaou A, Yassour M, Grabherr M, Blood PD, Bowden J, et al. *De novo* transcript sequence reconstruction from RNA-seq using the Trinity platform for reference generation and analysis. *Nat Protoc*. 2013;**8**:1494–512.
26 Altschul SF, Gish W, Miller W, Myers EW, Lipman DJ. Basic local alignment search tool. *J Mol Biol*. 1990;**215**:403–10.
27 National Center for Biotechnology Information. Building a BLAST database with local sequences. Bethesda, MD, USA; 2008. https://www.ncbi.nlm.nih.gov/books/NBK279688/
28 Langmead B. Aligning Short Sequencing Reads with Bowtie. *Curr Prot Bioinform*. 2010;**32**:1–24
29 Li B, Dewey CN. RSEM: Accurate transcript quantification from RNA-Seq data with or without a reference genome. *BMC Bioinformatics*. 2011;**12**:1–16.
30 Edgar R, Domrachev M, Lash AE. Gene Expression Omnibus: NCBI gene expression and hybridization array data repository. *Nucleic Acids Res*. 2002;**30**:207–10.
31 RStudio Team. *RStudio: Integrated Development for R*. PBC, Boston, MA, USA: RStudio; 2020. http://www.rstudio.com/.
32 R Core Team. *R: A language and environment for statistical computing*. Vienna, Austria: R Foundation for Statistical Computing; 2018. https://www.R-project.org/.
33 Love MI, Anders S, Huber W. Analyzing RNA-seq data with DESeq2. 2020. http://bioconductor.org/packages/release/bioc/html/DESeq2.html.
34 Love MI, Anders S, Kim V, Huber W. RNA-Seq workflow: gene-level exploratory analysis and differential expression. *F1000Res*. 2019;**4**:1070.
35 Love MI, Huber W, Anders S. Moderated estimation of fold change and dispersion for RNA-seq data with DESeq2. *Genome Biol*. 2014;**15**:1–21.
36 The Gene Ontology Consortium, Ashburner M, Ball CA, Blake JA, Botstein D, Butler H, Cherry JM, et al. Gene Ontology: tool for the unification of biology. *NIH Public Access*. 2000;**25**:25–9.
37 Carbon S, Douglass E, Good BM, Unni DR, Harris NL, Mungall CJ, et al. The Gene Ontology resource: Enriching a GOld mine. *Nucleic Acids Res*. 2021;**49**:D325–34.
38 Mi H, Muruganujan A, Ebert D, Huang X, Thomas PD. PANTHER version 14: More genomes, a new PANTHER GO-slim and improvements in enrichment analysis tools. *Nucleic Acids Res*. 2019;**47**:D419–26.

FEBS Open Bio (2021) © 2021 The Authors. *FEBS Open Bio* published by John Wiley & Sons Ltd on behalf of Federation of European Biochemical Societies.

39 Kovács KJ. Measurement of immediate-early gene activation- c-fos and beyond. *J Neuroendocrinol*. 2008;**20**:665–72.
40 Kovács KJ. c-Fos as a transcription factor: A stressful (re)view from a functional map. *Neurochem Int*. 1998;**33**:287–97.
41 Ebling FJP, Maywood ES, Mehta M, Hancock DC, McNulty S, De Bono J, et al. FOSB in the suprachiasmatic nucleus of the Syrian and Siberian Hamster. *Brain Res Bull*. 1996;**41**:257–68.
42 Fu R, Gillen AE, Grabek KR, Riemondy KA, Epperson LE, Bustamante CD, et al. Dynamic RNA regulation in the brain underlies physiological plasticity in a hibernating mammal. *Front Physiol*. 2021;**11**:1–18.
43 Mauger DM, Joseph Cabral B, Presnyak V, Su SV, Reid DW, Goodman B, et al. mRNA structure regulates protein expression through changes in functional half-life. *Proc Natl Acad Sci USA*. 2019;**116**:24075–83.
44 Carey HV, Andrews MT, Martin SL. Mammalian hibernation: Cellular and molecular responses to depressed metabolism and low temperature. *Physiol Rev*. 2003;**83**:1153–81.
45 O'Hara BF, Watson FL, Srere HK, Kumar H, Wiler SW, Welch SK, et al. Gene expression in the brain across the hibernation cycle. *J Neurosci*. 1999;**19**:3781–90.
46 Sharova LV, Sharov AA, Nedorezov T, Piao Y, Shaik N, Ko MSH. Database for mRNA half-life of 19 977 genes obtained by DNA microarray analysis of pluripotent and differentiating mouse embryonic stem cells. *DNA Res*. 2009;**16**:45–58.
47 Herwig A, Petri I, Barrett P. Hypothalamic gene expression rapidly changes in response to photoperiod in juvenile Siberian hamsters *(Phodopus sungorus)*. *J Neuroendocrinol*. 2012;**24**:991–8.
48 Murphy M, Jethwa PH, Warner A, Barrett P, Nilaweera KN, Brameld JM, et al. Effects of manipulating hypothalamic triiodothyronine concentrations on seasonal body weight and torpor cycles in Siberian hamsters. *Endocrinology*. 2012;**153**:101–12.
49 Barrett P, Ebling FJP, Schuhler S, Wilson D, Ross AW, Warner A, et al. Hypothalamic thyroid hormone catabolism acts as a gatekeeper for the seasonal control of body weight and reproduction. *Endocrinology*. 2007;**148**:3608–17.
50 Petri I, Diedrich V, Wilson D, Fernandez-Calleja J, Herwig A, Steinlechner S, et al. Orchestration of gene expression across the seasons: Hypothalamic gene expression in natural photoperiod throughout the year in the Siberian hamster. *Sci Rep*. 2016;**6**:1–9.
51 Bank JHH, Wilson D, Rijntjes E, Barrett P, Herwig A. Alternation between short- and long photoperiod reveals hypothalamic gene regulation linked to seasonal body weight changes in Djungarian hamsters *(Phodopus sungorus)*. *J Neuroendocrinol*. 2017;**29**:1–11.
52 Dardente H, Hazlerigg DG, Ebling FJP. Thyroid hormone and seasonal rhythmicity. *Front Endocrinol*. 2014;**5**:1–11.
53 Barrett P, Bolborea M. Molecular pathways involved in seasonal body weight and reproductive responses governed by melatonin. *J Pineal Res*. 2012;**52**:376–88.
54 Wittkowski W, Bergmann M, Hoffmann K, Pera F. Photoperiod-dependent changes in TSH-like immunoreactivity of cells in the hypophysial pars tuberalis of the Djungarian hamster, *Phodopus sungorus*. *Cell Tissue Res*. 1988;**251**:183–7.
55 West AC, Wood SH. Seasonal physiology: making the future a thing of the past. *Curr Opin Physiol*. 2018;**5**:1–8.
56 Dardente H, Wyse CA, Birnie MJ, Dupré SM, Loudon ASI, Lincoln GA, et al. A molecular switch for photoperiod responsiveness in mammals. *Curr Biol*. 2010;**20**:2193–8.
57 Unfried C, Ansari N, Yasuo S, Korf HW, Von Gall C. Impact of melatonin and molecular clockwork components on the expression of thyrotropin β-chain (Tshb) and the Tsh receptor in the mouse pars tuberalis. *Endocrinology*. 2009;**150**:4653–62.
58 Nakao N, Ono H, Yoshimura T. Thyroid hormones and seasonal reproductive neuroendocrine interactions. *Reproduction*. 2008;**136**:1–8.
59 Bernard DJ, Brûlé E. Anterior pituitary: glycoprotein hormones from gonadotrope (FSH and LH) and thyrotrope (TSH) cells. In Litwack G, ed *Hormonal signaling in biology and medicine*, pp. 119–44. Elsevier Inc; 2020.
60 Batten ML, Imanishi Y, Maeda T, Tu DC, Moise AR, Bronson D, et al. Lecithin-retinol acyltransferase is essential for accumulation of all-trans-retinyl esters in the eye and in the liver. *J Biol Chem*. 2004;**279**:10422–32.
61 Sprenger RJ, Tanumihardjo SA, Kurtz CC. Developing a model of Vitamin A deficiency in a hibernating mammal, the 13-lined ground squirrel *(Ictidomys tridecemlineatus)*. *Comp Med*. 2018;**68**:196–203.
62 Ross AW, Helfer G, Russell L, Darras VM, Morgan PJ. Thyroid hormone signalling genes are regulated by photoperiod in the hypothalamus of F344 rats. *PLoS One*. 2011;**6**:1–14.
63 Ross AW, Webster CA, Mercer JG, Moar KM, Ebling FJ, Schuhler S, et al. Photoperiodic regulation of hypothalamic retinoid signaling: association of retinoid X Receptor γ with body weight. *Endocrinology*. 2004;**145**:13–20.
64 Dardente H, Wood S, Ebling FJP, Sáenz de Miera C. An integrative view of mammalian seasonal neuroendocrinology. *J Neuroendocrinol*. 2019;**31**:1–17.

FEBS Open Bio (2021) © 2021 The Authors. *FEBS Open Bio* published by John Wiley & Sons Ltd on behalf of Federation of European Biochemical Societies.

65 Takahashi TM, Sunagawa GA, Soya S, Abe M, Sakurai K, Ishikawa K, et al. A discrete neuronal circuit induces a hibernation-like state in rodents. *Nature*. 2020;**583**:109–14.
66 Puram SV, Bonni A. Novel functions for the anaphase-promoting complex in neurobiology. *Semin Cell Dev Biol*. 2011;**22**:586–94.
67 Peretti D, Bastide A, Radford H, Verity N, Molloy C, Martin MG, et al. RBM3 mediates structural plasticity and protective effects of cooling in neurodegeneration. *Nature*. 2015;**518**:236–9.
68 Williams DR, Epperson LE, Li W, Hughes MA, Taylor R, Rogers J, et al. Seasonally hibernating phenotype assessed through transcript screening. *Physiol Genomics*. 2005;**24**:13–22.
69 Logan SM, Storey KB. Cold-inducible RNA-binding protein Cirp, but not Rbm3, may regulate transcript processing and protection in tissues of the hibernating ground squirrel. *Cell Stress Chaperones*. 2020;**25**:857–68.
70 Pamenter ME, Hall JE, Tanabe Y, Simonson TS. Cross-species insights into genomic adaptations to hypoxia. *Front Genet*. 2020;11.
71 Baik A, Olenchock B, Moslehi J, Kaelin WG. Acute hypoxia-inducible factor Egln1 inactivation protects against ischemia-reperfusion injury by regulation of glucose oxidation and reactive oxygen species generation. *J Am Coll Cardiol*. 2013;**61**:E28.
72 To KKW, Huang LE. Suppression of hypoxia-inducible factor 1α (HIF-1α) transcriptional activity by the HIF prolyl hydroxylase EGLN1. *J Biol Chem*. 2005;**280**:38102–7.
73 Quinones QJ, Zhang Z, Ma Q, Smith MP, Soderblom E, Moseley MA, et al. Proteomic profiling reveals adaptive responses to surgical myocardial ischemia-reperfusion in hibernating arctic ground squirrels compared to rats. *Anesthesiology*. 2016;**124**:1296–310.
74 Heldmaier G, Ortmann S, Elvert R. Natural hypometabolism during hibernation and daily torpor in mammals. *Respir Physiol Neurobiol*. 2004;**141**:317–29.
75 Knights AJ, Funnell AP, Pearson RC, Crossley M, Bell-Anderson KS. Adipokines and insulin action. *Adipocyte*. 2014;**3**:88–96.
76 Shao C, Ji C, Wang X, Hu B. Expression and significance of GRHL2 in esophageal cancer. *Onco Targets Ther*. 2017;**10**:2025–31.
77 Schwartz WJ, De La Iglesia HO, Zlomanczuk P, Illnerová H. Encoding le quattro stagioni within the mammalian brain: Photoperiodic orchestration through the suprachiasmatic nucleus. *J Biol Rhythms*. 2001;**16**:302–11.
78 Silver R, Schwartz WJ. The suprachiasmatic nucleus is a functionally heterogeneous timekeeping organ. *Methods Enzym*. 2005;**393**:451–65.
79 Mercer JG, Moar KM, Ross AW, Hoggard N, Morgan PJ. Photoperiod regulates arcuate nucleus POMC, AGRP, and leptin receptor mRNA in Siberian hamster hypothalamus. *Am J Physiol Regul Integr Comp Physiol*. 2000;**278**:R271–81.
80 Helwig M, Herwig A, Heldmaier G, Barrett P, Mercer JG, Klingenspor M. Photoperiod-dependent regulation of carboxypeptidase E affects the selective processing of neuropeptides in the seasonal Siberian hamster *(Phodopus sungorus)*. *J Neuroendocrinol*. 2013;**25**:190–7.
81 Herwig A, de Vries EM, Bolborea M, Wilson D, Mercer JG, Ebling FJP, et al. Hypothalamic ventricular ependymal thyroid hormone deiodinases are an important element of circannual timing in the Siberian hamster *(Phodopus sungorus)*. *PLoS One*. 2013;**8**:e62003.
82 Bechtold DA, Sidibe A, Saer BRC, Li J, Hand LE, Ivanova EA, et al. A role for the melatonin-related receptor GPR50 in leptin signaling, adaptive thermogenesis, and torpor. *Curr Biol*. 2012;**22**:70–7.
83 Ivanova EA, Bechtold DA, Dupré SM, Brennand J, Barrett P, Luckman SM, et al. Altered metabolism in the melatonin-related receptor (GPR50) knockout mouse. *Am J Physiol - Endocrinol Metab*. 2008;**294**:176–82.
84 Scherbarth F, Diedrich V, Dumbell RA, Schmid HA, Steinlechner S, Barrett P. Somatostatin receptor activation is involved in the control of daily torpor in a seasonal mammal. *Am J Physiol Integr Comp Physiol*. 2015;**309**:R668–74.
85 Nürnberger F, Pleschka K, Masson-Pévet M, Pévet P. The somatostatin system of the brain and hibernation in the European hamster *(Cricetus cricetus)*. *Cell Tissue Res*. 1997;**288**:441–7.
86 Heldmaier G, Klingenspor M, Werneyer M, Lampi BJ, Brooks SP, Storey KB. Metabolic adjustments during daily torpor in the Djungarian hamster. *Am J Physiol*. 1999;**276**:E896–906.
87 Dark J, Lewis DA, Zucker I. Hypoglycemia and torpor in Siberian hamsters. *Am J Physiol*. 1999;**276**:R776–81.
88 Walton JC, Grier AJ, Weil ZM, Nelson RJ. Photoperiod and stress regulation of corticosteroid receptor, brain-derived neurotrophic factor, and glucose transporter GLUT3 mRNA in the hippocampus of male Siberian hamsters *(Phodopus sungorus)*. *Neuroscience*. 2012;**213**:106–11.
89 Nilaweera KN, Herwig A, Bolborea M, Campbell G, Mayer C-D, Morgan PJ, et al. Photoperiodic regulation of glycogen metabolism, glycolysis, and glutamine synthesis in tanycytes of the Siberian hamster suggests novel roles of tanycytes in hypothalamic function. *Glia*. 2011;**59**:1695–705.
90 Yu J, Li J, Zhang S, Xu X, Zheng M, Jiang G, et al. IGF-1 induces hypoxia-inducible factor 1α-mediated

FEBS Open Bio (2021) © 2021 The Authors. *FEBS Open Bio* published by John Wiley & Sons Ltd on behalf of Federation of European Biochemical Societies.

GLUT3 expression through PI3K/Akt/mTOR dependent pathways in PC12 cells. *Brain Res*. 2012;**1430**:18–24.
91 Mimura I, Nangaku M, Kanki Y, Tsutsumi S, Inoue T, Kohro T, et al. Dynamic change of chromatin conformation in response to hypoxia enhances the expression of GLUT3 (SLC2A3) by cooperative interaction of hypoxia-inducible factor 1 and KDM3A. *Mol Cell Biol*. 2012;**32**:3018–32.
92 Miki T, Xu Z, Chen-Goodspeed M, Liu M, Van Oort-Jansen A, Rea MA, et al. PML regulates PER2 nuclear localization and circadian function. *EMBO J*. 2012;**31**:1427–39.
93 Lin HK, Bergmann S, Pandolfi PP. Cytoplasmic PML function in TGF-β signalling. *Nature*. 2004;**431**:205–11.
94 Nakashima A, Kawamoto T, Honda KK, Ueshima T, Noshiro M, Iwata T, et al. DEC1 modulates the circadian phase of clock gene expression. *Mol Cell Biol*. 2008;**28**:4080–92.
95 Kawamoto T, Noshiro M, Sato F, Maemura K, Takeda N, Nagai R, et al. A novel autofeedback loop of Dec1 transcription involved in circadian rhythm regulation. *Biochem Biophys Res Commun*. 2004;**313**:117–24.
96 Ceulemans H, Bollen M. Functional diversity of protein phosphatase-1, a cellular economizer and reset button. *Physiol Rev*. 2004;**84**:1–39.
97 Schmutz I, Wendt S, Schnell A, Kramer A, Mansuy IM, Albrecht U. Protein phosphatase 1 (PP1) is a post-translational regulator of the mammalian circadian clock. *PLoS One*. 2011;**6**:e21325.
98 Romanenko SA, Perelman PL, Trifonov VA, Graphodatsky AS. Chromosomal evolution in Rodentia. *Heredity*. 2012;**108**:4–16.
99 Filippucci MG, Rodino E, Nevo E, Capanna E. Evolutionary genetics and systematics of the garden dormouse, *Eliomys wagner*, 1840. 2 -allozyme diversity and differentiation of chromosomal races. *Bolletino Di Zool*. 1988;**55**:47–54.
100 Ideraabdullah FY, de la Casa-Esperón E, Bell TA, Detwiler DA, Magnuson T, Sapienza C, et al. Genetic and haplotype diversity among wild-derived mouse inbred strains. *Genome Res*. 2004;**14**:1880–7.
101 Weaver DR, Liu C, Reppert SM. Nature's Knockout: The Mel1b receptor is not necessary for reproductive and circadian responses to melatonin in siberian hamsters. *Mol Endocrinol*. 1996;**10**:1478–87.
102 Benford H, Bolborea M, Pollatzek E, Lossow K, Hermans-Borgmeyer I, Liu B, et al. A sweet taste receptor-dependent mechanism of glucosensing in hypothalamic tanycytes. *Glia*. 2017;**65**:773–89.
103 Paul MJ, Kauffman AS, Zucker I. Feeding schedule controls circadian timing of daily torpor in SCN-ablated Siberian hamsters. *J Biol Rhythms*. 2004;**19**:226–37.

Supporting information

Additional supporting information may be found online in the Supporting Information section at the end of the article.

Doc S1. Comparative transcriptomics of the djungarian hamster hypothalamus.

Doc S2. Processing pipeline - executed commands from trim-galore to rsem.

Doc S3. R script with R session info - executed normalization (from *P*-value to padj), statistics (pairwise group comparison), principal component analysis, heatmap, setup of the R-software and installed packages.

Fig. S1. Core body temperature patterns of SP-acclimated hamsters.

Table S1. Background information on hamsters.

Table S2. Quality control of RNA-Seq data and accession numbers of data depositories.

FEBS Open Bio (2021) © 2021 The Authors. *FEBS Open Bio* published by John Wiley & Sons Ltd on behalf of Federation of European Biochemical Societies.

3.2 Supplementary Material

3.2.1 Supplementary File 1: Supplementary Tables and Figures

Supplementary File 1

Haugg E, Borner J, Diedrich V, Herwig A (2021)
Comparative Transcriptomics of the Djungarian Hamster Hypothalamus during Short Photoperiod Acclimation and Spontaneous Torpor

Correspondence to: elena.haugg@uni-ulm.de

This file includes:

Supplementary Table 1:	Background information on hamsters.
Supplementary Figure 1:	Core body temperature patterns of SP-acclimated hamsters.
Supplementary Table 2:	Quality control of RNA-Seq data and accession numbers of data depositories.
Supplementary Table 3:	Results of the 68 predefined indicator genes.

Supplementary Table 1: Background information on hamsters (n = 12). Hamster identification number, gender (f for female, m for male), body mass, fur index, age, and duration of short photoperiod (SP) exposure at several key dates. Body mass and fur index are usual parameters to assess the acclimation state. The initial body mass was measured at the beginning of the experiment, when eight of twelve hamsters were transferred to SP. Until termination, hamsters in SP reduced body mass, while hamsters in LP retained or increased their body mass, yet with a high variation [1]. The fur index was assessed from 1 (brown light summer fur) to 6 (white isolating winter fur) according to Figala et al. 1973 [2]. All SP-acclimated hamsters were capable of torpor, while their torpor incidence, which is the number of torpor bouts per days of the observation interval, varied [1]. The terminal core body temperature (Tb) is indicated as plotted in **Supplementary Figure 1.** Several parameters were only assessed for hamsters which were transferred to SP, since four hamsters remained without radiotelemetry transmitter in long photoperiod (LP).

hamster ID	gender	body mass			fur index	age [weeks] at		
		initial [g]	sacrifice [g]	difference [%]	sacrifice	SP	surgery	sacrifice
EH03-26	m	41.9	28.7	-31.5	5.0	18.3	29.4	32.1
EH03-33	m	31.3	25.4	-18.8	3.0	15.6	27.4	29.6
EH03-10	m	42.3	26.4	-37.6	3.5	19.4	29.7	37.3
EH03-02	f	29.4	26.3	-10.5	5.5	22.4	33.6	40.4
EH03-36	f	28.3	25.8	-8.8	4.5	15.6	27.7	29.9
EH03-38	m	41.2	29.5	-28.4	3.5	13.6	25.9	28.0
EH03-37	f	25.4	25.5	0.4	3.0	15.6	27.9	29.9
EH03-19	m	37.1	25.8	-30.5	3.0	15.7	29.6	34.1
EH03-LP1	m	38.2	37.1	-2.9	1.0	-	-	32.0
EH03-LP2	f	30.0	32.5	8.3	1.0	-	-	30.0
EH03-LP3	m	32.2	36.9	14.6	1.0	-	-	29.9
EH03-LP5	f	29.6	29.0	-2.0	1.0	-	-	29.7

hamster ID	duration [weeks] in SP at		observation		torpor incidence		sampling group	terminal Tb [°C]
	surgery	sacrifice	interval [weeks]	torpor bouts [#]	observation interval	last 7 full days		
EH03-26	11.1	13.9	2.7	12	0.6	0.9	SPHT	23.6
EH03-33	11.9	14.0	2.1	4	0.3	0.4	SPHT	24.0
EH03-10	10.3	17.9	7.6	30	0.6	0.7	SPHT	25.0
EH03-02	11.1	18.0	6.9	14	0.3	0.4	SPHT	25.9
EH03-36	12.1	14.3	2.1	2	0.1	0.3	SPNT	34.9
EH03-38	12.3	14.4	2.1	6	0.4	0.3	SPNT	35.3
EH03-37	12.3	14.3	2.0	1	0.1	0.0	SPNT	35.4
EH03-19	13.9	18.4	4.6	10	0.3	0.7	SPNT	35.5
EH03-LP1	-	-	-	-	-	-	LPNT	-
EH03-LP2	-	-	-	-	-	-	LPNT	-
EH03-LP3	-	-	-	-	-	-	LPNT	-
EH03-LP5	-	-	-	-	-	-	LPNT	-

[1] Haugg E, Herwig A, Diedrich V (2021) Body temperature and activity adaptation of short photoperiod exposed Djungarian hamsters (Phodopus sungorus): Timing, traits, and torpor. Front Physiol. https://doi.org/10.3389/fphys.2021.626779

[2] Figala J, Hoffmann K, Goldau G (1973) Zur Jahresperiodik beim Dsungarischen Zwerghamster Phodopus sungorus Pallas. Oecologia 12:89–118. https://doi.org/10.1007/BF00345511

Supplementary Figure 1: Core body temperature patterns of SP-acclimated hamsters (n = 8). The graph shows the day of sacrifice and the day before. Time is given in *Zeitgeber* time (ZT), with lights on at ZT0 and lights off at ZT08. Photophases are indicated (grey bars on the x-axis). After at least one observed torpor bout per hamster (see also **Supplementary Table 1**), sacrifice was carried out approximately ZT04 (vertical line), either in deep torpor (HT, n = 4, black lines) or without torpor expression (NT; n = 4, grey lines).

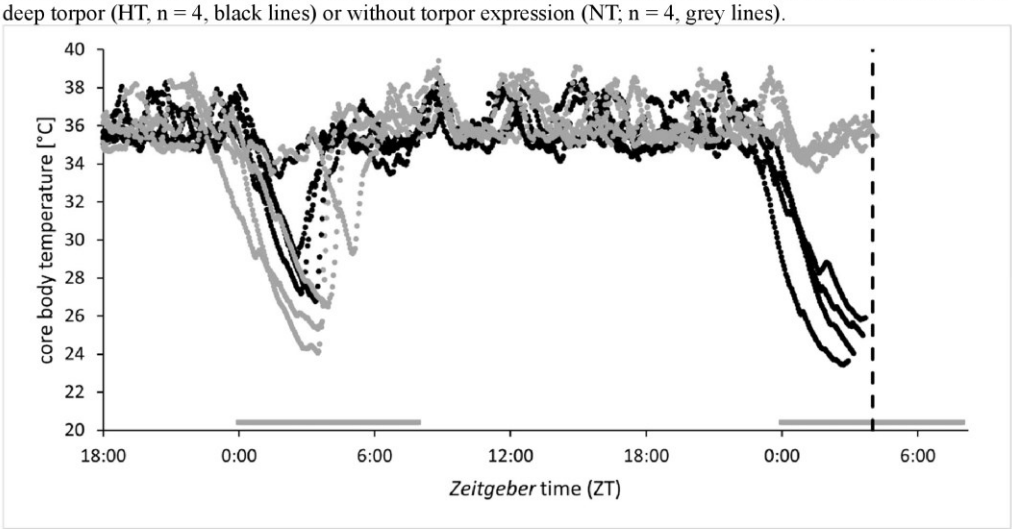

Supplementary Table 2: Quality control of RNA-Seq data and accession numbers of data depositories. Quality control was performed with FastQC [3]. Sequence length was throughout 151 base pairs. The GC-content was 48 or 49 % per file, per sample and in total. The number of total read pairs ranged from 30,375,548 to 35,052,887 with a mean of 32,717,097 per sample. In total, 392,605,160 read pairs were included in the original *de novo* assembly before mapping against the reference was performed. Each sample is indicated by the photoperiod (SP or LP), metabolic state at termination (HT or NT), and a running number within the cohort EH03. All data discussed in this study are accessible as indicated through GEO Series accession number GSE179663 (https://www.ncbi.nlm.nih.gov/geo/query/acc.cgi?acc=GSE179663).

read pairs	sample ID	BioSample in BioProject PRJNA743775	raw illumina data in SRA Study SRP326941	non-normalized gene expression in GEO Series GSE179663
33,069,666	SPHT02	SAMN20060157	SRR15041647	GSM5425878
30,498,292	SPHT10	SAMN20060158	SRR15041646	GSM5425879
31,130,806	SPHT26	SAMN20060159	SRR15041645	GSM5425880
30,375,548	SPHT33	SAMN20060160	SRR15041644	GSM5425881
34,994,187	SPNT19	SAMN20060161	SRR15041643	GSM5425882
35,006,001	SPNT36	SAMN20060162	SRR15041642	GSM5425883
34,055,106	SPNT37	SAMN20060163	SRR15041651	GSM5425884
35,052,887	SPNT38	SAMN20060164	SRR15041650	GSM5425885
32,690,972	LPNT01	SAMN20060153	SRR15041653	GSM5425874
32,951,578	LPNT02	SAMN20060154	SRR15041652	GSM5425875
31,571,032	LPNT03	SAMN20060155	SRR15041649	GSM5425876
31,209,085	LPNT05	SAMN20060156	SRR15041648	GSM5425877

Supplementary Table 3: Results of the 68 predefined indicator genes. (Table see next page). Results for both pairwise group comparisons, namely NT: SP vs LP and SP: HT vs NT. Indicator genes with padj < 0.05 (black fields with white labelling) were presented in the main document **(Table 4)**. A negative log2(FC) indicates downregulation (yellow), a positive log2(FC) upregulation (green) relative to the according baseline (LP-NT for photoperiodic comparison, SP-NT for torpor comparison). "Not present" (grey) marks genes which were not present in one or both pairwise group comparisons but annotated in the reference *Mus musculus*. "Outlier" (grey) replaces a padj-value given the outlying count according to the statistics performed with DESeq2 [4].

[3] Andrews S (2010) FastQC: A Quality Control Tool for High Throughput Sequence Data. https://www.bioinformatics.babraham.ac.uk/projects/fastqc/

[4] Love MI, Anders S, Huber W (2020) Analyzing RNA-seq data with DESeq2. http://bioconductor.org/packages/release/bioc/vignettes/DESeq2/inst/doc/DESeq2.html#pvaluesNA (20210622).

Supplementary Table 3: Results of the 68 predefined indicator genes. (Legend text see previous page).

	#	NT: SP vs LP			SP: HT vs NT			gene	gene product
		padj	-log10 (padj)	log2 (FC)	padj	-log10 (padj)	log2 (FC)		
transcription	1	0.991	0.0	-1.02	0.975	0.0	-0.02	*Fos*	proto-oncogene c-Fos
	2	0.992	0.0	-0.12	0.973	0.0	0.04	*Fosb*	protein fosB
	3	0.991	0.0	-0.13	0.000	5.4	-0.44	*Jun*	transcription factor AP-1 / c-Jun
	4	0.991	0.0	-0.25	0.817	0.1	0.07	*Junb*	transcription factor jun-B
	5	0.991	0.0	-0.03	0.926	0.0	-0.02	*Jund*	transcription factor jun-D
	6	0.996	0.0	-0.01	0.041	1.4	-0.16	*c-Jun1*	c-Jun-amino-terminal kinase-interacting protein 1
	7	0.991	0.0	0.04	0.052	1.3	-0.14	*c-Jun3*	c-Jun-amino-terminal kinase-interacting protein 3
clock	8	0.996	0.0	-0.03	0.322	0.5	0.60	*Avp*	vasopressin-neurophysin 2-copeptin
	9	0.967	0.0	-0.40	0.913	0.0	-0.07	*Avpr1a*	vasopressin V1a receptor
	10	0.073	1.1	-0.22	0.330	0.5	-0.16	*Bmal1*	brain and muscle ARNT-like 1
	11	0.997	0.0	0.00	0.768	0.1	0.21	*Bmal2*	brain and muscle ARNT-like 2
	12	0.991	0.0	0.11	0.000	13.0	-0.47	*Bhlhe40*	class E basic helix-loop-helix protein 40
	13	0.991	0.0	0.08	0.973	0.0	0.01	*Clock*	circadian locomoter output cycles protein kaput
	14	0.991	0.0	0.08	0.519	0.3	-0.10	*Cry1*	cryptochrome-1
	15	0.991	0.0	0.16	0.670	0.2	-0.09	*Cry2*	cryptochrome-2
	16	0.000	45.3	-1.85	0.721	0.1	-0.20	*Gpr50*	melatonin-related receptor
	17	0.837	0.1	-0.21	0.051	1.3	-0.38	*Id2*	DNA-binding protein inhibitor ID-2
	18	0.995	0.0	-0.02	0.607	0.2	0.09	*Mta1*	metastasis-associated protein MTA1
	19	0.991	0.0	-1.18	outlier			*Mtnr1a*	melatonin receptor type 1A
	20	not present			not present			*Mtnr1b*	melatonin receptor type 1B
	21	0.991	0.0	0.25	0.379	0.4	-0.24	*Per1*	period circadian protein homolog 1
	22	0.089	1.1	0.36	0.228	0.6	0.24	*Per2*	period circadian protein homolog 2
	23	0.000	3.9	0.68	0.814	0.1	0.08	*Per3*	period circadian protein homolog 3
	24	0.996	0.0	-0.02	0.008	2.1	0.55	*Pml*	protein PML
	25	0.996	0.0	-0.02	0.048	1.3	-0.14	*Ppp1cc*	serine/threonine-protein phosphatase
	26	0.991	0.0	0.19	0.871	0.1	0.14	*Timeless*	protein timeless homolog
	27	0.991	0.0	-0.28	0.353	0.5	0.21	*Vip*	vasoactive intestinal peptide
thyroid	28	0.991	0.0	0.90	0.433	0.4	0.73	*Dio1*	iodothyronine deiodinase type I
	29	0.952	0.0	-0.37	0.801	0.1	0.11	*Dio2*	iodothyronine deiodinase type II
	30	0.038	1.4	5.10	outlier			*Dio3*	thyroxine 5-deiodinase
	31	0.992	0.0	0.03	0.918	0.0	-0.04	*Mct8*	monocarboxylate transporter 8
	32	0.996	0.0	0.01	0.775	0.1	-0.04	*Thra*	thyroid hormone receptor alpha
	33	0.991	0.0	0.17	0.550	0.3	0.15	*Thrb*	thyroid hormone receptor beta
	34	0.991	0.0	0.10	0.614	0.2	0.10	*Trh*	pro-thyrotropin-releasing hormone
	35	0.991	0.0	0.14	0.449	0.3	0.21	*Trhr*	thyrotropin-releasing hormone receptor
	36	0.991	0.0	0.20	0.845	0.1	0.09	*Trhr2*	thyrotropin releasing hormone receptor 2
	37	0.991	0.0	-0.10	0.868	0.1	0.08	*Tshr*	thyrotropin receptor
	38	0.991	0.0	-0.13	0.143	0.8	-0.25	*Txnip*	thioredoxin-interacting protein
growth	39	outlier			not present			*GH*	somatotropin / growth hormone
	40	0.991	0.0	0.10	0.829	0.1	0.05	*Sst*	somatostatin
	41	0.632	0.2	-0.25	0.013	1.9	0.33	*Sstr1*	somatostatin receptor type 1
	42	0.991	0.0	-0.08	0.066	1.2	0.28	*Sstr2*	somatostatin receptor type 2
	43	0.997	0.0	0.00	0.560	0.3	0.16	*Sstr3*	somatostatin receptor type 3
	44	0.991	0.0	0.25	0.855	0.1	0.11	*Sstr4*	somatostatin receptor type 4
	45	0.991	0.0	-0.22	0.920	0.0	0.09	*Sstr5*	somatostatin receptor type 5
metabolism	46	0.991	0.0	-0.05	0.805	0.1	-0.08	*Tas1r3*	taste receptor type 1 member 3
	47	not present			not present			*Tas1r2*	taste receptor type 1 member 2
	48	0.997	0.0	0.01	0.304	0.5	-0.16	*Glut1*	glucose transporter member 1
	49	0.991	0.0	-0.08	0.043	1.4	0.23	*Glut3*	glucose transporter member 3
	50	0.991	0.0	0.24	0.790	0.1	-0.19	*Glut4*	glucose transporter member 4
	51	0.995	0.0	0.04	0.623	0.2	0.25	*Glut5*	glucose transporter member 5
	52	0.991	0.0	0.13	0.838	0.1	-0.06	*Glut6*	glucose transporter member 6
	53	0.991	0.0	0.30	0.418	0.4	0.24	*P2ry1*	P2Y purinoceptor 1
	54	0.997	0.0	0.00	0.836	0.1	-0.03	*Fgfr1*	fibroblast growth factor receptor 1
	55	0.991	0.0	0.08	0.803	0.1	-0.04	*Insr*	insulin receptor
	56	0.991	0.0	0.10	0.448	0.3	0.23	*Lepr*	leptin receptor
	57	0.996	0.0	-0.06	outlier			*Agrp*	agouti-related protein
	58	0.991	0.0	-0.10	0.398	0.4	0.28	*Cartpt*	cocaine- and amphetamine-regulated transcript protein
	59	0.015	1.8	-1.05	0.183	0.7	0.40	*Pomc*	pro-opiomelanocortin
	60	0.991	0.0	-0.21	0.829	0.1	0.11	*Mc3r*	melanocortin receptor 3
	61	0.869	0.1	-0.57	0.491	0.3	0.40	*Mc4r*	melanocortin receptor 4
	62	0.063	1.2	-0.62	0.061	1.2	-0.54	*Npy*	pro-neuropeptide Y
	63	0.991	0.0	-0.14	0.063	1.2	0.27	*Npy1r*	neuropeptide Y receptor type 1
	64	0.991	0.0	-0.23	0.442	0.4	0.36	*Npy2r*	neuropeptide Y receptor type 2
	65	0.996	0.0	-0.11	outlier			*Qrfp*	orexigenic neuropeptide QRFP
	66	0.991	0.0	0.46	0.479	0.3	0.47	*Qrfpr*	pyroglutamylated RF-amide peptide receptor
	67	0.991	0.0	0.05	0.379	0.4	-0.10	*Ncam1*	neural cell adhesion molecule 1
	68	0.991	0.0	-0.33	0.431	0.4	0.27	*Vim*	vimentin, cytosceleton of glial cells

3.8.2 Supplementary File 2: Processing Pipeline

```
# Bash-Script version of 13.02.2021 09:00 as provided by Elena Haugg, working group Annika Herwig, Institute of Neurobiology, Ulm University, Germany, 2021
# contact: elena.haugg@uni-ulm.de


#for each sample: prepare reads (here: paired end reads, 1 lane, from Illumina NextSeq 500)

#command: trim_galore –paired –cores <number of cores> <"forward / left" file(s) (read 1 = R1) in format .fastq.gz, space-separated> <"reverse / right" file(s) (read 2 = R2) in format .fastq.gz, space-separated>
trim_galore --paired --cores 1 *SPHT02_R1.fastq.gz *SPHT02_R2.fastq.gz &
trim_galore --paired --cores 1 *SPHT10_R1.fastq.gz *SPHT10_R2.fastq.gz &
trim_galore --paired --cores 1 *SPHT26_R1.fastq.gz *SPHT26_R2.fastq.gz &
trim_galore --paired --cores 1 *SPHT33_R1.fastq.gz *SPHT33_R2.fastq.gz &
trim_galore --paired --cores 1 *LPNT01_R1.fastq.gz *LPNT01_R2.fastq.gz &
trim_galore --paired --cores 1 *LPNT02_R1.fastq.gz *LPNT02_R2.fastq.gz &
trim_galore --paired --cores 1 *LPNT03_R1.fastq.gz *LPNT03_R2.fastq.gz &
trim_galore --paired --cores 1 *LPNT05_R1.fastq.gz *LPNT05_R2.fastq.gz &
trim_galore --paired --cores 1 *SPNT19_R1.fastq.gz *SPNT19_R2.fastq.gz &
trim_galore --paired --cores 1 *SPNT36_R1.fastq.gz *SPNT36_R2.fastq.gz &
trim_galore --paired --cores 1 *SPNT37_R1.fastq.gz *SPNT37_R2.fastq.gz &
trim_galore --paired --cores 1 *SPNT38_R1.fastq.gz *SPNT38_R2.fastq.gz &
wait
#output is a *val_1.fq.gz for all "forward / left" files and a *val_2.fq.gz for all "reverse / right" files


#for each organism: de novo assembly

#command: Trinity –seqType <file format> --max_memory <threshold> --CPU <all available CPU> --min_kmer_cov 2 --bflyCalculateCPU –left <R1 fastq files, comma-separated> <R2 fastq files, comma-separated>
#note: high performance computing (HPC) is needed! All other commands can be performed on a good linux computer.
Trinity --seqType fq --max_memory 100G --CPU 20 --min_kmer_cov 2 --bflyCalculateCPU --left SPHT02_R1_val_1.fq.gz,SPHT10_R1_val_1.fq.gz,SPHT26_R1_val_1.fq.gz,SPHT33_R1_val_1.fq.gz,LPNT01_R1_val_1.fq.gz,LPNT02_R1_val_1.fq.gz,LPNT03_R1_val_1.fq.gz,LPNT05_R1_val_1.fq.gz,SPNT19_R1_val_1.fq.gz,SPNT36_R1_val_1.fq.gz,SPNT37_R1_val_1.fq.gz,SPNT38_R1_val_1.fq.gz --right SPHT02_R2_val_2.fq.gz,SPHT10_R2_val_2.fq.gz,SPHT26_R2_val_2.fq.gz,SPHT33_R2_val_2.fq.gz,LPNT01_R2_val_2.fq.gz,LPNT02_R2_val_2.fq.gz,LPNT03_R2_val_2.fq.gz,LPNT05_R2_val_2.fq.gz,SPNT19_R2_val_2.fq.gz,SPNT36_R2_val_2.fq.gz,SPNT37_R2_val_2.fq.gz,SPNT38_R2_val_2.fq.gz
#rename output to e.g., Trinity-Hypothalamus-Phodopus-ZT04.fasta


#for each organism-reference-combination: mapping

#command: makeblastdb -in <reference proteome fasta> -parse_seqids -title <"name"> -dbtype <prot> -out <name of output>
#reference proteome of Mus musculus (GRCm39, Annotation Release 109) was downloaded via NCBI https://www.ncbi.nlm.nih.gov/genome/?term=txid10090[orgn]
makeblastdb -in GCF_000001635.27_GRCm39_protein.faa -parse_seqids -title "Mus musculus 39 proteome" -dbtype prot -out mus_proteome

#command: blastx -db <name of makeblastdb output> -query <Trinity-output> -out <name of output> -evalue <threshold> -outfmt <output-format, 6 is table> -num_threads <number of available CPU>
blastx -db mus_proteome -query Trinity-Hypothalamus-Phodopus-ZT04.fasta -out blastx_ham -evalue 1E-5 -outfmt 6 -num_threads 20
```

```
#command: ruby extract_hits_from_fasta.rb <Trinity-output> <blastx-output> <name of output>
ruby extract_hits_from_fasta.rb Trinity-Hypothalamus-Phodopus-ZT04.fasta blastx_ham Trinity-Hypothalamus-Phodopus-ZT04_aftermapping.fasta

#command: ruby hits_to_genemap.rb <blastx-output> <reference annotation> <name of output>
#Mus musculus (GRCm39, Annotation Release 109) was downloaded via NCBI in tabular format (.txt) https://www.ncbi.nlm.nih.gov/genome/?term=txid10090[orgn]
ruby hits_to_genemap.rb blastx_ham proteins_52_992563.txt genemap_ham.txt

#command: rsem-prepare-reference --bowtie --transcript-to-gene-map <name of genemap output> <name of extract hits output> <name of output>
rsem-prepare-reference --bowtie --transcript-to-gene-map genemap_ham.txt Trinity-Hypothalamus-Phodopus-ZT04_aftermapping.fasta preparedmap-ham


#for each sample: rsem-output

#gunzip output of trim-galore with command: gunzip *.fq.gz
gunzip SPHT02_R1_val_1.fq.gz
gunzip SPHT02_R2_val_2.fq.gz
gunzip SPHT10_R1_val_1.fq.gz
gunzip SPHT10_R2_val_2.fq.gz
gunzip SPHT26_R1_val_1.fq.gz
gunzip SPHT26_R2_val_2.fq.gz
gunzip SPHT33_R1_val_1.fq.gz
gunzip SPHT33_R2_val_2.fq.gz
gunzip SPNT19_R1_val_1.fq.gz
gunzip SPNT19_R2_val_2.fq.gz
gunzip SPNT36_R1_val_1.fq.gz
gunzip SPNT36_R2_val_2.fq.gz
gunzip SPNT37_R1_val_1.fq.gz
gunzip SPNT37_R2_val_2.fq.gz
gunzip SPNT38_R1_val_1.fq.gz
gunzip SPNT38_R2_val_2.fq.gz
gunzip LPNT01_R1_val_1.fq.gz
gunzip LPNT01_R2_val_2.fq.gz
gunzip LPNT02_R1_val_1.fq.gz
gunzip LPNT02_R2_val_2.fq.gz
gunzip LPNT03_R1_val_1.fq.gz
gunzip LPNT03_R2_val_2.fq.gz
gunzip LPNT05_R1_val_1.fq.gz
gunzip LPNT05_R2_val_2.fq.gz

#command: rsem-calculate-expression --paired-end -p <number of CPU> –left <forward file(s) (R1_val_1) in format .fq, comma-separated> <backward file(s) (R2_val_2) in format .fq, comma-separated> <name of rsem-prepare-reference-output> <name of the sample>
rsem-calculate-expression --paired-end -p 20 SPHT02_R1_val_1.fq SPHT02_R2_val_2.fq preparedmap-ham SPHT02
wait
rsem-calculate-expression --paired-end -p 20 SPHT10_R1_val_1.fq SPHT10_R2_val_2.fq preparedmap-ham SPHT10
wait
rsem-calculate-expression --paired-end -p 20 SPHT26_R1_val_1.fq SPHT26_R2_val_2.fq preparedmap-ham SPHT26
wait
```

```
rsem-calculate-expression --paired-end -p 20 SPHT33_R1_val_1.fq SPHT33_R2_val_2.fq preparedmap-ham
    SPHT33
wait
rsem-calculate-expression --paired-end -p 20 SPNT19_R1_val_1.fq SPNT19_R2_val_2.fq preparedmap-ham
    SPNT19
wait
rsem-calculate-expression --paired-end -p 20 SPNT36_R1_val_1.fq SPNT36_R2_val_2.fq preparedmap-ham
    SPNT36
wait
rsem-calculate-expression --paired-end -p 20 SPNT37_R1_val_1.fq SPNT37_R2_val_2.fq preparedmap-ham
    SPNT37
wait
rsem-calculate-expression --paired-end -p 20 SPNT38_R1_val_1.fq SPNT38_R2_val_2.fq preparedmap-ham
    SPNT38
wait
rsem-calculate-expression --paired-end -p 20 LPNT01_R1_val_1.fq LPNT01_R2_val_2.fq preparedmap-ham
    LPNT01
wait
rsem-calculate-expression --paired-end -p 20 LPNT02_R1_val_1.fq LPNT02_R2_val_2.fq preparedmap-ham
    LPNT02
wait
rsem-calculate-expression --paired-end -p 20 LPNT03_R1_val_1.fq LPNT03_R2_val_2.fq preparedmap-ham
    LPNT03
wait
rsem-calculate-expression --paired-end -p 20 LPNT05_R1_val_1.fq LPNT05_R2_val_2.fq preparedmap-ham
    LPNT05
wait
#rsem output per sample are two files, .isoforms.results (not used) and .genes.results (used)
```

3.8.3 Supplementary File 3: R-Statistics

```
# R-Script version of 20210214 as provided by Elena Haugg
# executed by Elena Haugg, working group Annika Herwig, Institute of Neurobiology, Ulm University, Germany, 2021
# Contact: elena.haugg@uni-ulm.de

# RStudio version 5.3.2 (R Core Team 2018; RStudio Team 2020)
# please find R session info at the end of this document


# activation of packages, which must be installed before
library("tximport") # (Soneson et al. 2015)
library("DESeq2") # (Love et al. 2014, 2019, 2020) # an alternative of DESeq2's dds is edgR's TMM
library("apeglm") # (Zhu et al. 2019)
library("RColorBrewer") # (Neuwirth 2014)
library("pheatmap") # (Kolde 2019)


######################
######### SP: HT vs NT
######################

### data import
setwd("H:/NGS-Business/Statistics/WH-Ham/SPHTvsSPNT") # set working directory to the pairwise group comparison folder. It contains a .csv where you state the sample document names and the group of each sample (see next command). Furthermore, this folder contains the rsem-output in format .genes.results within a sub-folder called "rsem".
samples <- read.csv(file.path("Samples_SPHTvsSPNT.csv")) # tell the sample names and the sample groups. The .csv has one column with header "id,group" (no space in between). It has one line per sample with the sample name (without file extention) and the sample group, comma separated without spaces. Take all samples for outlier assessment. To get the results of this pairwise comparison, state all samples except the outliers. Warning: The output file of this script is only correct for pairwise comparison of two groups.
files <- file.path("rsem", paste0(samples$id, ".genes.results")) # tell where to find the data, namely the folder "rsem" within the working directory. Use the exact terms of the .csv, expanded to the full document name inclusively the file format (.genes.results, which is an output file of rsem). There is no need to delete outliers within the subfolder "rsem".
names(files) <- samples$id # tell where to find the sample IDs, namely in column "id" of the .csv
txi.rsem <- tximport(files, type = "rsem") # import the data, which type is rsem (irrespectively of the subfolder name).

### First data normalization, for Likelihood ratio test (LRT)
dds <- DESeqDataSetFromTximport(txi.rsem, colData = samples, design = ~ group) # txi.sem is the count matrix. Table of sample information (colData) is the .csv. Design is comparing groups, with groups stated in the .csv.
keep <- rowSums(counts(dds)) >= 10 # threshold: same or more than 10 counts per column
dds <- dds[keep,] # dds is overwritten with data fulfilling threshold

### Likelihood ratio test (LRT), for Cook's Distance Outliers
dds.LRT <- DESeq(dds, test="LRT", reduced=~1)
res.LRT <- results(dds.LRT)
res.LRT.Ordered <- res.LRT[order(res.LRT$pvalue),]
# write.csv(as.data.frame(res.LRT.Ordered), file="DESeq_1resLRTOrdered.csv") # you might use this output as control

### Second data normalization, for RESULTS and Cook's Distance Outliers
dds <- DESeq(dds) # dds is overwritten
res <- results(dds)
```

```
summary(res) # when thousands of outliers, check for quality and removal
resOrdered <- res[order(res$pvalue),]
# write.csv(as.data.frame(resOrdered),file="Deseq_2resOrdered.csv") # you might use this output as control
res.SPHT.SPNT <- results(dds, contrast=c("group", "SPHT", "SPNT")) # refer to the groups as stated in the .csv
write.csv(as.data.frame(resOrdered),file="SPHTvsSPNT.csv") # name the output file according to the performed comparison
# the results .csv with the normalized differentially gene expression is for further procession (e.g. indicator genes, most extremely expressed genes).

### Cook's Distance Outliers, for PCA and Heatmap
vsd <- vst(dds, blind=FALSE)
vsd_assay <- assay(vsd) # find outliers with Cook's Distance (the bigger the distance, the more likely an outlier) and replace outlying values by trimmed mean
vsd_assay.Ordered <- assay(vsd)[order(match(row.names(vsd_assay),row.names(res.LRT.Ordered))),]
# write.csv(as.data.frame(vsd_assay.Ordered), file="Deseq_3vsdAssayOrdered.csv") # you might use this output as control
plotPCA(vsd, intgroup=c("group")) ### PCA – for outlier assessment

### Heatmap, as additional visualization
select <- order(rowMeans(counts(dds,normalized=TRUE)), decreasing=TRUE)[1:20]
df <- as.data.frame(colData(dds)[,c("group","id")])
sampleDists <- dist(t(assay(vsd)))
sampleDistMatrix <- as.matrix(sampleDists)
rownames(sampleDistMatrix) <- paste(vsd$group, vsd$id, sep="-")
colnames(sampleDistMatrix) <- NULL
colors <- colorRampPalette( rev(brewer.pal(9, "Blues")) )(255)
pheatmap(sampleDistMatrix, clustering_distance_columns=sampleDists, clustering_distance_cols=sampleDists, col=colors)

######################
######### NT: SP vs LP
######################

### data import
setwd("H:/NGS-Business/Statistics/WH-Ham/SPNTvsLPNT") # set working directory to the pairwise group comparison folder. It contains a .csv where you state the sample document names and the group of each sample (see next command). Furthermore, this folder contains the rsem-output in format .genes.results within a sub-folder called "rsem".
samples <- read.csv(file.path("Samples_SPNTvsLPNT.csv")) # tell the sample names and the sample groups. The .csv has one column with header “id,group” (no space in between). It has one line per sample with the sample name (without file extention) and the sample group, comma separated without spaces. Take all samples for outlier assessment. To get the results of this pairwise comparison, state all samples except the outliers. Warning: The output file of this script is only correct for pairwise comparison of two groups.
files <- file.path("rsem", paste0(samples$id, ".genes.results")) # tell where to find the data, namely the folder “rsem” within the working directory. Use the exact terms of the .csv, expanded to the full document name inclusively the file format (.genes.results, which is an output file of rsem). There is no need to delete outliers within the subfolder "rsem".
names(files) <- samples$id # tell where to find the sample IDs, namely in column "id" of the .csv
txi.rsem <- tximport(files, type = "rsem") # import the data, which type is rsem (irrespectively of the subfolder name).

### First data normalization, for Likelihood ratio test (LRT)
dds <- DESeqDataSetFromTximport(txi.rsem, colData = samples, design = ~ group) # txi.sem is the count matrix. Table of sample information (colData) is the .csv. Design is comparing groups, with groups stated in the .csv.
keep <- rowSums(counts(dds)) >= 10 # threshold: same or more than 10 counts per column
dds <- dds[keep,] # dds is overwritten with data fulfilling threshold
```

```
### Likelihood ratio test (LRT), for Cook's Distance Outliers
dds.LRT <- DESeq(dds, test="LRT", reduced=~1)
res.LRT <- results(dds.LRT)
res.LRT.Ordered <- res.LRT[order(res.LRT$pvalue),]
# write.csv(as.data.frame(res.LRT.Ordered), file="DESeq_1resLRTOrdered.csv") # you might use this output as control

### Second data normalization, for RESULTS and Cook's Distance Outliers
dds <- DESeq(dds) # dds is overwritten
res <- results(dds)
summary(res) # when thousands of outliers, check for quality and removal
resOrdered <- res[order(res$pvalue),]
# write.csv(as.data.frame(resOrdered),file="Deseq_2resOrdered.csv") # you might use this output as control
res.SPNT.LPNT <- results(dds, contrast=c("group", "SPNT", "LPNT")) # refer to the groups as stated in the .csv
write.csv(as.data.frame(resOrdered),file="SPNTvsLPNT.csv") # name the output file according to the performed comparison
# the results .csv with the normalized differentially gene expression is for further procession (e.g. indicator genes, most extremely expressed genes).

### Cook's Distance Outliers, for PCA and Heatmap
vsd <- vst(dds, blind=FALSE)
vsd_assay <- assay(vsd) # find outliers with Cook's Distance (the bigger the distance, the more likely an outlier) and replace outlying values by trimmed mean
vsd_assay.Ordered <- assay(vsd)[order(match(row.names(vsd_assay),row.names(res.LRT.Ordered))),]
# write.csv(as.data.frame(vsd_assay.Ordered), file="Deseq_3vsdAssayOrdered.csv") # you might use this output as control
plotPCA(vsd, intgroup=c("group")) ### PCA – for outlier assessment


### Heatmap, as additional visualization
select <- order(rowMeans(counts(dds,normalized=TRUE)), decreasing=TRUE)[1:20]
df <- as.data.frame(colData(dds)[,c("group","id")])
sampleDists <- dist(t(assay(vsd)))
sampleDistMatrix <- as.matrix(sampleDists)
rownames(sampleDistMatrix) <- paste(vsd$group, vsd$id, sep="-")
colnames(sampleDistMatrix) <- NULL
colors <- colorRampPalette( rev(brewer.pal(9, "Blues")) )(255)
pheatmap(sampleDistMatrix, clustering_distance_columns=sampleDists, clustering_distance_cols=sampleDists, col=colors)


##############################
### R session info (20210212)
##############################

# R version 3.5.2 (2018-12-20)
# Platform: x86_64-w64-mingw32/x64 (64-bit)
# Running under: Windows 10 x64 (build 17134)

# Matrix products: default

# locale:
#  [1] LC_COLLATE=German_Germany.1252  LC_CTYPE=German_Germany.1252  LC_MONETARY=German_Germany.1252
# [4] LC_NUMERIC=C                    LC_TIME=German_Germany.1252

# attached base packages:
```

```
# [1] stats4    parallel  stats     graphics  grDevices utils     datasets  methods   base

# other attached packages:
#  [1] RColorBrewer_1.1-2         pheatmap_1.0.12           apeglm_1.4.2              DESeq2_1.22.2
#  [5] SummarizedExperiment_1.12.0 DelayedArray_0.8.0        BiocParallel_1.16.6       matrixStats_0.56.0
#  [9] tximport_1.10.1            AnnotationDbi_1.44.0      Biobase_2.42.0            GenomicRanges_1.34.0
# [13] GenomeInfoDb_1.18.2        IRanges_2.16.0            S4Vectors_0.20.1          BiocGenerics_0.28.0

# loaded via a namespace (and not attached):
#  [1] bitops_1.0-6          bit64_0.9-7           progress_1.2.2        httr_1.4.1            numDeriv_2016.8-1.1
#  [6] tools_3.5.2           backports_1.1.6       R6_2.4.1              rpart_4.1-13          Hmisc_4.4-0
# [11] DBI_1.1.0             colorspace_1.4-1      nnet_7.3-12           tidyselect_1.0.0      gridExtra_2.3
# [16] prettyunits_1.1.1     bit_1.1-15.2          compiler_3.5.2        htmlTable_2.0.0       labeling_0.3
# [21] scales_1.1.1          checkmate_2.0.0       mvtnorm_1.1-0         readr_1.3.1           genefilter_1.64.0
# [26] stringr_1.4.0         digest_0.6.25         Rsamtools_1.34.1      foreign_0.8-71        XVector_0.22.0
# [31] base64enc_0.1-3       pkgconfig_2.0.3       htmltools_0.4.0       bbmle_1.0.23.1        htmlwidgets_1.5.1
# [36] rlang_0.4.5           rstudioapi_0.11       RSQLite_2.2.0         farver_2.0.3          acepack_1.4.1
# [41] dplyr_0.8.5           RCurl_1.98-1.2        magrittr_1.5          GenomeInfoDbData_1.2.0 Formula_1.2-3
# [46] Matrix_1.2-15         Rcpp_1.0.4.6          munsell_0.5.0         lifecycle_0.2.0       stringi_1.4.6
# [51] MASS_7.3-51.1         zlibbioc_1.28.0       plyr_1.8.6            grid_3.5.2            blob_1.2.1
# [56] bdsmatrix_1.3-4       crayon_1.3.4          lattice_0.20-38       Biostrings_2.50.2     splines_3.5.2
# [61] annotate_1.60.1       hms_0.5.3             locfit_1.5-9.4        knitr_1.25            pillar_1.4.4
# [66] geneplotter_1.60.0    biomaRt_2.38.0        XML_3.99-0.3          glue_1.4.0            latticeExtra_0.6-28
# [71] data.table_1.12.8     vctrs_0.2.4           gtable_0.3.0          purrr_0.3.4           assertthat_0.2.1
# [76] ggplot2_3.3.2         emdbook_1.3.12        xfun_0.13             xtable_1.8-4          coda_0.19-3
# [81] survival_2.43-3       tibble_3.0.1          memoise_1.1.0         cluster_2.0.7-1       ellipsis_0.3.0
```

Chapter 4

Time to Enter Torpor: Transcriptomics of the Djungarian Hamster Hypothalamic Core Areas Suprachiasmatic Nucleus and Paraventricular Nucleus

Authors: Elena Haugg, Janus Borner, Annika Herwig

This chapter was written as a manuscript for submission but is unpublished.

Contribution: All authors conceived the project. The author of this dissertation, EH, performed the animal work. EH performed the bioinformatics, statistics, and data analyses under supervision of JB. EH and AH interpreted the data. EH wrote the manuscript, which was carefully revised by AH. All authors agree to be accountable for the content of the work.

Keywords: RNA-Seq, gene expression, metabolism, spontaneous daily torpor, hypothermia, Siberian hamster, *Phodopus sungorus,* hypothalamus

Abbreviations:

HT: hypothermia

log2(FC): logarithm of a gene`s fold change to the base 2

NT: normothermia

padj: adjusted p-value of a gene`s expression

PVN: paraventricular nucleus

SCN: suprachiasmatic nucleus

Tb: core body temperature

ZT: *Zeitgeber*-time, here: lights on at ZT0

Acknowledgements: I like to thank supporters of Ulm University for their help and advice regarding the LMD-project in 2019 and 2020, in particular Elisabeth Picca and Sabine Schmidt for breeding and keeping of hamsters, Dr. Victoria Diedrich for assisting during implantation and sampling of animals, Dr. Carola Dreier for supervising the lab work, Diana Krattenmacher and Dr. Christoph Wiegreffe of the Core Facility Lasermicrodissection for their valuable contribution in developing an adequate sampling of hypothalamic core areas and coating the MembraneSlides, Dr. Karlheinz Holzmann of the Core Facility Genomics for assessment of the preliminary samples' RNA quality and quantity, and furthermore Dr. Sven-Ernö Bikar and Dr. Tilmann Laufs of StarSeq GmbH Mainz for their RNA-Seq service. The bioinformatics was performed on the computational resource bwForCluster NEMO. The authors acknowledge support by the state of Baden-Württemberg through bwHPC and the German Research Foundation (DFG) through grant no INST 39/963-1 FUGG (bwForCluster NEMO).

4.1 Abstract

Anticipating harsh environmental conditions, Djungarian hamsters *(Phodopus sungorus)* adapt to winter-like short photoperiod by morphological, behavioral, and physiological adaptations, including spontaneous torpor, a metabolic downstate to save additional energy. The nocturnal hamsters express torpor for several hours during the day and remain active on torpor-free days as well as every night. There is evidence, that these fine-tuned mechanisms in torpor control are orchestrated by feedback loops within the hypothalamus, which integrates external and internal signals to control circadian rhythms. Two hypothalamic core areas are particularly promising to be involved in torpor regulation. The suprachiasmatic nucleus (SCN) is the master circadian clock in all mammals, while the paraventricular nucleus (PVN) is a neuroendocrine interface between SCN, pituitary gland and bloodstream.

For this study, Djungarian hamsters were raised in long photoperiod (16:8 light:darkness). After 14 ± 1 weeks in short photoperiod (SP, 8:16 light:darkness), twelve animals were sampled one hour after lights on either hypothermic during torpor entry (HT, n = 6, Tb = 30.0 ± 0.3 °C) or normothermic on a torpor-free day (NT, n = 6, Tb = 35.9 ± 1.3 °C). SCN as well as the PVN were lasermicrodissected using cresyl violet stained cryosections of the hypothalamus. After purification of total RNA, isolation, and sequencing of mRNA, a *de novo* assembly of transcriptomes were generated and mapped against annotated genes of *Mus musculus*. The sampling groups HT and NT were compared pairwise for each SCN and PVN.

In HT-SCN, 181 genes were up- and 690 genes were downregulated. A GO enrichment analysis revealed enhanced metabolic processes. Several indicator genes from torpor-relevant systems screened for were downregulated, namely the transcription factor *Junb*, vasopressin and one of its receptors, the circadian clock genes *Mta1* and *Timeless*, monocarboxylate-transporter 8 and the P2Y purinoceptor 1. Furthermore, the 66 genes with a fold change of at least two were discussed. In HT-PVN, only 14 genes were regulated, yet with various functions. A downregulation of the E3 ubiquitin-protein ligase *Marchf1* might indicate a decreased degradation of insulin receptors leading to increased insulin sensitivity within PVN during torpor entry. These results point towards a severe remodeling of the circadian clockwork potentially altering clock output to induce torpor, while

mitochondria, systemic signaling and metabolism, transcription and modification, cell cycle, and brain plasticity might also be of relevance.

4.2 Introduction

Seasonal acclimatizations and metabolic downstates, like hibernation, spontaneous torpor, starvation torpor as well as estivation, are expressed by all orders of mammals to overcome harsh environmental conditions [23–25]. Knowledge about natural hypometabolism including hypothermia of endotherms is potentially applicable for medical use and long-distance space flights [26–28]. Mechanisms underlying torpor control however, are still unclear [2,22,44].

The photoperiodic Djungarian hamster *(Phodopus sungorus)*, spontaneously uses daily torpor as one of multiple reversible physiological, morphological, and behavioral changes to overcome winter. As soon as the daylength falls below 13 hours per day, regardless if in nature or due to a switch of light regime in artificial conditions, the fat, reproductive "summer" hamster with brown fur anticipates harsh winter-like conditions [60,61]. It gradually reduces locomotor activity, food intake, body mass, and mean body temperature, while reproductive organs are receded towards an optimization of the overall energy balance [63–66,119]. After about three months of acclimation to short photoperiod, the hamster has turned into a lean, non-reproductive "winter" hamster with white, dense, more insulating fur [60,61].

After the morphological adaptations have been largely completed, spontaneous torpor, a metabolic downstate, might be expressed to save additional energy, even when the hamster is provided with nesting material, food and water *ad libitum,* and 20 °C ambient temperature. Hereby, torpor is initialized, maintained, and reversed within the few hours of photophase, while the nocturnal Djungarian hamster is active during the scotophase and on torpor-free days [57,60,119].

Torpor is characterized by drastic, reversible reduction of metabolic rate, and, in turn, heart rate, ventilation, and body temperature [41,58,70]. There is evidence that the

hypothalamus is involved in torpor control. The hypothalamus controls circadian rhythms, homeostasis of body temperature, blood pressure and food intake, as well as reproduction, all of them relevant for photoperiodic acclimation, mediation of energy metabolism and torpor expression [29,44]. Hereby, the hypothalamic core areas and cell populations play distinct roles in these complex physiological processes [22,32].

The suprachiasmatic nucleus (SCN) is the mammalian master circadian clock within the hypothalamus and involved in the retinohypothalamic pathway [100,120]. The clockwork of nocturnal rodents like mice and hamster comprises a fine-tuned feedback loop. The Clock-Bmal1-heterodimer is enhancing and suppressed by the Per-Cry-heterodimer. This oscillating equilibrium is modulated by further major players of the circadian clock. Clock-Bmal1 is enhancing Rev-Erb and Ror, while Rev-Erb suppresses and Ror enhances Clock-Bmal1. Per proteins are phosphorylated by CK1δ/ε, while the role of Tim remains unclear. This clock circle is reset by external cues, as light, which alter transcription and protein turnover [98,121]. Day length is mediated by melatonin (Mel), in interaction with systemic neuropeptides and hormones, as the luteinizing hormone (LH), catecholamines, the gonadotropin-releasing hormone (GnRH), beta-endorphin, and opiates [66,79,80,110]. Hereby, brain anatomy, neuronal signaling and functional pathways are based on general principles, with species-specific character [99,122]. Therefore, knowledge gained from one model organism is not necessarily directly applicable to others.

The SCN is likely to synchronize the strongly circadian gated torpor bouts with the external light-dark-rhythm [54]. Given a short photoperiod of 8:16 hours light:darkness, the typical body temperature (Tb) pattern during a torpor bout is described with torpor entry ($T_b < 32$ °C) around ZT01, deep torpor ($T_b = 24$ °C) around ZT04, and torpor arousal ($T_b > 32$ °C) around ZT07, while ZT stands for *Zeitgeber*-time [42]. Timing of torpor entry and arousal with the external cues *lights on* and *lights off* might be explained by single-cell suprachiasmatic neurons. Although self-oscillating, they rely on the networks` information about the circadian rhythm [101,102,123]. There is evidence, that genes and proteins of the circadian clock maintain rhythmic expression in heart, lung, liver, pineal gland, and SCN during a torpor bout of the Djungarian hamster, yet with altered turnover resulting from inactivation and degradation [124,125]. SCN ablation can prevent acclimation to short photoperiod as well as torpor expression [110,126]. By contrast, SCN lesion in combination

with food restriction can cause the expression of multiple torpor bouts per day [127]. This points towards the relevance of SCN in timing of torpor onset, while the mechanisms to control course of the metabolic downstate do not lie exclusively within the SCN.

Downstream of the SCN, in interplay with the supraoptic nucleus, the paraventricular nucleus (PVN) mediates and modulates neuroendocrine signals and influences the sympathetic nervous system [103,104,106,107]. Transcription of the immediate early gene *c-Fos,* inducible by stimuli, such as light and dehydration, seem to allow the communication between SCN and PVN as well as between supraoptic nucleus and PVN [105,109]. Hereby, vasopressin (*Avp*) neurons of the SCN likely project to the oxytocin (*Oxt*) neurons of PVN. So, feeding and locomotor activity are suppressed during the resting phase [108].

In the Djungarian hamster, PVN lesions increased food intake and body mass, and prevented acclimation to short photoperiod [110,111]. Since the PVN regulates body mass and energy metabolism and is involved in circadian rhythm, an at least indirect influence of PVN on torpor expression is likely [112,113].

Aiming to investigate torpor orchestration on mRNA level, two transcriptomic studies analyzed the differential gene expression in the whole hypothalamus of hamsters sacrificed during torpor or on a torpor-free day. One study focused on torpor entry (ZT01) and the other on deep torpor (ZT04). Predominantly general adaptive mechanisms resulting from the metabolic depression and reduced body temperature have been found [118,128].

To target the hypothalamus in a higher anatomic resolution, the hypothalamic core areas SCN and PVN were lasermicrodissected from hamsters sacrificed around ZT01 either in torpor entry with a Tb of 30 °C or on a torpor-free day with normothermic Tb values. Animal work as well as the bioinformatics, statistics and analyses were performed analogous to a previous study [128]. We hypothesize, that altered SCN activity is an important factor driving the animal into torpor.

4.3 Materials and Methods

4.3.1 Animal work

4.3.1.1 Breeding and housing

The twelve Djungarian hamsters *(Phodopus sungorus)* used in this study were bred in summer 2019 and in February 2020 at the Institute of Neurobiology (Ulm University, Germany) in accordance with the local ethics committee (35/9185.46-3). Animals were housed under same conditions as described for earlier studies [119,128]. The indoors breeding colony was housed in summer-like long photoperiod (LP; 16:8 light:darkness) provided by artificial light (150 lux). Additional constant red light (<5 lux) enabled animal handling during the scotophase. From the age of six weeks, the hamsters were single housed in Makrolon Type III cages (26.5 x 42.5 x 18.0 cm) with wooden bedding and tissue as nesting material.

4.3.1.2 Experimental setup

Twelve adult hamsters (8 males, 4 females) were transferred to short photoperiod (SP; 8:16 light:darkness) at an age of 17 ± 2 weeks. Regardless of the light regime, the hamsters were housed at an ambient temperature of 20 ± 1 °C with tap water and food (Altromin hamster breeding diet 7014, Lage, Germany) *ad libitum*, and cucumber, oak flakes, and sunflower seeds once a week. The degree of adaptation was assessed weekly by body mass as well as fur index according to [60] with 1, light brown summer fur and 6, dense white winter fur. Background information on each hamster is provided (Supplementary Table 1).

4.3.1.3 Radiotelemetry

For organizational reasons, five hamsters were implanted with a radiotelemetry transmitter prior to the change of photoperiod at an age of 13± 1 weeks, while seven hamsters were implanted after the change of photoperiod at an age of 19 ± 2 weeks. Torpor was assessed using core body temperature (Tb), as previously described [119,128]. A radiotelemetry system (DSI - Data Sciences International, Harvard Bioscience Inc., St. Paul, MN, USA) with DataQuest™ ArtBronze software was used. The receiver board (RPC-1) was placed under each individual home cage. A transmitter (model TA-11TA-F10,

silicone-coated, 1.1 cc volume, 1.6 g weight, 0.15 °C accuracy) was implanted intraperitoneally under isoflurane anesthesia (2.5 % and 1 ml/min for induction, 0.75 – 2.0 % and 0.4 ml/min for maintenance) and carprofen analgesia (5 mg/kg i.p. Rimadyl®, Zoetis Deutschland GmbH, Berlin). Recovery from surgery was supported by additional oat flakes, sunflower seeds, cucumber, and nesting material. Body mass, coat care, posture, and behavior were monitored daily for about seven days until recovery. Experimental and surgical procedures were approved by the Regierungspräsidium Tübingen, Germany (1411).

4.3.1.4 Sampling scheme

Spontaneous daily torpor was defined as a core body temperature below 32 °C for at least 30 minutes [41,42,129]. All hamsters of this study expressed torpor at least once. The hamsters were sacrificed after 14 ± 1 weeks of SP-acclimation approximately one hour after the beginning of the photophase (*Zeitgeber*-time ZT01) either during torpor entry (HT, n = 6, 4 males, 2 females) or when normothermic on the day of sampling (NT, n = 6, 4 males, 2 females) (Figure 1). The body temperature patterns of the last day and the day before are provided (Supplementary Figure 1). Radiotelemetry data from ten of the twelve hamsters was analyzed previously [119]. The hamsters were sacrificed with carbon dioxide. After decapitation, the brain was shock-frozen using dry ice and stored at -80 °C.

4.3.2 Lab work

4.3.2.1 Preparations

To maintain lab work in a RNAse-poor environment, gloves, all surfaces, non-heat resistant instruments as well as the defrosted cryostat were cleaned prior to use with 70 % ethanol and Thermo Scientific™ RNase AWAY™ surface decontaminant (Fisher Scientific GmbH, Schwerte, Germany). Plastic instruments underwent incubation for at least 12 hours at 37 °C in 0.1 % DEPC-Aqua dd., followed by heating to 100 °C. Glass and metal ware was baked at least 3 hours at 180 °C. RNAse-free water was prepared by incubating 0.1 % DEPC-Aqua dd. for at least 12 hours at 37 °C, followed by autoclave. For staining solutions, this RNAse-free water and absolute ethanol (200 Proof, Molecular Biology Grade, Fisher BioReagents™; Fisher Scientific GmbH, Schwerte, Germany) were used. Per 250 mL,

2.5 g Cresyl violet powder with 50 % ethanol was stirred for 6 hours, filtered, and stored at 4 °C. 70 % ethanol was stored at -20 °C as well as at 4 °C. Absolute ethanol was stored at 4 °C. The Carl Zeiss™ MembraneSlides 1.0 PEN (Fisher Scientific GmbH, Schwerte, Germany) were coated with Poly-L-Lysine and UV-irradiated for 30 minutes just prior to usage.

4.3.2.2 Sectioning of the brain

Brains were sectioned and stained to lasermicrodissect the SCN and PVN. Within the chamber of a cryostat "Microm HM 560" (Thermo Scientific, Walldorf, Germany), the -19 °C brain was roughly trimmed with a hand-warm razor blade, mounted, and sectioned with the -17 °C steel blade from anterior to posterior. As soon as the anterior part of the anterior commissure fused at about Bregma -0.20 mm (according to the mouse brain atlas, Franklin and Paxinos 2008), the mounted brain was carefully fine-trimmed with a hand-warm razor blade to a hypothalamic column to sample the following 72 serial sections of about 5x3x0.02 mm in an 8x3 raster on not more than three prepared slides. This set of sections covered both the SCN, reaching from Bregma -0.22 mm to -0.82 mm, and the PVN, reaching from Bregma -0.22 mm to -1,06 mm. The sections were dried at ambient temperature.

4.3.2.3 Staining of cell nuclei and Nissl bodies

Using plastic screw cap cells with a volume of 50 mL, each slide was treated successively for one minute with frozen 70 % ethanol, for a half minute with cooled 1 % cresyl violet in 50 % ethanol dipped onto the horizontal slide by a disposable pipette, for one minute with cooled 70 % ethanol, and for one minute with cooled absolute ethanol. Each slide dried at room temperature while positioned vertically within a covered box. This cresyl violet enabled the detection of SCN and PVN at the lasermicroscope.

4.3.2.4 Lasermicrodissection of hypothalamic core areas

Of each brain, the hypothalamic core areas SCN and PVN were lasermicrodissected (Figure 2) from cresyl violet stained 0.02 mm thick sections spanning Bregma -0.22 mm to -1,06 mm (according to [99] using the PALM MicroBeam (Carl Zeiss Microscopy Deutschland GmbH, Oberkochen, Germany) with one Carl Zeiss™ adhesive-cap tube per sample (Fisher Scientific GmbH, Schwerte, Germany). First, the SCN was marked on 18 ± 4

sections using 260 ± 83 elements, followed by the lasercapturing of 1.1 ± 0.3 mm^2 area in total, resulting in a SCN sample volume of approximately 0.022 ± 0.006 mm^3. The tube with the SCN material was closed and incubated on ice. Second, the PVN was marked on 17 ± 2 sections using 243 ± 96 elements, followed by the lasercapturing of 1.0 ± 0.2 mm^2 area in total, resulting in a PVN sample volume of not more than 0.020 ± 0.005 mm^3. Values per sample are provided (Supplementary Table 2). Both the SCN sample and the PVN sample were filled with 50 µl RLT lysis buffer with 1:100 β-Mercaptoethanol, vortexed with lid downwards for 30 seconds, incubated with lid downwards on ice for 30 minutes, centrifuged at 12.000 rpm at room temperature for 5 minutes, and stored at -80°C.

4.3.2.5 From total RNA to sequencing of mRNA

The 24 samples (12 animals, 2 hypothalamic core areas) were thawed in a 37° C water bath 3 ± 2 days after lasermicrodissection. Total RNA was purified using the RNeasy Plus Micro Kit with gDNA eliminator spin column (Qiagen GmbH, Hilden, Germany) according to manufacturer's instructions. For further processing, the samples were sent to StarSEQ GmbH, Mainz, Germany. Total RNA was checked for quality (Bioanalyzer, Agilent Technologies, Waldbronn, Germany) and quantity (RNA 6000 Pico Kit for very small RNA amounts of 50–5000pg/µL, Agilent Technologies, Waldbronn, Germany). In SCN samples, the quality (RNA integrity number, RIN) was 8.8 ± 0.4, the quantity 424 ± 188 pg/µL, and the rRNA ratio (28s / 18s) 2.9 ± 1.1. In PVN samples, the quality (RNA integrity number, RIN) was 8.5 ± 0.6, the quantity 619 ± 312 pg/µL, and the rRNA ratio (28s / 18s) of 2.4 ± 1.3. Individual values are shown in Supplementary Table 3. The mRNA was isolated, the library prepared (NEBNext® Single Cell / Low Input RNA library Prep Kit dual index), and the RNA-Seq performed on an Illumina NextSeq 500 (1 lane, 2x25 mio reads, 2 x 150 nt, 7.5 gb).

4.3.3 Data work

4.3.3.1 Bioinformatics

The bioinformatical pipeline used in this study was identical with our previous transcriptomics approach [128]. Bioinformatics was performed on the bwForCluster NEMO of the Baden-Württemberg High Performance Computing (bwHPC) project. Data of raw Illumina data was controlled for quality using FastQC 0.11.9 [130] and prepared with trim-

galore 0.6.6 [131]. The read pairs from all samples were pooled to generate a single *de novo* transcriptome assembly using Trinity 2.8.5 [132,133]. The transcripts were mapped against the reference proteome of *Mus musculus* (GRCm39, Annotation Release 109) using blastx 2.5.0+ with an e-value < 1E-5 [134,135]. A reduced assembly containing only transcripts with a hit against a mouse protein was generated using "extract_hits_from_fasta.rb". A transcript-to-GeneID dictionary was generated based on the best hit to the mouse proteome by using "hits_to_genemap.rb". The reads from each sample were then mapped back to the reduced assembly using bowtie 1.3.0 [136]. So, data analysis was based on the numerical GeneID of the reference *Mus musculus.* One GeneID includes all isoforms, precursors, and preproproteins associated with a certain gene locus. Non-normalized differential gene expression per sample was calculated using rsem 1.3.1 [137].

4.3.3.2 Data depositories and supplied scripts

The raw Illumina data have been deposited as Bio-Samples SAMN20520422 to -45 at the NCBI Sequence Read Archive under SRA Study accession number SRP330843 within the Bioproject PRJNA751505. Both the original and the processed *de novo* assembly as well as the non-normalized gene expression (GSM5494442 to -65) have been deposited in NCBI's Gene Expression Omnibus [138].

These data are accessible through GEO Series accession number GSE181298. The data processing pipeline from raw Illumina data to non-normalized gene expression is attached as Supplementary File 2. Both ruby-scripts were uploaded to SourceForge (https://sourceforge.net/projects/prepare-transcript-to-gene-map/). The R-script with R-session info is attached as Supplementary File 3.

4.3.3.3 Statistics

The statistics applied for this study was identical with our previous transcriptomics approach [128]. Statistics and the principal component analyses were performed in RStudio 3.5.2 [139,140] using DESeq2 (Love et al. 2014, 2019, 2020). In this study, two pairwise group comparisons were made, namely SCN: HT vs NT and PVN: HT vs NT, respecting different hypothalamic core areas of the same individuals sampled either during torpor entry or on a torpor-free day. The statistical pipeline, as given in Supplementary File

3, comprises from a normalization of data across all samples included in a pairwise group comparison. Hereby, the counts of all genes of a sample were adjusted equally to level methodical bias, as different amount of tissue due to various brain sizes. This allowed a relative comparison between both sampling groups for each gene.

4.3.3.4 Data interpretation

Data was described by a gene's fold change, log2(FC), and the significance of this fold change (adjusted p-value, padj), for the HT-group relative to the NT-group. A negative log2(FC) indicates downregulation and a positive log2(FC) upregulation. All present genes with at least one count represent the entire data pool of a pairwise comparison. Genes with padj > 0.05 and any fold change were defined as not regulated. This includes outlying genes, for which the padj was not calculable during data normalization. Genes with padj< 0.05 and any fold change were defined as regulated genes.

4.3.3.5 Gene expression profiling

A principal component analysis (Figure 3) visualizes the distance between all samples of this study by their overall gene expression. Volcano plots for each pairwise group comparison (Figure 4) visualize each genes' fold change in dependence of its significance. Data processing and graphical representation was performed with Microsoft Excel (Office 365, 2016).

4.3.3.6 Regulated biological processes

To identify enriched biological processes in SCN and PVN during torpor entry, a GO enrichment analysis was performed separately for each pairwise group comparison. The regulated genes were tested, while all present genes were used as baseline to assess the expectable regulation of biological processes. The genes' fold change was irrelevant for this test, which output does not tell if an enriched biological process is up- or downregulated. Data were analyzed using the PANTHER Overrepresentation Test (Released 20210224) based on the GO Ontology database (DOI: 10.5281/zenodo.4495804 Released 20210201), with Fisher's Exact as test type and False Discovery Rate correction. (PANTHER-tool via http://geneontology.org/) [144–146].

4.3.3.7 Screening for indicator genes

As reviewed earlier, several hypothalamic systems including the circadian clock system, thyroid system, growth axis, and energy metabolism have been identified as relevant in photoperiodic acclimation and / or orchestration of torpor [2]. We specifically screened for differential expression of 68 genes as preselected in [128] and introduced in Table 1.

4.3.3.8 Regulated genes

For SCN-HT relative to SCN-NT, genes with padj< 0.05 and an extreme fold change of |log2(FC)| > 2.0 are discussed only. For PVN-HT relative to PVN-NT all genes with padj< 0.05 and an any fold change are discussed. Prior to literature research, the UniProt Knowledgebase (https://www.uniprot.org/) was used to get an overview of each genes biological function.

4.4 Results

After all hamsters had expressed a spontaneous torpor bout at least once, they were sacrificed about one hour after lights on (Figure 1) either hypothermic during torpor entry (HT, n = 6, Tb = 30 ± 0.3 °C) or normothermic on a torpor-free day (NT, n = 6, Tb = 35.9 ± 1.3 °C). The two sampling groups HT and NT differed only in terminal body temperature by about 6 °C (Supplementary Table 1). Of each hamster, the hypothalamic core areas SCN and PVN were lasermicrodissected (Supplementary Table 2). Quality and quantity of total RNA was comparable between SCN and PVN samples (Supplementary Table 3). On average 36.2 ± 6.2 mio read pairs of mRNA per SCN sample and 38.3 ± 6.4 mio read pairs of mRNA per PVN sample were sequenced. In total, 894,514,860 read pairs contributed to one single *de novo* transcriptome assembly (Supplementary Table 4). Of 696,614 transcripts in total, 144,567 were successfully mapped against the reference *Mus musculus*.

4.4.1 Gene expression profiling

The gene expression profiles of SCN samples were widely scattered in the principal component analysis, however with clear separation of SCN-HT and SCN-NT samples in the first dimension (Figure 3A). This results in high differential gene expression in the SCN during torpor entry as compared to normothermia of a torpor-free day (Figure 4A). In the principal component analysis of PVN samples, the PVN-HT samples scattered widely around the PVN-NT samples, which clustered on a small area. This high variance of the PVN-HT samples' gene expression profiles (Figure 3B) minimizes differential gene expression in the PVN during torpor entry as compared to normothermia (Figure 4B).

4.4.2 Regulated biological processes

The GO enrichment analyses revealed a regulation of metabolic processes within the SCN during torpor entry (Table 2), namely cellular metabolic process, metabolic process, nitrogen compound metabolic process, primary metabolic process, and organic substance metabolic process, with a fold enrich of 1.20 to 1.23 each. No biological processes were regulated during torpor entry in the PVN.

4.4.3 Screening for indicator genes

Of 68 indicator genes (Table 1), no gene was significantly upregulated in SCN-HT during torpor entry, while seven were significantly downregulated, namely *Junb, Avp, Avpr1a, Mta1, Timeless, Mct8,* and *P2ry1* (Table 3). In the PVN: HT vs NT comparison, none of the 68 indicator genes were regulated. For the results of all screened genes in both pairwise group comparisons see Supplementary Table 5.

4.4.4 Genes regulated in both SCN and PVN during torpor entry

Three genes were regulated in both SCN and PVN during torpor, compared to the respective non-torpid group (Table 4). Two of them were upregulated with padj < 0.001 and a log2(FC) > 2.0, namely *Gm773* and *Gsdme.* The other one was upregulated with less significance and a small fold change, namely *Mylip / Idol / Mir.* No further genes were regulated in both pairwise group comparisons.

4.4.5 Genes regulated in SCN during torpor entry

In SCN: HT vs NT with 15.158 present genes in total, 871 genes were significantly regulated with padj < 0.05 (Figure 4A). Of those, 181 genes were upregulated, and 690 genes were downregulated, which accounts for a 1:4 proportion of upregulated to downregulated genes.

A fold change threshold of |log2(FC)| > 2.0 was applied to concentrate on those 66 genes with the highest probability to be of biological relevance within the SCN of the Djungarian hamster during torpor entry. Two genes which fulfilled both level of significance and fold change were indicator genes (*Junb* and *Avp*). The remaining genes were assorted to six major topics. 12 genes play a role in mitochondria (Table 5), nine genes in systemic signaling and metabolism (Table 6), eleven genes in transcription and modification (Table 7), eight genes in cell cycle (Table 8), eight genes in brain plasticity (Table 9), while the biological functions of 14 genes are largely unknown (Table 10).

4.4.6 Genes regulated in PVN during torpor entry

In PVN: HT vs NT with 15.275 present genes in total, 14 genes were significantly regulated with padj < 0.05 (Figure 4B, Table 4, Table 11). Of those, nine genes were upregulated, and five genes were downregulated, which accounts for a 3:2 proportion of upregulated to downregulated genes.

4.5 Discussion

There is evidence, that spontaneous torpor of the Djungarian hamster adapted to winter-like short photoperiod is orchestrated within the hypothalamus. Earlier transcriptomics studies on differential gene expression in the whole hypothalamus revealed more general adaptive mechanisms to initialize and maintain torpor. We concluded that this approach was unable to unravel specific torpor-relevant mechanisms. It is likely, that gene regulation in one hypothalamic core area is levelled by the transcripts expressed in the other core areas of the hypothalamus [118,128]. In the given study, lasermicrodissection of the suprachiasmatic nucleus and the paraventricular nucleus

sampled at torpor entry enabled differential gene expression analyses in two important hypothalamic core areas at torpor induction.

The hamsters sampled either hypothermic during torpor entry or normothermic on a torpor-free day differed in terminal core body temperature only (Supplementary Table 1). The total area lasermicrodissected from sections with defined thickness allowed to conclude on similar approximate volumes of dissected material for both SCN and PVN samples (Supplementary Table 2). Although the time-lasting procedure of cryosectioning, staining and lasermicrodissection favored a degradation of mRNA, the maintenance of a RNAse-poor environment resulted in respectable quality and quantity of total RNA (Supplementary Table 3). Also, the amount of mRNA read pairs was comparable for SCN and PVN data (Supplementary Table 4), which both contributed to one *de novo* assembly. About one fifth of transcripts were mapped against the reference *Mus musculus,* as much as in an earlier study using the same methodological pipeline, yet with samples of fast-dissected hypothalamus [128]. Hence, the results of SCN and PVN data are comparable.

4.5.1 Gene expression profiling

Nevertheless, differential gene expression during torpor entry was more substantial in SCN than in PVN regarding distance in the principal component analysis (Figure 3) and number of regulated genes (Figure 4) from HT- in relation to NT-samples and sampling group. While the proportion of upregulated to downregulated genes was 3:2 in whole hypothalamus during deep torpor [128] as well as in whole hypothalamus [118] and in PVN during torpor entry, the proportion was 1:4 in SCN during torpor entry. The body temperature difference between the HT- and the NT- sampling group was 10 °C in the study on deep torpor and 6 °C in the studies on torpor entry. Although the extent of metabolic downstate is reasonable to cause a slowing of transcription and translation, less upregulated than downregulated genes were observed in SCN only. This does not tell a silencing of the SCN during torpor entry. Conversely, the SCN during torpor entry had the highest number of regulated genes (871) with padj < 0.05 among these studies, followed by whole hypothalamus during deep torpor (759) and torpor entry (284). In PVN, only 14 genes were regulated during torpor entry. Assuming an equal importance of a lack of than

a gain of transcribed genes, the SCN underlies these studies` greatest regulation. Hence, the SCN seems to be of highest importance gaining better insight into torpor mechanisms.

4.5.2 Regulated biological processes

The GO enrichment analysis identified enriched biological processes in SCN, but not in the PVN during torpor entry (Table 2). Hence, the overall clock output within the master circadian clock might be modulated by enriched metabolic processes, what has potential to induce torpor. Hereby, the gene regulation within SCN is not affecting gene expression within PVN, at least not during torpor entry. The SCN probably signals to other hypothalamic core areas relevant for torpor control. Furthermore, these results point to nucleus-specific changes in metabolism.

Previous transcriptomic data of the Djungarian hamsters also suggested enriched metabolic processes in whole hypothalamus during deep torpor (ZT04) compared to a torpor-free day [128]. Furthermore, transcriptional, biosynthetic, and cellular processes were enriched in whole hypothalamus during deep torpor (ZT04), which were not enriched in SCN and PVN during torpor entry (ZT01). Therefore, further transcriptomics on level of core areas sampled at different torpor stages probably might result in interesting findings contributing to understand torpor orchestration.

4.5.3 Screening for indicator genes

The list with 68 indicator genes of several key systems with potential regulatory function in photoperiodic status and torpor expression (Table 1) was developed for and used in an earlier transcriptomic study on the Djungarian hamsters' whole hypothalamus sampled at ZT04 facing torpor expression (deep torpor vs. torpor-free day) and photoperiodic status (SP vs LP) [128]. Here, we focus on gene regulation within hypothalamic core areas during torpor entry (ZT01) using hamsters with the same degree of adaptation to photoperiod (Supplementary Table 1). Hence, we did not expect all the indicator genes to be regulated. Nevertheless, the genes found to be regulated using this screening-approach allow a deeper insight into torpor orchestration (Table 3). Furthermore, indicator genes not expressed in SCN, PVN and / or whole hypothalamus verify the results of the respective study (Supplementary Table 5).

Seven indicator genes were regulated in SCN during torpor entry (Table 3). *Junb* and *Avp* were downregulated with a log2(FC) > -2.0, which accounts for less than 25 % of the mRNA-level in the torpid group compared to those of the non-torpid group, while *Avpr1a, Mta1, Tim*, *Mct8* and P2ry1 were downregulated with a smaller fold change of at least log2(FC) > -0.5, which accounts for at least a 75 % of the mRNA-level in the torpid group compared to those of the non-torpid group. Hence, this gene regulation is likely of biological relevance. None of these genes regulated in SCN during torpor entry were regulated in PVN during torpor entry, whole hypothalamus during deep torpor, and whole hypothalamus in the photoperiodic approach [128]. Hence, the regulation of these seven indicator genes is specific for SCN and / or torpor entry.

The transcription factor ***Junb*** is, like c-Jun and c-Fos, part of the Jun/Fos family. A heterodimer from Jun and Fos act together with the AP-1 complex not only as suppressor or activator of transcription, but also in cell-proliferation and differentiation [147]. Members of the Jun/Fos family are expressed within minutes as response to external stimulation, as a light pulse, which is processed in the SCN. Therefore, members of the Jun/Fos family are studied in the brain and SCN of e.g. rat, the hibernating golden- mantled ground squirrel, as well as the Djungarian hamster [148–150]. In an earlier study on transcriptomics of the Djungarian hamster, c-*Jun1* was downregulated during deep torpor (ZT04), while several other immediate early genes, including *Junb*, were not regulated in whole hypothalamus during deep spontaneous torpor or seasonal normothermia [128]. Finding *Junb* to be downregulated in SCN during torpor entry (ZT01) point towards a core-specific altered transcription.

In the SCN of the Djungarian hamster, vasopressin is a photoperiod- and clock-dependent neuropeptide, and signals time of day and year to subsequent core areas. The *Avp* level within the SCN is reduced in short photoperiod compared to long photoperiod, and fluctuates within 24 hours, having lowest values in the scotophase and peaking values during the photophase [151–154]. In the given study, sampling was controlled for both acclimation (short photoperiod) and time (ZT01) of the day, allowing an interpretation of the downregulation of *Avp* and its receptor during torpor entry.

An altered *Avp*-level might result from altered number of *Avp*-containing neurons. The number of vasopressin-containing neurons within the SCN of the European ground squirrel was increasing after hibernation analogous to the reappearance of circadian rhythmicity of locomotor activity and body temperature [155]. It would be of interest, whether the number of *Avp*-containing neurons can change in the much smaller temporal window during a torpor bout in the Djungarian hamster. Furthermore, the number of vasopressin receptors might probably alter the perception of vasopressin.

It has previously been shown that torpor expression did not affect the amount of *Avp* in the SCN on a day of a torpor bout, but resulted in a depressed amplitude of *Avp* the day after a torpor bout [125,153]. Finding extremely downregulated *Avp* in SCN during torpor entry might have been affected by torpor the day before. Since the given study design did not respect a torpor the day before sacrifice, some hamsters sampled in HT or NT expressed torpor the day before, others did not, as shown in Supplementary Figure 1. Future study designs might control for torpor the day before sampling and torpor incidence, which both potentially affect the results.

In mice, AVP-neurons project from the SCN to thirst neurons in the *organum vasculosum lamina terminalis,* a specialized structure within the wall of the third ventricle of the hypothalamus. In a clock-dependent manner, water uptake prior to sleep is triggered without physiological need [156]. In context of torpor entry of the Djungarian hamster, a downregulation of vasopressin and its receptor might suppress drinking and feeding behavior during this metabolic downstate.

Mta1 was downregulated in SCN during torpor entry. Interacting with the Clock-Bmal1 complex, ***Mta1*** regulates its own or the Cry transcription, impairing the Cry1-mediated negative feedback loop of the circadian system [157], yet, with a delay of approximately 12 to 24 hours. However, various manifestations of *Mta1* due to posttranslational modifications as well as their interactions with other genes and proteins have been described [158,159]. Hence, the effect of downregulated *Mta1* in the SCN during torpor entry on the circadian clock is hard to estimate. It may alter the circadian clock, what has potential to induce the next torpor bout. Besides this, diverse biological functions of *Mta1* in DNA repair and inflammation are discussed [160], which might be of importance regarding neuroprotection during metabolic downstates [30].

Timeless (***Tim***) is an essential part of the flies' circadian rhythm, while its role is unclear in the mammalian clockwork. Yet, there is evidence for several functions. The interaction between *Tim* and *Per1* negatively regulates *Clock-Bmal1*-induced activity of the *Per1* promoter [161]. Since *Tim* binds with the transcriptional repressor *Cry* and *Chk1*, it might influence the determination of period length and for light-independent resetting mechanism of the clock [162]. In the SCN of mouse neither mRNA nor protein of *Tim* do rhythmically oscillate or are to alter by light pulses [163]. Also in the hypothalamus of hibernating arctic squirrels, *Tim* is the only gene of the circadian system not regulated [164].

Mta1 and *Tim* also play a role in several pathways influencing a bride spectrum of biological functions in diverse systems investigated in specific organs [165]. Therefore, it is possible, that *Mta1* and *Tim* do not only affect the circadian clock, but are regulated in the light of e.g., DNA repair, protein degradation, or histone modification, like several other regulated genes found to be differentially expressed within the Djungarian hamsters` SCN and likely relevant for torpor induction.

The monocarboxylate transporter 8 ***(Mct8)*** is a thyroid hormone transporter of thyroxine (T4), triiodothyronine (T3), reverse triiodothyronine (rT3) and diiodothyronine [166]. Its level is increased in short photoperiod, but reduced during a torpor bout, which both in turn affects Dio2 and T3 levels [2,167–169]. *Mct8*-level of hypothalamus is decreased in deep torpor and post torpor, but remains unchanged during torpor entry and arousal [42], while the *Mct8*-level of SCN was decreased during torpor entry in the given study, indicating a core-specific regulation which might be of importance in torpor orchestration. *Mct8* plays a role in development of the brain in general [93]. For the thyroid system, the expression of monocarboxylate transporters may especially play a role in tanycytes lining the third ventricle [94].

Purinergic type 2 (P2y) receptors (P2ry) regulate diverse physiological functions, as neuronal excitation, inflammation, cell growth and apoptosis [170,171], which are likely to be of relevance also in the hypometabolic brain. Since the P2Y purinoceptor 1 (***P2ry1 or P2Y1)*** in astrocytes inhibits excitatory glutamatergic synaptic neurotransmission [172], a downregulation of *P2ry1* in SCN during torpor entry might point towards an increased

neuronal excitation. Since an application of P2Y1 in the ventromedial hypothalamic nucleus (VMH) and lateral hypothalamic nucleus (LH) increased food intake in rats [173], a downregulation of *P2ry1* in SCN during torpor entry suggests clock-dependent less drive to eat. P2Y1 receptors contribute to protect astrocytes from oxidative stress [174], yet, a downregulation of *P2ry1* in SCN during torpor entry seems to contra productive to overcome neurodegeneration and hypoxia / reperfusion. In tanycytes, P2Y1 receptors allow the ATP-mediated sensing of glucose. Intracellular Ca2+ level is increased, while a Ca2+ wave across neighboring tanycytes propagates the signal of energy state [175,176]. Complex alteration of the tanycytes` biology is discussed regarding disorders as obesity and anorexia [177–179], and naturally used to orchestrate seasonal acclimation and torpor expression, although mechanisms are not fully understood yet [86,180]. Other purinergic type 2 receptors also have interesting functions. For example, *P2ry12* contributes to microglial closure of the injured blood–brain barrier [181]. However, although present in SCN during torpor entry, the purinergic type 2 receptors 2, 6, 10b, 12, 13 and 14 were not regulated.

4.5.4 Genes regulated in both SCN and PVN during torpor entry

Three genes might play a role in both SCN and PVN during torpor entry. All of them are upregulated (Table 4). ***Gm773,*** a gene model, had the most extreme regulation of both fold change and significance in both pairwise group comparisons. *Gm773* might be encoded on the X-chromosome. However, in our study with four males and two females in each HT and NT sampling group, the number of sex chromosomes was balanced. While there are no studies on *Gm773*, So, reasons for this extreme upregulation of *Gm773* in SCN and PVN during torpor entry of the Djungarian hamster remain unclear.

Gsdme is the key element in the pryoptosis pathway, a form of regulated cell death [182]. Its upregulation may indicate necrosis in both SCN and PVN during torpor entry.

Mylip/*Idol/Mir* is a degrader of the LDL receptor, so, playing a role in cholesterol and therefore energy metabolism [183,184]. Its overexpression also inhibits neurite outgrowth [185].

4.5.5 Genes regulated in SCN during torpor entry

Besides the level of significance (padj < 0.05) which fulfilled 871 genes, a fold change threshold of |log2(FC)| > 2.0 was applied to concentrate on those 66 genes with the highest probability to be of biological relevance within the SCN of the Djungarian hamster during torpor entry. These are discussed along their potential roles in mitochondria, systemic signaling and metabolism, transcription and modification, cell cycle and brain plasticity. However, most genes have several biological functions, and not all of them have been reported in literature so far. Since genes can be repressors or enhancers of a biological function, the up- or downregulation played a minor role for the interpretation. Whenever possible, the regulatory direction was interpreted according to literature.

4.5.5.1 Mitochondria

Several genes with functions in mitochondria were regulated in SCN. All of them were downregulated during torpor entry compared to a torpor-free day (Table 5). According to the UniProt Knowledgebase (https://www.uniprot.org/), ***Bola1*** may act as a mitochondrial iron-sulfur cluster assembly factor [186], while ***Ndufaf8, Ndufb2*** and ***Cox6a1****/Cox6al* are likely part of the respiratory chain and therefore involved in the ATP energy metabolism [187]. ***Cox5b*** is component of the cytochrome c oxidase in mitochondria [188]. ***Gatc, Mrps28****/S28mt,* ***Mrps34****/S34mt,* and ***Mrpl3****/L3mt* are involved in mitochondrial translation. ***Mrpl3****/L3mt* was also downregulated in whole hypothalamus during deep torpor (ZT04) with a small fold change of log2(FC) = -0.3 and a high significance of -log10(padj) = 3.2 and padj = 0.0007 [128]. ***Efhd1/****Sws2* is a mitochondrial calcium binding protein expressed in neurons but not glial cells, which might be involved in neuronal development [189]. Furthermore, *Efhd1/Sws2* is a sensor for mitoflash activation, an electrical and chemical excitation of mitochondria which uncouples respiration from ATP production [190,191]. *Efhd1/Sws2* was also downregulated in whole hypothalamus during deep torpor (ZT04) with a small fold change of log2(FC) = -0.6 and a significance of -log10(padj) = 1.7 and padj = 0.0220 [128]. ***Bloc1s4*** is a subunit of the BLOC-1 complex, which contributes to intracellular membrane trafficking and organelle biogenesis [192]. ***Klc3***, a component of kinesin, plays a vital role in organelle transport [193].

Given the known importance of mitochondria in cell survival during hypoxia and hypothermia [194], our results on genes involved in respiratory chain and transcriptional machinery of mitochondria indicate a reduced mitochondrial performance in the Djungarian hamsters' SCN during torpor entry. This is obviously not the case for the PVN during torpor entry, and probably not the case for the whole model organism. Although there is a positive correlation of body temperature, metabolic rate and liver mitochondrial performance in Djungarian hamsters and ground squirrels [19,20,44], the mitochondrial performance in kidneys, skeletal muscle and heart is unchanged during torpor of the Djungarian hamster [195].

4.5.5.2 Systemic signaling and metabolism

Several genes involved in systemic signaling and metabolism were regulated in SCN. All of them were downregulated in torpor entry compared to a torpor-free day, except for *Inhbe, Rrad* and *Tlr4,* which were upregulated (Table 6). ***Kiss1r****/Gpr54* is the receptor for kisspeptin / metastin, which is investigated in rodents, sheep and primates including human [196,197]. Because kisspeptin regulates gonadotropin-released hormone physiology, its expression and role has been studied also in the photoperiodic model organism *Phodopus sungorus* in relation to seasonal fluctuation of reproduction and body mass in reliance on sex and age [198,199]. Recently, kisspeptin-expressing neurons in the arcuate hypothalamus were found to control food intake, sleep, activity, and core body temperature also in the circadian context [200], modulating the signals downstream of the SCN [201]. Therefore, a downregulation of its receptor *Kiss1r/Gpr54* during torpor entry in SCN might indicate an, at least temporal and spatial, insensitivity of kisspeptin, yet with unclear extent, duration, and consequences. An earlier study found, using radiotelemetry data of a representative SP-week in Djungarian hamsters, a reduction of mean core body temperature in general and activity during scotophase, the more often torpor is expressed. Also, a frequent torpor expression favors timing of torpor onset with lights on, torpor duration, body temperatures reduction, and probably energy saving [119]. Although the complex interactions between observed parameters are not fully understood, these results suggest a torpor-driven gene regulation in SCN is affecting the hamsters' morphology, physiology, behavior, and metabolism, which again modulate the SCN in transcriptional-translational feedback loops. While kisspeptin mRNA itself was not present in this study,

neither kisspeptin nor its receptor were regulated in the Djungarian hamsters' whole hypothalamus at ZT04 comparing deep torpor hypothermia with SP-normothermia as well as comparing SP-normothermia with LP-normothermia [128].

Apoe has diverse functions, e.g., it is involved in fat metabolism. *Apoe* is studied in relation to Alzheimer's disease because of its tau and amyloid-beta binding function [202], while the *Apoe*-mediated interaction between astrocytes and endothelial cells, induced by melatonin, is of interest for pathogenesis of stroke [203].

Cck is a hormone peptide of the complex gut-brain pathway, where it may play a role in food uptake and body weight [204]. The current understanding of the feedback loop to mediate satiety and adiposity signals from peripheral nerves within hypothalamic core areas including the PVN does not respect the SCN [205], at least not in the mouse, which is as nocturnal as the Djungarian hamster, but does not underly seasonal acclimatizations. In the photoperiodic Djungarian hamster, the SCN might noticeably be involved in the gut-brain pathway. Hereby, *Cck* was studied in the Djungarian hamster`s SCN and brainstem, yet hitherto regarding the seasonal, but not torpid state, whereby the number of *Cck*-containing neurons are reduced within SCN and nucleus of the brainstems' solitary tract, but not the brainstems' solitary parabrachial nucleus, during acclimation to short photoperiod, during which food intake and body mass are reduced [206,207]. *Cck* is a more effective food suppressor when administered intraperitoneally in SP- than in LP-acclimated Djungarian hamsters [208]. Further research is needed to assess, whether *Cck*-sensitivity is also altered during stages of a torpor bout. Interestingly, for the PVN, which likely mediates given and aimed energy level, only a small number *Cck*-containing neurons was reported [207]. Given a relevant regulation of *Cck* within the SCN, but not PVN, during torpor entry, the master circadian clock might be on top of systemic energy homeostasis in the Djungarian hamster. It is to consider, that food intake might acutely increase *Cck* within neurons to suppress further feeding, at least in rats [209]. This might have possibly been also the case in active and probably feeding hamsters sampled on a torpor-free day (NT-group). This might have caused the relative downregulation in inactive, non-eating hamsters sampled during torpor-entry (HT-group).

Ly6h is primarily expressed in brain, where it is possibly involved in glutamatergic signaling and neuronal plasticity due to modulation of nicotinic acetylcholine receptors [210]. ***Inhbe*** is a subunit of both, activin and inhibin, which modulate the pituitary function

together with follistatin regarding the reproductive axis [211], while its upregulation in the SCN during torpor entry is unclear. ***Rrad*** is involved in negative regulation of cell growth. Its voltage-gated calcium channel activity is important for hearth function, bone density and marrow adiposity [212,213], but has potential to play a role in neuronal signaling [214]. ***Tlr4/****Lps* plays a role in (neuro) inflammation [215]. An upregulation of *Tlr4****/****Lps* caused neurodegeneration in the mouse [216], which is probably also the case in the SCN during torpor entry of the Djungarian hamster. ***Cd320/****TCblR* plays a role in vitamin B12 transport and metabolism [217]. ***Fth1*** is a subunit of ferritin, which stores free iron. In the brain, it is important for astrocyte-mediated iron homeostasis from the blood, oligodendrocyte development and myelinization [218,219]. A false organization of iron within cells may lead to ferroptosis [220], as possible due to downregulation of *Fth1* within the SCN during torpor entry.

4.5.5.3 Transcription and modification

Several genes involved in transcription or modification were regulated in SCN. *Egr3* and *B3gnt4* were upregulated, while all others were downregulated in torpor entry compared to a torpor-free day (Table 7). ***Egr3*** is an immediate early gene and transcription factor that is upregulated by synaptic activity suggesting increased SCN activity during torpor entry [221,222]. *Egr3* is induced in the SCN by light [223,224], which should play no role in this study, since all hamsters were sacrificed one hour after lights on.

Dtd2/*Atd* is a hydrolase with proofreading activity involved in tRNA metabolic processes [225]. ***Osgep*** is a metal-ion binding transferase involved in tRNA processing, which is studied regarding neurodegeneration [226]. ***Dohh*** mediates post-translational hypusine modification of the eukaryotic initiation factor 5A (eIF5A) and essential for development and cell proliferation [227]. ***B3gnt4*** is an upregulated glycosyltransferase. Distribution and functions of ***Chst7/****Gst5* and similar sulfotransferases are studied, also in the rodent brain [228,229]. ***Josd2*** is involved in protein ubiquitination [230,231]. ***Usp14*** in involved in ubiquitin regeneration and recycling at the proteasome and plays a role at synapses [232].

Three histones were downregulated in SCN during torpor entry, ***H1f4/****H1-4/Hist1h1e,* ***H2bc22/****Hist1h2bp,* and ***Cenpa****.* Histones control transcription regulation, DNA repair, DNA replication, and are under research regarding epigenetics. Also in an earlier study comparing the transcriptome of whole hypothalamus in deep torpor (ZT04) to a torpor-

free day, ***H1f4/****H1-4/Hist1h1e* was downregulated with a small fold change of log2(FC) = -0.9 and a high significance of -log10(padj) = 2.9 and padj = 0.0014 [128]. Nevertheless, the role of histones in context of this study is unclear.

4.5.5.4 Cell cycle

Several genes involved in cell cycle were regulated in SCN. All of them were downregulated in torpor entry compared to a torpor-free day, except for the upregulated *Sertad1* and *Gaddad45b* (Table 8). ***Sertad1/****Sei-1/Trip-Br1* is a transcription factor involved in developmental and pathological neuronal death [233–235]. Hereby, the interplay between *Sertad1/Sei-1/Trip-Br1* and the ubiquitination of adenylyl cyclases in context of cAMP signaling is under research [236]. Interestingly, upregulation of *Sertad1/Sei-1/Trip-Br1* prevents hypoxia-induced cell death in breast cancer cell lines [237], hence might be relevant to maintain functionality of the SCN. ***Gadd45b****/Myd118,* is involved in negative regulation of cell growth as well as apoptosis. The rats' Gadd45 protein is upregulated in neurons sublethally injured by ischemia [238,239].

A downregulation of ***Rnf43*** in SCN during torpor entry might enhance the Wnt signaling pathway in hypothalamic glial cells, which might affect neural stem cell proliferation [240–243]. Also, by similarity, the downregulation of ***Rrm2,*** which mediates DNA synthesis and repair, might inhibit Wnt signaling and cause cell cycle arrest in SCN during torpor entry [244,245].

By similarity, the downregulated ***Nop53/****Gltscr2/Pict1* is involved in ribosome biogenesis and has diverse functions in several pathways. For example, its contribution to cell proliferation and apoptosis is of interest in tumor suppression [246]. Also, ***Trp53i13***, a potential tumor suppressor, was downregulated [247].

Two genes involved in DNA repair are downregulated. ***Mcm8*** is studied regarding infertility and cancer [248]. ***Babam1/****Merit40/Nba1* is part of the BRISC and BRCA1-A complex [249].

4.5.5.5 Brain plasticity

Several genes involved in brain plasticity were regulated in SCN. All of them were downregulated in torpor entry compared to a torpor-free day (Table 9). *Claudin-5* ***(Cldn5/****Bec1)* is the main and therefore essential component of the blood brain barrier

[250,251]. Studies in mouse and rat brains have shown downregulated claudin-5 in the first hours after ischemic stroke [252,253]. In hibernating thirteen-lined ground squirrel, it was shown that they underwent natural ischemia during a torpor bout, without suffering from neuropathological changes [9]. Furthermore, mouse hypothalamic tanycytes express claudin-5 [254], which might be investigated further in the Djungarian hamster in metabolic context [178]. ***Nkapl*** and ***Hes6*** are suppressors of the Notch pathway, which is important for brain morphology, synaptic plasticity and neuronal survival [255–257]. ***Anapc11*** contributes as subunit of the anaphase-promoting complex to protein ubiquitination, and is studied for more than a decade due to its major role in neuronal connectivity and brain plasticity [258]. ***Ppfia3*** is part of the liprin-alpha family, which regulates the development of dendrites and acts in formation and structure of synapses [259]. ***Gdf5****/Bmp14,* a member of the TGFβ superfamily, plays a role in development. It is investigated regarding neurodegenerative diseases due to its potential in neuro-protection and recovery [260–262]. ***Boc***, the "brother" of CDO (cell adhesion molecule-related / down regulated by oncogenesis), is a member of the Ig superfamily of cell adhesion molecules, and component of an axon-guiding, cell-cell-interacting receptor-like complex studied in muscle, but also developing brain of zebra fish embryos [263]. ***Pigh*** is essential for the glycosylphosphatidylinositol (GPI) synthesis important for neurogenesis and therefore of clinical relevance for neurodevelopmental disorders [264].

4.5.5.6 Unclear function

Several genes with unclear function were regulated in SCN. Besides *Otos* and *Ankub1*, all of them were downregulated during torpor entry compared to a torpor-free day (Table 10). ***Otos/****Ocp10* and *Ankub1* were upregulated. In the inner ear, a downregulation of ***Otos/****Ocp10* leads to deafness, while its regulatory function in other parts of the central nervous system is unclear, yet astrocyte-mediated repair mechanisms in neurons after traumatic injuries are assumed [265,266]. Although the detection of ***Ankub1*** was reported elsewhere, its function is completely unclear.

Following genes with unknown or assumed function were downregulated in SCN during torpor entry. ***Cmtm3****/Cklfsf3* is an evolutionary conserved cytokine with unknown function [267]. ***Tpgs1/****Gtrgeo22* may contribute to post-translational modification of tubulin, which is important for neuronal differentiation [268]. ***Sncb*** may be involved as pre-synaptic

protein in neuronal plasticity [269]. Also, ***Dmpk*** might influence synaptic plasticity [270]. Despite a similarity to the histone-binding *Ptma,* nothing is known about its pseudogene 2 ***Ptma-ps2.*** Although expressed in diverse tissue of several model organisms, the function of the protein-coding genes ***Fam216a*** and ***Fam71e1*** are uninvestigated***.*** Two zinc finger proteins were downregulated in SCN during torpor entry. ***Zfp879****/Znf879* may be involved in transcriptional translation (https://www.uniprot.org/). The function of ***Znhit2****/Orf6* is unknown. A related gene, *Znhit3/Trip3,* is named after its function, namely thyroid receptor-interacting protein 3, yet not regulated in this study [271]. ***Ccdc166*** is a novel imprinted gene [272]. Nothing is known about the uncharacterized protein C6orf226 homolog and the UPF0575 protein C19orf67 homolog.

4.5.6 Genes regulated in PVN during torpor entry

Both differential gene expression (Figure 4B, Table 11) as well as the interpretation of regulated genes and their products in this studies' context was limited for the pairwise group comparison PVN: HT vs NT. Besides ***Gm773*** and ***Gsdme,*** which were discussed earlier, four genes met the threshold $|\log2(FC)| > 2.0$. ***Atad2***, which expression amplification loop is in focus of cancer research, was upregulated in PVN [273]. The three other genes were downregulated. ***Armc4/Odad2*** in involved in cilia and sperm motility [274]. ***Efemp2,*** one of diverse fibulin-like extracellular matrix proteins, might be involved in tissue remodeling and cellular processes [275]. ***Kcng4*** modifies potassium voltage-gated channel properties, which might affect signaling in the PVN during torpor entry [276,277].

Using no threshold for the fold change, eight further genes fulfilled the padj < 0.05 significance threshold. ***Mylip/****Idol/Mir* was discussed earlier. ***Hmbox1,*** upregulated in PVN during torpor entry, was identified as positive regulator of telomere length, which is associated with aging [278]. In dependance of ambient temperature it was shown, that spontaneous torpor bouts in the Djungarian hamster as well as hibernation bouts in the dormouse seem to affect telomere length positively, so, aging might be slow down during or because of metabolic downstates [33,279]. ***Klf6/****Copeb/Cpbp,* upregulated, is a transcription factor and a tumor suppressor gene [280]. ***Obsl1,*** upregulated, is involved in cell–cell, cell–matrix, and internal cytoskeletal connections, and studied regarding clinical diseases [281]. ***Tmem74,*** upregulated, is an important regulator of autophagy under stress conditions [282], and should be investigated regarding torpor. ***Zc3h8/Fliz1,*** upregulated in

this study and, for hitherto unknown reasons, upregulated in cancer cells, is part of the Little Elongation Complex and therefore involved in snRNA biogenesis [283,284].

The downregulated ***Marchf1/****March1/March-1* degrades, besides others, MHC class II proteins and insulin receptors. *Marchf1* plays a role at least in dendritic cells, B cells and T cells. The gene expression of *Marchf1* and its biological functions are studied in context of malaria, obesity, diabetes, and cancer, besides others [285–290]. The role of *Marchf1* in the PVN, for the model organism *Phodopus,* and regarding metabolic downstates as torpor, is unknown. But it is tempting to speculate that decreased degradation of insulin receptors leading to increased insulin sensitivity might be an important factor in torpor control. ***Kdm2b****/Fbl10/Fbxl10/Jhdm1b/Kiaa3014*, downregulated, demethylates the important histone H3, and is studied regarding epigenetics, stem cells, neurological disorders, and cancer [291,292].

4.6 Conclusion

Data basis of SCN and PVN samples were comparable as in amount of lasermicrodissected tissue, number of sequenced read pairs, and number of matches with the mouse annotation. In SCN of the Djungarian hamster, 181 upregulated and 690 downregulated genes were found during torpor entry. At the same time, 14 genes with diverse functions were regulated in PVN. Despite the identification of specific enhanced biological functions, the comprehension of each single genes` contribution remained incomplete, given the large number of regulated genes in SCN, multiple functions of each transcript, and lacking information on translation. Here, a multi-omics approach might be feasible. For a more comprehensive insight into mechanisms of torpor orchestration, further hypothalamic core areas might be analyzed, also at further stages of torpor, as deep torpor, arousal, and post-torpor. However, the given transcriptomic data which were successfully mapped against the mouse reference sequences is promising for a successful application of templates designed for mouse to validate and expand knowledge by methods like in-situ hybridization and immunohistochemistry in the Djungarian hamster. Subsequently, markers might be designed which enable cell-sorting for e.g., tanycytes, *Avp*-expressing neurons, or mitochondria. Since spontaneous torpor is a metabolic downstate affected by and affecting the whole organism, the scale of focus should be fine-tuned as

well as enlarged. This study suggests processes on several levels to be of importance for torpor orchestration, as transcription, translation, modification of mRNA and proteins, metabolism within mitochondria and cells, cell cycle to face protection, repair, replacement, and structural flexibility, besides signaling in and plasticity of the brain on the large scale. Especially, the role of the circadian clock in SCN and the periphery might be in focus of future research to unravel torpor control mechanisms.

4.7 Tables and Figures

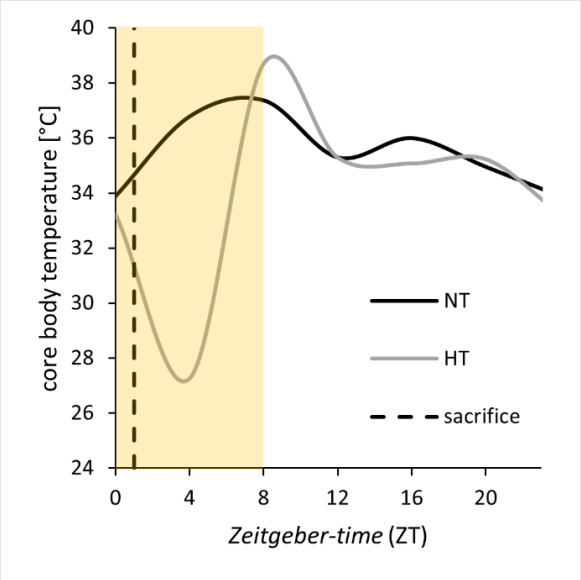

Figure 1: Sampling scheme. The twelve hamsters of this study were housed at 20 °C ambient temperature with food and water *ad libitum.* After 14 ± 1 weeks of adaptation to short photoperiod (SP, eight hours light per day, yellow field), the hamsters were sacrificed about one hour after lights on (ZT01, vertical line) either hypothermic during torpor entry (HT) or normothermic on a torpor-free day (NT). Individual core body temperature patterns of this studies' hamsters are attached in Supplementary Figure 1.
Body temperature data of hamster EH04-08, which was sampled for this studies' NT-group, were measured in intervals of three minutes, processed to mean values per hour and displayed in intervals of four hours. Radiotelemetry data of hamster EH04-08 were already shown [128] and analyzed [119].

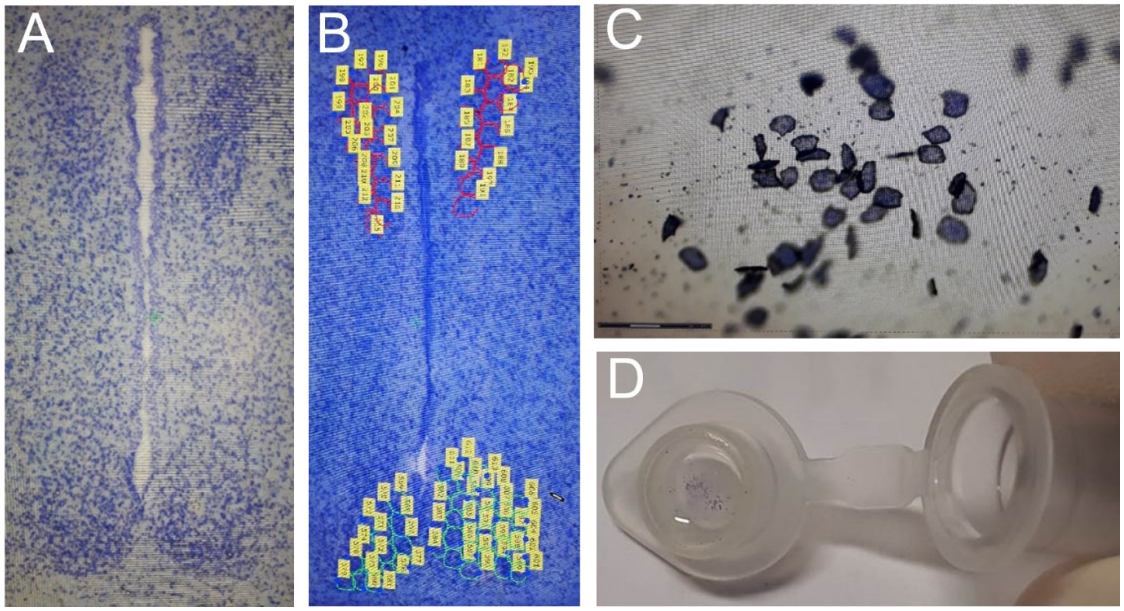

Figure 2: Insights into lasermicrodissection. (A) Cresyl violet staining of cell nuclei. Staining 20 µm coronal sections enables to identify the hypothalamic core areas SCN (top of picture, dorsal in hypothalamus) and PVN (bottom of picture, ventral in hypothalamus), both bilateral of third ventricle. **(B) Marked hypothalamic core areas on one section.** The SCN (red) and PVN (green) is marked manually in circles of about 0.0048 mm^2 on each of about 18 sections per brain. After lasering automatically along the line of each circle, the material is catapulted automatically by an air blast into the adhesive cap closely clamped above the marked area. **(D) Dissected material sticking to an adhesive cap.** During a sampling session, the technical setup is continuously checked for functionality. Between slice and adhesive cap should fit a sheet of paper, and the area within the adhesive cap focused by the air blast should be changed regularly to enable the sampling of all the dissected material. **(C) Adhesive cap tube.** The sum of sampled lasermicrodissected material, either from SCN or from PVN of an animal, is visible with bare eye within the adhesive cap.

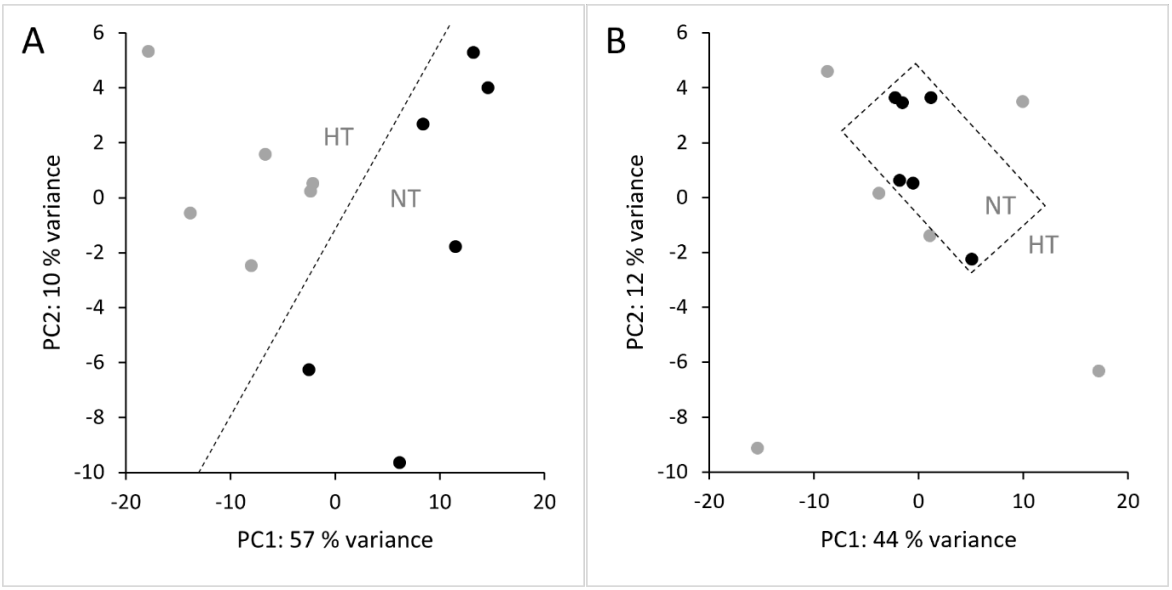

Figure 3: Principal component analyses of (A) SCN and (B) PVN. Differences in overall gene expression profiles of samples (dots) and sampling groups (HT: grey, NT: black; optically separated by dotted lines) in the first two dimensions. The higher the distance between two dots, the more different the gene expression profiles of two samples.

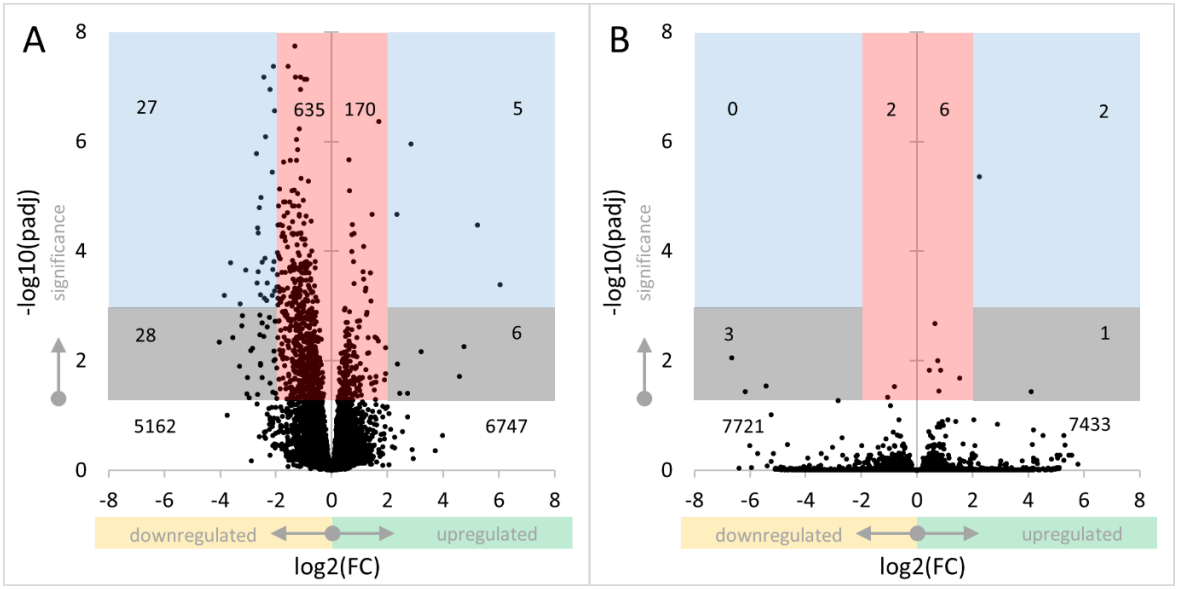

Figure 4: Volcano plots of SCN (A) and PVN (B). Differential gene expression for the HT-group in relation to the NT group of each pairwise group comparison. All mapped genes (dots) are represented by fold change (x-axis) in dependence on significance (y-axis). Differentially expressed genes are shown in the colored areas above the lower horizontal significance threshold (-log10(0.05) = 1.3). Genes indicated with padj < 0.001 throughout this study are shown above the upper significance threshold (-log10(0.001) = 3.0). The numbers of regulated genes per area are indicated respecting the direction (upregulated: green arrow, downregulated: yellow arrow). For SCN, the genes within the grey and blue areas are discussed only. For PVN, all regulated genes were discussed (red, grey and blue areas). One gene is not shown, namely Gm773, upregulated in both SCN with log2(FC) of 11.1 and -log10(padj) of 24.3 and PVN with log2(FC) of 10.6 and -log10(padj) of 23.9. For SCN, all genes with a padj < 0.05 and a |log2(FC)| > 2.0 are discussed (blue and grey areas). For PVN, all genes with a padj < 0.05 and any fold change are discussed (blue, grey and red areas).

Table 1: The 68 preselected indicator genes. (Table see next page). Genes of several key systems with potential regulatory function in torpor expression and photoperiodic status were screened for differential gene expression. This list was developed for and used in an earlier transcriptomic study on the Djungarian hamsters' whole hypothalamus [128].

Table 1: The 68 preselected indicator genes. (Legend text see previous page).

system	#	gene	gene product
transcription	1 + 2	*Fos + Fosb*	proto-oncogene c-Fos + protein fosB
	3 + 4 + 5	*Jun + Junb + Jund*	transcription factor AP-1 / c-Jun + jun-B + jun-D
	6 + 7	*c-Jun1 + c-Jun3*	c-Jun-amino-terminal kinase-interacting protein 1 + 3
clock	8	*Avp*	vasopressin-neurophysin 2-copeptin
	9	*Avpr1a*	vasopressin V1a receptor
	10 + 11	*Bmal1 + Bmal2*	brain and muscle ARNT-like 1 + 2
	12	*Bhlhe40*	class E basic helix-loop-helix protein 40
	13	*Clock*	circadian locomoter output cycles protein kaput
	14 + 15	*Cry1 + Cry2*	cryptochrome 1 + 2
	16	*Gpr50*	melatonin-related receptor
	17	*Id2*	DNA-binding protein inhibitor ID-2
	18	*Mta1*	metastasis-associated protein MTA1
	19 + 20	*Mtnr1a + Mtnr1b*	melatonin receptor type 1A + 1B
	21 + 22 + 23	*Per1 + Per2 + Per3*	period circadian protein homolog 1 + 2 + 3
	24	*Pml*	protein PML
	25	*Ppp1cc*	serine/threonine-protein phosphatase
	26	*Timeless*	protein timeless homolog
	27	*Vip*	vasoactive intestinal peptide
thyroid	28 + 29	*Dio1 + Dio2*	iodothyronine deiodinase type I + II
	30	*Dio3*	thyroxine 5-deiodinase
	31	*Mct8*	monocarboxylate transporter 8
	32 + 33	*Thra + Thrb*	thyroid hormone receptor alpha + beta
	34	*Trh*	pro-thyrotropin-releasing hormone
	35 + 36	*Trhr + Trhr2*	thyrotropin-releasing hormone receptor 1 + 2
	37	*Tshr*	thyrotropin receptor
	38	*Txnip*	thioredoxin-interacting protein
growth	39	*GH*	somatotropin / growth hormone
	40	*Sst*	somatostatin
	41 - 45	*Sstr1 - Sstr5*	somatostatin receptor type 1 - 5
metabolism	46 + 47	*Tas1r3 + Tas1r2*	taste receptor type 1 member 3 + 2
	48	*Glut1*	glucose transporter member 1
	49 - 52	*Glut3 - 6*	glucose transporter member 3 - 6
	53	*P2ry1*	P2Y purinoceptor 1
	54	*Fgfr1*	fibroblast growth factor receptor 1
	55	*Insr*	insulin receptor
	56	*Lepr*	leptin receptor
	57	*Agrp*	agouti-related protein
	58	*Cartpt*	cocaine- and amphetamine-regulated transcript protein
	59	*Pomc*	pro-opiomelanocortin
	60 + 61	*Mc3r + Mc4r*	melanocortin receptor 3 + 4
	62	*Npy*	pro-neuropeptide Y
	63 + 64	*Npy1r + Npy2r*	neuropeptide Y receptor type 1 + 2
	65	*Qrfp*	orexigenic neuropeptide QRFP
	66	*Qrfpr*	pyroglutamylated RF-amide peptide receptor
	67	*Ncam1*	neural cell adhesion molecule 1
	68	*Vim*	vimentin, cytosceleton of glial cells

Table 2: GO enrichment analysis of SCN: HT vs NT. Regulated genes with padj < 0.05 were tested, while all present genes were used as background. Listed are GO terms of those biological processes found to be regulated by less or more genes than expected using a false discovery rate (FDR) < 0.05.

GO biological process complete	reference	test				
	hits		expected	fold enrich	raw p-value	FDR
total	15632	843	-	-	-	-
cellular metabolic process	5607	401	327	1.23	6.10E-07	4.63E-03
metabolic process	6198	437	362	1.21	5.19E-07	7.89E-03
nitrogen compound metabolic process	4982	354	291	1.22	1.23E-05	3.73E-02
primary metabolic process	5401	381	315	1.21	7.54E-06	2.86E-02
organic substance metabolic process	5841	409	341	1.20	5.13E-06	2.60E-02

Table 3: Indicator genes regulated in SCN during torpor entry. A negative log2(FC) indicates downregulation, a positive log2(FC) upregulation of the HT-group relative to the NT-group. No indicator genes were regulated in the PVN during torpor entry. All 68 indicator genes screened for are listed in Table 1. Results of all screening indicator genes of both SCN and PVN data are shown in Supplementary Table 5.

indicator #	-log10(padj)	padj	log2(FC)	gene	gene product
4	2.2	0.007	-2.88	*Junb*	transcription factor jun-B
8	3.4	0.000	-2.66	*Avp*	vasopressin-neurophysin 2-copeptin
9	1.5	0.034	-0.69	*Avpr1a*	vasopressin V1a receptor
18	1.5	0.032	-0.82	*Mta1*	metastasis-associated protein MTA1
26	2.9	0.001	-1.00	*Timeless*	protein timeless homolog
31	1.4	0.043	-0.56	*Mct8*	monocarboxylate transporter 8
53	4.9	< 0.000	-1.66	*P2ry1*	P2Y purinoceptor 1

Table 4: Genes regulated in both SCN and PVN during torpor entry. Values are given for the HT-sampling group (torpor entry) relative to the NT-sampling group (torpor-free day). All listed genes fulfil the level of significance (padj < 0.05) with any fold change. Color code as used for the Vulcano Plots (Figure 4).

comparison	-log10(padj)	padj	log2(FC)	gene	gene product
SCN	11.09	< 0.001	24.3	*Gm773*	uncharacterized protein LOC331416 / gene model 773
PVN	10.6	< 0.001	23.9		
SCN	5.95	< 0.001	2.9	*Gsdme*	gasdermin-E
PVN	5.4	< 0.001	2.3		
SCN	2.3	0.0049	0.7	*Mylip / Idol / Mir*	E3 ubiquitin-protein ligase MYLIP / inducible degrader of the LDL-receptor / myosin regulatory light chain-interacting protein
PVN	1.8	0.0151	0.8		

Table 5: Mitochondrial genes regulated in SCN during torpor entry. Values are given for the HT-sampling group (torpor entry) relative to the NT-sampling group (torpor-free day). All listed genes fulfil the level of significance (padj < 0.05) and the fold change threshold (|log2(FC)| > 2.0). Color code as used for the Vulcano Plots (Figure 4).

-log10(padj)	padj	log2(FC)	gene	gene product
3.80	< 0.001	-2.5	*Bola1*	bolA-like protein 1
2.68	0.002	-2.5	*Ndufaf8*	mitochondrial NADH dehydrogenase
3.04	< 0.001	-3.3	*Ndufb2*	mitochondrial NADH dehydrogenase 1 beta subcomplex subunit 2 / NADH-ubiquinone oxidoreductase AGGG subunit and complex I-AGGG
3.65	< 0.001	-3.1	*Cox6a1 / Cox6al*	mitochondrial cytochrome c oxidase subunit 6A1
2.68	0.002	-2.5	*Cox5b / Gm34962*	mitochondrial cytochrome c oxidase subunit 5B
4.97	< 0.001	-2.5	*Gatc*	mitochondrial glutamyl-tRNA(Gln) amidotransferase subunit C / cytochrome c oxidase assembly factor PET112 homolog
3.20	< 0.001	-2.6	*Mrps28 / S28mt*	mitochondrial 28S ribosomal protein S28
3.62	< 0.001	-2.6	*Mrps34 / S34mt*	mitochondrial 28S ribosomal protein S34
7.37	< 0.001	-2.1	*Mrpl3 / L3mt*	mitochondrial 39S ribosomal protein L3
5.78	< 0.001	-2.7	*Efhd1 / Sws2*	EF-hand domain-containing protein D1 / mitocalcin / swiprosin-2
1.99	0.010	-2.1	*Bloc1s4*	biogenesis of lysosome-related organelles complex 1 subunit 4 / BLOC-1 subunit 4 / protein cappuccino homolog
1.90	0.013	-3.3	*Klc3*	kinesin light chain 3

Table 6: Signaling genes regulated in SCN during torpor entry. Values are given for the HT-sampling group (torpor entry) relative to the NT-sampling group (torpor-free day). All listed genes fulfil the level of significance (padj < 0.05) and the fold change threshold (|log2(FC)| > 2.0). Color code as used for the Vulcano Plots (Figure 4).

-log10(padj)	padj	log2(FC)	gene	gene product
1.94	0.011	-2.5	*Kiss1r / Gpr54*	kiSS-1 receptor / G-protein coupled receptor 54 or OT7T175 / kisspeptins or metastin receptor
2.23	0.006	-2.8	*Apoe*	apolipoprotein E
3.14	< 0.001	-2.4	*Cck*	cholecystokinin
3.27	< 0.001	-2.0	*Ly6h*	lymphocyte antigen 6H
1.40	0.040	2.7	*Inhbe*	inhibin beta E chain / activin beta-E chain
2.16	0.007	3.2	*Rrad*	GTP-binding protein RAD
4.47	< 0.001	5.2	*Tlr4*	toll-like receptor 4
3.87	< 0.001	-2.4	*Cd320 / TCblR*	CD320 antigen / transcobalamin receptor
3.19	< 0.001	-2.1	*Fth1*	ferritin heavy chain

Table 7: Transcribing and modifying genes regulated in SCN during torpor entry. Values are given for the HT-sampling group (torpor entry) relative to the NT-sampling group (torpor-free day). All listed genes fulfil the level of significance (padj < 0.05) and the fold change threshold (|log2(FC)| > 2.0). Color code as used for the Vulcano Plots (Figure 4).

-log10(padj)	padj	log2(FC)	gene	gene product
3.38	< 0.001	6.0	*Egr3*	early growth response protein 3
3.80	< 0.001	-2.1	*Dtd2 / Atd*	D-aminoacyl-tRNA deacylase 2 / animalia-specific tRNA deacylase
6.55	< 0.001	-2.0	*Osgep*	probable tRNA N6-adenosine threonylcarbamoyltransferase
2.47	0.003	-2.6	*Dohh*	deoxyhypusine hydroxylase
1.40	0.040	2.4	*B3gnt4*	N-acetyllactosaminide beta-1,3-N-acetylglucosaminyltransferase 4
1.38	0.041	-2.6	*Chst7 / Gst5*	carbohydrate sulfotransferase 7
3.10	< 0.001	-2.3	*Josd2*	josephin-2
1.32	0.048	-3.0	*Usp14*	ubiquitin carboxyl-terminal hydrolase 14
1.59	0.026	-2.2	*H1f4 / H1-4 / Hist1h1e*	histone H1.4
2.34	0.005	-4.0	*H2bc22 / Hist1h2bp*	histone H2B type 1-P
1.69	0.020	-3.0	*Cenpa*	histone H3-like centromeric protein A / centromere protein A

Table 8: Cell cycle genes regulated in SCN during torpor entry. Values are given for the HT-sampling group (torpor entry) relative to the NT-sampling group (torpor-free day). All listed genes fulfil the level of significance (padj < 0.05) and the fold change threshold (|log2(FC)| > 2.0). Color code as used for the Vulcano Plots (Figure 4).

-log10(padj)	padj	log2(FC)	gene	gene product
4.67	< 0.001	2.3	*Sertad1 / Sei-1 / Trp-Br1*	SERTA domain-containing protein 1 / CDK4-binding protein p34SEI1 / transcriptional regulator interacting with the PHD-bromodomain 1
1.93	0.012	2.4	*Gadd45b / Myd118*	growth arrest and DNA damage-inducible protein GADD45 beta / myeloid differentiation primary response protein MyD118 / negative growth regulatory protein MyD118
1.39	0.041	-3.0	*Rnf43*	E3 ubiquitin-protein ligase RNF43 / RING finger protein 43
1.69	0.020	-2.5	*Rrm2*	ribonucleoside-diphosphate reductase subunit M2
2.61	0.002	-2.3	*Nop53 / Gltscr2 / Pict1*	ribosome biogenesis protein NOP53 / glioma tumor suppressor candidate region gene 2 protein / PreS1-binding protein
2.64	0.002	-3.2	*Trp53i13*	tumor protein p53-inducible protein 13
1.92	0.012	-2.6	*Mcm8*	DNA helicase MCM8
6.95	< 0.001	-2.2	*Babam1 / Merit40 / Nba1*	BRISC and BRCA1-A complex member 1

Table 9: Brain plasticity genes regulated in SCN during torpor entry. Values are given for the HT-sampling group (torpor entry) relative to the NT-sampling group (torpor-free day). All listed genes fulfil the level of significance (padj < 0.05) and the fold change threshold (|log2(FC)| > 2.0). Color code as used for the Vulcano Plots (Figure 4).

-log10(padj)	padj	log2(FC)	gene	gene product
4.42	< 0.001	-2.6	*Cldn5 / Bec1*	claudin-5 / brain endothelial cell clone 1 protein
4.79	< 0.001	-2.6	*Nkapl*	NKAP-like protein
4.33	< 0.001	-2.6	*Hes6*	transcription cofactor HES-6 / hairy and enhancer of split 6
2.81	0.002	-3.2	*Anapc11*	anaphase-promoting complex subunit 11 / APC11 / cyclosome subunit 11
2.43	0.004	-2.4	*Ppfia3*	liprin-alpha-3
2.71	0.002	-2.0	*Gdf5 / Bmp14*	growth/differentiation factor 5
1.42	0.038	-2.1	*Boc*	brother of CDO (cell adhesion molecule-related / down regulated by oncogenesis)
5.43	< 0.001	-2.1	*Pigh*	phosphatidylinositol N-acetylglucosaminyltransferase subunit H / phosphatidylinositol-glycan biosynthesis class H protein

Table 10: Unresearched genes regulated in SCN during torpor entry. Values are given for the HT-sampling group (torpor entry) relative to the NT-sampling group (torpor-free day). All listed genes fulfil the level of significance (padj < 0.05) and the fold change threshold (|log2(FC)| > 2.0). Color code as used for the Vulcano Plots (Figure 4).

-log10(padj)	padj	log2(FC)	gene	gene product
2.26	0.006	4.7	*Otos / Ocp10*	otospiralin / organ of Corti 10 kDa protein
1.71	0.019	4.6	*Ankub1*	protein ANKUB1 / ankyrin repeat and ubiquitin domain-containing 1
6.09	< 0.001	-2.4	*Cmtm3 / Cklfsf3*	CKLF-like MARVEL transmembrane domain-containing protein 3 / chemokine-like factor superfamily member 3
3.79	< 0.001	-3.6	*Tpgs1 / Gtrgeo22*	tubulin polyglutamylase complex subunit 1 / PGs1 / p32
2.17	0.007	-2.1	*Sncb*	beta-synuclein
1.41	0.039	-2.0	*Dmpk*	myotonin-protein kinase
2.01	0.010	-2.0	*Ptma-ps2*	prothymosin alpha, pseudogene 2
2.79	0.002	-2.2	*Fam71e1*	family with sequence similarity 71 member E1 / protein FAM71E1
2.42	0.004	-3.5	*Fam216a*	family with sequence similarity 216 member a / protein FAM216A
3.41	< 0.001	-2.3	*Znhit2 / Orf6*	zinc finger HIT domain-containing protein 2 / protein FON
3.66	< 0.001	-2.1	*Zfp879 / Znf879*	zinc finger protein 879
7.17	< 0.001	-2.4	*Ccdc166*	coiled-coil domain-containing protein 166 / domain of unknown function (DUF) 4515
3.18	< 0.001	-3.8		uncharacterized protein C6orf226 homolog
2.83	0.001	-2.6		UPF0575 protein C19orf67 homolog

Table 11: Genes regulated in PVN during torpor entry. Values are given for the HT-sampling group (torpor entry) with relative to the NT-sampling group (torpor-free day). All listed genes fulfil the level of significance (padj < 0.05) with any fold change. Color code as used for the Vulcano Plots (Figure 4).

-log10(padj)	padj	log2(FC)	gene	gene product
1.4	0.037	4.1	*Atad2*	ATPase family AAA domain-containing protein 2
1.5	0.029	-5.4	*Armc4 / Odad2*	armadillo repeat-containing protein 4 / outer dynein arm-docking complex subunit 2
1.4	0.037	-6.2	*Efemp2*	EGF-containing fibulin-like extracellular matrix protein 2
2.1	0.009	-6.7	*Kcng4*	potassium voltage-gated channel subfamily G member 4
1.8	0.015	0.4	*Hmbox1*	homeobox-containing protein 1
2.0	0.010	0.8	*Klf6 / Copeb / Cpbp*	Krueppel-like factor 6 / core promoter element-binding protein
1.4	0.036	0.8	*Obsl1*	obscurin-like protein 1
1.7	0.021	1.5	*Tmem74*	transmembrane protein 74
2.7	0.002	0.7	*Zc3h8 / Fliz1*	zinc finger CCCH domain-containing protein 8 / fetal liver zinc finger protein 1
1.3	0.047	-1.0	*Marchf1 / March1 / March-1*	E3 ubiquitin-protein ligase MARCHF1 / membrane-associated RING finger protein 1
1.5	0.030	-0.8	*Kdm2b / Fbl10 / Fbxl10 / Jhdm1b / Kiaa3014*	lysine-specific demethylase 2B / F box and leucine-rich repeat protein 10 / JmjC domain-containing histone demethylation protein 1B

4.8 Supplementary Material

4.8.1 Supplementary File 1: Supplementary Tables and Figures

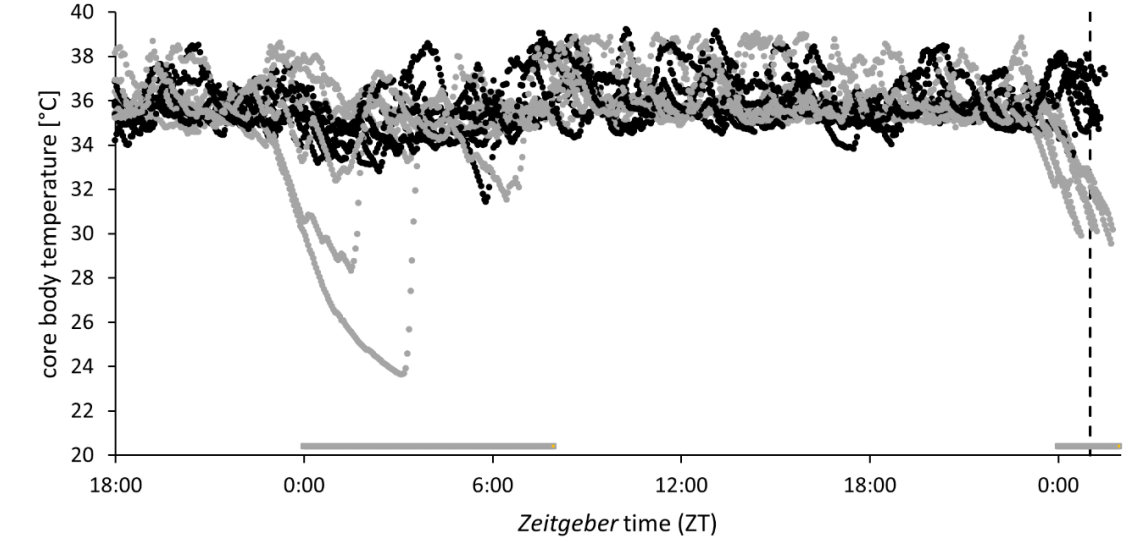

Supplementary Figure 1: Terminal body temperature pattern. The graph shows the day of sacrifice and the day before. Time is given in *Zeitgeber*-time (ZT), with lights on at ZT0 and lights off at ZT08. Photophases are indicated (grey bars on the x-axis). After at least one observed torpor bout per hamster (see also Supplementary Table 1), sacrifice was carried out approximately one hour after lights on at *Zeitgeber*-time ZT01 (vertical line) either hypothermic in torpor entry (HT, n = 6, grey lines) or normothermic on a torpor-free day (NT; n = 6, black lines). Radiotelemetry data of ten hamsters were analyzed previously [119]. Please find an analogous pattern in a study on the hypothalamic transcriptomics of hamsters sampled at ZT04 in deep torpor, on a torpor-free day or LP-normothermia [128].

Supplementary Table 1: Background information on hamsters. Each hamster (n = 12) is indicated by the cohort (EH03 and EH04) and a running number within the cohort. Listed are gender (f for female, m for male) as well as body mass, fur index, age, and duration in short photoperiod (SP) for several key dates, namely SP-start, surgery to implant the radiotelemetry transmitter, and sacrifice. The fur index was assessed from 1, brown light summer fur, to 6, white isolating winter fur, according to Figala et al. 1973 [60]. Cohort EH04 was implanted already in LP prior to SP-adaptation, while EH03 was implanted when adapted to SP. The number of torpor bouts are based on all torpor bouts with a body temperature below 32 °C for at least 30 minutes expressed during the individual observation interval. The torpor incidence is defined as the number of torpor bouts expressed during the number of observation days, and is given for the last seven full days after at least seven days of recovery from surgery. Adaptation, body temperature and activity of this studies' hamsters, except for EH03-29 and EH03-22, were analyzed previously [119]. Mean values and standard deviation of the mean values (Std.Dev.) are given for the HT-sampling group (n = 6), the NT-sampling group (n = 6), and all hamsters (n = 12). After sampling about one hour after lights on (*Zeitgeber*-time ZT01, given 3 min = 0.05 and 1h = 1.00) either hypothermic during torpor entry (HT) or normothermic on a torpor-free day (NT), a running number per sampling group (from 1 to 6) was assigned to indicate the SCN and PVN sample gained from each animal.

hamster ID	gender	body mass			terminal fur index	age [weeks] at		
		at SP [g]	at sacrifice [g]	difference [%]		SP	surgery	sacrifice
EH03-08	m	40.4	33.2	-17.8	4.0	19.4	29.4	32.7
EH03-30	m	34.2	31.9	-6.7	4.5	15.9	27.0	29.1
EH04-11	f	29.0	23.4	-19.3	5.0	14.0	11.7	26.7
EH04-07	m	39.5	29.0	-26.6	4.0	14.9	12.4	28.4
EH04-06	f	29.4	23.3	-20.7	4.0	15.9	13.4	29.9
EH04-10	m	32.0	24.2	-24.4	5.0	14.0	11.7	28.3
EH03-05	m	33.6	26.5	-21.1	3.0	21.1	35.1	37.4
EH03-29	f	35.4	26.9	-24.0	3.0	18.3	29.4	31.1
EH03-22	m	32.1	25.7	-19.9	4.5	19.3	30.3	32.3
EH04-09	f	30.4	23.4	-23.0	3.0	14.9	12.6	28.4
EH04-08	m	23.3	19.5	-16.3	5.0	14.9	12.4	29.1
EH04-05	m	38.5	27.4	-28.8	5.0	15.9	13.4	30.3
mean HT		34.1	27.5	-19.3	4.4	15.7	17.6	29.2
Std.Dev. HT		4.9	4.5	6.9	0.5	2.0	8.3	2.0
mean NT		32.2	24.9	-22.2	3.9	17.4	22.2	31.5
Std.Dev. NT		5.2	3.0	4.2	1.0	2.6	10.5	3.2
mean all		**33.2**	**26.2**	**-20.7**	**4.2**	**16.5**	**19.9**	**30.3**
Std.Dev. all		**4.9**	**3.9**	**5.7**	**0.8**	**2.4**	**9.3**	**2.8**

hamster ID	duration in SP [weeks] at		observation		torpor incidence last 7 full days	sampling time [ZT]	terminal Tb [°C]	sampling ID
	surgery	sacrifice	interval [weeks]	torpor bouts [#]				
EH03-08	10.0	13.3	3.3	5	0.3	0.85	29.5	HT01
EH03-30	11.1	13.3	2.1	5	0.4	1.75	30.2	HT02
EH04-11	-2.3	12.7	15.0	2	0.0	0.75	29.9	HT03
EH04-07	-2.4	13.6	16.0	1	0.1	1.25	30.1	HT04
EH04-06	-2.4	14.0	16.4	9	0.7	0.70	30.1	HT05
EH04-10	-2.3	14.3	16.6	7	0.6	1.10	30.2	HT06
EH03-05	14.0	16.3	2.3	5	0.6	1.35	35.2	NT01
EH03-29	11.1	12.9	1.7	3	-	1.30	34.7	NT02
EH03-22	11.0	13.0	2.0	5	-	1.25	35.5	NT03
EH04-09	-2.3	13.6	15.9	1	0.1	1.50	37.2	NT04
EH04-08	-2.4	14.3	16.7	3	0.1	1.35	35.2	NT05
EH04-05	-2.4	14.4	16.9	2	0.0	0.90	37.9	NT06
mean HT	2.0	13.5	11.6	5	0.4	1.1	30.0	
Std.Dev. HT	6.7	0.6	6.9	3	0.3	0.4	0.3	
mean NT	4.8	14.1	9.2	3	0.2	1.3	35.9	
Std.Dev. NT	8.0	1.3	7.9	2	0.2	0.2	1.3	
mean all	**3.4**	**13.8**	**10.4**	**4**	**0.3**	**1.2**		
Std.Dev. All	**7.2**	**1.0**	**7.2**	**2**	**0.3**	**0.3**		

Supplementary Table 2: Validation of lasermicrodissection. Using the PALM MicroBeam software (Carl Zeiss Microscopy Deutschland GmbH, Oberkochen, Germany), three parameters were documented per sample. Using the visual overview of the "Navigator", the number of sections each hypothalamic core area expanded to were counted. The "Element List" provided the number of marked elements and the total marked area per sample. Knowing the sections to be 0.02 mm thick, the total volume of each sample was calculated. These values are approximations, while the amount of sampled material was not investigated.

animal ID	SCN					PVN				
	sections [#]	elements [#]	area [mm²]	volume [mm³]	sample ID	sections [#]	elements [#]	area [mm²]	volume [mm³]	sample ID
EH03_08	20	214	1.7	0.034	SCN_HT01	15	148	1.3	0.026	PVN_HT01
EH03_30	14	124	0.7	0.015	SCN_HT02	13	107	0.6	0.013	PVN_HT02
EH04_11	15	365	0.9	0.018	SCN_HT03	19	312	0.8	0.017	PVN_HT03
EH04_07	16	267	1.0	0.020	SCN_HT04	20	332	1.1	0.023	PVN_HT04
EH04_06	18	370	0.9	0.018	SCN_HT05	16	347	1.0	0.019	PVN_HT05
EH04_10	21	254	1.4	0.027	SCN_HT06	15	122	0.5	0.010	PVN_HT06
EH03_05	21	269	1.5	0.030	SCN_NT01	15	216	1.0	0.021	PVN_NT01
EH03_29	15	123	1.1	0.022	SCN_NT02	17	148	1.2	0.024	PVN_NT02
EH03_22	22	296	1.4	0.028	SCN_NT03	20	258	1.1	0.022	PVN_NT03
EH04_09	16	304	1.1	0.021	SCN_NT04	15	292	1.0	0.021	PVN_NT04
EH04_08	12	199	0.8	0.017	SCN_NT05	17	242	1.0	0.019	PVN_NT05
EH04_05	28	337	1.1	0.021	SCN_NT06	19	395	1.1	0.022	PVN_NT06
min	12	123	0.7	0.015		13	107	0.5	0.010	
max	28	370	1.7	0.034		20	395	1.3	0.026	
mean	**18**	**260**	**1.1**	**0.022**		**17**	**243**	**1.0**	**0.020**	
Std. Dev.	**4**	**83**	**0.3**	**0.006**		**2**	**96**	**0.2**	**0.005**	

Supplementary Table 3: Quality and quantity of total RNA. Total RNA was purified using the RNeasy Plus Micro Kit with gDNA eliminator spin column (Qiagen GmbH, Hilden, Germany), and checked for quality (Bioanalyzer, Agilent Technologies, Waldbronn, Germany) and quantity (RNA 6000 Pico Kit for very small RNA amounts of 50 – 5000pg/µL, Agilent Technologies, Waldbronn, Germany).

animal ID	SCN				PVN			
	sample ID	quality (RIN)	quantity [pg / µL]	rRNA ratio [28s / 18s]	sample ID	quality (RIN)	quantity [pg / µL]	rRNA ratio [28s / 18s]
EH03_08	SCN_HT01	8.2	440	1.2	PVN_HT01	9.5	764	3.3
EH03_30	SCN_HT02	8.7	267	4.2	PVN_HT02	8.9	313	4.5
EH04_11	SCN_HT03	8.7	312	1.6	PVN_HT03	8.0	821	1.3
EH04_07	SCN_HT04	9.0	338	3.7	PVN_HT04	9.2	851	2.7
EH04_06	SCN_HT05	8.6	168	3.6	PVN_HT05	7.8	804	1.2
EH04_10	SCN_HT06	9.1	442	2.9	PVN_HT06	8.7	216	3.5
EH03_05	SCN_NT01	9.2	802	2.6	PVN_NT01	7.9	991	1.2
EH03_29	SCN_NT02	8.9	465	3.7	PVN_NT02	9.1	424	4.1
EH03_22	SCN_NT03	9.0	339	4.2	PVN_NT03	8.3	164	1.3
EH04_09	SCN_NT04	8.1	741	1.3	PVN_NT04	8.7	1102	2.8
EH04_08	SCN_NT05	9.2	283	2.7	PVN_NT05	8.3	577	1.3
EH04_05	SCN_NT06	9.2	496	2.6	PVN_NT06	8.1	403	1.3
min		8.1	168	1.2		7.8	164	1.2
max		9.2	802	4.2		9.5	1102	4.5
mean		**8.8**	**424**	**2.9**		**8.5**	**619**	**2.4**
Std. Dev.		**0.4**	**188**	**1.1**		**0.6**	**312**	**1.3**

Supplementary Table 4: Quality control of RNA-Seq data. The mRNA was isolated, the library prepared (NEBNext® Single Cell / Low Input RNA library Prep Kit dual index), and the RNA-Seq performed on an Illumina NextSeq 500 (1 lane, 2x25 mio reads, 2 x 150 nt, 7.5 gb). Quality control was performed with FastQC [130]. There were zero reads flagged as poor quality. The sequence length was throughout 151 base pairs. The GC-content was 45 ± 1 %. The number of total read pairs ranged from 27.4 mio to 48.9 mio with a mean of 36.2 ± 6.2 mio per SCN sample and a mean of 38.3 ± 6.4 mio per PVN sample. In total, 894,514,860 read pairs from both SCN and PVN were included in the original *de novo* assembly before mapping against the reference was performed. All data discussed in this study are accessible through GEO Series accession number GSE181298.

animal ID	SCN		PVN	
	sample ID	read pairs [#]	sample ID	read pairs [#]
EH03_08	SCN_HT01	33,359,816	PVN_HT01	32,285,924
EH03_30	SCN_HT02	45,628,975	PVN_HT02	29,720,901
EH04_11	SCN_HT03	33,220,396	PVN_HT03	30,632,110
EH04_07	SCN_HT04	36,574,578	PVN_HT04	27,404,626
EH04_06	SCN_HT05	48,872,922	PVN_HT05	32,679,724
EH04_10	SCN_HT06	32,529,918	PVN_HT06	43,362,931
EH03_05	SCN_NT01	39,123,835	PVN_NT01	37,864,734
EH03_29	SCN_NT02	47,709,353	PVN_NT02	37,424,340
EH03_22	SCN_NT03	42,090,945	PVN_NT03	43,203,384
EH04_09	SCN_NT04	29,036,245	PVN_NT04	47,527,760
EH04_08	SCN_NT05	33,995,779	PVN_NT05	33,751,737
EH04_05	SCN_NT06	37,575,691	PVN_NT06	38,938,236
sum per area	**459,718,453**		**434,796,407**	
total sum	**894,514,860**			

Supplementary Table 5: Results of all 68 predefined indicator genes. (Table see next page). Results for both pairwise group comparisons, namely SCN: HT vs NT and PVN: HT vs NT. Indicator genes with padj < 0.05 (black fields with white labelling) were presented in the main document (Table 3). A negative log2(FC) indicates downregulation (yellow), a positive log2(FC) upregulation (green) of the HT-group relative to the NT-group. "Not present" (grey) marks genes which were not present in one or both pairwise group comparisons but annotated in the reference *Mus musculus*. "Outlier" (grey) replaces a padj-value given the outlying count according to the statistics performed with DESeq2 [141].

Supplementary Table 5: Results of all 68 predefined indicator genes. (Legend text see previous page).

	#	SCN: HT vs NT			PVN: HT vs NT			gene	gene product
		padj	-log10 (padj)	log2(FC)	padj	-log10 (padj)	log2(FC)		
transcription	1	0.314	0.5	-0.54	0.999	0.0	0.52	*Fos*	proto-oncogene c-Fos
	2	outlier			0.999	0.0	-1.05	*Fosb*	protein fosB
	3	0.653	0.2	0.60	0.773	0.1	0.64	*Jun*	transcription factor AP-1 / c-Jun
	4	0.007	2.2	-2.88	0.540	0.3	-2.15	*Junb*	transcription factor jun-B
	5	0.059	1.2	-1.16	0.917	0.0	-0.76	*Jund*	transcription factor jun-D
	6	0.365	0.4	-0.25	0.999	0.0	-0.06	*c-Jun1*	c-Jun-amino-terminal kinase-interacting protein 1
	7	0.186	0.7	-0.34	0.999	0.0	-0.04	*c-Jun3*	c-Jun-amino-terminal kinase-interacting protein 3
clock	8	0.000	3.4	-2.66	0.999	0.0	0.11	*Avp*	vasopressin-neurophysin 2-copeptin
	9	0.034	1.5	-0.69	0.976	0.0	-0.78	*Avpr1a*	vasopressin V1a receptor
	10	0.411	0.4	-0.26	0.999	0.0	0.24	*Bmal1*	brain and muscle ARNT-like 1
	11	0.824	0.1	0.57	0.999	0.0	0.45	*Bmal2*	brain and muscle ARNT-like 2
	12	0.961	0.0	0.02	0.999	0.0	-0.17	*Bhlhe40*	class E basic helix-loop-helix protein 40
	13	0.941	0.0	0.07	0.999	0.0	0.03	*Clock*	circadian locomoter output cycles protein kaput
	14	0.719	0.1	0.19	0.999	0.0	0.19	*Cry1*	cryptochrome-1
	15	0.743	0.1	-0.16	0.999	0.0	0.01	*Cry2*	cryptochrome-2
	16	0.875	0.1	-0.24	0.937	0.0	2.92	*Gpr50*	melatonin-related receptor
	17	0.404	0.4	0.42	0.999	0.0	-0.26	*Id2*	DNA-binding protein inhibitor ID-2
	18	0.032	1.5	-0.82	0.999	0.0	0.22	*Mta1*	metastasis-associated protein MTA1
	19	0.973	0.0	0.05	0.999	0.0	-2.45	*Mtnr1a*	melatonin receptor type 1A
	20	not present			not present			*Mtnr1b*	melatonin receptor type 1B
	21	0.506	0.3	0.41	0.999	0.0	0.04	*Per1*	period circadian protein homolog 1
	22	0.162	0.8	0.60	0.999	0.0	0.21	*Per2*	period circadian protein homolog 2
	23	0.587	0.2	0.65	0.999	0.0	-0.74	*Per3*	period circadian protein homolog 3
	24	0.455	0.3	0.48	0.999	0.0	-0.61	*Pml*	protein PML
	25	0.824	0.1	0.10	0.999	0.0	0.20	*Ppp1cc*	serine/threonine-protein phosphatase
	26	0.001	2.9	-1.00	0.999	0.0	-0.43	*Timeless*	protein timeless homolog
	27	0.982	0.0	-0.01	0.999	0.0	-1.32	*Vip*	vasoactive intestinal peptide
thyroid	28	not present			not present			*Dio1*	iodothyronine deiodinase type I
	29	0.735	0.1	0.79	0.999	0.0	1.07	*Dio2*	iodothyronine deiodinase type II
	30	not present			not present			*Dio3*	thyroxine 5-deiodinase
	31	0.043	1.4	-0.56	0.999	0.0	-0.16	*Mct8*	monocarboxylate transporter 8
	32	0.941	0.0	-0.03	0.999	0.0	0.08	*Thra*	thyroid hormone receptor alpha
	33	0.831	0.1	0.12	0.999	0.0	0.01	*Thrb*	thyroid hormone receptor beta
	34	0.713	0.1	0.67	0.999	0.0	0.20	*Trh*	pro-thyrotropin-releasing hormone
	35	0.963	0.0	0.05	0.999	0.0	-0.47	*Trhr*	thyrotropin-releasing hormone receptor
	36	not present			0.999	0.0	1.37	*Trhr2*	thyrotropin releasing hormone receptor 2
	37	outlier			0.999	0.0	-3.32	*Tshr*	thyrotropin receptor
	38	0.221	0.7	0.87	0.999	0.0	-0.08	*Txnip*	thioredoxin-interacting protein
growth	39	outlier			not present			*GH*	somatotropin / growth hormone
	40	0.272	0.6	-1.09	0.999	0.0	-0.05	*Sst*	somatostatin
	41	0.074	1.1	-0.58	0.999	0.0	0.06	*Sstr1*	somatostatin receptor type 1
	42	0.604	0.2	0.47	0.999	0.0	0.03	*Sstr2*	somatostatin receptor type 2
	43	outlier			0.999	0.0	0.35	*Sstr3*	somatostatin receptor type 3
	44	0.491	0.3	1.26	0.943	0.0	-1.29	*Sstr4*	somatostatin receptor type 4
	45	outlier			0.999	0.0	0.01	*Sstr5*	somatostatin receptor type 5
metabolism	46	outlier			0.999	0.0	-0.54	*Tas1r3*	taste receptor type 1 member 3
	47	not present			not present			*Tas1r2*	taste receptor type 1 member 2
	48	0.570	0.2	0.18	0.999	0.0	-0.10	*Glut1*	glucose transporter member 1
	49	0.093	1.0	0.40	0.999	0.0	0.04	*Glut3*	glucose transporter member 3
	50	0.818	0.1	0.59	0.999	0.0	-1.37	*Glut4*	glucose transporter member 4
	51	0.435	0.4	0.96	0.999	0.0	-0.12	*Glut5*	glucose transporter member 5
	52	0.840	0.1	-0.20	0.999	0.0	0.14	*Glut6*	glucose transporter member 6
	53	0.000	4.9	-1.66	0.999	0.0	-0.91	*P2ry1*	P2Y purinoceptor 1
	54	0.788	0.1	0.12	0.999	0.0	0.16	*Fgfr1*	fibroblast growth factor receptor 1
	55	0.832	0.1	0.29	0.999	0.0	0.18	*Insr*	insulin receptor
	56	outlier			0.999	0.0	0.38	*Lepr*	leptin receptor
	57	outlier			0.999	0.0	0.01	*Agrp*	agouti-related protein
	58	0.969	0.0	-0.08	0.999	0.0	-0.08	*Cartpt*	cocaine- and amphetamine-regulated transcript protein
	59	0.870	0.1	0.12	0.999	0.0	0.32	*Pomc*	pro-opiomelanocortin
	60	outlier			0.999	0.0	1.40	*Mc3r*	melanocortin receptor 3
	61	0.782	0.1	0.51	0.999	0.0	0.05	*Mc4r*	melanocortin receptor 4
	62	0.357	0.4	0.95	0.999	0.0	0.39	*Npy*	pro-neuropeptide Y
	63	0.761	0.1	0.19	0.999	0.0	-0.18	*Npy1r*	neuropeptide Y receptor type 1
	64	0.425	0.4	-1.66	0.910	0.0	-1.98	*Npy2r*	neuropeptide Y receptor type 2
	65	outlier			not present			*Qrfp*	orexigenic neuropeptide QRFP
	66	outlier			0.999	0.0	-0.04	*Qrfpr*	pyroglutamylated RF-amide peptide receptor
	67	0.783	0.1	0.12	0.999	0.0	0.08	*Ncam1*	neural cell adhesion molecule 1
	68	0.824	0.1	-0.14	0.999	0.0	-0.16	*Vim*	vimentin, cytosceleton of glial cells

4.8.2 Supplementary File 2: Processing Pipeline

```
# Bash-Script version of 13.02.2021 09:00 as provided by Elena Haugg, working group Annika Herwig, Institute of Neurobiology, Ulm University, Germany, 2021
# contact: elena.haugg@uni-ulm.de


#for each sample: prepare reads (here: paired end reads, 1 lane, from Illumina NextSeq 500)

#command: trim_galore –paired –cores <number of cores> <"forward / left" file(s) (read 1 = R1) in format .fastq.gz, space-separated> <"reverse / right" file(s) (read 2 = R2) in format .fastq.gz, space-separated>
trim_galore --paired --cores 1 *SCN_HT01_R1.fastq.gz *SCN_HT01_R2.fastq.gz &
trim_galore --paired --cores 1 *SCN_HT02_R1.fastq.gz *SCN_HT02_R2.fastq.gz &
trim_galore --paired --cores 1 *SCN_HT03_R1.fastq.gz *SCN_HT03_R2.fastq.gz &
trim_galore --paired --cores 1 *SCN_HT04_R1.fastq.gz *SCN_HT04_R2.fastq.gz &
trim_galore --paired --cores 1 *SCN_HT05_R1.fastq.gz *SCN_HT05_R2.fastq.gz &
trim_galore --paired --cores 1 *SCN_HT06_R1.fastq.gz *SCN_HT06_R2.fastq.gz &
trim_galore --paired --cores 1 *SCN_NT01_R1.fastq.gz *SCN_NT01_R2.fastq.gz &
trim_galore --paired --cores 1 *SCN_NT02_R1.fastq.gz *SCN_NT02_R2.fastq.gz &
trim_galore --paired --cores 1 *SCN_NT03_R1.fastq.gz *SCN_NT03_R2.fastq.gz &
trim_galore --paired --cores 1 *SCN_NT04_R1.fastq.gz *SCN_NT04_R2.fastq.gz &
trim_galore --paired --cores 1 *SCN_NT05_R1.fastq.gz *SCN_NT05_R2.fastq.gz &
trim_galore --paired --cores 1 *SCN_NT06_R1.fastq.gz *SCN_NT06_R2.fastq.gz &
trim_galore --paired --cores 1 *PVN_HT01_R1.fastq.gz *PVN_HT01_R2.fastq.gz &
trim_galore --paired --cores 1 *PVN_HT02_R1.fastq.gz *PVN_HT02_R2.fastq.gz &
trim_galore --paired --cores 1 *PVN_HT03_R1.fastq.gz *PVN_HT03_R2.fastq.gz &
trim_galore --paired --cores 1 *PVN_HT04_R1.fastq.gz *PVN_HT04_R2.fastq.gz &
trim_galore --paired --cores 1 *PVN_HT05_R1.fastq.gz *PVN_HT05_R2.fastq.gz &
trim_galore --paired --cores 1 *PVN_HT06_R1.fastq.gz *PVN_HT06_R2.fastq.gz &
trim_galore --paired --cores 1 *PVN_NT01_R1.fastq.gz *PVN_NT01_R2.fastq.gz &
trim_galore --paired --cores 1 *PVN_NT02_R1.fastq.gz *PVN_NT02_R2.fastq.gz &
trim_galore --paired --cores 1 *PVN_NT03_R1.fastq.gz *PVN_NT03_R2.fastq.gz &
trim_galore --paired --cores 1 *PVN_NT04_R1.fastq.gz *PVN_NT04_R2.fastq.gz &
trim_galore --paired --cores 1 *PVN_NT05_R1.fastq.gz *PVN_NT05_R2.fastq.gz &
trim_galore --paired --cores 1 *PVN_NT06_R1.fastq.gz *PVN_NT06_R2.fastq.gz &
wait
#output is a *val_1.fq.gz for all "forward / left" files and a *val_2.fq.gz for all "reverse / right" files


#for each organism: de novo assembly

#command: Trinity –seqType <file format> --max_memory <threshold> --CPU <all available CPU> --min_kmer_cov 2 --bflyCalculateCPU –left <R1 fastq files, comma-separated> <R2 fastq files, comma-separated>
#note: high performance computing (HPC) is needed! All other commands can be performed on a good linux computer.
Trinity --seqType fq --max_memory 100G --CPU 20 --min_kmer_cov 2 --bflyCalculateCPU --left SCN_HT01_R1_val_1.fq.gz,SCN_HT02_R1_val_1.fq.gz,SCN_HT03_R1_val_1.fq.gz,SCN_HT04_R1_val_1.fq.gz,SCN_HT05_R1_val_1.fq.gz,SCN_HT06_R1_val_1.fq.gz,SCN_NT01_R1_val_1.fq.gz,SCN_NT02_R1_val_1.fq.gz,SCN_NT03_R1_val_1.fq.gz,SCN_NT04_R1_val_1.fq.gz,SCN_NT05_R1_val_1.fq.gz,SCN_NT06_R1_val_1.fq.gz,PVN_HT01_R1_val_1.fq.gz,PVN_HT02_R1_val_1.fq.gz,PVN_HT03_R1_val_1.fq.gz,PVN_HT04_R1_val_1.fq.gz,PVN_HT05_R1_val_1.fq.gz,PVN_HT06_R1_val_1.fq.gz,PVN_NT01_R1_val_1.fq.gz,PVN_NT02_R1_val_1.fq.gz,PVN_NT03_R1_val_1.fq.gz,PVN_NT04_R1_val_1.fq.gz,PVN_NT05_R1_val_1.fq.gz,PVN_NT06_R1_val_1.fq.gz --right SCN_HT01_R2_val_2.fq.gz,SCN_HT02_R2_val_2.fq.gz,SCN_HT03_R2_val_2.fq.gz,SCN_HT04_R2_val_2.fq.gz,SCN_HT05_R2_val_2.fq.gz,SCN_HT06_R2_val_2.fq.gz,SCN_NT01_R2_val_2.fq.gz,SCN_NT02_R2_val_2.fq.gz,SCN_NT03_R2_val_2.fq.gz,SCN_NT04_R2_val_2.fq.gz,SCN_NT05_R2_val_2.fq.gz,SCN_NT06_R2_
```

```
    val_2.fq.gz,PVN_HT01_R2_val_2.fq.gz,PVN_HT02_R2_val_2.fq.gz,PVN_HT03_R2_val_2.fq.gz,PVN_HT04_
    R2_val_2.fq.gz,PVN_HT05_R2_val_2.fq.gz,PVN_HT06_R2_val_2.fq.gz,PVN_NT01_R2_val_2.fq.gz,PVN_N
    T02_R2_val_2.fq.gz,PVN_NT03_R2_val_2.fq.gz,PVN_NT04_R2_val_2.fq.gz,PVN_NT05_R2_val_2.fq.gz,PV
    N_NT06_R2_val_2.fq.gz
#rename output to e.g., Trinity_SCN-PVN_Phodopus-ZT01.fasta


#for each organism-reference-combination: mapping

#command: makeblastdb -in <reference proteome fasta> -parse_seqids -title <"name"> -dbtype <prot> -out
    <name of output>
#reference proteome of Mus musculus (GRCm39, Annotation Release 109) was downloaded via NCBI
    https://www.ncbi.nlm.nih.gov/genome/?term=txid10090[orgn]
makeblastdb -in GCF_000001635.27_GRCm39_protein.faa -parse_seqids -title "Mus musculus 39 proteome"
    -dbtype prot -out mus_proteome

#command: blastx -db <name of makeblastdb output> -query <Trinity-output> -out <name of output> -evalue
    <threshold> -outfmt <output-format, 6 is table> -num_threads <number of available CPU>
blastx -db mus_proteome -query Trinity_SCN-PVN_Phodopus-ZT01.fasta -out blastx_LMD -evalue 1E-5 -
    outfmt 6 -num_threads 20

#command: ruby extract_hits_from_fasta.rb <Trinity-output> <blastx-output> <name of output>
ruby extract_hits_from_fasta.rb Trinity_SCN-PVN_Phodopus-ZT01.fasta blastx_LMD Trinity_SCN-
    PVN_Phodopus-ZT01_aftermapping.fasta

#command: ruby hits_to_genemap.rb <blastx-output> <reference annotation> <name of output>
#Mus musculus (GRCm39, Annotation Release 109) was downloaded via NCBI in tabular format (.txt)
    https://www.ncbi.nlm.nih.gov/genome/?term=txid10090[orgn]
ruby hits_to_genemap.rb blastx_LMD proteins_52_992563.txt genemap_LMD.txt

#command: rsem-prepare-reference --bowtie --transcript-to-gene-map <name of genemap output> <name
    of extract hits output> <name of output>
rsem-prepare-reference --bowtie --transcript-to-gene-map genemap_LMD.txt Trinity_SCN-PVN_Phodopus-
    ZT01_aftermapping.fasta preparedmap-LMD


#for each sample: rsem-output

#gunzip output of trim-galore with command: gunzip *.fq.gz
gunzip SCN_HT01_R1_val_1.fq.gz
gunzip SCN_HT01_R2_val_2.fq.gz
gunzip SCN_HT02_R1_val_1.fq.gz
gunzip SCN_HT02_R2_val_2.fq.gz
gunzip SCN_HT03_R1_val_1.fq.gz
gunzip SCN_HT03_R2_val_2.fq.gz
gunzip SCN_HT04_R1_val_1.fq.gz
gunzip SCN_HT04_R2_val_2.fq.gz
gunzip SCN_HT05_R1_val_1.fq.gz
gunzip SCN_HT05_R2_val_2.fq.gz
gunzip SCN_HT06_R1_val_1.fq.gz
gunzip SCN_HT06_R2_val_2.fq.gz
gunzip SCN_NT01_R1_val_1.fq.gz
gunzip SCN_NT01_R2_val_2.fq.gz
gunzip SCN_NT02_R1_val_1.fq.gz
gunzip SCN_NT02_R2_val_2.fq.gz
gunzip SCN_NT03_R1_val_1.fq.gz
gunzip SCN_NT03_R2_val_2.fq.gz
```

```
gunzip SCN_NT04_R1_val_1.fq.gz
gunzip SCN_NT04_R2_val_2.fq.gz
gunzip SCN_NT05_R1_val_1.fq.gz
gunzip SCN_NT05_R2_val_2.fq.gz
gunzip SCN_NT06_R1_val_1.fq.gz
gunzip SCN_NT06_R2_val_2.fq.gz
gunzip PVN_HT01_R1_val_1.fq.gz
gunzip PVN_HT01_R2_val_2.fq.gz
gunzip PVN_HT02_R1_val_1.fq.gz
gunzip PVN_HT02_R2_val_2.fq.gz
gunzip PVN_HT03_R1_val_1.fq.gz
gunzip PVN_HT03_R2_val_2.fq.gz
gunzip PVN_HT04_R1_val_1.fq.gz
gunzip PVN_HT04_R2_val_2.fq.gz
gunzip PVN_HT05_R1_val_1.fq.gz
gunzip PVN_HT05_R2_val_2.fq.gz
gunzip PVN_HT06_R1_val_1.fq.gz
gunzip PVN_HT06_R2_val_2.fq.gz
gunzip PVN_NT01_R1_val_1.fq.gz
gunzip PVN_NT01_R2_val_2.fq.gz
gunzip PVN_NT02_R1_val_1.fq.gz
gunzip PVN_NT02_R2_val_2.fq.gz
gunzip PVN_NT03_R1_val_1.fq.gz
gunzip PVN_NT03_R2_val_2.fq.gz
gunzip PVN_NT04_R1_val_1.fq.gz
gunzip PVN_NT04_R2_val_2.fq.gz
gunzip PVN_NT05_R1_val_1.fq.gz
gunzip PVN_NT05_R2_val_2.fq.gz
gunzip PVN_NT06_R1_val_1.fq.gz
gunzip PVN_NT06_R2_val_2.fq.gz


#command: rsem-calculate-expression --paired-end -p <number of CPU> –left <forward file(s) (R1_val_1) in
    format .fq, comma-separated> <backward file(s) (R2_val_2) in format .fq, comma-separated> <name of
    rsem-prepare-reference-output> <name of the sample>
rsem-calculate-expression --paired-end -p 20 SCN_HT01_R1_val_1.fq SCN_HT01_R2_val_2.fq preparedmap-
    LMD SCN_HT01
wait
rsem-calculate-expression --paired-end -p 20 SCN_HT02_R1_val_1.fq SCN_HT02_R2_val_2.fq preparedmap-
    LMD SCN_HT02
wait
rsem-calculate-expression --paired-end -p 20 SCN_HT03_R1_val_1.fq SCN_HT03_R2_val_2.fq preparedmap-
    LMD SCN_HT03
wait
rsem-calculate-expression --paired-end -p 20 SCN_HT04_R1_val_1.fq SCN_HT04_R2_val_2.fq preparedmap-
    LMD SCN_HT04
wait
rsem-calculate-expression --paired-end -p 20 SCN_HT05_R1_val_1.fq SCN_HT05_R2_val_2.fq preparedmap-
    LMD SCN_HT05
wait
rsem-calculate-expression --paired-end -p 20 SCN_HT06_R1_val_1.fq SCN_HT06_R2_val_2.fq preparedmap-
    LMD SCN_HT06
wait
rsem-calculate-expression --paired-end -p 20 SCN_NT01_R1_val_1.fq SCN_NT01_R2_val_2.fq preparedmap-
    LMD SCN_NT01
wait
```

```
rsem-calculate-expression --paired-end -p 20 SCN_NT02_R1_val_1.fq SCN_NT02_R2_val_2.fq preparedmap-
    LMD SCN_NT02
wait
rsem-calculate-expression --paired-end -p 20 SCN_NT03_R1_val_1.fq SCN_NT03_R2_val_2.fq preparedmap-
    LMD SCN_NT03
wait
rsem-calculate-expression --paired-end -p 20 SCN_NT04_R1_val_1.fq SCN_NT04_R2_val_2.fq preparedmap-
    LMD SCN_NT04
wait
rsem-calculate-expression --paired-end -p 20 SCN_NT05_R1_val_1.fq SCN_NT05_R2_val_2.fq preparedmap-
    LMD SCN_NT05
wait
rsem-calculate-expression --paired-end -p 20 SCN_NT06_R1_val_1.fq SCN_NT06_R2_val_2.fq preparedmap-
    LMD SCN_NT06
wait
rsem-calculate-expression --paired-end -p 20 PVN_HT01_R1_val_1.fq PVN_HT01_R2_val_2.fq preparedmap-
    LMD PVN_HT01
wait
rsem-calculate-expression --paired-end -p 20 PVN_HT02_R1_val_1.fq PVN_HT02_R2_val_2.fq preparedmap-
    LMD PVN_HT02
wait
rsem-calculate-expression --paired-end -p 20 PVN_HT03_R1_val_1.fq PVN_HT03_R2_val_2.fq preparedmap-
    LMD PVN_HT03
wait
rsem-calculate-expression --paired-end -p 20 PVN_HT04_R1_val_1.fq PVN_HT04_R2_val_2.fq preparedmap-
    LMD PVN_HT04
wait
rsem-calculate-expression --paired-end -p 20 PVN_HT05_R1_val_1.fq PVN_HT05_R2_val_2.fq preparedmap-
    LMD PVN_HT05
wait
rsem-calculate-expression --paired-end -p 20 PVN_HT06_R1_val_1.fq PVN_HT06_R2_val_2.fq preparedmap-
    LMD PVN_HT06
wait
rsem-calculate-expression --paired-end -p 20 PVN_NT01_R1_val_1.fq PVN_NT01_R2_val_2.fq preparedmap-
    LMD PVN_NT01
wait
rsem-calculate-expression --paired-end -p 20 PVN_NT02_R1_val_1.fq PVN_NT02_R2_val_2.fq preparedmap-
    LMD PVN_NT02
wait
rsem-calculate-expression --paired-end -p 20 PVN_NT03_R1_val_1.fq PVN_NT03_R2_val_2.fq preparedmap-
    LMD PVN_NT03
wait
rsem-calculate-expression --paired-end -p 20 PVN_NT04_R1_val_1.fq PVN_NT04_R2_val_2.fq preparedmap-
    LMD PVN_NT04
wait
rsem-calculate-expression --paired-end -p 20 PVN_NT05_R1_val_1.fq PVN_NT05_R2_val_2.fq preparedmap-
    LMD PVN_NT05
wait
rsem-calculate-expression --paired-end -p 20 PVN_NT06_R1_val_1.fq PVN_NT06_R2_val_2.fq preparedmap-
    LMD PVN_NT06
wait
#rsem output per sample are two files, .isoforms.results (not used) and .genes.results (used)
```

4.8.3 Supplementary File 3: R-Statistics

```
# R-Script version of 20210214 as provided by Elena Haugg
# executed by Elena Haugg, working group Annika Herwig, Institute of Neurobiology, Ulm University, Germany, 2021
# Contact: elena.haugg@uni-ulm.de

# RStudio version 5.3.2 (R Core Team 2018; RStudio Team 2020)
# please find R session info at the end of this document


# activation of packages, which must be installed before
library("tximport") # (Soneson et al. 2015)
library("DESeq2") # (Love et al. 2014, 2019, 2020) # an alternative of DESeq2's dds is edgR's TMM
library("apeglm") # (Zhu et al. 2019)
library("RColorBrewer") # (Neuwirth 2014)
library("pheatmap") # (Kolde 2019)


######################
######### SCN: HT vs NT
######################

### data import
setwd("H:/NGS-Business/Statistics/LMD") # set working directory to the pairwise group comparison folder. It contains a .csv where you state the sample document names and the group of each sample (see next command). Furthermore, this folder contains the rsem-output in format .genes.results within a sub-folder called "rsem".
samples <- read.csv(file.path("Samples_LMD-SCN-HTvsNT.csv")) # tell the sample names and the sample groups. The .csv has one column with header "id,group" (no space in between). It has one line per sample with the sample name (without file extention) and the sample group, comma separated without spaces. Take all samples for outlier assessment. To get the results of this pairwise comparison, state all samples except the outliers. Warning: The output file of this script is only correct for pairwise comparison of two groups.
files <- file.path("rsem", paste0(samples$id, ".genes.results")) # tell where to find the data, namely the folder "rsem" within the working directory. Use the exact terms of the .csv, expanded to the full document name inclusively the file format (.genes.results, which is an output file of rsem). There is no need to delete outliers within the subfolder "rsem".
names(files) <- samples$id # tell where to find the sample IDs, namely in column "id" of the .csv
txi.rsem <- tximport(files, type = "rsem") # import the data, which type is rsem (irrespectively of the subfolder name).

### First data normalization, for Likelihood ratio test (LRT)
dds <- DESeqDataSetFromTximport(txi.rsem, colData = samples, design = ~ group) # txi.sem is the count matrix. Table of sample information (colData) is the .csv. Design is comparing groups, with groups stated in the .csv.
keep <- rowSums(counts(dds)) >= 10 # threshold: same or more than 10 counts per column
dds <- dds[keep,] # dds is overwritten with data fulfilling threshold

### Likelihood ratio test (LRT), for Cook's Distance Outliers
dds.LRT <- DESeq(dds, test="LRT", reduced=~1)
res.LRT <- results(dds.LRT)
res.LRT.Ordered <- res.LRT[order(res.LRT$pvalue),]
# write.csv(as.data.frame(res.LRT.Ordered), file="DESeq_1resLRTOrdered.csv") # you might use this output as control

### Second data normalization, for RESULTS and Cook's Distance Outliers
```

```
dds <- DESeq(dds) # dds is overwritten
res <- results(dds)
summary(res) # when thousands of outliers, check for quality and removal
resOrdered <- res[order(res$pvalue),]
# write.csv(as.data.frame(resOrdered),file="Deseq_2resOrdered.csv") # you might use this output as control
res.SPHT.SPNT <- results(dds, contrast=c("group", "HT", "NT")) # refer to the groups as stated in the .csv
write.csv(as.data.frame(resOrdered),file="Results_LMD-SCN-HTvsNT.csv") # name the output file according to the performed comparison
# the results .csv with the normalized differentially gene expression is for further procession (e.g. indicator genes, most extremely expressed genes).

### Cook's Distance Outliers, for PCA and Heatmap
vsd <- vst(dds, blind=FALSE)
vsd_assay <- assay(vsd) # find outliers with Cook's Distance (the bigger the distance, the more likely an outlier) and replace outlying values by trimmed mean
vsd_assay.Ordered <- assay(vsd)[order(match(row.names(vsd_assay),row.names(res.LRT.Ordered))),]
# write.csv(as.data.frame(vsd_assay.Ordered), file="Deseq_3vsdAssayOrdered.csv") # you might use this output as control
plotPCA(vsd, intgroup=c("group")) ### PCA – for outlier assessment

### Heatmap, as additional visualization
select <- order(rowMeans(counts(dds,normalized=TRUE)), decreasing=TRUE)[1:20]
df <- as.data.frame(colData(dds)[,c("group","id")])
sampleDists <- dist(t(assay(vsd)))
sampleDistMatrix <- as.matrix(sampleDists)
rownames(sampleDistMatrix) <- paste(vsd$group, vsd$id, sep="-")
colnames(sampleDistMatrix) <- NULL
colors <- colorRampPalette( rev(brewer.pal(9, "Blues")) )(255)
pheatmap(sampleDistMatrix, clustering_distance_columns=sampleDists, clustering_distance_cols=sampleDists, col=colors)


######################
######### PVN: HT vs NT
######################

### data import
setwd("H:/NGS-Business/Statistics/LMD") # set working directory to the pairwise group comparison folder. It contains a .csv where you state the sample document names and the group of each sample (see next command). Furthermore, this folder contains the rsem-output in format .genes.results within a sub-folder called "rsem".
samples <- read.csv(file.path("Samples_LMD-PVN-HTvsNT.csv")) # tell the sample names and the sample groups. The .csv has one column with header “id,group” (no space in between). It has one line per sample with the sample name (without file extention) and the sample group, comma separated without spaces. Take all samples for outlier assessment. To get the results of this pairwise comparison, state all samples except the outliers. Warning: The output file of this script is only correct for pairwise comparison of two groups.
files <- file.path("rsem", paste0(samples$id, ".genes.results")) # tell where to find the data, namely the folder “rsem” within the working directory. Use the exact terms of the .csv, expanded to the full document name inclusively the file format (.genes.results, which is an output file of rsem). There is no need to delete outliers within the subfolder "rsem".
names(files) <- samples$id # tell where to find the sample IDs, namely in column "id" of the .csv
txi.rsem <- tximport(files, type = "rsem") # import the data, which type is rsem (irrespectively of the subfolder name).

### First data normalization, for Likelihood ratio test (LRT)
```

```
dds <- DESeqDataSetFromTximport(txi.rsem, colData = samples, design = ~ group) # txi.sem is the count matrix. Table of sample information (colData) is the .csv. Design is comparing groups, with groups stated in the .csv.
keep <- rowSums(counts(dds)) >= 10 # threshold: same or more than 10 counts per column
dds <- dds[keep,] # dds is overwritten with data fulfilling threshold

### Likelihood ratio test (LRT), for Cook's Distance Outliers
dds.LRT <- DESeq(dds, test="LRT", reduced=~1)
res.LRT <- results(dds.LRT)
res.LRT.Ordered <- res.LRT[order(res.LRT$pvalue),]
# write.csv(as.data.frame(res.LRT.Ordered), file="DESeq_1resLRTOrdered.csv") # you might use this output as control

### Second data normalization, for RESULTS and Cook's Distance Outliers
dds <- DESeq(dds) # dds is overwritten
res <- results(dds)
summary(res) # when thousands of outliers, check for quality and removal
resOrdered <- res[order(res$pvalue),]
# write.csv(as.data.frame(resOrdered),file="Deseq_2resOrdered.csv") # you might use this output as control
res.SPHT.SPNT <- results(dds, contrast=c("group", "HT", "NT")) # refer to the groups as stated in the .csv
write.csv(as.data.frame(resOrdered),file="Results_LMD-PVN-HTvsNT.csv") # name the output file according to the performed comparison
# the results .csv with the normalized differentially gene expression is for further procession (e.g. indicator genes, most extremely expressed genes).

### Cook's Distance Outliers, for PCA and Heatmap
vsd <- vst(dds, blind=FALSE)
vsd_assay <- assay(vsd) # find outliers with Cook's Distance (the bigger the distance, the more likely an outlier) and replace outlying values by trimmed mean
vsd_assay.Ordered <- assay(vsd)[order(match(row.names(vsd_assay),row.names(res.LRT.Ordered))),]
# write.csv(as.data.frame(vsd_assay.Ordered), file="Deseq_3vsdAssayOrdered.csv") # you might use this output as control
plotPCA(vsd, intgroup=c("group")) ### PCA – for outlier assessment

### Heatmap, as additional visualization
select <- order(rowMeans(counts(dds,normalized=TRUE)), decreasing=TRUE)[1:20]
df <- as.data.frame(colData(dds)[,c("group","id")])
sampleDists <- dist(t(assay(vsd)))
sampleDistMatrix <- as.matrix(sampleDists)
rownames(sampleDistMatrix) <- paste(vsd$group, vsd$id, sep="-")
colnames(sampleDistMatrix) <- NULL
colors <- colorRampPalette( rev(brewer.pal(9, "Blues")) )(255)
pheatmap(sampleDistMatrix, clustering_distance_columns=sampleDists, clustering_distance_cols=sampleDists, col=colors)


##############################
### R session info (20210212)
##############################

# R version 3.5.2 (2018-12-20)
# Platform: x86_64-w64-mingw32/x64 (64-bit)
# Running under: Windows 10 x64 (build 17134)

# Matrix products: default

# locale:
```

```
#          [1]          LC_COLLATE=German_Germany.1252                    LC_CTYPE=German_Germany.1252
    LC_MONETARY=German_Germany.1252
# [4] LC_NUMERIC=C                LC_TIME=German_Germany.1252

# attached base packages:
# [1] stats4    parallel  stats     graphics  grDevices utils     datasets  methods   base

# other attached packages:
#  [1] RColorBrewer_1.1-2         pheatmap_1.0.12           apeglm_1.4.2              DESeq2_1.22.2
#  [5] SummarizedExperiment_1.12.0 DelayedArray_0.8.0        BiocParallel_1.16.6       matrixStats_0.56.0
#  [9] tximport_1.10.1            AnnotationDbi_1.44.0      Biobase_2.42.0            GenomicRanges_1.34.0
# [13] GenomeInfoDb_1.18.2        IRanges_2.16.0            S4Vectors_0.20.1          BiocGenerics_0.28.0

# loaded via a namespace (and not attached):
#  [1] bitops_1.0-6          bit64_0.9-7           progress_1.2.2        httr_1.4.1            numDeriv_2016.8-1.1
#  [6] tools_3.5.2           backports_1.1.6       R6_2.4.1              rpart_4.1-13          Hmisc_4.4-0
# [11] DBI_1.1.0             colorspace_1.4-1      nnet_7.3-12           tidyselect_1.0.0      gridExtra_2.3
# [16] prettyunits_1.1.1     bit_1.1-15.2          compiler_3.5.2        htmlTable_2.0.0       labeling_0.3
# [21] scales_1.1.1          checkmate_2.0.0       mvtnorm_1.1-0         readr_1.3.1           genefilter_1.64.0
# [26] stringr_1.4.0         digest_0.6.25         Rsamtools_1.34.1      foreign_0.8-71        XVector_0.22.0
# [31] base64enc_0.1-3       pkgconfig_2.0.3       htmltools_0.4.0       bbmle_1.0.23.1        htmlwidgets_1.5.1
# [36] rlang_0.4.5           rstudioapi_0.11       RSQLite_2.2.0         farver_2.0.3          acepack_1.4.1
# [41] dplyr_0.8.5           RCurl_1.98-1.2        magrittr_1.5          GenomeInfoDbData_1.2.0 Formula_1.2-3
# [46] Matrix_1.2-15         Rcpp_1.0.4.6          munsell_0.5.0         lifecycle_0.2.0       stringi_1.4.6
# [51] MASS_7.3-51.1         zlibbioc_1.28.0       plyr_1.8.6            grid_3.5.2            blob_1.2.1
# [56] bdsmatrix_1.3-4       crayon_1.3.4          lattice_0.20-38       Biostrings_2.50.2     splines_3.5.2
# [61] annotate_1.60.1       hms_0.5.3             locfit_1.5-9.4        knitr_1.25            pillar_1.4.4
# [66] geneplotter_1.60.0    biomaRt_2.38.0        XML_3.99-0.3          glue_1.4.0            latticeExtra_0.6-28
# [71] data.table_1.12.8     vctrs_0.2.4           gtable_0.3.0          purrr_0.3.4           assertthat_0.2.1
# [76] ggplot2_3.3.2         emdbook_1.3.12        xfun_0.13             xtable_1.8-4          coda_0.19-3
# [81] survival_2.43-3       tibble_3.0.1          memoise_1.1.0         cluster_2.0.7-1       ellipsis_0.3.0
```

Chapter 5

General Discussion



5.1 Early prediction of torpor behavior using radiotelemetry data

Fascination Djungarian hamster. A change in light regime from summer-like long photoperiod (LP) to winter-like short photoperiod (SP) induces a gradual, reversible physiological, morphological, and behavioral change from the fat, reproductive "summer" hamster with brown fur to a slim, non-reproductive "winter" hamster with white fur, while the expression of spontaneous torpor is not obligate. In a cohort as well as in a litter with the same genetics, epigenetics, environment and experiences, the pace and extent of acclimations to SP cover the whole possible spectrum, from no over slow and weak to fast and strong response. In nature, this flexibility of the population likely guarantees a survival of the fittest during the Siberian winter conditions with its individual, hard to prognose pace and extent. In torpor research, the complex acclimation and torpor behavior must be considered regarding study design and interpretation of results.

Classification. In Chapter 2, weekly measurements of body mass and fur index throughout the acclimation to SP were combined with radiotelemetry data, which were measured in three-minute intervals and broke down to mean values per weekly time frame. The analyses of experiment 1 were designed to improve sampling for molecular analyses.

Hereby, four torpor incidence groups were characterized. The results underline systemic differences which coincide with a certain torpor incidence. To level methodological bias, there is need to distribute hamsters with different traits equally to the sampling groups “hypothermia” (HT), sampled in torpor, and “normothermia” (NT), sampled on a torpor-free day. Hereby, a weekly measurement of body mass and fur index to assess the speed and strength of acclimation to SP might help as well as radiotelemetry analyses of a torpor-week. Planning of sampling can be refined in analyzing each hamsters’ torpor incidence of the week before, which also allows assumptions, at which time torpor entry will take place.

Polymorphism. Experiment 2 showed that the locomotor activity and the core body temperature (Tb), and therefore likely the metabolic rate [41,58,70], are reduced during scotophase (nighttime hours) as immediate response to SP, while acclimation of body mass and fur is observable weeks later. However, within the cohort, there was a large spectrum in each of the parameters over the entire course of acclimation to SP. Between manifestations of the observed parameters, there were assumable interconnections, however, no determinable inevitabilities. This confirms a phenotype continuum in the Djungarian hamster [24,293,294].

Early signs. As became obvious in experiment 2, locomotor activity and Tb data is meaningful especially in the comparison between the last week in LP and the first week in SP. It is assumable, that the more pronounced the decline of values as immediate response to the light regime change, the more likely is torpor expression three months later. The body mass change pace and extent during acclimation to SP as well as the variability of Tb values, and probably metabolic rate values [41,58,70], during scotophase have potential to indicate the torpor incidence, however, assumably at a late stage of SP-acclimation. For now, the best way is to start with at least 18 % more lab animals to ensure a sufficient number of torpor expressing hamsters, and to conclude from the torpor incidence of one week on the expectable torpor incidence of the following week.

5.1.1 Why is torpor expressed in artificial, rich conditions?

Winter is coming. Since seasonal acclimations take time, an early anticipation of upcoming harsh conditions must be made in advance. Therefore, one can “trick” the Djungarian hamster into changing from its summer to its winter state, even while providing an ambient temperature of 20 °C, nesting material, and food and water *ad libitium*.

However, the expression of spontaneous daily torpor without an obvious need to save energy is puzzling.

Torpor purpose. There are few ways to explain spontaneous torpor expression in artificial, rich conditions. Either there is or there is no acute energetic bottleneck. The Djungarian hamsters' pronounced acclimation to SP including vast body mass reduction might indeed require an acute need to save energy [44,75]. Alternatively, there is not necessarily an energetic requirement to express torpor, but torpor is expressed as a kind of program, written in the hamsters` (epi)genome, that cannot be not executed. Hereby, further or other potentially functions of torpor aiming to increase fitness of the individual or the population might play a role. Favorable effects of torpor expression on reproduction, development, water conservation, migration, and inter-specific competition are discussed [3,35].

Torpor obligation. There are even less ways to explain the cohorts' polymorphism regarding torpor incidence. Hereby, the two extremes of the phenotype continuum can be differentiated in torpor expression and no torpor expression. As shown in Chapter 2, a strong response to SP, in terms of a reduced locomotor activity and probably food intake given the pronounced body mass loss, seem to come along with torpor expression. By contrast, hamsters with a weak response to SP, in terms of a probably high food intake given the relatively high locomotor activity and minor body mass loss, seem often to not express torpor. From the deterministic view, a hamster, given its individual combination of traits, is not flexible enough to gain energy from food instead of saving energy with torpor expression, and vice versa. Furthermore, it is unlikely the hamster is able to consider the long-term stable artificial environment without any threats. Even generations of indoor breeding cannot make some of the hamsters confident enough, that harsh winter-like conditions will never happen, since there is no need to acclimate to SP and to express torpor.

Torpor habit. It is hard to imagine, that the hamster does spontaneous torpor voluntarily just because it can, while some kind of individual behavior favors a particular torpor incidence. In a study on nonresponders, partial responders and full responders to SP, these observed winter phenotypes are not related to differences in aspects of observable animal personalities [293]. A classification of animals according to shared parameter values into artificial groups is clearly useful for descriptive research, like also done in Chapter 2 using

torpor incidence groups as well as a differentiation of hamsters with and without torpor expression. Nevertheless, the continuum of diverse traits in the Djungarian hamster as well as in hibernators must be and is acknowledged [24,293–295].

5.1.2 Does torpor influence circadian rhythm?

Short torpor bouts. As shown in Chapter 2, the smaller the torpor incidence, the shorter and shallower the torpor bouts, and the less synchronized torpor onset with onset of photophase. The energy saved must compensate or exceed the energetic investment to initiate, maintain and especially terminate a torpor bout. This might not be the case for short and shallow torpor bouts, which would explain rare torpor expression. Hamster which are, for any reason, not able to synchronize its circadian rhythms inclusively torpor expression to the external clock properly might have no benefit or even disadvantage of torpor expression. Consequently, rhythmicity of other circadian rhythms, as locomotor activity and feeding bouts, might allow conclusions on torpor behavior.

Torpor vortex. As shown in Chapter 2, a high torpor incidence comes along with long torpor bouts and extreme minimal Tb reached throughout the bout. Hereby, the high torpor incidence comes along with low Tb values even throughout the middle of scotophase, and consequently a probably overall reduced level of metabolic rate [41,58,70]. In practical expertise of animal experiments as well as in theory, frequent torpor bouts cause a prolongation of torpor duration with even smaller Tb values and therefore probably even more energy saved, but likely also a higher energy demand. Though, the hamster must catch up of sleep [73], as also displayed in reduced locomotor activity in the first half of scotophase [119,296], and consequently less time to consume food. This negative feedback loop might cause a further extent of torpor bouts.

Long torpor bouts. In theory, torpor extent from late scotophase to the early scotophase might affect perception of light cues, as *lights on (Zeitgeber*-time zero, ZT00), and *lights off* (ZT08 in 8:16h light:darkness). Torpor extent beyond photophase (daytime hours) has potential to cause issues reading the clock properly and synchronize to the 24h-rhythm. Indeed, there is evidence, that torpor causes a shortening of circadian periods [297]. Hereby, onset of photophase seems to be a more important cue than onset of scotophase. When daylength is shortened, torpor is still synchronized to *lights on* [55]. By contrast, keeping the Djungarian hamster in complete darkness, like in a natural burrow, resulted in

unchanged torpor incidence, but increased torpor duration, while the endogenous rhythm of torpor timing grew more than 24 hours [54,58].

5.1.3 Is a certain phenotype inherited?

Breed with SP-responders. In the breeding colony of the Herwig lab, only those hamsters are selected for breeding in LP, which responded in body mass and fur index to the previously applied SP. Empirically, there is, with about 2 out of 100 hamsters, almost no SP-nonresponsive offspring. However, as shown in Chapter 2, up to 18 % (14 out of 80) of SP-responders did not express torpor throughout their individual observation duration. This information is to respect for the major counterparts “reduction of lab animals” and “statistically valuable sample sizes” in study design development, approvals, and breeding.

Breed randomly. Another working group, which paired Djungarian hamsters randomly, found the entire acclimation spectrum within offspring per breeding pair. However, within a litter, there was a dominant phenotype [298]. This indicates an influence of genetic disposition towards a certain acclimation strength and torpor proneness, while simultaneously a potential survival of the fittest mechanism is inherited in the hamster population. So, in theory, the individual hamster might not be adapted best to the given external conditions, which may reach from mild to harsh Siberian winters. But the hamster population with its wide spectrum of life history traits has a sufficient number of fit individuals, so, some will survive and breed in the next summer [299].

5.1.4 Are there forever normothermic hamsters?

Wrong wording. To avoid bias due to study design, hamsters dedicated to molecular torpor studies must fulfil the criteria “expression of at least one torpor bout” prior to sacrifice. Accordingly, responders without torpor expression cannot be sacrificed for neither the HT nor the NT sampling group. Hereby, hamsters were internally classified into “capable of torpor” (COTs), which can already be sacrificed, and “forever normothermic” (FNTs), which cannot. While COT is an eligible term, given reliable radiotelemetry data proving torpor expression according to the mathematical torpor definition “Tb smaller than 32 °C for at least 30 minutes”, the use of the term FNT is notoriously unscientific given “never say never”. A hamster might have expressed torpor before implantation of a

radiotelemetry transmitter. A hamster might have expressed torpor later in this or a following winter-like SP. A hamster would probably express torpor given more severe winter-like conditions in terms of ambient temperature and food scarcity.

Correct meaning. Nevertheless, working with the Djungarian hamsters suggests, that responders without torpor expression will never express torpor, given an obviously less pronounced acclimation in terms of body mass reduction and winter fur growth, an estimated high locomotor activity, and an estimated high Tb. After collecting enough data and after the development of appropriate analysis methods, the study in Chapter 2 confirmed, that the responders without torpor expression indeed differed from responders with torpor expression, mainly in a less pronounced initial response to SP in terms of Tb and locomotor activity reduction and a weaker decline of body mass during acclimation to SP. Responders without torpor expression were to discriminate in advance by the less pronounced relative body mass change from responders which were capable of torpor, but rarely expressed torpor (no or one torpor bout during a late SP-week). Furthermore, the standard deviation of the mean, or, in other words, the variability of Tb values, during middle of scotophase might be of use to estimate the expectable torpor behavior.

Future investigations. Extent of response to SP and torpor orchestration might be caused by many aspects, which were reviewed previously in the neuroendocrine context [2]. Whether weak responders without torpor expression are less able to read the clock might be investigated. To test, whether a certain torpor behavior is reflected in brain anatomy, a staining of cell nuclei might be applied to assess neuronal density and volumes of hypothalamic core areas relevant in torpor orchestration. Hereby, labelling of specific cells in combination of a 3D-reconstruction of the brain might be beneficial [300,301]. Approaches to determine neuronal activity in the Djungarian hamster might be developed. The transcriptional activity is assessable via *in situ* hybridization and immunohistochemistry targeting members of the c-Fos/c-Jun-superfamily (see also bachelor thesis of Carina Praisler in 2019: "Immunhistochemischer Nachweis der neuronalen Aktivität im suprachiasmatischen Nukleus des Dsungarischen Zwerghamsters *(Phodopus sungorus)* nach Lichtimpuls").

5.1.5 Is the next torpor bout predictable?

Maybe. As shown in Chapter 2, a hamster is more likely to express torpor after about ten weeks of acclimation to SP, the stronger its initial response to the light regime change from LP to SP, and the more pronounced the relative body mass reduction during acclimation to SP. So far, a hamsters' torpor incidence is best to forecast by its torpor incidence of the previous week. Despite a fruitful approach in sugar gliders [302], own efforts to predict the day and time of the next torpor bout in the Djungarian hamster were unsuccessful. Using available data and analysis methods, we found no cues, whether and in which parameters torpor becomes apparent in advance (see also bachelor thesis of Insa Krey in 2019/2020: "Aktivitätsanalyse von Dsungarischen Zwerghamstern *(Phodopus sungorus)* im Kurztag: Vorhersage eines spontanen täglichen Torporbouts"). Tools and approaches of scientists of other scientific fields, as informatics, mathematics, and statistics, might contribute to an interdisciplinary project on acute torpor prediction. Hereby, (ar)rhythmia of circadian rhythms have potential to allow conclusions to torpor timing and pattern. This might combined with mathematical models using monitoring data developed to explain extent of metabolic downstates of several species including dormouse and Djungarian hamster [43].

5.1.6 Is locomotor activity data reliable?

Technical setup. There are more calm and more active hamsters, as observed during animal work and underlined with locomotor activity data in Chapter 2. Nevertheless, good scientific practice requires continuous questioning [303]. Technical interference might be in fact responsible for differences between hamsters. To assess this, available radiotelemetry data was analyzed. Pairs of hamsters equipped with the same combination of transmitter and receiver had no similarity in activity level and pattern. The orientation of transmitter within the hamsters` intraperitoneal cavity might influence recorded signal strength. To test this, transmitters were moved manually across a receiver. Data of one transmitter did basically not differ, regardless its orientation to the receiver. Also, a fold-higher signal of a fold-times faster movement underpins comparable measurements. Since technical bias seems to be minimal, there is valid activity data per hamster and an acceptable comparability between hamsters. Accordingly, there is no need to normalize

the activity data across all values of a hamster, a certain transmitter-receiver-combination, a hamster cohort for which the same technical setup was used, or experiment using data of several hamster cohorts.

Verification. To assess locomotor activity patterns in the Djungarian hamster, a non-invasive method, namely passive infrared motion detector to monitor convulsions of a running wheel, were used elsewhere [67,68,304,305]. Regardless of the method, the typical Djungarian hamster is nocturnal, with decreasing activity level over the course of the scotophase. Also, the activity level decreases over the course of acclimation to SP. Despite the typical locomotor activity pattern in the Djungarian hamster can be verified using both non-invasive and invasive methods, the locomotor activity level is not comparable between systems given different units.

Transmitter mass. The intraperitoneal implantation of a radiotelemetry transmitter might affect an animal. While the anesthesia and the analgesia are metabolized, the transmitter with a weight of 1.6 g remains. Though, this accounts for a body mass gain of about 6 % in a hamster of 25.0 g weight. The hamster might integrate this weight in its overall energy balance in terms of an altered food consumption and exercise. With the transmitter weight, the center of gravity and therefore posture and behavior might be changed. As reviewed elsewhere regarding, the small, non-flying mammals' performance after an implantation is not impeded, provided the implant mass is less than the neonate litter mass [3]. In the Djungarian hamster, litter mass is at least 2.5 g at the third day after birth [298].

Surgery. Body-to-transmitter size ratio as well as anesthesia have potential to impact short- and long-term body mass, food and water intake, as well as circadian rhythms in mice and rats [306]. In addition, analgesia and the suture and its scaring might impact an animals' short- and long-term behavior and posture, which would in turn affect Tb and locomotor activity data. To some extent, radiotelemetry data allows to review the justifiability of a surgery to implant a transmitter. In Chapter 2, radiotelemetry data monitored during the first week after surgery to implant the transmitter were excluded from analyses. Analyzing these and further data confirmed the assumption, that the animals do fully recover from surgery within a week, since afterwards, locomotor activity as well as Tb level and pattern did not change any more (see also master thesis of Alexandra Hintrichs in 2020: "Surgical recovery in Djungarian hamsters *(Phodopus sungorus):* effects

of photoperiod and surgical invasiveness on body mass, Tb and locomotor activity patterns"). Further research might be done to assess effects of transmitter implantation and consequences of the required surgery. Hereby, available data might be analyzed. There are plenty of systems in use, where transmitters, thermologgers or transponders of diverse sizes and weights are implanted into the intraperitoneal cavity or under the skin of diverse species for remote, retrospective, or acute measurements of several parameters [3].

5.1.7 How to express relative locomotor activity data?

Approaches. Several approaches were made to turn absolute activity data [cpm] into relative values [%]. Doing so, within-animal changes over weeks of acclimation as well as across-animal differences at the same moment of acclimation might be expressed and compared. Hereby, the mean, median, third quartile, or most extreme activity value was set to 100 %, aiming to express all other values as portions. This method, with and without e.g., Z-transformation, is restricted by two reasons.

Artificial bias. First, the most extreme activity value caused by a hamster itself is unknown. Contrary to the Tb, which must have physiologically meaningful values below 42 °C, the cutoff of activity values is unclear. That handling affected single activity values is obvious. To clean the cage, weigh or sacrifice the hamster, the cage with hamster including transmitter was pulled across the receiver, resulting in an artificially increased activity value within this three-minute bin. However, these occasions took place relatively rarely, considering 480 data points per day. By contrast, frequency and extent of outlying activity values due to technical reasons of the radiotelemetry system itself are unclear, and therefore their effect on key values which were set to 100 %.

Missing baseline. Second, there is no real baseline. To assess e.g., effects of a drug, a lab animal is recorded prior and after application. Hence, each animal is its own reference. In torpor research, the “experiment” consists of a change of light regime or other external parameters to observe natural processes. As shown in Chapter 2, the Djungarian hamster has no stable “standard” condition, but underlies continuous behavioral, physiological, and metabolic changes in response to the light regime change.

Ratio. The photo- to scotophase activity ratio, as developed in consequence in Chapter 2, enabled a within-hamster relative value characterizing nocturnality, which

became less pronounced throughout acclimation to SP because of a reduction of locomotor activity during scotophase, but not photophase. Further ratios might be developed.

5.1.8 How do locomotor activity and body temperature relate?

Value range. To sacrifice the hamster during a certain stage of torpor, a transmitter was intraperitoneally implanted (Chapter 2, 3, 4). This allows the hamster to live undisturbed in its home cage, while the observer can monitor its values in real-time from outside the animals` room. The used radiotelemetry system records Tb and activity data in intervals of three minutes. The value range of core Tb at an ambient temperature of about 20 °C spans about 24 °C during deep torpor, and a vertebrate`s maximal Tb of 42 °C. Higher and therefore unrealistic Tb values were removed as technical artefacts from the data set. The value range of activity spans zero activity during resting or torpor, and a hamsters' maximal activity, e.g., during climbing the food manger or jumping in a corner (Figure 1, inlay).

Connection. As shown previously, the activity data becomes more meaningful, the bigger the data bin. In Chapter 2, we worked with time windows, e.g., scotophase and photophase, which expanded over one week of analysis (Chapter 2, Figures 1 and 2). So, an impressive common drop of activity and Tb values from last LP to first SP week became aware for scotophase (Chapter2, Figures 6A and 8A). Interestingly, activity and Tb values of scotophase, but not of photophase, did develop analogously during acclimation to SP. Hence, activity and Tb do somehow relate, but not at any circumstances.

Approach. To assess the degree of connection between activity and Tb, further analyses were made. The smallest unit of use are mean activity values per hour. Hourly means of activity and Tb were correlated. Regression lines per hamster and week of analysis (7 * 24 value pairs) turned out to have a logarithmically shape. A transformation of values using the natural logarithm resulted in linear correlations. Interestingly, they seem to become steeper, the more progressed the experimental week and degree of acclimation to SP (Figure 1). Obviously, this is due to the progressing activity reduction and a growing use of torpor expression after about SP10. Also, the reduced body mass, accompanied by the growth of a more insulating fur, have potential to influence the correlation of Tb and activity, besides the use of brown adipose tissue for shivering-free thermogenesis and the systemic fine-adjustment of energy homeostasis itself.

Limitations. Yet, these assumptions left unpresented in Chapter 2, since three analytical problems remained. First, according the critical value table of the University of Connecticut (https://researchbasics.education.uconn.edu/r_critical_value_table/, 09.10.2020), a linear correlation with level of significance of $p < 0.05$ and 54 degrees of freedom (8 hours * 7 days, minus 2) is given at a correlation coefficient of $r > 0.273$. Yet, the correlation of transformed value pairs does not have a linear correlation in some analysis weeks (Figure 2). It is unclear how to deal with this. Statistical tests require linear correlations. So, either data must be removed from the analyses, which might be interpreted as data manipulation, or another or a further transformation method must be found. Second, the natural logarithm of zero activity is mathematically not defined. An eradication of data by a hamster- and week-dependent one-digit percentage does not only reduce validity of the analysis but complicates an adequate application of statistical tests, which require an equal amount of value pairs from each hamster and week. Here, either each activity value of 0.000 cpm is set at 0.333 cpm, a manipulation of data which would be valid provided a communication, or a data transformation must be found which can handle zero activity. Third, the validity of analyses is reduced by the fact, that there is a delay in the intercourse of activity and Tb, e.g., a hypothermic hamster can move, and a highly active hamster can stop its movements, while still being heated up. So far, activity bursts, feeding bouts and torpor bouts are not respected in the rigid separation of one-hour bins. A more flexible approach must be found. Hereby, methods as Fourier-transformation might be useful [307].

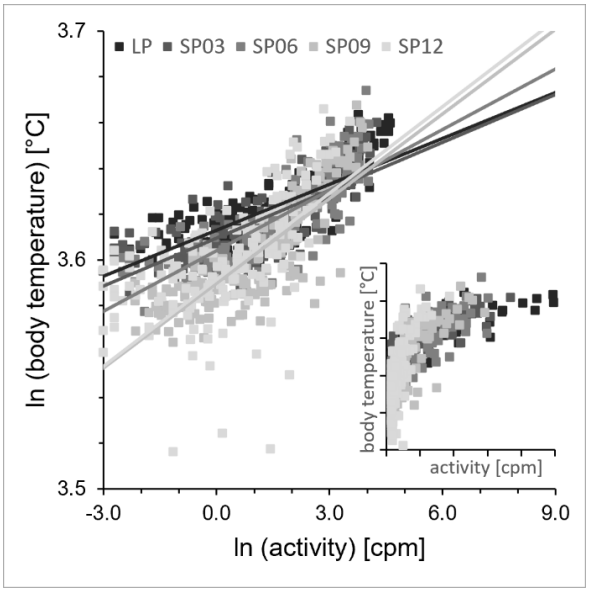

Figure 1: Correlation of locomotor activity and body temperature. Exemplary logarithmic correlation of one-hour-bin value pairs per day and experimental week (24 hours * 7 days for each experimental week LP, SP03, SP06, SP09, and SP12, from dark to light grey) of hamster #05 (Chapter 2, experiment 2). Linear trend lines for each week visualize steeper slopes with progressing SP adaptation. The inlay shows the same data prior to transformation. SP12 contained torpor episodes with zero activity and Tb down to 24.3 °C (not shown). Unpublished data (2021 Haugg Diedrich Herwig) due to mathematical and statistical limitations (see text).

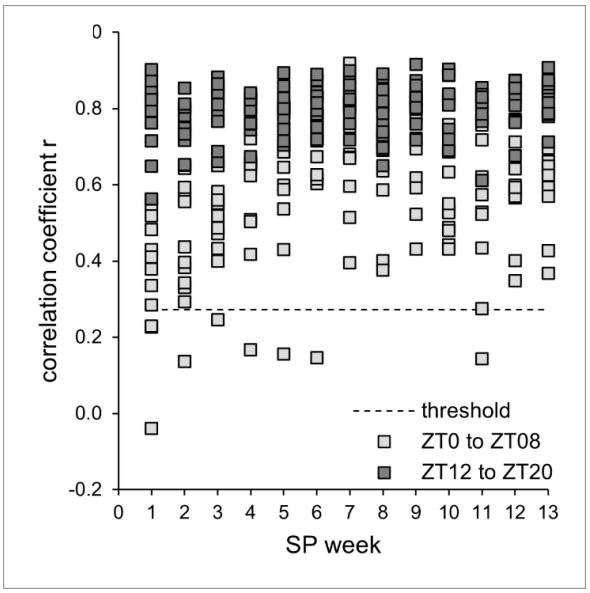

Figure 2: Correlation coefficients r of locomotor activity and body temperature. For each hamster (n = 11, chapter 2, experiment 2), experimental week (SP00 to SP13), and time frame (photophase from ZT0 to ZT08 as well as middle of scotophase from ZT12 to ZT20), the correlation coefficient r was calculated. Data basis were 56 value pairs (8 hours * 7 days) of logarithmized mean activity per hour and logarithmized mean Tb per hour. The coefficients of all weeks and animals were higher during the middle eight hours of scotophase from ZT12 to ZT20 (median: 0.809) than during the eight hours lasting photophase from ZT0 to ZT08 (median: 0.594, Mann-Whitney Rank Sum Test, U = 2170, T = 12466, $p < 0.001$). Values below the threshold at 0.273 are not statistically significant correlations. Unpublished data (2021 Haugg Diedrich Herwig) due to mathematical and statistical limitations (see text).

5.1.9 Are there alternatives to radiotelemetry?

Radiotelemetry. For molecular approaches in research on circadian rhythms and torpor, Djungarian hamsters are sacrificed in a certain state (e.g., torpor vs. torpor-free day) at a certain time (ZT) [42,150,153]. For my work, this was done using real-time Tb data, provided by a radiotelemetry transmitter which had to be implanted intraperitoneally in a small surgery using anesthesia and analgesia (Chapter 3 and 4). All available Tb and locomotor activity data was processed in Chapter 2. The benefit of this method is, that the hamster is kept undisturbed in its home cage, where it has potentially normal behavior, physiology, and metabolism.

Indirect calorimetry and infrared camera. As suggested in Chapter 2, there are non-invasive methods as alternatives to radiotelemetry. Especially, the sacrifice might be timed using indirect calorimetry, which delivers metabolic rate data [41]. An infrared camera allows to assess behavior beyond locomotor activity, as well as surface body temperature, which is, however, a limited approach due to insulating winter fur and masking nesting material. Both indirect calorimetry and infrared cameras are used in our working group. Nevertheless, these non-invasive methods also have potential to be stressful for the animals. Indirect calorimetry requires a specialized cuvette smaller than the usual home cage, while sounds of the technical equipment might irritate the hamster. The use of an infrared camera requires a removal of the metal food manger and would require a deposition of food pellets on the cage's floor when used in the long-term. Accordingly,

these unfamiliar conditions are not allowed to be permanently maintained. Hence, a frequent manipulation of the animals surrounding or a transfer of the animal from one cage into another is indicated, usually performed by a team of alternating experimenters.

Progress. Although the Djungarian hamster habituates quickly and most of the hamsters display a curious behavior, regardless of the circumstances, the choice between invasive and non-invasive methods is debatable regarding animal welfare, research question, and progress of technology. Especially in the beginning of torpor research, rectal thermometers were in use [64]. Nowadays, advanced systems are developed which can collect e.g., body temperature, locomotor activity, respiratory rate, blood pressure, heart rate, blood flow, electrocardiogram and other biopotentials [303]. For example, LABORAS™ (laboratory animal behavior observation registration and analysis system, Metris b.v., Hoofddorp, The Netherlands) allows to conclude from vibration signatures alone, without the use of implants or cameras, on e.g., resting, grooming, eating and moving of the rodent within its home cage [308]. However, in torpor research, the important parameters will stay metabolic rate and body temperature.

5.1.10 Can radiotelemetry help to refine animal husbandry and reduce animal numbers?

Understanding. Radiotelemetry data contributes to a refinement of animal husbandry. The Djungarian hamsters' immediate response to a light regime change in at least locomotor activity and Tb, as shown in experiment 2 of Chapter 2, underlines the previously known importance to strictly avoid any potentially irritating light signals. Furthermore, our hamsters` locomotor activity patterns allow to respect their natural circadian rhythm in practice, e.g., by cleaning the cage at the end of photophase instead of the beginning.

Planning. The use of radiotelemetry contributes to torpor research and indirect reduction of animal numbers. Primarily, radiotelemetry enables to sacrifice the hamsters in a certain metabolic state (torpor vs. torpor-free day) at a certain time (ZT) to use tissues in molecular approaches. As described in experiment 1 of Chapter 2, radiotelemetry data allowed considerations regarding a refinement of the sampling scheme. These considerations improve validity of experimental data, and, in turn, reduce the need to perform an animal experiment again. Furthermore, knowing about 18 % of responders

without torpor expression, an acclimation of 18 % more animals to SP allows the sacrifice of as many hamsters capable of torpor as planned. This spares delay and a potential batch effect due to a subsequent experiment aiming to reach the needed sample size and therefore significance.

Awareness. So far, radiotelemetry did not allow a direct reduction of animal numbers. Chapter 2 helps to raise awareness of weak responders without torpor expression. These hamsters might be involved in studies on prerequisites and proximate stimuli of torpor expression in Djungarian hamsters acclimated to SP. A third sampling group might be added to the common comparison of torpid animals with animals on a torpor-free day. This requires a reliable identification of responders without torpor expression, which is still limited, as discussed in Chapter 2. A further improvement of data collection and analysis is needed, possibly developed also in the context of torpor prediction.

Data. Data depositories allow students as well as scientists to iterate and extent analyses without performing animal experiments themselves. The radiotelemetry data used in Chapter 2 is available on request to guarantee a correct use and interpretation, also in the light of possible collaborative project ideas. The transcriptomic data inclusively bioinformatical as well as statistical pipelines used in Chapters 3 and 4 are deposited for immediate review and use by everybody.

5.2 Investigation of hypothalamic control mechanisms by transcriptomics

Whole hypothalamus. In Chapter 3, a bioinformatical and statistical pipeline was developed to investigate hypothalamic control mechanisms. Since knowledge on photoperiodic-driven gene regulation in the hypothalamus of the Djungarian hamster existed, data and therefore methods of our analytic approach were validated to also assess the less investigated torpor-driven gene regulation. Interestingly, the maintenance of the normothermic winter-like state on mRNA-level required few gene regulation within the hypothalamus (15 upregulated, 17 downregulated genes), while the maintenance of deep torpor at ZT04 was actively regulated (456 upregulated, 303 downregulated genes). Despite or because of the hypometabolic and therefore hypothermic state, transcriptional, biosynthetic, cellular, and metabolic processes were altered in the hypothalamus during

deep torpor. In this study, regulated genes and biological functions with evident or interesting functions in photoperiodic and torpor maintenance came to the fore. Results point towards adaptive and protective mechanisms of the Djungarian hamsters' hypothalamus to the severe metabolic downstate, while the picture of proximate stimuli to orchestrate torpor remained incomplete.

Hypothalamic nuclei. In Chapter 4, the hypothalamic core areas suprachiasmatic nucleus (SCN) and paraventricular nucleus (PVN) were lasermicrodissected towards a more targeted approach. Hereby, mRNA-Seq data was gained from tissue of SP-acclimated hamsters sacrificed around ZT01 either in torpor entry or on a torpor-free day. The methods developed in Chapter 3 were applied. The transcriptional activity was highest in SCN (181 upregulated, 690 downregulated genes) and lowest in PVN (9 upregulated, 5 downregulated genes). Several metabolic processes were altered in SCN. According to literature research regarding potential biological functions of many regulated genes, mitochondria, systemic signaling and metabolism, transcription and modification, cell cycle, and brain plasticity might be of relevance to orchestrate torpor entry in SCN. Especially, a remodeling of the circadian clockwork seems to alter the clock output to induce torpor.

5.2.1 What is mapping of transcriptomes good for?

Reference data. In Chapters 3 and 4, a *de novo* assembly of transcriptomes was performed. So far, there is no annotated genome of the Djungarian hamster. Hence, the transcripts are meaningless sequences, which are or are not regulated. Therefore, the studies' mRNA sequences were translated into amino acid sequences, which were mapped against reference sequences of the house mouse *(Mus musculus)* using blastx [134,135]. In both Chapter 3 and 4, about one fifth of transcripts were successfully mapped (171,923 of 868,657 transcripts; 144,567 of 696,614 transcripts). In other studies, several databases were used at once to map [309,310]. Bao and colleagues mapped transcripts of the Djungarian hamster not only against the annotated genome of one species, but of three: mouse, rat and human [117]. This allowed 11.8 % hamster genes to be mapped (476,208 transcripts in total, 285,851 hamster genes, 33,711 annotated genes), including an identification of that organism with the best sequence match.

Mapped data. Mapping of transcripts is furthermore beneficial for a successful selection of anti-mRNA and antibodies to verify, anatomically locate, and expand results of transcriptomic and proteomic studies in Djungarian hamsters. Commercially available anti-mRNA and antibodies were originally designed for application in the classical model organisms mouse, rat and human. Applying them in tissue of Djungarian hamster may not work at all, or do work, but may unnoticeably label additional or other molecular structures than intended. Hence, valuable, open-access transcriptome data favors reduction of lab animals and further resources since approaches with molecular templates without a successful mapping become redundant to test experimentally.

5.2.2 How to unravel torpor-genes?

Limitations. In Chapter 3 and 4, many transcripts remained unmapped, although potentially of interest in studies facing seasonal acclimation and metabolic downstates as torpor. In general, using mouse, rat or human as reference appear to be limited. None of these organisms is seasonal, and only mouse and rat are nocturnal as the Djungarian hamster. Drastic natural metabolic downstates are not known in rat and human. The mouse as well as the Djungarian hamster expresses fasting-induced torpor, aligned with feeding rhythm, after an involuntary body mass reduction by about 20 % [37,38]. By contrast, spontaneous torpor in the Djungarian hamster is aligned with circadian rhythm after a body mass reduction by about 20 % during acclimation to short photoperiod. Hence, fasting-induced torpor might be based on somehow different mechanisms than spontaneous torpor [42].

Potential. However, mouse, rat and human are the best studied mammalian organisms. Their annotated genomes were performed and are regularly updated by specialist using state-of-art methods and best resources. Given the intense use of data by the international scientific community from all conceivable scientific fields, possible irregularities would attract attention and cause communication and improvement soon. Furthermore, extreme metabolic downstates are developed independently from each other in species covering all orders of the animal kingdom [24]. Hence, there is a chance, that mouse, rat and human have the genetic code necessary to express metabolic downstates, but torpor-important genes are silenced.

Situation. Interestingly, the hibernating thirteen-lined ground squirrel liver and brain sequencing data is prepared in an own software tool for further data analyses and visualization (SquirrelBox, https://raysinensis.shinyapps.io/squirrelBox/) [115]. Further genomes of species expressing metabolic downstates were annotated, yet often years ago with one organ or one non-representative animal only, according to eukaryotic genomes annotated at NCBI. Hence, these annotated genomes are partly limited in quality, quantity and validity from today`s view. State-of-the-art approaches and tools will be realized.

Progress. From my point of view, able scientists might create a directory with annotated genes from all species capable to express extreme metabolic downstates for a mapping against all of them at once. This dictionary might reveal torpor-relevant genes simply not present in mouse, rat and human, but in one of several species with a closer kinship, yet less annotated genomes. To my knowledge, this dictionary might also help to annotate the Djungarian hamsters' genome [311]. So far, the use of nonredundant protein databases and their analyses tools is recommended for newly targeted transcriptomes without an annotated genome of the given species or a close, well-annotated reference species [133,312]. Hereby, the Database for Annotation, Visualization and Integrated Discovery (DAVID, https://david.ncifcrf.gov/), fuses not only several databases, but also helpful tools to handle and interpret data [313].

5.2.3 How to identify the relevant data?

Separated parameters. Differential gene expression is expressed in two parameters, both given for the test group in relation to the control group. The genes' fold change is stated as -log2(FC). The adjusted p-value, short padj, states the significance of a genes' regulation after normalization of counts over all samples of a pairwise group comparison. In Chapter 3 and 4, a padj threshold (padj < 0.05) was applied to discriminate between regulated and not regulated genes.

Thresholds. To focus on those genes with an extreme and therefore biologically most meaningful regulation, a fold change threshold (|log2(FC)| > 2.0) was applied. This resulted in a manageable number of "most extremely regulated" genes in Chapter 3 (whole hypothalamus at ZT04), where seven genes were regulated by photoperiod (NT: SP vs LP) and five by torpor (SP: HT vs NT). Applying the same thresholds in Chapter 4 (hypothalamic nuclei at ZT01) resulted in the need to discuss 66 and 6 genes regulated within SCN and

PVN, respectively. Hence, instead of supporting comparability between studies, the application of the same fold change threshold in several studies can contradict clarity of results. In literature, the application of a fold change threshold in addition to the traditional significance threshold is common to concentrate on the most relevant subset of transcriptomic data [289,309,314], while a stricter padj threshold would be a novelty. In my own opinion, a genes' significance (padj) is of high importance for its biological relevance. Therefore, not only the threshold (padj = 0.05) differentiating not regulated from regulated genes was marked in the volcano plots of Chapters 3 and 4, but also a stricter threshold (padj = 0.001). However, the application of thresholds are always debatable, as for torpor definitions like "core Tb must be below 32 °C for at least 30 minutes" [315–317]. Indeed, the volcano plots of Chapters 3 and 4, which display each gene's significance by its fold change, allow to doubt a satisfactorily selection of the most relevant genes using thresholds. Hereby, genes with an extreme fold change, yet reaching significance closely, were discussed, while genes with an outstanding significance, yet minor fold change, were ignored.

Fused parameters. To focus on the "widest and highest catapulted lava" instead, values of fold change (x-axis, "widest") and significance (y-axis, "highest") must be combined in a standardized, meaningful way. I suggest a simple ranking method. Hereby, the set of regulated genes might be split in two subsets of up- and downregulated genes. These two subsets of genes might each be ranked by 1a) the padj and 1b) the fold change, before 2) both ranks are e.g., summed to the final rank, from which 3) a certain number of genes with the highest final rank values are selected. Since transcriptomic studies are of growing popularity, but the identification of most relevant data is still unclear, it will be important to make more advanced bioinformatics, mathematics, and statistics available for a wider range of scientists. Hereby, analytical methods will be developed which avoid the use of thresholds [318].

Screening. The screening method is promising to verify and validate genes found to be regulated using other methods, as immunohistochemistry, *in situ* hybridization, quantitative real-time PCR (RT-qPCR), and cell-sorting (FACS, fluorescence activated cell scanning) [42,69,90,118,207,319–321]. Interestingly, so-called indicator genes were rarely present in data subsets of genes with an extreme fold change. Hence there might be other, more important genes responsible to initialize torpor in distinct nuclei (Chapter 4) and

maintain winter-like state and torpor in whole hypothalamus (Chapters 3) than hitherto suspected.

Transferability of knowledge. As shown in Chapter 3 and 4, a manual literature research is required to evaluate potential roles of regulated genes. Of course, knowledge regarding a gene's biological function is limited, especially regarding seasonal acclimation and metabolic downstates. Most studies were performed in mouse, rat or human, and not necessarily in hypothalamus and its core areas. Hereby, assignability to the given studies in the Djungarian hamster ranges between vague suggestions of a gene's possible role and overinterpretation of biological functions which perfectly make sense in this certain context.

Interpretation. However, it is to consider that transcripts, as analyzed in Chapter 3 and 4, are not necessarily translated into proteins at all, and not necessarily into those which were successfully mapped using the house mouse as reference. There are countless cell type and species-specific pre- and posttranslational modifications, and the effects of a reduced metabolism and Tb during a metabolic downstate as torpor are unratable. In addition, a substantial number of genes were regulated which serve a degradation of mRNA and proteins. Hence, valuable statements regarding systemic effects of single regulated genes are limited to impossible using a manual literature research alone. A GO enrichment analysis, or further potentially applicable methods as pathway analyses [227,288], can help to understand interactions of genes within a bigger context. Hereby, the automatically breaking down of regulated genes to GO classes and e.g., biological functions is still methodologically limited, since based on findings which were communicated in scientific manuscripts and manually fed in databases.

5.2.4 Are transcriptome studies in hibernators and Djungarian hamsters comparable?

General mechanisms. As introduced in Chapter 1, there are several forms of hypometabolism to overcome energetic bottlenecks. It is likely, that the deep, multi-day torpor bouts as obligately expressed during hibernation are orchestrated differently from the shallow, daily torpor of Djungarian hamster, which is expressed spontaneously and

synchronized to photophase. However, there might be interesting similarities, which might be valid for metabolic downstates in general.

Studies. Several transcriptome studies were performed using tissue, e.g., bone marrow, heart, skeletal muscle, white and brown adipose tissue, medulla, forebrain, cerebral cortex and hypothalamus, of a hibernator, namely the thirteen-lined ground squirrel *(Ictidomys tridecemlineatus)* [39,115,116,322–324]. Nevertheless, these studies are not readily comparable with each other and the transcriptome studies of the Djungarian hamster [117,118,128].

Compatibility. This is not only because all studies differed in relevant aspects, as RNA extraction kits, sequencer, mapping method, reference organism, statistics, and ways to identify the relevant data. Moreover, the study design is different. In the photoperiodic Djungarian hamster, sacrifice takes place at the same *Zeitgeber*-time to level ultradian effects of gene regulation. Since hamsters acclimated to winter-like conditions do not express torpor daily, they can be sacrificed either in torpor (SP-HT) or on a torpor-free day (SP-NT). In a seasonal hibernator acclimated to winter-like conditions, all animals express multi-day torpor bouts, which are regularly interrupted by interbout arousals of few hours. Hereby, the animals can be sacrificed at certain stages, e.g., torpor entry, deep torpor, torpor arousal, and interbout arousal, but not on a torpor-free day. So, as also performed in Chapter 3, a sampling group with animals acclimated to summer-like conditions can be useful to determine some kind of baseline, which is impeded, since photoperiodic as well as seasonal species underly a constant, gradual and hard to individually characterize acclimation to external conditions. Furthermore, a pairwise comparison of sampling groups is available only, since statistical tests are designed to compare a treated test group with an untreated control group. Hence, the more sampling groups involved in a transcriptome study, the more superficial the communicated results must be, what counteracts the aim to unravel torpor orchestration in detail. The communication of limitations and their handling is especially important for methods as transcriptomics to favor review and comparison [116].

5.3 Further Perspectives

Current position. Seasonal acclimatizations and metabolic downstates of endotherms are fascinating. Although they enable a survival of energetic bottlenecks due to harsh environmental conditions, they also represent a challenge for each animal. The photoperiodic Djungarian hamster *(Phodopus sungorus)* is an ideal model organism to investigate underlying mechanisms also in artificial conditions. Although the knowledge on prerequisites and proximate stimuli for acclimations and torpor expression has increased, the complexity is far not completely understood.

Systems biology. Further studies might unravel, whether a lower basal metabolic rate enables torpor expression, why and how. Practicable tools to forecast torpor behavior and the next torpor bout might possibly be developed. The locomotor activity, accessible when mean values per large time bin are used, allows interesting approaches. Methods to correlate locomotor activity and Tb or metabolic rate would result in valuable findings regarding the interplay of parameters as well as torpor control. For deeper insights into a hamsters' strategy to survive, multi-factorial models might also integrate more and partly hard to assessable parameters, as food consumption, which is impeded by food hording in nest and cheek pouches, and brown adipose tissue, which is measurable only once, namely after sacrifice.

Chronobiology. The appropriate regulation of the Djungarian hamsters' clockwork is essential for prerequisites and proximate stimuli of torpor, as locomotor activity level and pattern throughout the course of acclimation to SP as well as differentially expressed clock genes in SCN during torpor entry indicated in Chapter 2 and 4. To find out details, the SCNs transcriptome might be analyzed at further key moments, as deep torpor (ZT04), torpor arousal (ZT07) and post-torpor (ZT16). Since the gene regulation of the hypothalamus is likely not caused by SCN and PVN alone, as shown in profound differences between Chapter 3 and 4, the transcriptome of further hypothalamic nuclei, besides further brain areas which are also likely involved in torpor orchestration, might be analyzed.

Molecular biology. Apart from analyses of further brain areas, specialized cell populations, as tanycytes, or organelles, as mitochondria, might be analyzed. This is possible on level of lab work, as well as on level of computational work. Lasermicrodissection has a high resolution yet requires cells which are to differentiate by

simple and fast staining methods. Successfully mapped transcriptomics data might favor to find working markers for methods as immunohistochemistry and *in situ* hybridization to assess and locate gene expression within brain tissue as well as for various single-cell isolation techniques prior to transcriptomics in the course of scRNA-seq [325]. Hereby, digital spatial profiling has potential to unravel time- and nuclei-specific gene expression relevant for torpor orchestration. Ideally, novel multi-omics approaches including pathways analyses allow the interpretation of transcriptomic and proteomic data which was gained from the same tissue [326]. Hereby, anomalies in brain anatomy or gene expression might unravel reasons for the broad spectrum of response to short photoperiod and torpor incidence within a cohort of the Djungarian hamster.

Outlook. Technological advancements will enable more detailed analysis of further parameters while respecting animal welfare. Furthermore, interdisciplinary teams will make advances in mathematical modelling, statistics and data analysis. Given a trend towards open access of scientific manuscripts and data sets, entries in knowledge bases will be refined and extended, while number of lab animals can be reduced. However, in foreseeable time, it will remain unresolved, why one certain animal performs the way it does.

IV References

[1] A. Silvani, Editorial: The Integrative Physiology of Metabolic Downstates, Front. Physiol. 12 (2021) 1–2. https://doi.org/10.3389/fphys.2021.758972.

[2] V. Diedrich, E. Haugg, C. Dreier, A. Herwig, What can seasonal models teach us about energy balance?, J. Endocrinol. 244 (2020) R17–R32. https://doi.org/10.1530/JOE-19-0502.

[3] F. Geiser, Ecological Physiology of Daily Torpor and Hibernation, Springer International Publishing, Cham, 2021. https://doi.org/10.1007/978-3-030-75525-6.

[4] A. Masuda, T. Oishi, Effects of photoperiod and temperature on body weight, food intake, food storage, and pelage color in the Djungarian hamster, *Phodopus sungorus,* J. Exp. Zool. 248 (1988) 133–139. https://doi.org/10.1002/jez.1402480202.

[5] T. Ruf, A. Stieglitz, S. Steinlechner, J.L. Blank, G. Heldmaier, Cold exposure and food restriction facilitate physiological responses to short photoperiod in Djungarian hamsters *(Phodopus sungorus),* J. Exp. Zool. 267 (1993) 104–112. https://doi.org/10.1002/jez.1402670203.

[6] G. Heldmaier, S. Steinlechner, J. Rafael, B. Latteier, Photoperiod and ambient temperature as environmental cues for seasonal thermogenic adaptation in the Djungarian hamster, *Phodopus sungorus,* Int. J. Biometeorol. 26 (1982) 339–345. https://doi.org/10.1007/BF02219505.

[7] D.A. Zysling, A.D. Garst, G.E. Demas, Photoperiod and food restriction differentially affect reproductive and immune responses in Siberian Hamsters *Phodopus sungorus,* Funct. Ecol. 23 (2009) 979–988. https://doi.org/10.1111/j.1365-2435.2009.01572.x.

[8] N. Huber, S. Vetter, G. Stalder, H. Gerritsmann, S. Giroud, Dynamic Function and Composition Shift in Circulating Innate Immune Cells in Hibernating Garden Dormice, Front. Physiol. 12 (2021) 1–12. https://doi.org/10.3389/fphys.2021.620614.

[9] K.U. Frerichs, C. Kennedy, L. Sokoloff, J.M. Hallenbeck, Local Cerebral Blood Flow during Hibernation, a Model of Natural Tolerance to “Cerebral Ischemia,” J. Cereb. Blood Flow Metab. 14 (1994) 193–205. https://doi.org/10.1038/jcbfm.1994.26.

[10] E.L. De Vrij, P.C. Vogelaar, M. Goris, M.C. Houwertjes, A. Herwig, G.J. Dugbartey, A.S. Boerema, A.M. Strijkstra, H.R. Bouma, R.H. Henning, Platelet dynamics during natural and pharmacologically induced torpor and forced hypothermia, PLoS One. 9 (2014) 1–12. https://doi.org/10.1371/journal.pone.0093218.

[11] H.R. Bouma, F.G.M. Kroese, J.W. Kok, F. Talaei, A.S. Boerema, A. Herwig, O. Draghiciu, A. van Buiten, A.H. Epema, A. van Dam, A.M. Strijkstra, R.H. Henning, Low body temperature governs the decline of circulating lymphocytes during hibernation through sphingosine-1-phosphate, Proc. Natl. Acad. Sci. 108 (2011) 2052–2057. https://doi.org/10.1073/pnas.1008823108.

[12] H.R. Bouma, G.J. Dugbartey, A.S. Boerema, F. Talaei, A. Herwig, M. Goris, A. van

Buiten, A.M. Strijkstra, H. V. Carey, R.H. Henning, F.G.M. Kroese, Reduction of body temperature governs neutrophil retention in hibernating and nonhibernating animals by margination, J. Leukoc. Biol. 94 (2013) 431–437. https://doi.org/10.1189/jlb.0611298.

[13] H. V. Carey, C.L. Frank, J.P. Seifert, Hibernation induces oxidative stress and activation of NF-κB in ground squirrel intestine, J. Comp. Physiol. B Biochem. Syst. Environ. Physiol. 170 (2000) 551–559. https://doi.org/10.1007/s003600000135.

[14] A.L. Orr, L.A. Lohse, K.L. Drew, M. Hermes-Lima, Physiological oxidative stress after arousal from hibernation in Arctic ground squirrel, Comp. Biochem. Physiol. Part A Mol. Integr. Physiol. 153 (2009) 213–221. https://doi.org/10.1016/j.cbpa.2009.02.016.

[15] Y. Wei, J. Zhang, S. Xu, X. Peng, X. Yan, X. Li, H. Wang, H. Chang, Y. Gao, Controllable oxidative stress and tissue specificity in major tissues during the torpor–arousal cycle in hibernating Daurian ground squirrels, Open Biol. 8 (2018) 180068. https://doi.org/10.1098/rsob.180068.

[16] F. Van Breukelen, S.L. Martin, Translational initiation is uncoupled from elongation at 18°C during mammalian hibernation, Am. J. Physiol. - Regul. Integr. Comp. Physiol. 281 (2001) 1374–1379. https://doi.org/10.1152/ajpregu.2001.281.5.r1374.

[17] F. van Breukelen, S.L. Martin, Reversible depression of transcription during hibernation, J. Comp. Physiol. B Biochem. Syst. Environ. Physiol. 172 (2002) 355–361. https://doi.org/10.1007/s00360-002-0256-1.

[18] Y.J. Lee, S.I. Miyake, H. Wakita, D.C. McMullen, Y. Azuma, S. Auh, J.M. Hallenbeck, Protein SUMOylation is massively increased in hibernation torpor and is critical for the cytoprotection provided by ischemic preconditioning and hypothermia in SHSY5Y cells, J. Cereb. Blood Flow Metab. 27 (2007) 950–962. https://doi.org/10.1038/sj.jcbfm.9600395.

[19] J.F. Staples, Metabolic suppression in mammalian hibernation: The role of mitochondria, J. Exp. Biol. 217 (2014) 2032–2036. https://doi.org/10.1242/jeb.092973.

[20] J.C.L. Brown, A.R. Gerson, J.F. Staples, Mitochondrial metabolism during daily torpor in the dwarf Siberian hamster: Role of active regulated changes and passive thermal effects, Am. J. Physiol. - Regul. Integr. Comp. Physiol. 293 (2007) 1833–1845. https://doi.org/10.1152/ajpregu.00310.2007.

[21] S. Giroud, C. Habold, R.F. Nespolo, C. Mejías, J. Terrien, S.M. Logan, R.H. Henning, K.B. Storey, The Torpid State: Recent Advances in Metabolic Adaptations and Protective Mechanisms, Front. Physiol. 11 (2021) 1–24. https://doi.org/10.3389/fphys.2020.623665.

[22] C. Cubuk, J.H.H. Bank, A. Herwig, The Chemistry of Cold: Mechanisms of Torpor Regulation in the Siberian Hamster, Physiology. 31 (2016) 51–59. https://doi.org/10.1152/physiol.00028.2015.

[23] R.G. Melvin, M.T. Andrews, Torpor induction in mammals: recent discoveries fueling new ideas, Trends Endocrinol. Metab. 20 (2009) 490–498. https://doi.org/10.1016/j.tem.2009.09.005.

[24] T. Ruf, F. Geiser, Daily torpor and hibernation in birds and mammals, Biol. Rev. 90 (2015) 891–926. https://doi.org/10.1111/brv.12137.

[25] F. Geiser, Ontogeny and phylogeny of endothermy and torpor in mammals and birds, Comp. Biochem. Physiol. - A Mol. Integr. Physiol. 150 (2008) 176–180. https://doi.org/10.1016/j.cbpa.2007.02.041.

[26] H.R. Bouma, E.M. Verhaag, J.P. Otis, G. Heldmaier, S.J. Swoap, A.M. Strijkstra, R.H. Henning, H. V. Carey, Induction of torpor: Mimicking natural metabolic suppression for biomedical applications, J. Cell. Physiol. 227 (2012) 1285–1290. https://doi.org/10.1002/jcp.22850.

[27] M. Cerri, The central control of energy expenditure: Exploiting torpor for medical applications, Annu. Rev. Physiol. 79 (2017) 167–186. https://doi.org/10.1146/annurev-physiol-022516-034133.

[28] Z. Shi, M. Qin, L. Huang, T. Xu, Y. Chen, Q. Hu, S. Peng, Z. Peng, L.N. Qu, S.G. Chen, Q.H. Tuo, D.F. Liao, X.P. Wang, R.R. Wu, T.F. Yuan, Y.H. Li, X.M. Liu, Human torpor: translating insights from nature into manned deep space expedition, Biol. Rev. 96 (2021) 642–672. https://doi.org/10.1111/brv.12671.

[29] F.N. Buijs, L. León-Mercado, M. Guzmán-Ruiz, N.N. Guerrero-Vargas, F. Romo-Nava, R.M. Buijs, The circadian system: A regulatory feedback network of periphery and brain, Physiology. 31 (2016) 170–181. https://doi.org/10.1152/physiol.00037.2015.

[30] K.R. Dave, S.L. Christian, M.A. Perez-Pinzon, K.L. Drew, Neuroprotection: Lessons from hibernators, Comp. Biochem. Physiol. - B Biochem. Mol. Biol. 162 (2012) 1–9. https://doi.org/10.1016/j.cbpb.2012.01.008.

[31] Y.S. Tarahovsky, I.S. Fadeeva, N.P. Komelina, M.O. Khrenov, N.M. Zakharova, Antipsychotic inductors of brain hypothermia and torpor-like states: perspectives of application, Psychopharmacology (Berl). 234 (2017) 173–184. https://doi.org/10.1007/s00213-016-4496-2.

[32] A. Choukèr, J. Bereiter-Hahn, D. Singer, G. Heldmaier, Hibernating astronauts — science or fiction ?, Eur. J. Physiol. 471 (2019) 819–828. https://doi.org/10.1007/s00424-018-2244-7.

[33] J. Nowack, I. Tarmann, F. Hoelzl, S. Smith, S. Giroud, T. Ruf, Always a price to pay: Hibernation at low temperatures comes with a trade-off between energy savings and telomere damage, Biol. Lett. 15 (2019). https://doi.org/10.1098/rsbl.2019.0466.

[34] E. Millesi, H. Prossinger, J.P. Dittami, M. Fieder, Hibernation effects on memory in European ground squirrels *(Spermophilus citellus),* J. Biol. Rhythms. 16 (2001) 264–271. https://doi.org/10.1177/074873001129001971.

[35] F. Geiser, R.M. Brigham, The Other Functions of Torpor, in: T. Ruf, C. Bieber, W. Arnold, E. Millesi (Eds.), Living a Seas. World, Springer Berlin Heidelberg, Berlin, Heidelberg, 2012: pp. 109–121. https://doi.org/10.1007/978-3-642-28678-0_10.

[36] C.J. Cotton, H.J. Harlow, Do hypothermic tissue tolerances limit torpor expression?, J. Therm. Biol. 34 (2009) 206–211. https://doi.org/10.1016/j.jtherbio.2009.02.003.

[37] T. Hitrec, M. Luppi, S. Bastianini, F. Squarcio, C. Berteotti, V. Lo Martire, D. Martelli,

A. Occhinegro, D. Tupone, G. Zoccoli, R. Amici, M. Cerri, Neural control of fasting-induced torpor in mice, Sci. Rep. 9 (2019) 1–12. https://doi.org/10.1038/s41598-019-51841-2.

[38] G.P. Webb, S.A. Jagot, M.E. Jakobson, Fasting-induced torpor in Mus musculus and its implications in the use of murine models for human obesity studies, Comp. Biochem. Physiol. -- Part A Physiol. 72 (1982) 211–219. https://doi.org/10.1016/0300-9629(82)90035-4.

[39] M. Hampton, R.G. Melvin, A.H. Kendall, B.R. Kirkpatrick, N. Peterson, M.T. Andrews, Deep sequencing the transcriptome reveals seasonal adaptive mechanisms in a hibernating mammal, PLoS One. 6 (2011). https://doi.org/10.1371/journal.pone.0027021.

[40] M. Wilz, G. Heldmaier, Comparison of hibernation, estivation and daily torpor in the edible dormouse, *Glis glis,* J. Comp. Physiol. - B Biochem. Syst. Environ. Physiol. 170 (2000) 511–521. https://doi.org/10.1007/s003600000129.

[41] V. Diedrich, S. Kumstel, S. Steinlechner, Spontaneous daily torpor and fasting-induced torpor in Djungarian hamsters are characterized by distinct patterns of metabolic rate, J. Comp. Physiol. B Biochem. Syst. Environ. Physiol. 185 (2015) 355–366. https://doi.org/10.1007/s00360-014-0882-4.

[42] C. Cubuk, H. Markowsky, A. Herwig, Hypothalamic control systems show differential gene expression during spontaneous daily torpor and fasting-induced torpor in the Djungarian hamster *(Phodopus sungorus),* PLoS One. 12 (2017) e0186299. https://doi.org/10.1371/journal.pone.0186299.

[43] G. Heldmaier, T. Ruf, Body temperature and metabolic rate during natural hypothermia in endotherms, J. Comp. Physiol. B. 162 (1992) 696–706. https://doi.org/10.1007/BF00301619.

[44] M. Jastroch, S. Giroud, P. Barrett, F. Geiser, G. Heldmaier, A. Herwig, Seasonal control of mammalian energy balance: recent advances in the understanding of daily torpor and hibernation, J. Neuroendocrinol. 28 (2016) 1–10. https://doi.org/10.1111/jne.12437.

[45] M.J. Paul, I. Zucker, W.J. Schwartz, Tracking the seasons: The internal calendars of vertebrates, Philos. Trans. R. Soc. B Biol. Sci. 363 (2008) 341–361. https://doi.org/10.1098/rstb.2007.2143.

[46] I. Pajunen, Ambient temperature dependence of the body temperature and of the duration of the hibernation periods in the garden dormouse, *Eliomys quercinus L,* Cryobiology. 20 (1983) 690–697. https://doi.org/10.1016/0011-2240(83)90073-1.

[47] P.J. Morgan, A.W. Ross, J.G. Mercer, P. Barrett, Photoperiodic programming of body weight through the neuroendocrine hypothalamus, J. Endocrinol. 177 (2003) 27–34. https://doi.org/10.1677/joe.0.1770027.

[48] F.H. Bronson, Mammalian Reproduction: An Ecological Perspective, Biol. Reprod. 32 (1985) 1–26. https://doi.org/10.1095/biolreprod32.1.1.

[49] A.C. West, S.H. Wood, Seasonal physiology: making the future a thing of the past, Curr. Opin. Physiol. 5 (2018) 1–8. https://doi.org/10.1016/j.cophys.2018.04.006.

[50] S. Bertolino, C. Viano, I. Currado, Population dynamics, breeding patterns and spatial use of the garden dormouse *(Eliomys quercinus)* in an Alpine habitat, J. Zool. 253 (2001) 513–521. https://doi.org/10.1017/S0952836901000474.

[51] S. Stumpfel, C. Bieber, S. Blanc, T. Ruf, S. Giroud, Differences in growth rates and pre-hibernation body mass gain between early and late-born juvenile garden dormice, J. Comp. Physiol. B Biochem. Syst. Environ. Physiol. 187 (2017) 253–263. https://doi.org/10.1007/s00360-016-1017-x.

[52] E. Piscitiello, A. Herwig, E. Haugg, B. Schröder, G. Breves, S. Steinlechner, V. Diedrich, Acclimation of intestinal morphology and function in Djungarian hamsters *(Phodopus sungorus)* related to seasonal and acute energy balance, J. Exp. Biol. 224 (2021) 1–13. https://doi.org/10.1242/jeb.232876.

[53] T. Ruf, K. Gasch, G. Stalder, H. Gerritsmann, S. Giroud, An hourglass mechanism controls torpor bout length in hibernating garden dormice, J. Exp. Biol. 224 (2021). https://doi.org/10.1242/jeb.243456.

[54] R. Kirsch, A. Ouarour, P. Pévet, Daily torpor in the Djungarian hamster *(Phodopus sungorus):* photoperiodic regulation, characteristics and circadian organization, J. Comp. Physiol. A. 168 (1991) 121–128. https://doi.org/10.1007/BF00217110.

[55] T. Ruf, S. Steinlechner, G. Heldmaier, Rhythmicity of body temperature and torpor in the Djungarian hamster, *Phodopus sungorus,* in: A. Malan, B. Canguilhem (Eds.), Living Cold 2nd Int. Symp., 193rd ed., Colloques INSERM/John Libbey Eurotext Ldt, Le Hohwald, France, 1989: pp. 53–61.

[56] M. Jefimow, M. Wojciechowski, A. Masuda, T. Oishi, Correlation between torpor frequency and capacity for non-shivering thermogenesis in the Siberian hamster *(Phodopus sungorus),* J. Therm. Biol. 29 (2004) 641–647. https://doi.org/10.1016/j.jtherbio.2004.08.033.

[57] G. Heldmaier, S. Steinlechner, Seasonal pattern and energetics of short daily torpor in the Djungarian hamster, *Phodopus sungorus,* Oecologia. 48 (1981) 265–270. https://doi.org/10.1007/BF00347975.

[58] T. Ruf, G. Heldmaier, The impact of daily torpor on energy requirements in the Djungarian hamster, *Phodopus sungorus,* Physiol. Zool. 65 (1992) 994–1010. https://doi.org/10.2307/30158554.

[59] T. Ruf, M. Klingenspor, H. Preis, G. Heldmaier, Daily torpor in the Djungarian hamster *(Phodopus sungorus):* interactions with food intake, activity, and social behaviour, J. Comp. Physiol. B. 160 (1991) 609–615. https://doi.org/10.1007/BF00571257.

[60] J. Figala, K. Hoffmann, G. Goldau, Zur Jahresperiodik beim Dsungarischen Zwerghamster *Phodopus sungorus* Pallas, Oecologia. 12 (1973) 89–118. https://doi.org/10.1007/BF00345511.

[61] S. Steinlechner, Endokrine Mechanismen bei der jahreszeitlichen Klimaanpassung Fallstudie : Jahreszeitliche Anpassungen, in: S. Hirzel (Ed.), Endokrinol. IV Vor. Im Rahmen Des Proj. "Zeitstrukturen Endokriner Syst. Abhandlungen Der Sächsischen Akad. Der Wissenschaften Zu Leipzig. Math. Klasse, E. Peschke, Stuttgart, Germany, 2009: pp. 99–112.

[62] K. Hoffmann, The Critical Photoperiod in the Djungarian Hamster *Phodopus sungorus,* in: J. Aschoff, S. Daan, G. Groos (Eds.), Vertebr. Circadian Syst., Berlin, 1982: pp. 297–304. https://doi.org/10.1007/978-3-642-68651-1_33.

[63] A.S. Kauffman, A. Cabrera, I. Zucker, Energy intake and fur in summer- and winter-acclimated Siberian hamsters *(Phodopus sungorus),* Am. J. Physiol. - Regul. Integr. Comp. Physiol. 281 (2001) 519–527. https://doi.org/10.1152/ajpregu.2001.281.2.r519.

[64] G. Heldmaier, S. Steinlechner, Seasonal control of energy requirements for thermoregulation in the Djungarian hamster *(Phodopus sungorus),* living in natural photoperiod, J. Comp. Physiol. B Biochem. Syst. Environ. Physiol. 142 (1981) 429–437. https://doi.org/10.1007/BF00688972.

[65] P. Barrett, F.J.P. Ebling, S. Schuhler, D. Wilson, A.W. Ross, A. Warner, P.H. Jethwa, A. Boelen, T.J. Visser, D.M. Ozanne, Z.A. Archer, J.G. Mercer, P.J. Morgan, Hypothalamic thyroid hormone catabolism acts as a gatekeeper for the seasonal control of body weight and reproduction, Endocrinology. 148 (2007) 3608–3617. https://doi.org/10.1210/en.2007-0316.

[66] K. Hoffmann, The influence of photoperiod and melatonin on testis size, body weight, and pelage colour in the Djungarian hamster *(Phodopus sungorus),* J. Comp. Physiol. 85 (1973) 267–282. https://doi.org/10.1007/BF00694233.

[67] D. Weinert, K. Schöttner, A. V. Surov, P. Fritzsche, N.Y. Feoktistova, M. V. Ushakova, G.B. Ryurikov, Circadian activity rhythms of dwarf hamsters *(Phodopus spp.)* under laboratory and semi-natural conditions, Russ. J. Theriol. 8 (2009) 47–58. https://doi.org/10.15298/rusjtheriol.08.1.05.

[68] D. Müller, J. Hauer, K. Schöttner, P. Fritzsche, D. Weinert, Seasonal adaptation of dwarf hamsters (Genus *Phodopus*): differences between species and their geographic origin, J. Comp. Physiol. B Biochem. Syst. Environ. Physiol. 185 (2015) 917–930. https://doi.org/10.1007/s00360-015-0926-4.

[69] J.H.H. Bank, J. Kemmling, E. Rijntjes, E.K. Wirth, A. Herwig, Thyroid hormone status affects expression of daily torpor and gene transcription in Djungarian hamsters *(Phodopus sungorus),* Horm. Behav. 75 (2015) 120–129. https://doi.org/10.1016/j.yhbeh.2015.09.006.

[70] G. Heldmaier, M. Klingenspor, M. Werneyer, B.J. Lampi, S.P. Brooks, K.B. Storey, Metabolic adjustments during daily torpor in the Djungarian hamster, Am. J. Physiol. 276 (1999) E896–E906. https://doi.org/10.1152/ajpendo.1999.276.5.E896.

[71] F. Scherbarth, S. Steinlechner, Endocrine mechanisms of seasonal adaptation in small mammals: From early results to present understanding, J. Comp. Physiol. B Biochem. Syst. Environ. Physiol. 180 (2010) 935–952. https://doi.org/10.1007/s00360-010-0498-2.

[72] H.C. Heller, N.F. Ruby, Sleep and circadian rhythms in mammalian torpor, Annu. Rev. Physiol. 66 (2004) 275–289. https://doi.org/10.1146/annurev.physiol.66.032102.115313.

[73] T. Deboer, I. Tobler, Sleep regulation in the Djungarian hamster: Comparison of the dynamics leading to the slow-wave activity increase after sleep deprivation and

daily torpor, Sleep. 26 (2003) 567–572. https://doi.org/10.1093/sleep/26.5.567.

[74] S. Palchykova, T. Deboer, I. Tobler, Selective sleep deprivation after daily torpor in the Djungarian hamster, J. Sleep Res. 11 (2002) 313–319. https://doi.org/10.1046/j.1365-2869.2002.00310.x.

[75] G. Heldmaier, S. Ortmann, R. Elvert, Natural hypometabolism during hibernation and daily torpor in mammals, Respir. Physiol. Neurobiol. 141 (2004) 317–329. https://doi.org/10.1016/j.resp.2004.03.014.

[76] G. Heldmaier, A. Buchberger, Sources of heat during nonshivering thermogenesis in Djungarian hamsters: a dominant role of brown adipose tissue during cold adaptation, J. Comp. Physiol. B. 156 (1985) 237–245. https://doi.org/10.1007/BF00695778.

[77] H. Dardente, D.G. Hazlerigg, F.J.P. Ebling, Thyroid hormone and seasonal rhythmicity, Front. Endocrinol. (Lausanne). 5 (2014) 1–11. https://doi.org/10.3389/fendo.2014.00019.

[78] S. Steinlechner, G. Heldmaier, Role of photoperiod and melatonin in seasonal acclimatization of the Djungarian Hamster, *Phodopus sungorus,* Int. J. Biometeorol. 26 (1982) 329–337. https://doi.org/10.1007/BF02219503.

[79] P. Niklowitz, A. Lerchl, E. Nieschlag, Photoperiodic Responses in Djungarian Hamsters *(Phodopus sungorus):* Importance of Light History for Pineal and Serum Melatonin Profiles1, Biol. Reprod. 51 (1994) 714–724. https://doi.org/10.1095/biolreprod51.4.714.

[80] T. Korhonen, A.-M. Mustonen, P. Nieminen, S. Saarela, Effects of cold exposure, exogenous melatonin and short-day treatment on the weight-regulation and body temperature of the Siberian Hamster *(Phodopus sungorus),* Regul. Pept. 149 (2008) 60–66. https://doi.org/10.1016/j.regpep.2007.09.033.

[81] G.C. Wagner, J.D. Johnston, B.B. Tournier, F.J.P. Ebling, D.G. Hazlerigg, Melatonin induces gene-specific effects on rhythmic mRNA expression in the pars tuberalis of the Siberian hamster *(Phodopus sungorus),* Eur. J. Neurosci. 25 (2007) 485–490. https://doi.org/10.1111/j.1460-9568.2006.05291.x.

[82] A. Herwig, P. Pévet, B. Bothorel, S. Steinlechner, M. Saboureau, Trans-pineal microdialysis in the Djungarian hamster *(Phodopus sungorus):* A tool to study seasonal changes of circadian clock activities, J. Pineal Res. 40 (2006) 177–183. https://doi.org/10.1111/j.1600-079X.2005.00296.x.

[83] T.J. Bartness, B.D. Goldman, E.L. Bittman, SCN lesions block responses to systemic melatonin infusions in Siberian hamsters, Am. J. Physiol. Integr. Comp. Physiol. 260 (1991) R102–R112. https://doi.org/10.1152/ajpregu.1991.260.1.r102.

[84] P. Pevet, E. Challet, Melatonin: Both master clock output and internal time-giver in the circadian clocks network, J. Physiol. Paris. 105 (2011) 170–182. https://doi.org/10.1016/j.jphysparis.2011.07.001.

[85] J. Recio, P. Pévet, B. Vivien-Roels, J.M. Míguez, M. Masson-Pévet, Daily and photoperiodic melatonin binding changes in the suprachiasmatic nuclei, paraventricular thalamic nuclei, and pars tuberalis of the female Siberian hamster *(Phodopus sungorus),* J. Biol. Rhythms. 11 (1996) 325–332.

https://doi.org/10.1177/074873049601100406.

[86] J.E. Lewis, F.J.P. Ebling, Tanycytes as regulators of seasonal cycles in neuroendocrine function, Front. Neurol. 8:79 (2017) 1–7. https://doi.org/10.3389/fneur.2017.00079.

[87] J. Bockmann, T.M. Böckers, B. Vennemann, P. Niklowitz, J. Müller, W. Wittkowski, B. Sabel, M.R. Kreutz, Short photoperiod-dependent down-regulation of thyrotropin-alpha and -beta in hamster pars tuberalis-specific cells is prevented by pinealectomy., Endocrinology. 137 (1996) 1804–1813. https://doi.org/10.1210/endo.137.5.8612518.

[88] N. Nakao, H. Ono, T. Yamamura, T. Anraku, T. Takagi, K. Higashi, S. Yasuo, Y. Katou, S. Kageyama, Y. Uno, T. Kasukawa, M. Iigo, P.J. Sharp, A. Iwasawa, Y. Suzuki, S. Sugano, T. Niimi, M. Mizutani, T. Namikawa, S. Ebihara, H.R. Ueda, T. Yoshimura, Thyrotrophin in the pars tuberalis triggers photoperiodic response, Nature. 452 (2008) 317–322. https://doi.org/10.1038/nature06738.

[89] E.A. Hanon, G.A. Lincoln, J.M. Fustin, H. Dardente, M. Masson-Pévet, P.J. Morgan, D.G. Hazlerigg, Ancestral TSH mechanism signals summer in a photoperiodic mammal, Curr. Biol. 18 (2008) 1147–1152. https://doi.org/10.1016/j.cub.2008.06.076.

[90] F. Langlet, Tanycytes: A gateway to the metabolic hypothalamus, J. Neuroendocrinol. 26 (2014) 753–760. https://doi.org/10.1111/jne.12191.

[91] H. Dardente, S. Wood, F.J.P. Ebling, C. Sáenz de Miera, An integrative view of mammalian seasonal neuroendocrinology, J. Neuroendocrinol. 31 (2019) 1–17. https://doi.org/10.1111/jne.12729.

[92] G. Helfer, P. Barrett, P.J. Morgan, A unifying hypothesis for control of body weight and reproduction in seasonally breeding mammals, J. Neuroendocrinol. 31 (2019) 1–12. https://doi.org/10.1111/jne.12680.

[93] A. Herwig, A.W. Ross, K.N. Nilaweera, P.J. Morgan, P. Barrett, Hypothalamic thyroid hormone in energy balance regulation, Obes. Facts. 1 (2008) 71–79. https://doi.org/10.1159/000123428.

[94] K.N. Nilaweera, A. Herwig, M. Bolborea, G. Campbell, C.-D. Mayer, P.J. Morgan, F.J.P. Ebling, P. Barrett, Photoperiodic regulation of glycogen metabolism, glycolysis, and glutamine synthesis in tanycytes of the Siberian hamster suggests novel roles of tanycytes in hypothalamic function, Glia. 59 (2011) 1695–1705. https://doi.org/10.1002/glia.21216.

[95] J.E. Silva, Thermogenic mechanisms and their hormonal regulation, Physiol. Rev. 86 (2006) 435–464. https://doi.org/10.1152/physrev.00009.2005.

[96] A. Tups, C. Ellis, K.M. Moar, T.J. Logie, C.L. Adam, J.G. Mercer, M. Klingenspor, Photoperiodic regulation of leptin sensitivity in the Siberian hamster, *Phodopus sungorus,* is reflected in arcuate nucleus SOCS-3 (suppressor of cytokine signaling) gene expression, Endocrinology. 145 (2004) 1185–1193. https://doi.org/10.1210/en.2003-1382.

[97] T.J. Bartness, G.E. Demas, C.K. Song, Seasonal Changes in Adiposity: the Roles of the Photoperiod, Melatonin and Other Hormones, and Sympathetic Nervous

System, Exp. Biol. Med. 227 (2002) 363–376. https://doi.org/10.1177/153537020222700601.

[98] V. Pilorz, C. Helfrich-Förster, H. Oster, The role of the circadian clock system in physiology, Pflügers Arch. - Eur. J. Physiol. 470 (2018) 227–239. https://doi.org/10.1007/s00424-017-2103-y.

[99] K. Franklin, G. Paxinos, The mouse brain in stereotaxic coordinates, 3rd ed., 2008. https://doi.org/10.1016/S0306-4530(03)00088-X.

[100] A.C. Liu, W.G. Lewis, S.A. Kay, Mammalian circadian signaling networks and therapeutic targets, Nat. Chem. Biol. 3 (2007) 630–639. https://doi.org/10.1038/nchembio.2007.37.

[101] D.K. Welsh, D.E. Logothetis, M. Meister, S.M. Reppert, Individual neurons dissociated from rat suprachiasmatic nucleus express independently phased circadian firing rhythms, Neuron. 14 (1995) 697–706. https://doi.org/10.1016/0896-6273(95)90214-7.

[102] A.B. Webb, N. Angelo, J.E. Huettner, E.D. Herzog, Intrinsic, nondeterministic circadian rhythm generation in identified mammalian neurons, Proc. Natl. Acad. Sci. U. S. A. 106 (2009) 16493–16498. https://doi.org/10.1073/pnas.0902768106.

[103] C.B. Saper, A.D. Loewy, L.W. Swanson, W.M. Cowan, Direct hypothalamo-autonomic connections, Brain Res. 117 (1976) 305–312. https://doi.org/10.1016/0006-8993(76)90738-1.

[104] H. Kawano, S. Masuko, β-endorphin-, adrenocorticotrophic hormone- and neuropeptide y-containing projection fibers from the arcuate hypothalamic nucleus make synaptic contacts on to nucleus preopticus medianus neurons projecting to the paraventricular hypothalamic nucleus in the rat, Neuroscience. 98 (2000) 555–565. https://doi.org/10.1016/S0306-4522(00)00134-2.

[105] I.C. Munch, M. Mller, P.J. Larsen, N. Vrang, Light-induced c-Fos expression in suprachiasmatic nuclei neurons targeting the paraventricular nucleus of the hamster hypothalamus: Phase dependence and immunochemical identification, J. Comp. Neurol. 442 (2002) 48–62. https://doi.org/10.1002/cne.1421.

[106] T.J. Bartness, G.N. Wade, Photoperiodic control of seasonal body weight cycles in hamsters, Neurosci. Biobehav. Rev. 9 (1985) 599–612. https://doi.org/10.1016/0149-7634(85)90006-5.

[107] T. Llewellyn, H. Zheng, X. Liu, B. Xu, K.P. Patel, Median preoptic nucleus and subfornical organ drive renal sympathetic nerve activity via a glutamatergic mechanism within the paraventricular nucleus, Am. J. Physiol. Integr. Comp. Physiol. 302 (2012) R424–R432. https://doi.org/10.1152/ajpregu.00403.2011.

[108] P. Santoso, M. Nakata, Y. Ueta, T. Yada, CNS control of metabolism: Suprachiasmatic vasopressin to paraventricular oxytocin neurocircuit in the hypothalamus relays light reception to inhibit feeding behavior, Am. J. Physiol. - Endocrinol. Metab. 315 (2018) E478–E488. https://doi.org/10.1152/ajpendo.00338.2016.

[109] S.M. Sagar, F.R. Sharp, T. Curran, Expression of c-fos protein in brain: Metabolic mapping at the cellular level, Sci. Sci. 240 (1988) 1328–1331.

https://doi.org/10.1126/science.3131879.

[110] E.L. Bittman, T.J. Bartness, B.D. Goldman, G.J. DeVries, Suprachiasmatic and paraventricular control of photoperiodism in Siberian hamsters, Am. J. Physiol. Integr. Comp. Physiol. 260 (1991) R90–R101. https://doi.org/10.1152/ajpregu.1991.260.1.r90.

[111] M.T. Foster, C.K. Song, T.J. Bartness, Hypothalamic paraventricular nucleus lesion involvement in the sympathetic control of lipid mobilization, Obesity. 18 (2010) 682–689. https://doi.org/10.1038/oby.2009.345.

[112] D.C. Klein, R. Smoot, J.L. Weller, S. Higa, S.P. Markey, G.J. Creed, D.M. Jacobowitz, Lesions of the paraventricular nucleus area of the hypothalamus disrupt the suprachiasmatic→ spinal cord circuit in the melatonin rhythm generating system, Brain Res. Bull. 10 (1983) 647–652. https://doi.org/10.1016/0361-9230(83)90033-3.

[113] N.F. Ruby, Paraventricular nucleus ablation disrupts daily torpor in Siberian hamsters, Brain Res. Bull. 37 (1995) 193–198. https://doi.org/10.1016/0361-9230(94)00279-A.

[114] R.M. Kliman, G.R. Lynch, Evidence for independence of circadian characters and extent of photoresponsiveness in the Djungarian Hamster, *Phodopus sungorus,* J. Biol. Rhythms. 6 (1991) 159–166. https://doi.org/10.1177/074873049100600206.

[115] R. Fu, A.E. Gillen, K.R. Grabek, K.A. Riemondy, L.E. Epperson, C.D. Bustamante, J.R. Hesselberth, S.L. Martin, Dynamic RNA Regulation in the Brain Underlies Physiological Plasticity in a Hibernating Mammal, Front. Physiol. 11 (2021) 1–18. https://doi.org/10.3389/fphys.2020.624677.

[116] C. Schwartz, M. Hampton, M.T. Andrews, Seasonal and regional differences in gene expression in the brain of a hibernating mammal, PLoS One. 8 (2013). https://doi.org/10.1371/journal.pone.0058427.

[117] R. Bao, K.G. Onishi, E. Tolla, F.J.P. Ebling, J.E. Lewis, R.L. Anderson, P. Barrett, B.J. Prendergast, T.J. Stevenson, Genome sequencing and transcriptome analyses of the Siberian hamster hypothalamus identify mechanisms for seasonal energy balance, Proc. Natl. Acad. Sci. (2019) 201902896. https://doi.org/10.1073/pnas.1902896116.

[118] C. Cubuk, J. Kemmling, A. Fabrizius, A. Herwig, Transcriptome analysis of hypothalamic gene expression during daily torpor in Djungarian hamsters *(Phodopus sungorus),* Front. Neurosci. 11 (2017) 122. https://doi.org/10.3389/fnins.2017.00122.

[119] E. Haugg, A. Herwig, V. Diedrich, Body Temperature and Activity Adaptation of Short Photoperiod-Exposed Djungarian Hamsters *(Phodopus sungorus):* Timing, Traits, and Torpor, Front. Physiol. 12 (2021). https://doi.org/10.3389/fphys.2021.626779.

[120] J.S. Takahashi, H.K. Hong, C.H. Ko, E.L. McDearmon, The genetics of mammalian circadian order and disorder: Implications for physiology and disease, Nat. Rev. Genet. 9 (2008) 764–775. https://doi.org/10.1038/nrg2430.

[121] J.C. Dunlap, Molecular bases for circadian clocks, Cell. 96 (1999) 271–290.

https://doi.org/10.1016/S0092-8674(00)80566-8.

[122] L.P. Morin, C.N. Allen, The circadian visual system, 2005, Brain Res. Rev. 51 (2006) 1–60. https://doi.org/10.1016/j.brainresrev.2005.08.003.

[123] R. Silver, W.J. Schwartz, The Suprachiasmatic Nucleus is a Functionally Heterogeneous Timekeeping Organ, in: Methods Enzym., 2005: pp. 451–465. https://doi.org/10.1016/S0076-6879(05)93022-X.

[124] F.I.J. Crawford, C.L. Hodgkinson, E.A. Ivanova, L.B. Logunova, G.J. Evans, S. Steinlechner, A.S.I. Loudon, Influence of torpor on cardiac expression of genes involved in the circadian clock and protein turnover in the Siberian hamster *(Phodopus sungorus),* Physiol. Genomics. 31 (2007) 521–530. https://doi.org/10.1152/physiolgenomics.00131.2007.

[125] A. Herwig, M. Saboureau, P. Pévet, S. Steinlechner, Daily torpor affects the molecular machinery of the circadian clock in Djungarian hamsters (*Phodopus sungorus),* Eur. J. Neurosci. 26 (2007) 2739–2746. https://doi.org/10.1111/j.1460-9568.2007.05927.x.

[126] N.F. Ruby, I. Zucker, Daily torpor in the absence of the suprachiasmatic nucleus in Siberian hamsters, Am. J. Physiol. - Regul. Integr. Comp. Physiol. 263 (1992) 353–362. https://doi.org/10.1152/ajpregu.1992.263.2.r353.

[127] N.F. Ruby, I. Zucker, Daily torpor in the absence of the suprachiasmatic nucleus in Siberian hamsters, Am. J. Physiol. 263 (1992) R353–R362. https://doi.org/10.1152/ajpregu.1992.263.2.R353.

[128] E. Haugg, J. Borner, V. Diedrich, A. Herwig, Comparative transcriptomics of the Djungarian hamster hypothalamus during short photoperiod acclimation and spontaneous torpor, FEBS Open Bio. 12 (2021) 443–459. https://doi.org/10.1002/2211-5463.13350.

[129] M.J. Paul, D.A. Freeman, H.P. Jin, J. Dark, Neuropeptide Y induces torpor-like hypothermia in Siberian hamsters, Brain Res. 1055 (2005) 83–92. https://doi.org/10.1016/j.brainres.2005.06.090.

[130] S. Andrews, FastQC: A Quality Control Tool for High Throughput Sequence Data, (2010). https://www.bioinformatics.babraham.ac.uk/projects/fastqc/.

[131] F. Krueger, TrimGalore, (2020). https://github.com/FelixKrueger/TrimGalore.

[132] M.G. Grabherr, B.J. Haas, M. Yassour, J.Z. Levin, D.A. Thompson, I. Amit, X. Adiconis, L. Fan, R. Raychowdhury, Q. Zeng, Z. Chen, E. Mauceli, N. Hacohen, A. Gnirke, N. Rhind, F. di Palma, B. W., N. Friedman, A. Regev, Trinity: reconstructing a full-length transcriptome without a genome from RNA-Seq data, Nat. Biotechnol. 29 (2013) 644–652. https://doi.org/10.1038/nbt.1883.Trinity.

[133] B.J. Haas, A. Papanicolaou, M. Yassour, M. Grabherr, P.D. Blood, J. Bowden, M.B. Couger, D. Eccles, B. Li, M. Lieber, M.D. Macmanes, M. Ott, J. Orvis, N. Pochet, F. Strozzi, N. Weeks, R. Westerman, T. William, C.N. Dewey, R. Henschel, R.D. Leduc, N. Friedman, A. Regev, *De novo* transcript sequence reconstruction from RNA-seq using the Trinity platform for reference generation and analysis, Nat. Protoc. 8 (2013) 1494–1512. https://doi.org/10.1038/nprot.2013.084.

[134] S.F. Altschul, W. Gish, W. Miller, E.W. Myers, D.J. Lipman, Basic local alignment search tool, J. Mol. Biol. 215 (1990) 403–410. https://doi.org/10.1016/S0022-2836(05)80360-2.

[135] National Center for Biotechnology Information Bethesda MD USA, Building a BLAST database with local sequences, (2008). https://www.ncbi.nlm.nih.gov/books/NBK279688/.

[136] B. Langmead, Aligning short sequencing reads with Bowtie. http://bowtie-bio.sourceforge.net/manual.shtml, Curr. Protoc. Bioinforma. (2010) 1–24. https://doi.org/10.1002/0471250953.bi1107s32.

[137] B. Li, C.N. Dewey, RSEM: Accurate transcript quantification from RNA-Seq data with or without a reference genome. http://deweylab.github.io/RSEM/, BMC Bioinformatics. 12 (2011) 1–16. https://doi.org/10.1186/1471-2105-12-323.

[138] R. Edgar, M. Domrachev, A.E. Lash, Gene Expression Omnibus: NCBI gene expression and hybridization array data repository, Nucleic Acids Res. 30 (2002) 207–210. https://doi.org/10.1093/nar/30.1.207.

[139] RStudio Team, RStudio: Integrated Development for R, (2020). http://www.rstudio.com/.

[140] R Core Team, R: A language and environment for statistical computing. R Foundation for Statistical Computing, Vienna, Austria. https://www.R-project.org/, (2018). https://www.r-project.org/.

[141] M.I. Love, S. Anders, W. Huber, Analyzing RNA-seq data with DESeq2, 2020. https://www.bioconductor.org/packages/devel/bioc/vignettes/DESeq2/inst/doc/DESeq2_pdf.pdf.

[142] M.I. Love, S. Anders, V. Kim, W. Huber, RNA-Seq workflow: gene-level exploratory analysis and differential expression, 2019. https://bioconductor.org/packages/release/workflows/vignettes/rnaseqGene/inst/doc/rnaseqGene.html#starting-from-summarizedexperiment.

[143] M.I. Love, W. Huber, S. Anders, Moderated estimation of fold change and dispersion for RNA-seq data with DESeq2, Genome Biol. 15 (2014) 1–21. https://doi.org/10.1186/s13059-014-0550-8.

[144] The Gene Ontology Consortium, M. Ashburner, C.A. Ball, J.A. Blake, D. Botstein, H. Butler, J.M. Cherry, A.P. Davis, K. Dolinski, S.S. Dwight, J.T. Eppig, M.A. Harris, D.P. Hill, L. Issel-Tarver, A. Kasarskis, S. Lewis, J.C. Matese, J.E. Richardson, M. Ringwald, Gene Ontology: tool for the unification of biology, NIH Public Access. 25 (2000) 25–29. https://doi.org/10.1038/75556.

[145] S. Carbon, E. Douglass, B.M. Good, D.R. Unni, N.L. Harris, C.J. Mungall, S. Basu, R.L. Chisholm, R.J. Dodson, E. Hartline, P. Fey, P.D. Thomas, L.P. Albou, D. Ebert, M.J. Kesling, H. Mi, A. Muruganujan, X. Huang, T. Mushayahama, S.A. LaBonte, D.A. Siegele, G. Antonazzo, H. Attrill, N.H. Brown, P. Garapati, S.J. Marygold, V. Trovisco, G. dos Santos, K. Falls, C. Tabone, P. Zhou, J.L. Goodman, V.B. Strelets, J. Thurmond, P. Garmiri, R. Ishtiaq, M. Rodríguez-López, M.L. Acencio, M. Kuiper, A. Lægreid, C. Logie, R.C. Lovering, B. Kramarz, S.C.C. Saverimuttu, S.M. Pinheiro, H. Gunn, R. Su, K.E. Thurlow, M. Chibucos, M. Giglio, S. Nadendla, J. Munro, R.

Jackson, M.J. Duesbury, N. Del-Toro, B.H.M. Meldal, K. Paneerselvam, L. Perfetto, P. Porras, S. Orchard, A. Shrivastava, H.Y. Chang, R.D. Finn, A.L. Mitchell, N.D. Rawlings, L. Richardson, A. Sangrador-Vegas, J.A. Blake, K.R. Christie, M.E. Dolan, H.J. Drabkin, D.P. Hill, L. Ni, D.M. Sitnikov, M.A. Harris, S.G. Oliver, K. Rutherford, V. Wood, J. Hayles, J. Bähler, E.R. Bolton, J.L. de Pons, M.R. Dwinell, G.T. Hayman, M.L. Kaldunski, A.E. Kwitek, S.J.F. Laulederkind, C. Plasterer, M.A. Tutaj, M. Vedi, S.J. Wang, P. D'Eustachio, L. Matthews, J.P. Balhoff, S.A. Aleksander, M.J. Alexander, J.M. Cherry, S.R. Engel, F. Gondwe, K. Karra, S.R. Miyasato, R.S. Nash, M. Simison, M.S. Skrzypek, S. Weng, E.D. Wong, M. Feuermann, P. Gaudet, A. Morgat, E. Bakker, T.Z. Berardini, L. Reiser, S. Subramaniam, E. Huala, C.N. Arighi, A. Auchincloss, K. Axelsen, G. Argoud-Puy, A. Bateman, M.C. Blatter, E. Boutet, E. Bowler, L. Breuza, A. Bridge, R. Britto, H. Bye-A-Jee, C.C. Casas, E. Coudert, P. Denny, A. Es-Treicher, M.L. Famiglietti, G. Georghiou, A.N. Gos, N. Gruaz-Gumowski, E. Hatton-Ellis, C. Hulo, A. Ignatchenko, F. Jungo, K. Laiho, P. Le Mercier, D. Lieberherr, A. Lock, Y. Lussi, A. MacDougall, M. Ma-Grane, M.J. Martin, P. Masson, D.A. Natale, N. Hyka-Nouspikel, S. Orchard, I. Pedruzzi, L. Pourcel, S. Poux, S. Pundir, C. Rivoire, E. Speretta, S. Sundaram, N. Tyagi, K. Warner, R. Zaru, C.H. Wu, A.D. Diehl, J.N. Chan, C. Grove, R.Y.N. Lee, H.M. Muller, D. Raciti, K. van Auken, P.W. Sternberg, M. Berriman, M. Paulini, K. Howe, S. Gao, A. Wright, L. Stein, D.G. Howe, S. Toro, M. Westerfield, P. Jaiswal, L. Cooper, J. Elser, The Gene Ontology resource: Enriching a GOld mine, Nucleic Acids Res. 49 (2021) D325–D334. https://doi.org/10.1093/nar/gkaa1113.

[146] H. Mi, A. Muruganujan, D. Ebert, X. Huang, P.D. Thomas, PANTHER version 14: More genomes, a new PANTHER GO-slim and improvements in enrichment analysis tools, Nucleic Acids Res. 47 (2019) D419–D426. https://doi.org/10.1093/nar/gky1038.

[147] P. Angel, M. Karin, The role of Jun, Fos and the AP-1 complex in cell-proliferation and transformation, BBA - Rev. Cancer. 1072 (1991) 129–157. https://doi.org/10.1016/0304-419X(91)90011-9.

[148] B. Rusak, L. McNaughton, H.A. Robertson, S.P. Hunt, Circadian variation in photic regulation of immediate-early gene mRNAs in rat suprachiasmatic nucleus cells, Mol. Brain Res. 14 (1992) 124–130. https://doi.org/10.1016/0169-328X(92)90019-8.

[149] B.F. O'Hara, F.L. Watson, H.K. Srere, H. Kumar, S.W. Wiler, S.K. Welch, L. Bitting, H.C. Heller, T.S. Kilduff, Gene expression in the brain across the hibernation cycle, J. Neurosci. 19 (1999) 3781–3790. https://doi.org/10.1016/S0006-8993(00)03008-0.

[150] F.J.P. Ebling, E.S. Maywood, M. Mehta, D.C. Hancock, S. McNulty, J. De Bono, S.J. Bray, M.H. Hastings, FosB in the Suprachiasmatic Nucleus of the Syrian and Siberian Hamster, Brain Res. Bull. 41 (1996) 257–268. https://doi.org/10.1016/S0361-9230(96)00192-X.

[151] J.D. Johnston, F.J.P. Ebling, D.G. Hazlerigg, Photoperiod regulates multiple gene expression in the suprachiasmatic nuclei and pars tuberalis of the Siberian hamster *(Phodopus sungorus),* Eur. J. Neurosci. 21 (2005) 2967–2974. https://doi.org/10.1111/j.1460-9568.2005.04148.x.

[152] M.J. Duncan, X. Cheng, K.S. Heller, Photoperiodic exposure and time of day

modulate the expression of arginine vasopressin mRNA and vasoactive intestinal peptide mRNA in the suprachiasmatic nuclei of Siberian hamsters, Mol. Brain Res. 32 (1995) 181–186. https://doi.org/10.1016/0169-328X(95)00072-Z.

[153] A. Herwig, F.G. Revel, M. Saboureau, P. Pévet, S. Steinlechner, Daily torpor alters multiple gene expression in the suprachiasmatic nucleus and pineal gland of the Djungarian hamster *(Phodopus sungorus),* Chronobiol. Int. 23 (2006) 269–276. https://doi.org/10.1080/07420520500522424.

[154] M.J. Duncan, Photoperiodic regulation of hypothalamic neuropeptide messenger RNA expression: Effect of pinealectomy and neuroanatomical location, Mol. Brain Res. 57 (1998) 142–148. https://doi.org/10.1016/S0169-328X(98)00084-9.

[155] R.A. Hut, E.A. Van der Zee, K. Jansen, M.P. Gerkema, S. Daan, Gradual reappearance of post-hibernation circadian rhythmicity correlates with numbers of vasopressin-containing neurons in the suprachiasmatic nuclei of European ground squirrels, J. Comp. Physiol. B Biochem. Syst. Environ. Physiol. 172 (2002) 59–70. https://doi.org/10.1007/s003600100227.

[156] C. Gizowski, C. Zaelzer, C.W. Bourque, Clock-driven vasopressin neurotransmission mediates anticipatory thirst prior to sleep, Nature. 537 (2016) 685–688. https://doi.org/10.1038/nature19756.

[157] D.Q. Li, S.B. Pakala, S.D.N. Reddy, S. Peng, S. Balasenthil, C.X. Deng, C.C. Lee, M.A. Rea, R. Kumar, Metastasis-associated protein 1 is an integral component of the circadian molecular machinery, Nat. Commun. 4 (2013) 1–13. https://doi.org/10.1038/ncomms3545.

[158] N. Sen, B. Gui, R. Kumar, Role of MTA1 in cancer progression and metastasis, Cancer Metastasis Rev. 33 (2014) 879–889. https://doi.org/10.1007/s10555-014-9515-3.

[159] R. Kumar, R.A. Wang, Structure, expression and functions of MTA genes, Gene. 582 (2016) 112–121. https://doi.org/10.1016/j.gene.2016.02.012.

[160] D.Q. Li, S.B. Pakala, S.S. Nair, J. Eswaran, R. Kumar, Metastasis-associated protein 1/nucleosome remodeling and histone deacetylase complex in cancer, Cancer Res. 72 (2012) 387–394. https://doi.org/10.1158/0008-5472.CAN-11-2345.

[161] A.M. Sangoram, L. Saez, M.P. Antoch, N. Gekakis, D. Staknis, A. Whiteley, E.M. Fruechte, M.H. Vitaterna, K. Shimomura, D.P. King, M.W. Young, C.J. Weitz, J.S. Takahashi, Mammalian circadian autoregulatory loop: A timeless ortholog and mPer1 interact and negatively regulate CLOCK-BMAL1-induced transcription, Neuron. 21 (1998) 1101–1113. https://doi.org/10.1016/S0896-6273(00)80627-3.

[162] E. Engelen, R.C. Janssens, K. Yagita, V.A.J. Smits, G.T.J. van der Horst, F. Tamanini, Mammalian TIMELESS Is Involved in Period Determination and DNA Damage-Dependent Phase Advancing of the Circadian Clock, PLoS One. 8 (2013). https://doi.org/10.1371/journal.pone.0056623.

[163] A.L. Gotter, T. Manganaro, D.R. Weaver, L.F. Kolakowski, B. Possidente, S. Sriram, D.T. MacLaughlin, S.M. Reppert, A time-less function for mouse Timeless, Nat. Neurosci. 3 (2000) 755–756. https://doi.org/10.1038/77653.

[164] J. Yan, B.M. Barnes, F. Kohl, T.G. Marr, Modulation of gene expression in

hibernating arctic ground squirrels, Physiol. Genomics. 32 (2008) 170–181. https://doi.org/10.1152/physiolgenomics.00075.2007.

[165] N. Sen, B. Gui, R. Kumar, Physiological functions of MTA family of proteins, Cancer Metastasis Rev. 33 (2014) 869–877. https://doi.org/10.1007/s10555-014-9514-4.

[166] W.E. Visser, E.C.H. Friesema, T.J. Visser, Minireview: Thyroid hormone transporters: The knowns and the unknowns, Mol. Endocrinol. 25 (2011) 1–14. https://doi.org/10.1210/me.2010-0095.

[167] A. Herwig, D. Wilson, T.J. Logie, A. Boelen, P.J. Morgan, J.G. Mercer, P. Barrett, Photoperiod and acute energy deficits interact on components of the thyroid hormone system in hypothalamic tanycytes of the Siberian hamster, Am. J. Physiol. Regul. Integr. Comp. Physiol. 296 (2009) R1307–R1315. https://doi.org/10.1152/ajpregu.90755.2008.

[168] A. Herwig, E.M. de Vries, M. Bolborea, D. Wilson, J.G. Mercer, F.J.P. Ebling, P.J. Morgan, P. Barrett, Hypothalamic ventricular ependymal thyroid hormone deiodinases are an important element of circannual timing in the Siberian hamster *(Phodopus sungorus),* PLoS One. 8 (2013) e62003. https://doi.org/10.1371/journal.pone.0062003.

[169] I. Petri, V. Diedrich, D. Wilson, J. Fernandez-Calleja, A. Herwig, S. Steinlechner, P. Barrett, Orchestration of gene expression across the seasons: Hypothalamic gene expression in natural photoperiod throughout the year in the Siberian hamster, Sci. Rep. 6 (2016) 1–9. https://doi.org/10.1038/srep29689.

[170] K. Inoue, S. Koizumi, M. Tsuda, Y. Shigemoto-Mogami, Signaling of ATP receptors in glia-neuron interaction and pain, Life Sci. 74 (2003) 189–197. https://doi.org/10.1016/j.lfs.2003.09.006.

[171] C. Matute, F. Cavaliere, Neuroglial interactions mediated by purinergic signalling in the pathophysiology of CNS disorders, Semin. Cell Dev. Biol. 22 (2011) 252–259. https://doi.org/10.1016/j.semcdb.2011.02.011.

[172] I. von Kügelgen, Pharmacological profiles of cloned mammalian P2Y-receptor subtypes, Pharmacol. Ther. 110 (2006) 415–432. https://doi.org/10.1016/j.pharmthera.2005.08.014.

[173] H. Kittner, H. Franke, J.I. Harsch, I.M. El-Ashmawy, B. Seidel, U. Krügel, P. Illes, Enhanced food intake after stimulation of hypothalamic P2Y1 receptors in rats: Modulation of feeding behaviour by extracellular nucleotides, Eur. J. Neurosci. 24 (2006) 2049–2056. https://doi.org/10.1111/j.1460-9568.2006.05071.x.

[174] Y. Shinozaki, S. Koizumi, S. Ishida, J.I. Sawada, Y. Ohno, K. Inoue, Cytoprotection against oxidative stress-induced damage of astrocytes by extracellular ATP via P2Y1 receptors, Glia. 49 (2005) 288–300. https://doi.org/10.1002/glia.20118.

[175] C. Frayling, R. Britton, N. Dale, ATP-mediated glucosensing by hypothalamic tanycytes, J. Physiol. 589 (2011) 2275–2286. https://doi.org/10.1113/jphysiol.2010.202051.

[176] J.A. Orellana, P.J. Saez, C. Cortes-Campos, R.J. Elizondo, K.F. Shoji, S. Contreras-Duarte, V. Figueroa, V. Velarde, J.X. Jiang, F. Nualart, J.C. Saez, M.A. Garcia, Glucose increases intracellular free Ca 2+ in tanycytes via ATP released through connexin 43

hemichannels, Glia. 60 (2012) 53–68. https://doi.org/10.1002/glia.21246.

[177] M. Bolborea, N. Dale, Hypothalamic tanycytes: Potential roles in the control of feeding and energy balance, Trends Neurosci. 36 (2013) 91–100. https://doi.org/10.1016/j.tins.2012.12.008.

[178] M. Bolborea, F. Langlet, What is the physiological role of hypothalamic tanycytes in metabolism?, Am. J. Physiol. Integr. Comp. Physiol. (2021). https://doi.org/10.1152/ajpregu.00296.2020.

[179] T. Goodman, M.K. Hajihosseini, Hypothalamic tanycytes-masters and servants of metabolic, neuroendocrine, and neurogenic functions, Front. Neurosci. 9 (2015) 1–9. https://doi.org/10.3389/fnins.2015.00387.

[180] F.J.P. Ebling, J.E. Lewis, Tanycytes and hypothalamic control of energy metabolism, Glia. 66 (2018) 1176–1184. https://doi.org/10.1002/glia.23303.

[181] N. Lou, T. Takano, Y. Pei, A.L. Xavier, S.A. Goldman, M. Nedergaard, Purinergic receptor P2RY12-dependent microglial closure of the injured blood-brain barrier, Proc. Natl. Acad. Sci. U. S. A. 113 (2016) 1074–1079. https://doi.org/10.1073/pnas.1520398113.

[182] W. Tonnus, A. Belavgeni, F. Beuschlein, G. Eisenhofer, M. Fassnacht, M. Kroiss, N.P. Krone, M. Reincke, S.R. Bornstein, A. Linkermann, The role of regulated necrosis in endocrine diseases, Nat. Rev. Endocrinol. 17 (2021) 497–510. https://doi.org/10.1038/s41574-021-00499-w.

[183] D. Lindholm, B.C. Bornhauser, L. Korhonen, Mylip makes an Idol turn into regulation of LDL receptor, Cell. Mol. Life Sci. 66 (2009) 3399–3402. https://doi.org/10.1007/s00018-009-0127-y.

[184] N.M. Van Loon, D. Lindholm, N. Zelcer, The E3 ubiquitin ligase inducible degrader of the LDL receptor/myosin light chain interacting protein in health and disease, Curr. Opin. Lipidol. 30 (2019) 192–197. https://doi.org/10.1097/MOL.0000000000000593.

[185] P.A. Olsson, L. Korhonen, E.A. Mercer, D. Lindholm, MIR is a novel ERM-like protein that interacts with myosin regulatory light chain and inhibits neurite outgrowth, J. Biol. Chem. 274 (1999) 36288–36392. https://doi.org/10.1074/jbc.274.51.36288.

[186] O. Stehling, C. Wilbrecht, R. Lill, Mitochondrial iron-sulfur protein biogenesis and human disease, Biochimie. 100 (2014) 61–77. https://doi.org/10.1016/j.biochi.2014.01.010.

[187] S. Guerrero-Castillo, F. Baertling, D. Kownatzki, H.J. Wessels, S. Arnold, U. Brandt, L. Nijtmans, The Assembly Pathway of Mitochondrial Respiratory Chain Complex I, Cell Metab. 25 (2017) 128–139. https://doi.org/10.1016/j.cmet.2016.09.002.

[188] Y. De Chu, W.R. Lin, Y.H. Lin, W.H. Kuo, C.J. Tseng, S.N. Lim, Y.L. Huang, S.C. Huang, T.J. Wu, K.H. Lin, C.T. Yeh, Cox5b-mediated bioenergetic alteration regulates tumor growth and migration by modulating ampk-uhmk1-erk cascade in hepatoma, Cancers (Basel). 12 (2020) 1–23. https://doi.org/10.3390/cancers12061646.

[189] M. Tominaga, H. Kurihara, S. Honda, G. Amakawa, T. Sakai, Y. Tomooka, Molecular characterization of mitocalcin, a novel mitochondrial Ca 2+-binding protein with EF-

hand and coiled-coil domains, J. Neurochem. 96 (2006) 292–304. https://doi.org/10.1111/j.1471-4159.2005.03554.x.

[190] T. Hou, C. Jian, J. Xu, A.Y. Huang, J. Xi, K. Hu, L. Wei, H. Cheng, X. Wang, Identification of EFHD1 as a novel Ca2+ sensor for mitoflash activation, Cell Calcium. 59 (2016) 262–270. https://doi.org/10.1016/j.ceca.2016.03.002.

[191] G. Feng, B. Liu, J. Li, T. Cheng, Z. Huang, X. Wang, H.P. Cheng, Mitoflash biogenesis and its role in the autoregulation of mitochondrial proton electrochemical potential, J. Gen. Physiol. 151 (2019) 727–737. https://doi.org/10.1085/jgp.201812176.

[192] C.A. Ghiani, M. Starcevic, I.A. Rodriguez-Fernandez, R. Nazarian, V.T. Cheli, L.N. Chan, J.S. Malvar, J. De Vellis, C. Sabatti, E.C. Dell'Angelica, The dysbindin-containing complex (BLOC-1) in brain: Developmental regulation, interaction with SNARE proteins and role in neurite outgrowth, Mol. Psychiatry. 15 (2010) 204–215. https://doi.org/10.1038/mp.2009.58.

[193] Z. Abraham, E. Hawley, D. Hayosh, V.A. Webster-Wood, O. Akkus, Kinesin and Dynein Mechanics: Measurement Methods and Research Applications, J. Biomech. Eng. 140 (2018) 1–11. https://doi.org/10.1115/1.4037886.

[194] R.G. Boutilier, Mechanisms of cell survival in hypoxia and hypothermia, J. Exp. Biol. 204 (2001) 3171–3181. https://doi.org/10.1242/jeb.204.18.3171.

[195] M. Kutschke, K. Grimpo, A. Kastl, S. Schneider, G. Heldmaier, C. Exner, M. Jastroch, Depression of mitochondrial respiration during daily torpor of the Djungarian hamster, *Phodopus sungorus,* is specific for liver and correlates with body temperature, Comp. Biochem. Physiol. - A Mol. Integr. Physiol. 164 (2013) 584–589. https://doi.org/10.1016/j.cbpa.2013.01.008.

[196] A.S. Kauffman, D.K. Clifton, R.A. Steiner, Emerging ideas about kisspeptin- GPR54 signaling in the neuroendocrine regulation of reproduction, Trends Neurosci. 30 (2007) 504–511. https://doi.org/10.1016/j.tins.2007.08.001.

[197] F.G. Revel, M. Saboureau, M. Masson-Pévet, P. Pévet, J.D. Mikkelsen, V. Simonneaux, KiSS-1: A likely candidate for the photoperiodic control of reproduction in seasonal breeders, Chronobiol. Int. 23 (2006) 277–287. https://doi.org/10.1080/07420520500521939.

[198] K. Rasri-Klosen, V. Simonneaux, P. Klosen, Differential response patterns of kisspeptin and RFamide-related peptide to photoperiod and sex steroid feedback in the Djungarian hamster *(Phodopus sungorus),* J. Neuroendocrinol. 29 (2017) e12529. https://doi.org/10.1111/jne.12529.

[199] T.J. Greives, K.L. Long, C.M. Bergeon Burns, G.E. Demas, Response to exogenous kisspeptin varies according to sex and reproductive condition in Siberian hamsters *(Phodopus sungorus),* Gen. Comp. Endocrinol. 170 (2011) 172–179. https://doi.org/10.1016/j.ygcen.2010.10.001.

[200] S.L. Padilla, J.G. Perez, M. Ben-hamo, C.W. Johnson, R. Sanchez, I. Bussi, R.D. Palmiter, H.O. De La Iglesia, Kisspeptin Neurons in the Arcuate Nucleus of the Hypothalamus Orchestrate Circadian Rhythms and Metabolism, Curr Biol. 29 (2019) 592–604. https://doi.org/10.1016/j.cub.2019.01.022.Kisspeptin.

[201] T.J. Greives, A.O. Mason, M.A.L. Scotti, J. Levine, E.D. Ketterson, L.J. Kriegsfeld, G.E. Demas, Environmental control of kisspeptin: Implications for seasonal reproduction, Endocrinology. 148 (2007) 1158–1166. https://doi.org/10.1210/en.2006-1249.

[202] T. Wisniewski, E. Drummond, APOE-amyloid interaction: Therapeutic targets, Neurobiol. Dis. 138 (2020). https://doi.org/10.1016/j.nbd.2020.104784.

[203] J. Xiang, W. Zhu, F. Yang, Z.H. Yu, M. Cai, X.T. Li, J.S. Zhang, W. Zhang, D.F. Cai, Melatonin-induced ApoE expression in mouse astrocytes protects endothelial cells from OGD-R induced injuries, Transl. Psychiatry. 10 (2020). https://doi.org/10.1038/s41398-020-00864-9.

[204] H.E. Raybould, Mechanisms of CCK signaling from gut to brain, Curr. Opin. Pharmacol. 7 (2007) 570–574. https://doi.org/10.1016/j.coph.2007.09.006.

[205] M.W. Schwartz, S.C. Woods, D. Porte, R.J. Seeley, D.G. Baskin, Central nervous system control of food intake, Nature. 404 (2000) 661–671. https://doi.org/10.1038/35007534.

[206] M. Helwig, Z.A. Archer, G. Heldmaier, A. Tups, J.G. Mercer, M. Klingenspor, Photoperiodic regulation of satiety mediating neuropeptides in the brainstem of the seasonal Siberian hamster *(Phodopus sungorus),* J. Comp. Physiol. A Neuroethol. Sensory, Neural, Behav. Physiol. 195 (2009) 631–642. https://doi.org/10.1007/s00359-009-0438-3.

[207] S. Reuss, Photoperiod effects on bombesin- and cholecystokinin-like immunoreactivity in the suprachiasmatic nuclei of the Djungarian hamster *(Phodopus sungorus),* Neurosci. Lett. 128 (1991) 13–16. https://doi.org/10.1016/0304-3940(91)90749-J.

[208] T.J. Bartness, J.E. Morley, A.S. Levine, Photoperiod-peptide interactions in the energy intake of Siberian hamsters, Peptides. 7 (1986) 1079–1085. https://doi.org/10.1016/0196-9781(86)90137-3.

[209] R.R. Schick, G.J. Harty, T.L. Yaksh, V.L.W. Go, Sites in the brain at which cholecystokinin octapeptide (CCK-8) acts to suppress feeding in rats: A mapping study, Neuropharmacology. 29 (1990) 109–118. https://doi.org/10.1016/0028-3908(90)90050-2.

[210] C.A. Puddifoot, M. Wu, R.J. Sung, W.J. Joiner, Ly6h regulates trafficking of alpha7 nicotinic acetylcholine receptors and nicotine-induced potentiation of glutamatergic signaling, J. Neurosci. 35 (2015) 3420–3430. https://doi.org/10.1523/JNEUROSCI.3630-14.2015.

[211] L.M. Bilezikjian, A.L. Blount, A.M.O. Leal, C.J. Donaldson, W.H. Fischer, W.W. Vale, Autocrine/paracrine regulation of pituitary function by activin, inhibin and follistatin, Mol. Cell. Endocrinol. 225 (2004) 29–36. https://doi.org/10.1016/j.mce.2004.02.010.

[212] C.N. Withers, D.M. Brown, I. Byiringiro, M.R. Allen, K.W. Condon, J. Satin, D.A. Andres, Rad GTPase is essential for the regulation of bone density and bone marrow adipose tissue in mice, Bone. 103 (2017) 270–280. https://doi.org/10.1016/j.bone.2017.07.018.

[213] H. Yada, M. Murata, K. Shimoda, S. Yuasa, H. Kawaguchi, M. Ieda, T. Adachi, M. Murata, S. Ogawa, K. Fukuda, Dominant negative suppression of Rad leads to QT prolongation and causes ventricular arrhythmias via modulation of L-type Ca2+ channels in the heart, Circ. Res. 101 (2007) 69–77. https://doi.org/10.1161/CIRCRESAHA.106.146399.

[214] B.A. Simms, G.W. Zamponi, Neuronal voltage-gated calcium channels: Structure, function, and dysfunction, Neuron. 82 (2014) 24–45. https://doi.org/10.1016/j.neuron.2014.03.016.

[215] O. Lykhmus, N. Mishra, L. Koval, O. Kalashnyk, G. Gergalova, K. Uspenska, S. Komisarenko, H. Soreq, M. Skok, Molecular mechanisms regulating LPS-induced inflammation in the brain, Front. Mol. Neurosci. 9 (2016) 1–13. https://doi.org/10.3389/fnmol.2016.00019.

[216] S. Lehnardt, L. Massillon, P. Follett, F.E. Jensen, R. Ratan, P.A. Rosenberg, J.J. Volpe, T. Vartanian, Activation of innate immunity in the CNS triggers neurodegeneration through a Toll-like receptor 4-dependent pathway, Proc. Natl. Acad. Sci. U. S. A. 100 (2003) 8514–8519. https://doi.org/10.1073/pnas.1432609100.

[217] E. V. Quadros, J.M. Sequeira, Cellular uptake of cobalamin: Transcobalamin and the TCblR/CD320 receptor, Biochimie. 95 (2013) 1008–1018. https://doi.org/10.1016/j.biochi.2013.02.004.

[218] N. Zhang, X. Yu, J. Xie, H. Xu, New Insights into the Role of Ferritin in Iron Homeostasis and Neurodegenerative Diseases, Mol. Neurobiol. 58 (2021) 2812–2823. https://doi.org/10.1007/s12035-020-02277-7.

[219] V.T. Cheli, D.A. Santiago González, Q. Wan, G. Denaroso, R. Wan, S.L. Rosenblum, P.M. Paez, H-ferritin expression in astrocytes is necessary for proper oligodendrocyte development and myelination, Glia. (2021) 1–18. https://doi.org/10.1002/glia.24083.

[220] X. Jiang, B.R. Stockwell, M. Conrad, Ferroptosis: mechanisms, biology and role in disease, Nat. Rev. Mol. Cell Biol. 22 (2021) 266–282. https://doi.org/10.1038/s41580-020-00324-8.

[221] L. Li, S.H. Yun, J. Keblesh, B.L. Trommer, H. Xiong, J. Radulovic, W.G. Tourtellotte, Egr3, a synaptic activity regulated transcription factor that is essential for learning and memory, Mol. Cell. Neurosci. 35 (2007) 76–88. https://doi.org/10.1016/j.mcn.2007.02.004.

[222] J.H. Kim, D.S. Roberts, Y. Hu, G.C. Lau, A.R. Brooks-Kayal, D.H. Farb, S.J. Russek, Brain-derived neurotrophic factor uses CREB and Egr3 to regulate NMDA receptor levels in cortical neurons, J. Neurochem. 120 (2012) 210–219. https://doi.org/10.1111/j.1471-4159.2011.07555.x.

[223] M.E. Morris, N. Viswanathan, S. Kuhlman, F.C. Davis, C.J. Weitz, A screen for genes induced in the suprachiasmatic nucleus by light, Science (80-.). 279 (1998) 1544–1547. https://doi.org/10.1126/science.279.5356.1544.

[224] V.M. Porterfield, H. Piontkivska, E.M. Mintz, Identification of novel light-induced genes in the suprachiasmatic nucleus, BMC Neurosci. 8 (2007) 1–10. https://doi.org/10.1186/1471-2202-8-98.

[225] S.K. Kuncha, M. Mazeed, R. Singh, B. Kattula, S.B. Routh, R. Sankaranarayanan, A chiral selectivity relaxed paralog of DTD for proofreading tRNA mischarging in Animalia, Nat. Commun. 9 (2018) 1–13. https://doi.org/10.1038/s41467-017-02204-w.

[226] S. Edvardson, L. Prunetti, A. Arraf, D. Haas, J.M. Bacusmo, J.F. Hu, A. Ta-Shma, P.C. Dedon, V. De Crécy-Lagard, O. Elpeleg, tRNA N6-adenosine threonylcarbamoyltransferase defect due to KAE1/TCS3 (OSGEP) mutation manifest by neurodegeneration and renal tubulopathy, Eur. J. Hum. Genet. 25 (2017) 545–551. https://doi.org/10.1038/ejhg.2017.30.

[227] H. Sievert, N. Pällmann, K.K. Miller, I. Hermans-Borgmeyer, S. Venz, A. Sendoel, M. Preukschas, M. Schweizer, S. Boettcher, P.C. Janiesch, T. Streichert, R. Walther, M.O. Hengartner, M.G. Manz, T.H. Brümmendorf, C. Bokemeyer, M. Braig, J. Hauber, K.E. Duncan, S. Balabanov, A novel mouse model for inhibition of DOHH-mediated hypusine modification reveals a crucial function in embryonic development, proliferation and oncogenic transformation, DMM Dis. Model. Mech. 7 (2014) 963–976. https://doi.org/10.1242/dmm.014449.

[228] K. Uchimura, F. Fasakhany, K. Kadomatsu, T. Matsukawa, T. Yamakawa, N. Kurosawa, T. Muramatsu, Diversity of N-acetylglucosamine-6-O-sulfotransferases: Molecular cloning of a novel enzyme with different distribution and specificities, Biochem. Biophys. Res. Commun. 274 (2000) 291–296. https://doi.org/10.1006/bbrc.2000.3141.

[229] Narentuya, Y. Takeda-Uchimura, T. Foyez, Z. Zhang, T.O. Akama, H. Yagi, K. Kato, Y. Komatsu, K. Kadomatsu, K. Uchimura, GlcNAc6ST3 is a keratan sulfate sulfotransferase for the protein-tyrosine phosphatase PTPRZ in the adult brain, Sci. Rep. 9 (2019) 1–11. https://doi.org/10.1038/s41598-019-40901-2.

[230] K.C. Grasty, S.D. Weeks, P.J. Loll, Structural insights into the activity and regulation of human Josephin-2, J. Struct. Biol. X. 3 (2019) 100011. https://doi.org/10.1016/j.yjsbx.2019.100011.

[231] V. de Cesare, D.C. Lopez, P.D. Mabbitt, A.J. Fletcher, M. Soetens, O. Antico, N.T. Wood, S. Virdee, Deubiquitinating enzyme amino acid profiling reveals a class of ubiquitin esterases, Proc. Natl. Acad. Sci. U. S. A. 118 (2021) 1–12. https://doi.org/10.1073/pnas.2006947118.

[232] P.C. Chen, L.N. Qin, X.M. Li, B.J. Walters, J.A. Wilson, L. Mei, S.M. Wilson, The proteasome-associated deubiquitinating enzyme Usp14 is essential for the maintenance of synaptic ubiquitin levels and the development of neuromuscular junctions, J. Neurosci. 29 (2009) 10909–10919. https://doi.org/10.1523/JNEUROSCI.2635-09.2009.

[233] S.C. Biswas, Y. Zhang, G. Iyirhiaro, R.T. Willett, Y.R. Gonzalez, S.P. Cregan, R.S. Slack, D.S. Park, L.A. Greene, Sertad1 plays an essential role in developmental and pathological neuron death, J. Neurosci. 30 (2010) 3973–3982. https://doi.org/10.1523/JNEUROSCI.6421-09.2010.

[234] R.K. Mongre, S. Jung, C.B. Mishra, B.S. Lee, S. Kumari, M.S. Lee, Prognostic and clinicopathological significance of sertad1 in various types of cancer risk: A systematic review and retrospective analysis, Cancers (Basel). 11 (2019) 1–23.

https://doi.org/10.3390/cancers11030337.

[235] E.A. Vuono, E. Ramirez-Medina, P. Azzinaro, K.A. Berggren, A. Rai, S. Pruitt, E. Silva, L. Velazquez-Salinas, M. V Borca, D.P. Gladue, SERTA Domain Containing Protein 1 (SERTAD1) Interacts with Classical Swine Fever Virus Structural Glycoprotein E2, Which Is Involved in Virus Virulence in Swine, Viruses. 12 (2020) 421. https://doi.org/10.3390/v12040421.

[236] W. Hu, X. Yu, Z. Liu, Y. Sun, X. Chen, X. Yang, X. Li, W.K. Lam, Y. Duan, X. Cao, H. Steller, K. Liu, P. Huang, The complex of TRIP-Br1 and XIAP ubiquitinates and degrades multiple adenylyl cyclase isoforms, Elife. 6 (2017) 1–25. https://doi.org/10.7554/eLife.28021.

[237] C. Li, S. Jung, Y. Yang, K. Il Kim, J.S. Lim, C. Il Cheon, M.S. Lee, Inhibitory role of TRIP-Br1 oncoprotein in hypoxia-induced apoptosis in breast cancer cell lines, Int. J. Oncol. 48 (2016) 2639–2646. https://doi.org/10.3892/ijo.2016.3454.

[238] K. Jin, J. Chen, K. Kawaguchi, R.L. Zhu, R.A. Stetler, R.P. Simon, S.H. Graham, Focal ischemia induces expression of the DNA damage-inducible gene GADD45 in the rat brain, Neuroreport. 7 (1996) 1797–1802. https://doi.org/10.1097/00001756-199607290-00022.

[239] M. Vairapandi, N. Azam, A.G. Balliet, B. Hoffman, D.A. Liebermann, Characterization of MyD118, Gadd45, and proliferating cell nuclear antigen (PCNA) interacting domains. PCNA impedes MyD118 and Gadd45-mediated negative growth control, J. Biol. Chem. 275 (2000) 16810–16819. https://doi.org/10.1074/jbc.275.22.16810.

[240] C.Y. Logan, R. Nusse, The Wnt signaling pathway in development and disease, Annu. Rev. Cell Dev. Biol. 20 (2004) 781–810. https://doi.org/10.1146/annurev.cellbio.20.010403.113126.

[241] B.K. Koo, M. Spit, I. Jordens, T.Y. Low, D.E. Stange, M. Van De Wetering, J.H. Van Es, S. Mohammed, A.J.R. Heck, M.M. Maurice, H. Clevers, Tumour suppressor RNF43 is a stem-cell E3 ligase that induces endocytosis of Wnt receptors, Nature. 488 (2012) 665–669. https://doi.org/10.1038/nature11308.

[242] R. Noelanders, K. Vleminckx, How Wnt Signaling Builds the Brain: Bridging Development and Disease, Neuroscientist. 23 (2017) 314–329. https://doi.org/10.1177/1073858416667270.

[243] R.N. Duncan, Y. Xie, A.D. McPherson, A. V. Taibi, J.L. Bonkowsky, A.D. Douglass, R.I. Dorsky, Hypothalamic radial glia function as self-renewing neural progenitors in the absence of Wnt/β-catenin signaling, Co. Biol. 143 (2016) 45–53. https://doi.org/10.1242/dev.126813.

[244] J. Li, J. Pang, Y. Liu, J. Zhang, C. Zhang, G. Shen, L. Song, Suppression of RRM2 inhibits cell proliferation, causes cell cycle arrest and promotes the apoptosis of human neuroblastoma cells and in human neuroblastoma RRM2 is suppressed following chemotherapy, Oncol. Rep. 40 (2018) 355–360. https://doi.org/10.3892/or.2018.6420.

[245] X. Liu, J. Peng, Y. Zhou, B. Xie, J. Wang, Silencing RRM2 inhibits multiple myeloma by targeting the Wnt/β-catenin signaling pathway, Mol. Med. Rep. 20 (2019) 2159–

2166. https://doi.org/10.3892/mmr.2019.10465.

[246] M. Sasaki, K. Kawahara, M. Nishio, K. Mimori, R. Kogo, K. Hamada, B. Itoh, J. Wang, Y. Komatsu, Y.R. Yang, H. Hikasa, Y. Horie, T. Yamashita, T. Kamijo, Y. Zhang, Y. Zhu, C. Prives, T. Nakano, T.W. Mak, T. Sasaki, T. Maehama, M. Mori, A. Suzuki, Regulation of the MDM2-P53 pathway and tumor growth by PICT1 via nucleolar RPL11, Nat. Med. 17 (2011) 944–951. https://doi.org/10.1038/nm.2392.

[247] A. V. Snezhkina, E.N. Lukyanova, D. V. Kalinin, A. V. Pokrovsky, A.A. Dmitriev, N. V. Koroban, E.A. Pudova, M.S. Fedorova, N.N. Volchenko, O.A. Stepanov, E.A. Zhevelyuk, S.L. Kharitonov, A. V. Lipatova, I.S. Abramov, A. V. Golovyuk, Y.E. Yegorov, K.S. Vishnyakova, A.A. Moskalev, G.S. Krasnov, N. V. Melnikova, D.S. Shcherbo, M. V. Kiseleva, A.D. Kaprin, B.Y. Alekseev, A.R. Zaretsky, A. V. Kudryavtseva, Exome analysis of carotid body tumor, BMC Med. Genomics. 11 (2018). https://doi.org/10.1186/s12920-018-0327-0.

[248] W.C. Griffin, M.A. Trakselis, The MCM8/9 complex: A recent recruit to the roster of helicases involved in genome maintenance, DNA Repair (Amst). 76 (2019) 1–10. https://doi.org/10.1016/j.dnarep.2019.02.003.

[249] J. Rabl, Brca1-a and brisc: Multifunctional molecular machines for ubiquitin signaling, Biomolecules. 10 (2020) 1–20. https://doi.org/10.3390/biom10111503.

[250] P. Berndt, L. Winkler, J. Cording, O. Breitkreuz-Korff, A. Rex, S. Dithmer, V. Rausch, R. Blasig, M. Richter, A. Sporbert, H. Wolburg, I.E. Blasig, R.F. Haseloff, Tight junction proteins at the blood–brain barrier: far more than claudin-5, Cell. Mol. Life Sci. 76 (2019) 1987–2002. https://doi.org/10.1007/s00018-019-03030-7.

[251] C.P. Profaci, R.N. Munji, R.S. Pulido, R. Daneman, The blood–brain barrier in health and disease: Important unanswered questions, J. Exp. Med. 217 (2020) 1–16. https://doi.org/10.1084/jem.20190062.

[252] Y. Yang, E.Y. Estrada, J.F. Thompson, W. Liu, G.A. Rosenberg, Matrix metalloproteinase-mediated disruption of tight junction proteins in cerebral vessels is reversed by synthetic matrix metalloproteinase inhibitor in focal ischemia in rat, J. Cereb. Blood Flow Metab. 27 (2007) 697–709. https://doi.org/10.1038/sj.jcbfm.9600375.

[253] F. Teng, V. Beray-Berthat, B. Coqueran, C. Lesbats, M. Kuntz, B. Palmier, M. Garraud, C. Bedfert, N. Slane, V. Bérézowski, F. Szeremeta, J. Hachani, D. Scherman, M. Plotkine, B.T. Doan, C. Marchand-Leroux, I. Margaill, Prevention of rt-PA induced blood-brain barrier component degradation by the poly(ADP-ribose)polymerase inhibitor PJ34 after ischemic stroke in mice, Exp. Neurol. 248 (2013) 416–428. https://doi.org/10.1016/j.expneurol.2013.07.007.

[254] A. Mullier, S.G. Bouret, V. Prevot, B. Dehouck, Differential distribution of tight junction proteins suggests a role for tanycytes in blood-hypothalamus barrier regulation in the adult mouse brain, J. Comp. Neurol. 518 (2010) 943–962. https://doi.org/10.1002/cne.22273.

[255] J.L. Ables, J.J. Breunig, A.J. Eisch, P. Rakic, Not(ch) just development: Notch signalling in the adult brain, Nat. Rev. Neurosci. 12 (2011) 269–283. https://doi.org/10.1038/nrn3024.

[256] H. Okuda, H. Kiuchi, T. Takao, Y. Miyagawa, A. Tsujimura, N. Nonomura, H. Miyata, M. Okabe, M. Ikawa, Y. Kawakami, N. Goshima, M. Wada, H. Tanaka, A novel transcriptional factor Nkapl is a germ cell-specific suppressor of Notch signaling and is indispensable for spermatogenesis, PLoS One. 10 (2015) 1–19. https://doi.org/10.1371/journal.pone.0124293.

[257] R. Fior, D. Henrique, A novel hes5/hes6 circuitry of negative regulation controls Notch activity during neurogenesis, Dev. Biol. 281 (2005) 318–333. https://doi.org/10.1016/j.ydbio.2005.03.017.

[258] J. Huang, A. Bonni, A decade of the anaphase-promoting complex in the nervous system, Genes Dev. 30 (2016) 622–638. https://doi.org/10.1101/gad.274324.115.

[259] M. Zürner, S. Schoch, The mouse and human Liprin-α family of scaffolding proteins: Genomic organization, expression profiling and regulation by alternative splicing, Genomics. 93 (2009) 243–253. https://doi.org/10.1016/j.ygeno.2008.10.007.

[260] A.M. Sullivan, G.W. O'Keeffe, The role of growth/differentiation factor 5 (GDF5) in the induction and survival of midbrain dopaminergic neurones: Relevance to Parkinson's disease treatment, J. Anat. 207 (2005) 219–226. https://doi.org/10.1111/j.1469-7580.2005.00447.x.

[261] H. Wu, J. Li, D. Xu, Q. Zhang, T. Cui, Growth differentiation factor 5 improves neurogenesis and functional recovery in adult mouse hippocampus following traumatic brain injury, Front. Neurol. 9 (2018) 1–10. https://doi.org/10.3389/fneur.2018.00592.

[262] Y. Zhao, M. Zhang, H. Liu, J. Wang, Signaling by growth/differentiation factor 5 through the bone morphogenetic protein receptor type IB protects neurons against kainic acid-induced neurodegeneration, Neurosci. Lett. 651 (2017) 36–42. https://doi.org/10.1016/j.neulet.2017.04.055.

[263] R.M. Connor, C.L. Allen, C.A. Devine, C. Claxton, B. Key, BOC, brother of CDO, is a dorsoventral axon-guidance molecule in the embryonic vertebrate brain, J. Comp. Neurol. 485 (2005) 32–42. https://doi.org/10.1002/cne.20503.

[264] C. Tremblay-Laganière, R. Kaiyrzhanov, R. Maroofian, T.T.M. Nguyen, K. Salayev, I.T. Chilton, W.K. Chung, J.A. Madden, C. Phornphutkul, P.B. Agrawal, H. Houlden, P.M. Campeau, PIGH deficiency can be associated with severe neurodevelopmental and skeletal manifestations, Clin. Genet. 99 (2021) 313–317. https://doi.org/10.1111/cge.13877.

[265] E. Mulry, K. Parham, Inner Ear Proteins as Potential Biomarkers, Otol. Neurotol. 41 (2020) 145–152. https://doi.org/10.1097/MAO.0000000000002466.

[266] B. Decourt, D. Hillman, Y. Bouleau, D. Dulon, A. Hafidi, Is otospiralin inner ear specific? Evidence for its expression in mouse brain, Int. J. Dev. Neurosci. 27 (2009) 87–96. https://doi.org/10.1016/j.ijdevneu.2008.09.001.

[267] J. Zhong, Y. Wang, X. Qiu, X. Mo, Y. Liu, T. Li, Q. Song, D. Ma, W. Han, Characterization and Expression Profile of CMTM3/CKLFSF3, BMB Rep. 39 (2006) 537–545. https://doi.org/10.5483/BMBRep.2006.39.5.537.

[268] C. Regnard, D. Fesquet, C. Janke, D. Boucher, E. Desbruyères, A. Koulakoff, C. Insina, P. Travo, B. Eddé, Characterisation of PGs1, a subunit of a protein complex

co-purfying with tubulin polyglutamylase, J. Cell Sci. 116 (2003) 4181–4190. https://doi.org/10.1242/jcs.00743.

[269] M.K. Janowska, K.P. Wu, J. Baum, Unveiling transient protein-protein interactions that modulate inhibition of alpha-synuclein aggregation by beta-synuclein, a pre-synaptic protein that co-localizes with alpha-synuclein, Sci. Rep. 5 (2015) 1–10. https://doi.org/10.1038/srep15164.

[270] P.E. Schulz, A.D. McIntosh, M.R. Kasten, B. Wieringa, H.F. Epstein, A role for myotonic dystrophy protein kinase in synaptic plasticity, J. Neurophysiol. 89 (2003) 1177–1186. https://doi.org/10.1152/jn.00504.2002.

[271] F. He, T. Umehara, K. Tsuda, M. Inoue, T. Kigawa, T. Matsuda, T. Yabuki, M. Aoki, E. Seki, T. Terada, M. Shirouzu, A. Tanaka, S. Sugano, Y. Muto, S. Yokoyama, Solution structure of the zinc finger HIT domain in protein FON, Protein Sci. 16 (2007) 1577–1587. https://doi.org/10.1110/ps.062635107.

[272] A. Bonaldi, A. Kashiwabara, É.S. d. Araújo, L. V. Pereira, A.R. Paschoal, M.B. Andozia, D. Villela, M.P. Rivas, C.K. Suemoto, C.A. Pasqualucci, L.T. Grinberg, H. Brentani, S.S. Maria-Engler, D.M. Carraro, A.M. Vianna-Morgante, C. Rosenberg, L.R. Vasques, A. Krepischi, Mining Novel Candidate Imprinted Genes Using Genome-Wide Methylation Screening and Literature Review, Epigenomes. 1 (2017) 13. https://doi.org/10.3390/epigenomes1020013.

[273] F. Boussouar, M. Jamshidikia, Y. Morozumi, S. Rousseaux, S. Khochbin, Malignant genome reprogramming by ATAD2, Biochim. Biophys. Acta - Gene Regul. Mech. 1829 (2013) 1010–1014. https://doi.org/10.1016/j.bbagrm.2013.06.003.

[274] A. Onoufriadis, A. Shoemark, M.M. Munye, C.T. James, M. Schmidts, M. Patel, E.M. Rosser, C. Bacchelli, P.L. Beales, P.J. Scambler, S.L. Hart, J.E. Danke-Roelse, J.J. Sloper, S. Hull, C. Hogg, R.D. Emes, G. Pals, A.T. Moore, E.M.K. Chung, H.M. Mitchison, Combined exome and whole-genome sequencing identifies mutations in ARMC4 as a cause of primary ciliary dyskinesia with defects in the outer dynein arm, J. Med. Genet. 51 (2014) 61–67. https://doi.org/10.1136/jmedgenet-2013-101938.

[275] S. De Vega, T. Iwamoto, Y. Yamada, Fibulins: Multiple roles in matrix structures and tissue functions, Cell. Mol. Life Sci. 66 (2009) 1890–1902. https://doi.org/10.1007/s00018-009-8632-6.

[276] O. Pongs, Voltage-gated potassium channels: From hyperexcitability to excitement, FEBS Lett. 452 (1999) 31–35. https://doi.org/10.1016/S0014-5793(99)00535-9.

[277] B. Rudy, J. Maffie, Y. Amarillo, B. Clark, E.M. Goldberg, H.Y. Jeong, I. Kruglikov, E. Kwon, M. Nadal, E. Zagha, Voltage Gated Potassium Channels: Structure and Function of Kv1 to Kv9 Subfamilies, Encycl. Neurosci. 10 (2009) 397–425. https://doi.org/10.1016/B978-008045046-9.01630-2.

[278] D. Kappei, F. Butter, C. Benda, M. Scheibe, I. Draškovič, M. Stevense, C.L. Novo, C. Basquin, M. Araki, K. Araki, D.B. Krastev, R. Kittler, R. Jessberger, J.A. Londoño-Vallejo, M. Mann, F. Buchholz, HOT1 is a mammalian direct telomere repeat-binding protein contributing to telomerase recruitment, EMBO J. 32 (2013) 1681–1701. https://doi.org/10.1038/emboj.2013.105.

[279] C. Turbill, S. Smith, C. Deimel, T. Ruf, Daily torpor is associated with telomere length change over winter in Djungarian Hamsters, Biol. Lett. 8 (2012) 304–307. https://doi.org/10.1098/rsbl.2011.0758.

[280] V. Andreoli, R.C. Gehrau, J.L. Bocco, Biology of Krüppel-like factor 6 transcriptional regulator in cell life and death, IUBMB Life. 62 (2010) 896–905. https://doi.org/10.1002/iub.396.

[281] S.B. Geisler, D. Robinson, M. Hauringa, M.O. Raeker, A.B. Borisov, M. V. Westfall, M.W. Russell, Obscurin-like 1, OBSL1, is a novel cytoskeletal protein related to obscurin, Genomics. 89 (2007) 521–531. https://doi.org/10.1016/j.ygeno.2006.12.004.

[282] C. Yu, L. Wang, B. Lv, Y. Lu, L. Zeng, Y. Chen, D. Ma, T. Shi, L. Wang, TMEM74, a lysosome and autophagosome protein, regulates autophagy, Biochem. Biophys. Res. Commun. 369 (2008) 622–629. https://doi.org/10.1016/j.bbrc.2008.02.055.

[283] J.A. Schmidt, K.G. Danielson, E.R. Duffner, S.G. Radecki, G.T. Walker, A. Shelton, T. Wang, J.E. Knepper, Regulation of the oncogenic phenotype by the nuclear body protein ZC3H8, BMC Cancer. 18 (2018) 1–15. https://doi.org/10.1186/s12885-018-4674-1.

[284] D. Hu, E.R. Smith, A.S. Garruss, N. Mohaghegh, M. Joseph, C. Lin, J. Jackson, X. Gao, A. Saraf, L. Florens, M.P. Washburn, J.C. Eissenberg, A. Shilatifard, The Little Elongation Complex functions at initiation and elongation phases of snRNA gene transcription, Mol Cell. 51 (2014) 493–505. https://doi.org/10.1016/j.molcel.2013.07.003.The.

[285] J. Oh, J.S. Shin, Molecular mechanism and cellular function of MHCII ubiquitination, Immunol. Rev. 266 (2015) 134–144. https://doi.org/10.1111/imr.12303.

[286] A. Nagarajan, M.C. Petersen, A.R. Nasiri, G. Butrico, A. Fung, H. Bin Ruan, R. Kursawe, S. Caprio, J. Thibodeau, M.C. Bourgeois-Daigneault, L. Sun, G. Gao, S. Bhanot, M.J. Jurczak, M.R. Green, G.I. Shulman, N. Wajapeyee, MARCH1 regulates insulin sensitivity by controlling cell surface insulin receptor levels, Nat. Commun. 7 (2016). https://doi.org/10.1038/ncomms12639.

[287] A. Majdoubi, J.S. Lee, O.A. Kishta, M. Balood, M.A. Moulefera, S. Ishido, S. Talbot, C. Cheong, T. Alquier, J. Thibodeau, Lack of the E3 Ubiquitin Ligase March1 Affects CD8 T Cell Fate and Exacerbates Insulin Resistance in Obese Mice, Front. Immunol. 11 (2020) 1–14. https://doi.org/10.3389/fimmu.2020.01953.

[288] J. Wu, L. Xia, X. Yao, X. Yu, K.C. Tumas, W. Sun, Y. Cheng, X. He, Y.C. Peng, B.K. Singh, C. Zhang, C.F. Qi, S. Bolland, S.M. Best, C. Gowda, R. Huang, T.G. Myers, C.A. Long, R.F. Wang, X.Z. Su, The E3 ubiquitin ligase MARCH1 regulates antimalaria immunity through interferon signaling and T cell activation, Proc. Natl. Acad. Sci. U. S. A. 117 (2020) 16567–16578. https://doi.org/10.1073/pnas.2004332117.

[289] H.J. Kim, J. Bandola-Simon, S. Ishido, N.W. Wong, V.N. Koparde, M. Cam, P.A. Roche, Ubiquitination of MHC Class II by March-I Regulates Dendritic Cell Fitness, J. Immunol. 206 (2021) 494–504. https://doi.org/10.4049/jimmunol.2000975.

[290] X. Zhou, S.C. Sun, Targeting ubiquitin signaling for cancer immunotherapy, Signal Transduct. Target. Ther. 6 (2021). https://doi.org/10.1038/s41392-020-00421-2.

[291] M. Yan, X. Yang, H. Wang, Q. Shao, The critical role of histone lysine demethylase KDM2B in cancer, Am. J. Transl. Res. 10 (2018) 2222–2233. https://pubmed.ncbi.nlm.nih.gov/30210666/.

[292] M.T. Pedersen, K. Helin, Histone demethylases in development and disease, Trends Cell Biol. 20 (2010) 662–671. https://doi.org/10.1016/j.tcb.2010.08.011.

[293] A.S. Przybylska, M.S. Wojciechowski, M. Jefimow, Physiological differences between winter phenotypes of Siberian hamsters do not correlate with their behaviour, Anim. Behav. 147 (2019) 105–114. https://doi.org/10.1016/j.anbehav.2018.11.007.

[294] F. van Breukelen, S.L. Martin, The hibernation continuum: Physiological and molecular aspects of metabolic plasticity in mammals, Physiology. 30 (2015) 273–281. https://doi.org/10.1152/physiol.00010.2015.

[295] J.G. Boyles, B. Smit, A.E. McKechnie, A new comparative metric for estimating heterothermy in endotherms, Physiol. Biochem. Zool. 84 (2011) 115–123. https://doi.org/10.1086/656724.

[296] T. Ruf, G. Heldmaier, Reduced locomotor activity following daily torpor in the Djungarian hamster: recovery from hypothermia?, Naturwissenschaften. 79 (1992) 574–575. https://doi.org/10.1007/BF01131417.

[297] E.M. Thomas, M.E. Jewett, I. Zucker, Torpor shortens the period of Siberian hamster circadian rhythms, Am. J. Physiol. - Regul. Integr. Comp. Physiol. 265 (1993) 951–956. https://doi.org/10.1152/ajpregu.1993.265.4.r951.

[298] A.S. Przybylska-Piech, M.S. Wojciechowski, M. Jefimow, Polymorphism of winter phenotype in Siberian hamster: consecutive litters do not differ in photoresponsiveness but prolonged acclimation to long photoperiod inhibits winter molt, Front. Zool. 18 (2021) 1–15. https://doi.org/10.1186/s12983-021-00391-3.

[299] A.S. Przybylska, M.S. Wojciechowski, M. Jefimow, Photoresponsiveness affects life history traits but not oxidative status in a seasonal rodent, Front. Zool. 16 (2019). https://doi.org/10.1186/s12983-019-0311-3.

[300] J. Rybak, A. Kuß, H. Lamecker, S. Zachow, H.C. Hege, M. Lienhard, J. Singer, K. Neubert, R. Menzel, The digital bee brain: Integrating and managing neurons in a common 3D reference system, Front. Syst. Neurosci. 4 (2010) 1–15. https://doi.org/10.3389/fnsys.2010.00030.

[301] J.K. Mai, O. Kedziora, L. Teckhaus, M. V. Sofroniew, Evidence for subdivisions in the human suprachiasmatic nucleus, J. Comp. Neurol. 305 (1991) 508–525. https://doi.org/10.1002/cne.903050312.

[302] N. Christian, F. Geiser, To use or not to use torpor? Activity and body temperature as predictors, Naturwissenschaften. 94 (2007) 483–487. https://doi.org/10.1007/s00114-007-0215-5.

[303] K. Kramer, L.B. Kinter, Evaluation and applications of radiotelemetry in small laboratory animals, Physiol. Genomics. 13 (2003) 197–205. https://doi.org/10.1152/physiolgenomics.00164.2002.

[304] K.E. Wynne-Edwards, A. V. Surov, A.Y. Telitzina, Differences in endogenous activity within the genus *Phodopus*, J. Mammal. 80 (1999) 855–865. https://doi.org/10.2307/1383254.

[305] D. Weinert, K. Schottner, An inbred lineage of Djungarian hamsters with a strongly attenuated ability to synchronize, Chronobiol. Int. 24 (2007) 1065–1079. https://doi.org/10.1080/07420520701791588.

[306] L.R. Leon, L.D. Walker, D.A. DuBose, L.A. Stephenson, Biotelemetry transmitter implantation in rodents: Impact on growth and circadian rhythms, Am. J. Physiol. - Regul. Integr. Comp. Physiol. 286 (2004) 967–974. https://doi.org/10.1152/ajpregu.00380.2003.

[307] H. Dowse, J. Umemori, T. Koide, Ultradian components in the locomotor activity rhythms of the genetically normal mouse, *Mus musculus,* J. Exp. Biol. 213 (2010) 1788–1795. https://doi.org/10.1242/jeb.038877.

[308] L.P. Quinn, T.O. Stean, B. Trail, M.S. Duxon, S.C. Stratton, A. Billinton, N. Upton, LABORAS^{TM}: Initial pharmacological validation of a system allowing continuous monitoring of laboratory rodent behaviour, J. Neurosci. Methods. 130 (2003) 83–92. https://doi.org/10.1016/S0165-0270(03)00227-9.

[309] R.F. Nespolo, J.D. Gaitan-Espitia, J.F. Quintero-Galvis, F. V. Fernandez, A.X. Silva, C. Molina, K.B. Storey, F. Bozinovic, A functional transcriptomic analysis in the relict marsupial *Dromiciops gliroides* reveals adaptive regulation of protective functions during hibernation, Mol. Ecol. 27 (2018) 4489–4500. https://doi.org/10.1111/mec.14876.

[310] N. Koike, A. Hida, R. Numano, M. Hirose, Y. Sakaki, H. Tei, Identification of the mammalian homologues of the *Drosophila* timeless gene, Timeless1, FEBS Lett. 441 (1998) 427–431. https://doi.org/10.1016/S0014-5793(98)01597-X.

[311] M. Yandell, D. Ence, A beginner's guide to eukaryotic genome annotation, Nat. Rev. Genet. 13 (2012) 329–342. https://doi.org/10.1038/nrg3174.

[312] H. Bagheri, R. Dyer, A. Severin, H. Rajan, Comprehensive Analysis of Non Redundant Protein Database, Res. Sq. (2019) 1–9. https://doi.org/https://doi.org/10.21203/rs.3.rs-54568/v1.

[313] G. Dennis, B.T. Sherman, D.A. Hosack, J. Yang, W. Gao, H.C. Lane, R.A. Lempicki, DAVID: Database for Annotation, Visualization, and Integrated Discovery, Genome Biol. 4 (2003). https://doi.org/10.1186/gb-2003-4-9-r60.

[314] J. Zhang, R. Cai, J. Liang, A. Izaz, Y. Shu, T. Pan, X. Wu, Molecular mechanism of Chinese alligator *(Alligator sinensis)* adapting to hibernation, J. Exp. Zool. Part B Mol. Dev. Evol. 336 (2021) 32–49. https://doi.org/10.1002/jez.b.23013.

[315] R.M. Brigham, C.K.R. Willis, F. Geiser, N. Mzilikazi, Baby in the bathwater: Should we abandon the use of body temperature thresholds to quantify expression of torpor?, J. Therm. Biol. 36 (2011) 376–379. https://doi.org/10.1016/j.jtherbio.2011.08.001.

[316] J.G. Boyles, B. Smit, A.E. McKechnie, Does use of the torpor cut-off method to analyze variation in body temperature cause more problems than it solves?, J. Therm. Biol. 36 (2011) 373–375. https://doi.org/10.1016/j.jtherbio.2011.07.007.

[317] R.M.R. Barclay, C.L. Lausen, L. Hollis, What's hot and what's not: defining torpor in free-ranging birds and mammals, Can. J. Zool. 79 (2001) 1885–1890. https://doi.org/10.1139/cjz-79-10-1885.

[318] A. Zhu, J.G. Ibrahim, M.I. Love, Heavy-Tailed prior distributions for sequence count data: Removing the noise and preserving large differences, Bioinformatics. 35 (2019) 2084–2092. https://doi.org/10.1093/bioinformatics/bty895.

[319] J.G. Mercer, K.M. Moar, A.W. Ross, N. Hoggard, P.J. Morgan, Photoperiod regulates arcuate nucleus POMC, AGRP, and leptin receptor mRNA in Siberian hamster hypothalamus, Am. J. Physiol. Integr. Comp. Physiol. 278 (2000) R271–R281. https://doi.org/10.1152/ajpregu.2000.278.1.R271.

[320] F. Langlet, Tanycyte gene expression dynamics in the regulation of energy homeostasis, Front. Endocrinol. (Lausanne). 10 (2019). https://doi.org/10.3389/fendo.2019.00286.

[321] Y. Kameda, Y. Arai, T. Nishimaki, Ultrastructural localization of vimentin immunoreactivity and gene expression in tanycytes and their alterations in hamsters kept under different photoperiods, Cell Tissue Res. 314 (2003) 251–262. https://doi.org/10.1007/s00441-003-0789-y.

[322] S.T. Cooper, S.S. Sell, M. Fahrenkrog, K. Wilkinson, D.R. Howard, H. Bergen, E. Cruz, S.E. Cash, M.T. Andrews, M. Hampton, Effects of hibernation on bone marrow transcriptome in thirteen-lined ground squirrels, Physiol. Genomics. 48 (2016) 513–525. https://doi.org/10.1152/physiolgenomics.00120.2015.

[323] M. Hampton, R.G. Melvin, M.T. Andrews, Transcriptomic analysis of brown adipose tissue across the physiological extremes of natural hibernation, PLoS One. 8 (2013) 1–12. https://doi.org/10.1371/journal.pone.0085157.

[324] C. Schwartz, M. Hampton, M.T. Andrews, Hypothalamic gene expression underlying pre-hibernation satiety, Genes, Brain Behav. 14 (2015) 310–318. https://doi.org/10.1111/gbb.12199.

[325] B. Hwang, J.H. Lee, D. Bang, Single-cell RNA sequencing technologies and bioinformatics pipelines, Exp. Mol. Med. (2018) 1–14. https://doi.org/10.1038/s12276-018-0071-8.

[326] C.R. Merritt, G.T. Ong, S.E. Church, K. Barker, P. Danaher, G. Geiss, M. Hoang, J. Jung, Y. Liang, J. McKay-Fleisch, K. Nguyen, Z. Norgaard, K. Sorg, I. Sprague, C. Warren, S. Warren, P.J. Webster, Z. Zhou, D.R. Zollinger, D.L. Dunaway, G.B. Mills, J.M. Beechem, Multiplex digital spatial profiling of proteins and RNA in fixed tissue, Nat. Biotechnol. 38 (2020) 586–599. https://doi.org/10.1038/s41587-020-0472-9.

V Statement of Contribution

The author of this dissertation contributed to each manuscript as follows:

task	contribution [%]		
	chapter 2 radiotelemetry	chapter 3 hypothalamus	chapter 4 core areas
study design	90	90	20
animal experiment	100	90	100
sample collection	100	90	100
laboratory work	-	100	100
data analysis	90	80	100
data presentation	90	100	100
data interpretation	80	90	90
manuscript preparation	70	80	90

VI Approvals and Funding

The Djungarian hamsters *(Phodopus sungorus)*, model organism of this dissertation, were bred and housed in accordance with the local ethics committee **(35/9185.46-3)**. Experimental and surgical procedures on hamsters were approved by the regional council Tübingen, Germany **(1411)** and performed by trained personnel **(FELASA B / EU Tätigkeit A).**

This dissertation was funded by a grant from the German Research Foundation **[HE 6382/2-1]**.

The bioinformatics of chapter 3 and 4 was performed on the computational resource bwForCluster NEMO. The authors acknowledge support by the state of Baden-Württemberg through bwHPC and the German Research Foundation (DFG) through grant no **INST 39/963-1 FUGG** (bwForCluster NEMO).

VII Scientific Curriculum Vitae

Personal data

Name:	Elena Haugg (M.Sc.)
Year and Place of Birth:	1991, Pfaffenhofen an der Ilm, Germany
Institutional Address:	Ulm University, Institute of Neurobiology, Albert-Einstein-Allee 11, M25 - Niveau 5, 89081 Ulm, Germany
ORCiD:	https://orcid.org/0000-0001-7426-2546
Research Gate:	https://www.researchgate.net/profile/Elena-Haugg

Parts of the *Personal data* have been removed from this version of the doctoral thesis for reasons of data protection.

Career

since Mar 2018	**Research Associate (wissenschaftliche Mitarbeiterin)** Herwig Lab, Institute of Neurobiology, Ulm University, Ulm, Germany
Sep 2017 - Feb 2018	**Scientific Assistant (Hilfswissenschaftlerin)** Wolf Lab, Institute of Neurobiology, Ulm University, Ulm, Germany

Parts of the *Career* have been removed from this version of the doctoral thesis for reasons of data protection.

Education

since Mar 2018	**Doctoral Candidate (Doktorandin)** with Specialization on Radiotelemetry and Transcriptomics Faculty of Natural Sciences, Ulm University, Ulm, Germany
Nov 2015 - Aug 2017	**Master Studies in Biology (M.Sc.)** with Specialization on Neurobiology, Ecology, Human Genetics Faculty of Natural Sciences, Ulm University, Ulm, Germany
Oct 2012 - Oct 2015	**Bachelor Studies in Biology (B.Sc.)** with Specialization on Physiology Faculty of Natural Sciences, Ulm University, Ulm, Germany

Parts of the *Education* have been removed from this version of the doctoral thesis for reasons of data protection.

Publications

Haugg E, Borner J, Diedrich V, Herwig A (2021) **Comparative transcriptomics of the Djungarian hamster hypothalamus during short photoperiod acclimation and spontaneous torpor.** FEBS Open Bio 12:443–459. https://doi.org/10.1002/2211-5463.13350

Haugg E, Herwig A & Diedrich V (2021) **Body temperature and activity adaptation of short photoperiod-exposed Djungarian hamsters *(Phodopus sungorus):* Timing, traits, and torpor.** Front Physiol. https://doi.org/10.3389/fphys.2021.626779

Piscitiello E, Herwig A, Haugg E, et al (2021) **Acclimation of intestinal morphology and function in Djungarian hamsters *(Phodopus sungorus)* related to seasonal and acute energy balance.** J Exp Biol 224 https://doi.org/10.1242/jeb.232876

Diedrich V, Haugg E, Dreier C, Herwig A (2020) **What can seasonal models teach us about energy balance?** J Endocrinol 244(2): R17-R32 https://doi.org/10.1530/JOE-19-0502

Scientific Talks

Nov 2021: **"Body temperature and activity adaptation of short photoperiod-exposed Djungarian hamsters *(Phodopus sungorus):* Timing, traits, and torpor",** NeuroCon - Science+ 2021 of the Young German Neuroscience Society (jNWG), Günzburg, Germany

Aug 2021: **"Differences in hypothalamic transcriptomics comparing hibernation and spontaneous daily torpor",** 16th International Hibernation Symposium (IHS) 2021, virtual

Poster Presentations

Poster "Differential gene expression in the hypothalamus of hibernating garden dormice *(Eliomys quercinus)*"

- Mar 2021: 14th Göttingen Meeting of the German Neuroscience Society (NWG), virtual

Poster "Neuroanatomical mapping of hypothalamic core areas involved in the regulation of spontaneous daily torpor in Djungarian hamsters *(Phodopus sungorus)*"

- May 2019: 12th Student Symposium on Molecular Medicine, Ulm, Germany
- Mar 2019: 13th Göttingen Meeting of the German Neuroscience Society (NWG), Göttingen, Germany
- Mar 2019: 6th Schram Foundation Symposium, Göttingen, Germany

Poster "Continuous monitoring of core body temperature to assess hypothermia during spontaneous daily torpor in Djungarian hamsters *(Phodopus sungorus)*"

- Mar 2019: European User Group meeting of Data Science International (DSI), Berlin, Germany

Poster "Nail down torpor-related genes in the brain"

- May 2018, 11th Student Symposium on Molecular Medicine, Ulm, Germany

Memberships in Scientific Societies

since Aug 2021	International Hibernation Society (IHS)
since Jun 2019	Life Sciences Studierendeninitiative e.V. (btS)
since Feb 2019	British Society for Neuroendocrinology (BSN)
since Oct 2018	Federation of European Neuroscience Society (FENS)
since Oct 2018	German Neuroscience Society (NWG)

VIII Danksagung

The *Danksagung* has been removed from this version of the doctoral thesis for reasons of data protection.